FINAL REPORT

Biobased Carbon Fibers and Thermosetting Resins for Use in DoD Composites Applications

SERDP Project WP-1758

MARCH 2017

John J. La Scala
Joshua Sadler
Faye R. Toulan
Anh-Phuong Lam
Christopher Annunziato
US Army Research Laboratory

Amod Ogale
Meng Zhang
Annel Greene
Steven Chambers
Clemson University

Joseph Stanzione III
Kaleigh Reno
Richard Wool
University of Delaware

Fengshuo Hu
Donghun Koo
Giuseppe Palmese
Drexel University

Eric Hernandez
Joseph Stanzione III
Rowan University

SERDP
DOD ▪ EPA ▪ DOE

Page Intentionally Left Blank

Page Intentionally Left Blank

NOTICES

Disclaimers

The findings in this report are not to be construed as an official Department of the Army position unless so designated by other authorized documents.

Citation of manufacturer's or trade names does not constitute an official endorsement or approval of the use thereof.

Destroy this report when it is no longer needed. Do not return it to the originator.

Page Intentionally Left Blank

REPORT DOCUMENTATION PAGE

Form Approved
OMB No. 0704-0188

1. REPORT DATE *(DD-MM-YYYY)*	2. REPORT TYPE	3. DATES COVERED (From - To)
March 2017	Technical Report	1 January 2010–31 June 2015

4. TITLE AND SUBTITLE
Biobased Carbon Fibers and Thermosetting Resins for Use in DOD Composites Applications: SERDP WP-1758 Final Report

5a. CONTRACT NUMBER

5b. GRANT NUMBER

5c. PROGRAM ELEMENT NUMBER

6. AUTHOR(S)
John J La Scala, Joshua Sadler, Faye R Toulan, Anh-Phuong Lam, Christopher Annunziato, Amod Ogale, Meng Zhang, Annel Greene, Steven Chambers, Joseph Stanzione III, Kaleigh Reno, Richard Wool, Fengshuo Hu, Eric Hernandez, Donghun Koo, and Giuseppe Palmese

5d. PROJECT NUMBER
SERDP WP-1758

5e. TASK NUMBER

5f. WORK UNIT NUMBER

7. PERFORMING ORGANIZATION NAME(S) AND ADDRESS(ES)
US Army Research Laboratory
ATTN: RDRL-WMM-C
Aberdeen Proving Ground, MD 21005-5069

8. PERFORMING ORGANIZATION REPORT NUMBER
ARL-TR-7969

9. SPONSORING/MONITORING AGENCY NAME(S) AND ADDRESS(ES)

10. SPONSOR/MONITOR'S ACRONYM(S)
SERDP

11. SPONSOR/MONITOR'S REPORT NUMBER(S)

12. DISTRIBUTION/AVAILABILITY STATEMENT
Approved for public release; distribution is unlimited.

13. SUPPLEMENTARY NOTES

14. ABSTRACT
Current constituent materials used to produce composites for the military are often made from both fibers and resins that are derived from petrochemical feedstocks. The use of biological resources to make advanced fibers and high-performance thermosetting resins will help reduce the dependence of military composites on the volatile cost of petroleum, result in significant technological gains, and reduce toxicity of composite materials. We have used both bacterial and chemical decomposition of lignin to make tractable structures that are capable of fiber spinning. Efforts to stabilize and carbonize lignin have resulted in the highest-performing lignin-based carbon fibers to date. However, new developments in commercial polyacrylonitrile-carbon fiber technology have eliminated the need for lignin-based carbon fibers altogether. Unsaturated polyester, vinyl ester, epoxy, and polyurethane resin thermosets have been developed. Isosorbide-based vinyl ester resins have the highest-ever glass transition temperatures for a vinyl ester system. Bisguaiacol F has very promising properties as a replacement for bisphenol A with significantly reduced toxicity. Furan epoxies have shown high promise with good thermal properties and excellent toughness. Many of these resin systems have low costs and even lower life cycle costs relative to commercial resins, and thus they have good potential for transition to commercial industry.

15. SUBJECT TERMS
thermoset, environmentally friendly, renewable resources, carbon fiber, lignin

16. SECURITY CLASSIFICATION OF:			17. LIMITATION OF ABSTRACT	18. NUMBER OF PAGES	19a. NAME OF RESPONSIBLE PERSON
a. REPORT	b. ABSTRACT	c. THIS PAGE			John J La Scala
Unclassified	Unclassified	Unclassified	UU	308	19b. TELEPHONE NUMBER (Include area code) 410-306-0687

Page Intentionally Left Blank

Contents

List of Figures

List of Tables

Acknowledgments

The authors would like to thank Cytec Industries for providing the RDX-26936 (methacrylated epoxy) vinyl ester; Applied Poleramics Incorporated for providing methacrylated lauric acid; and West Vaaco for supplying lignin samples. This research was supported by the US Department of Defense through the Strategic Environmental Research and Development Program (SERDP WP-1758). This research was also supported in part by an appointment to the Postgraduate Research Participation Program at the US Army Research Laboratory (ARL) administered by the Oak Ridge Institute for Science and Education through an interagency agreement between the US Department of Energy and ARL.

INTENTIONALLY LEFT BLANK.

Executive Summary

The goal of this work is to use renewable resources derived from plants and other sources to prepare high-performance carbon fiber and thermosetting matrix resins with high-strength and high-thermal resistance. The scientific objectives of this work are to 1) develop methods for breaking down, modifying, and processing renewable resources to make epoxy resins, vinyl resins, and carbon fibers and 2) determine structure-property relationships for these novel materials.

We have developed numerous scientific and engineering advancements in this project. Bacteria can successfully decompose lignin into useable structures for the formation of small filaments that might be able to be converted into carbon fibers. Approximately 300 strains of bacteria that decompose lignin were identified, and some have the potential to make lignin into fiber-forming oligomers, including newly identified species of *Serratia.* However, scale-up of this process proved problematic and unfeasible for completion in this project.

We chemically fractionated lignin to alter its molecular weight distribution and alter its usefulness for separating chemically modified lignin. Various chemical modifications of lignin have been used successfully in carbon fiber development. These methods include acetylation and methacrylation, and we have developed separation strategies to produce carbon fiber precursors. Both melt- and solution-spinnable lignin-based fibers were produced. Thermo-oxidation and UV curing were successful stabilization methods for these fibers. Carbon fibers were produced from a few types of lignin and chemically modified lignin. The resulting mechanical properties were relatively poor, but there are obvious steps that need to be taken to improve these properties. Electrical conductivity of these fibers ranged from moderately conductive, similar to that of polyacrylonitrile (PAN)-based fibers, to highly conductive, indicating a significant graphitic content. The highest mechanical properties were achieved for lignin-based carbon fibers by stretching the fibers during processing resulting in modulus of 35 GPa, strength of 1 GPa, and elongation to failure of 3%, significantly exceeding the state of the art in lignin-based fibers. However, life cycle analysis of the lignin-based carbon fibers is not favorable due to the recent reduction in cost of PAN-based carbon fibers.

Numerous biobased resins were developed, including epoxies, vinyl esters (VEs), unsaturated polyesters (UPEs), and polyurethanes, many with excellent properties that can be used in high-performance polymers, composites, and coatings applications. Lignin-based cross-linkers have been prepared that have performance similar to that of bisphenol A cross-linkers while having significantly reduced toxicity. We have developed isosorbide methacrylate with the highest ever

transition temperature of greater than 250 °C for a VE system. This work has produced numerous reactive diluents and viscosity reducers for VE and UPE technology based on fatty acids, lignin, and isosorbide that will maintain or increase polymer performance while reducing hazardous emissions. The isosorbide-based viscosity reducer and lignin-based reactive diluents are promising for scale-up and commercialization. We have identified biobased lignin-derived resins with high-bioatomic efficiency that are good for the lower end of high-performance composites and most coatings applications. Furan epoxies are very promising with good thermomechanical properties and very high toughness, making them excellent candidates for composites and coatings applications. We have developed higher-performing UPE resins using isosorbide as an additive or component, but the feasibility for scale-up is low due to the long reaction times required. Life cycle analysis of these resins shows that many of these renewable technologies have lower or similar cost relative to commercial resin technologies and thus have high potential for commercial transition.

This work has benefited the Department of Defense by developing fibers and resins to reduce reliance on petroleum-derived materials, developing materials with properties unachievable using petroleum, offering solutions to reducing hazardous emissions, and reducing the toxicity of high-performance polymers and fibers.

1. Objective

The goal of this work was to use renewable resources derived from plants and other sources to prepare high-performance carbon fiber and thermosetting matrix resins with high strength and high thermal resistance. The scientific objectives of this work are to 1) develop methods for breaking down, modifying, and processing renewable resources to make epoxy resins, vinyl resins, and carbon fibers and 2) determine structure-property relationships for these novel materials.

There are a number of specific project areas and goals for each of these areas:

- Microbial degradation of lignin
    - Demonstrate that microbial degradation of lignin is feasible for producing carbon fiber precursors.
    - Identify optimum bacteria for decomposition of lignin.
    - Produce microbially degraded lignin at a small-to-moderate scale.
    - Perform life cycle cost analysis for production of microbially degraded lignin as carbon fiber precursors relative to polyacrylonitrile (PAN).
- Chemical modification/degradation/fractionation of lignin
    - Identify optimum chemical methods to obtain lignin-based carbon fiber precursors.
    - Produce chemically modified lignin at small-to-moderate scale.
- Lignin-based carbon fiber development
    - Identify modified lignin samples with optimum rheological properties for fiber spinning.
    - Identify modified lignin samples that can be stabilized to prevent fusion of fibers during carbonization.
    - Identify modified lignin samples that can be used to produce carbon fibers with high modulus and high strength.
    - Produce high-performance carbon fiber at small-to-moderate scale.
    - Perform life cycle cost analysis for production of chemically modified lignin as carbon fiber precursors relative to PAN.

- High-performance biobased resins
    - Identify biobased epoxy, polyamine, unsaturated polyester (UPE), and vinyl ester (VE) cross-linkers that produce glass transition temperature (T_g) greater than 150 °C when used in conjunction with standard resin components or other biobased components.
    - Identify biobased reactive diluents for UPE and VE resins that produce T_g no less than 10 °C lower than that of styrene-based resins.
    - Produce optimum biobased resins at 250-g scale for composite production.
    - Perform life cycle cost analysis for biobased resins relative to comparable epoxies, UPEs, and VE resins.
- High-performance biobased composites
    - Demonstrate composite production using biobased carbon fiber and biobased resins.
    - Develop biobased composites with properties similar to that of comparable nonbiobased composites.

Each of these goals was met during the course of this project. The timelines for these accomplishments are discussed in the following section.

2. Background

2.1 Strategic Environmental Research Development Program (SERDP) Relevance*

SERDP is the US Department of Defense's (DOD) environmental science and technology program, planned and executed in partnership with the US Department of Energy (DOE) and the Environmental Protection Agency (EPA), with participation by numerous other federal and nonfederal organizations. SERDP invests across a broad spectrum of basic and applied research, as well as advanced development.

SERDP focuses on cross-service requirements and pursues solutions to the DOD's environmental challenges. The development and application of innovative

* Portions of this section were originally published in the US Army Research Laboratory (ARL) report: La Scala et al. Biobased carbon fibers and high-performance thermosetting resins for use in us department of defense applications. Aberdeen Proving Ground (MD): Army Research Laboratory (US); 2012 June. Report No.: ARL-SR-245.

environmental technologies will reduce the costs, environmental risks, and time required to resolve environmental problems while, at the same time, enhancing and sustaining military readiness.

Current constituent materials used to produce composites for the military (Fig. 1) are often made from both fibers and resins that are derived from petrochemical feedstocks. Because advanced fibers and thermosetting resins are derived from petroleum, their costs are tied strongly to the price of oil. This was evidenced over the past few years where the cost of oil rose to unprecedented levels, causing a similar cost increase in advanced fibers and thermosetting resins. Furthermore, some of these processes produce environmental toxins. The use of biological resources to make advanced fibers and high-performance thermosetting resins will help reduce the dependence of military composites on the volatile cost of petroleum, thereby helping to reduce the cost of composite materials for the DOD. In addition, the processes used to make these fibers and resins from biological sources should have reduced environmental effects. There have been previous developments in biobased composite resins, including fatty acid VEs[1] and acrylated or maleinized soybean oil,[2] but these have a reduced T_g relative to commercial epoxy and VE resins typically used in DOD composites, limiting their use. High-performance macroscale fibers have not yet been developed successfully from biological sources. Thus, newly developed biobased fibers and resins must have the high performance necessary for DOD applications. This work will benefit the DOD by providing critical, high-performance composite materials for DOD systems that are based on sustainable resources and processes, are not dependent upon fossil fuel feedstocks, and have reduced environmental effects.

Fig. 1 Various weapons platforms that use composite materials including the Apache helicopter, the high-mobility multipurpose wheeled vehicle, Stiletto, F-22, and USS *Radford*

This work will further enable us to reach the goals articulated in Executive Order 13423 (Strengthening Federal Environmental, Energy, and Transportation Management), the Department of Defense Green Procurement Program, and the 2007 Army Environmental Requirements and Technology Assessments by developing biobased, environmentally friendly composite materials.

Current constituent materials used to produce composites for the military are often made from both fibers and resins that are derived from petrochemical feedstocks. In the Army, rotor blades for rotorcraft helicopters and turbo propeller-driven aircraft are composite designs based on high-strength carbon fiber technology.[3] The lower mass of the blades increases both the revolutions per minute and the thrust and payload capacity for these platforms.[3] Composite sabots are the largest use of composite materials in the US military at over 800,000 lb annually, because the transition from aluminum to carbon fiber–reinforced composites allows extended range and velocity to be achieved.[3]

The US Air Force uses composite materials in many of its fighter jets, including the B-2, F-16, F-18, and F-22.[4] In fact, the use of composites has grown considerably in the Air Force, as the F-14 was only composed of approximately 2 weight-percent (wt%) composite materials, while the newer F-22 contains approximately 24 wt% composites.[4] Specifically, carbon-epoxy composites are used in the center and aft fuselage, wing and tail skins, and other areas for the F-18 and F-22.[4]

The Navy is also increasing its use of composite materials on ships. The Advanced Enclosed Mast/Sensor, a composite structure that was installed on the USS *Radford*, has a reduced weight, reduced structure and sensor maintenance, and higher performance relative to steel masts.[5] The M80 Stiletto is a new ship made using mostly carbon fiber-epoxy composites to reduce weight and meet other performance criteria.[6] In addition, a composite rudder is used on the MCM-9 and is being evaluated for use on DDG ships to reduce cavitation damage and minimize rudder maintenance.[7] UPE radomes are used in the Navy and Air Force to protect sensitive electronics from environmental hazards while allowing the transmission of radio waves.

Overall, composites outperform traditional materials for these applications because of their light weight, high strength, high toughness, resistance to plastic deformation, and inherent corrosion resistance. Therefore, future classes of vehicles and equipment will use significantly higher amounts of composite materials, making these vehicles lighter, faster, more efficient, and more maneuverable.

2.2 Fibers Background

Commonly used fibers in the DOD for reinforcement of composite structures are glass fibers, Kevlar, and carbon fibers. Important properties of these fibers are listed in Table 1. Glass fibers come in a variety of types, including E-glass, R-glass, and S-glass, that have slightly different chemical compositions. S-glass is generally superior to that of E-glass, while R-glass has properties intermediate of E- and S-glass. Glass fibers have relatively low moduli, especially when considering specific properties, because of their relatively high densities (~2.5 g/cm^3). Kevlar, or aramid fibers, is slightly stiffer than glass but with a lower strength. Kevlar comes in a few varieties, but Kevlar 49 is the most commonly used. Kevlar is most often used in body armor,[3] and because it has approximately half the density of glass fibers, it is also used to substitute for glass when lighter-weight parts are needed. Carbon fibers are the stiffest fibers used for typical composite applications and also have lower densities relative to glass. Thus, carbon fibers are typically used when high stiffness and low weight are needed. Carbon fibers come in a variety of types, but AS4 and IM7 are among the most commonly used in DOD composites. IM7 generally performs higher than AS4. Higher-performing carbon fibers do exist, such as Dialead K13D2U fibers, which have a modulus of approximately 700 GPa and strength of approximately 4,000 MPa. High-strength fibers such as Hexcel's IM9 have a strength of approximately 6,500 MPa with about the same modulus of IM7.[8–10]

Table 1 Properties of important composite fibers[8-10]

Property	E Glass	S2 Glass	K-49 Kevlar	AS4 Carbon	IM7 Carbon
Density (g/cm^3)	2.55	2.47	1.44	1.8	1.8
Tensile modulus (GPa)	70	88	130	230	280
Tensile strength (MPa)	5,300	8,300	4,000	4,300	5,200
Ultimate elongation (%)	5.5	4.7	2.7	1.8	1.9
Toughness (GPa)	65	85	50	3.7	4.0

High-strength carbon fibers used in structural composite applications, such as IM7 and AS4, are almost exclusively derived from solution-spinning of PAN precursor fibers.[11,12] In actuality, PAN-based carbon fibers are produced from copolymers of acrylonitrile and other monomers, such as acetic acid, vinyl acetate, and methacrylic acid, rather than pure PAN.[11] Acrylonitrile is produced from propene generated during the refining of fossil fuels,[11] and the other comonomers are produced from petroleum refining. The precursor fibers have to be produced by solution-spinning because ordinary grades of PAN degrade before melting. This strategy has been successfully used in the past to thermo-oxidatively stabilize precursor fibers into an intractable form by intra-chain cyclization of the CN moieties. This intractable form of precursor fiber is critical to the subsequent

carbonization step.[11] The fibers are carbonized at moderate temperature (~1,000–1,500 °C) to favor turbostratic carbon formation rather than graphite formation.[11]

The solution-based process to produce carbon fiber suffers from 3 inherent limitations: 1) use of hazardous solvents, 2) creation of voids within the precursor fibers due to the removal of solvent, and 3) production of hydrogen cyanide (HCN) during the thermal stabilization and carbonization steps. To avoid the use of solvents, prior research has focused on the development of carbon fibers from melt-spinnable PAN precursor fibers.[13] However, most organic fibers, including PAN and biobased precursors, melt below the oxidative stabilization temperature range of 250–270 °C. Our prior research has led to the development of UV radiation curing of a photosensitive termonomer to stabilize the precursor fibers.[14,15] A high-power UV irradiation chamber was designed and constructed. Subsequently, the fibers were thermo-oxidatively cyclized. High-temperature graphitization furnaces were then used to successfully produce carbon fibers. UV-assisted cross-linking and cyclization of terpolymer composition was successfully demonstrated. These carbon fibers displayed good tensile modulus (~130 GPa) but low strength (~700 MPa).[14,15] Although progress has been made in the elimination of solvents during precursor fiber-spinning, the precursor still remains PAN, which produces HCN and other toxic gases during the thermal stabilization and carbonization steps. Therefore, additional studies need to investigate the replacement of PAN by an environmentally friendly/sustainable precursor.

Although numerous hydrocarbons can be converted to carbon, very few have been actually converted to structural carbon fibers. Besides PAN, mesophase pitch (MP) and rayon are the only other precursors that have produced carbon fibers. MP produces highly graphitic carbon fibers with high modulus and high thermal conductivity, but low strength. The highly polynuclear aromatic structure of MP, in conjunction with limited alkyl side groups, has been successfully exploited in melt-spinning of the MP precursor. Melt-spinning is followed by thermo-oxidative cross-linking at the alkyl groups at fairly high temperatures (such as 250 °C) because the softening point of MP is quite high at 300 °C and then followed by very high graphitization temperatures (Fig. 2).[12] The highly aromatic molecular architecture facilitates 3-D graphitic crystal formation, which leads to ultrahigh thermal conductivity of over 1,100 W/m·K and high tensile modulus of approximately 700 GPa, but only moderate tensile strength of 2 GPa and poor compressive strength of approximately 0.7 GPa (due to flaw sensitivity of the highly crystalline structure and microbuckling of graphene layers). As a result, MP carbon fibers are not often used in structural applications but are used in electronic applications because of their high conductivities.

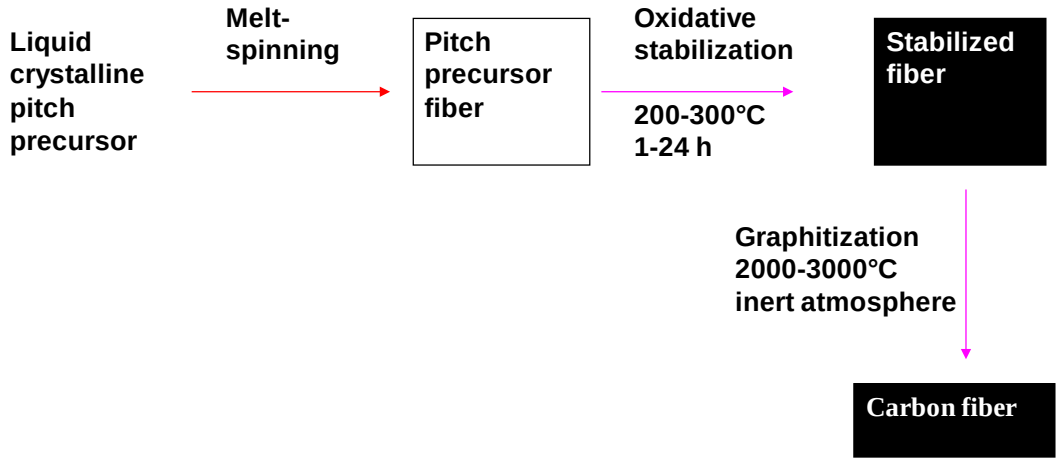

Fig. 2 Commercial pitch-based carbon fiber production[11,12]

Current materials technology and processing techniques do not allow for carbon fibers that achieve both high modulus and high strength.[11] The function is larger for PAN-based fibers, but also PAN-based fibers are able to achieve much higher strengths than pitch-based fibers, while pitch-based fibers can achieve higher moduli.[11] It is generally accepted that stresses created by high-temperature heat treatment cause splitting, reducing the mechanical and thermal properties of the fibers. Figure 3 shows these defects that limit the strength and modulus of these materials. PAN-based carbon fibers are typically much cheaper than pitch-based fibers.[11,12] In addition, high-modulus fibers generally cost more than lower-modulus fibers for 2 reasons: 1) higher-modulus fibers are made with reduced fiber diameter, improving both modulus and strength, but requiring increased processing of the starting fibers (PAN or pitch) and 2) high-modulus materials require higher carbonization temperatures, increasing processing costs.

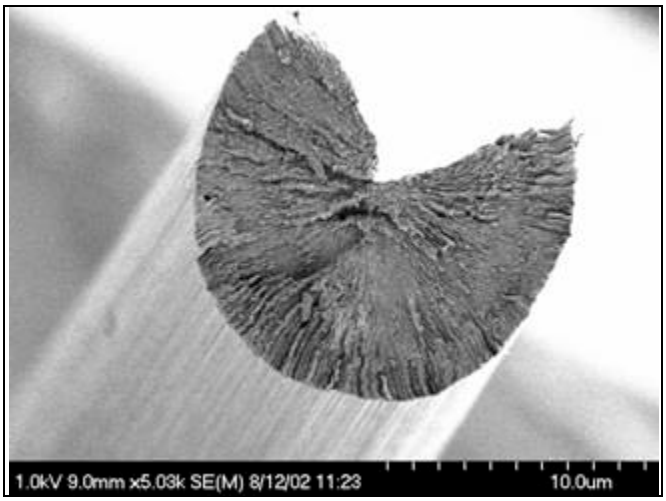

Fig. 3 Defects seen in carbon fibers that limit strength and modulus of these materials as shown for MP-based fibers produced at Clemson University

Rayon, on the hand, uses naturally occurring cellulose, but its conversion to carbon is limited to carbon fibers with poor strength and low thermal conductivity. Removal of noncarbon elements from the main chain severely limits its ability to form a 3-D graphitic crystalline structure.[13] Therefore, rayon-based carbon fibers cannot be used in primary reinforcement applications; instead, they find niche applications in ablative composites in rocket nozzles due to their low thermal conductivity.[12]

Carbon fibers are used in a number of defense applications.[16] PAN-based carbon fibers have the widest use and are found in rotary and fixed-wing aircraft, missiles, and space platforms. Pitch-based carbon fibers are not used in rotary aircraft, launch vehicles, and tactical missiles but are used in jets, strategic missiles, and satellites when increased stiffness is necessary. Rayon-based fibers are primarily used in missiles. Their overall demand for commercial and defense applications is estimated at 100,000,000 lb/yr in 2011.[17]

Numerous biobased fibers are used in composites, including jute, hemp, flax, sisal, and others. These fibers are based on cellulose and have specific moduli higher than that of glass fiber.[18] However, these fibers tend to have defects due to processing that cause them to have low strengths. Cellulosic nanofibers have been developed recently.[19] These nanofibers have dimensions of 20- to 100-nm-thick rods with lengths on the order of 1 μm. On the individual nanofiber scale, these nanofibers have excellent properties, including very high specific stiffness and strengths. However, the short length of these fibers does not allow for load transfer across the part, severely limiting the properties of the resulting composite.

2.3 Resins Background

The DOD uses various resin systems for composite materials, including epoxies, VEs, UPEs, bismaleimides, cyanate esters, and phenolics. Bismaleimides and cyanate esters are used typically for aircraft composites requiring very high-temperature performance (>250 °C). Phenolics are mainly used as spall liners in Army vehicles.[3]

Epoxy resins are among the most highly used matrix materials.[20] Epoxy resins are typically bisphenol-based monomers that are cross-linked using diamine curing agents (Fig. 4). Aliphatic epoxies also exist but produce low-temperature, flexible, and tough epoxies. Bisphenol epoxies and novolac epoxies, also based on phenol rings, are used to produce rigid, high-temperature epoxies. Similarly, aliphatic curing agents are used to produce tough low-temperature epoxies, while cyclic curing agents, such as Amicure bis(p-aminocyclohexyl) methane (PACM), are used to produce higher-temperature epoxies. Thus, epoxy resins can have viscosities of

100–10,000 cP at room temperature, T_g's ranging from below freezing to as high as 250 °C, moduli ranging from approximately MPa to 3 GPa, strengths of less than 1 MPa to greater than 100 MPa, and elongation to failure ranging from 1% to more than 50%.[20] Rigid epoxy resins for typical DOD applications have viscosities of 100–1,000 cP, T_g's greater than 100 °C, moduli greater than 2 GPa, strengths greater than 100 MPa, and elongation to failure of approximately 5%.[20] Novolac epoxies have T_g's greater than 200 °C, elongation to failure of approximately 3%, and strengths slightly less than 100 MPa.[20] Epoxy resins are produced from the reaction of a diol, such as bisphenol, or polyol and epichlorohydrin.[20] Both bisphenol and epichlorohydrin produce known health problems and are currently entirely derived from chemicals produced during petroleum refining.[20]

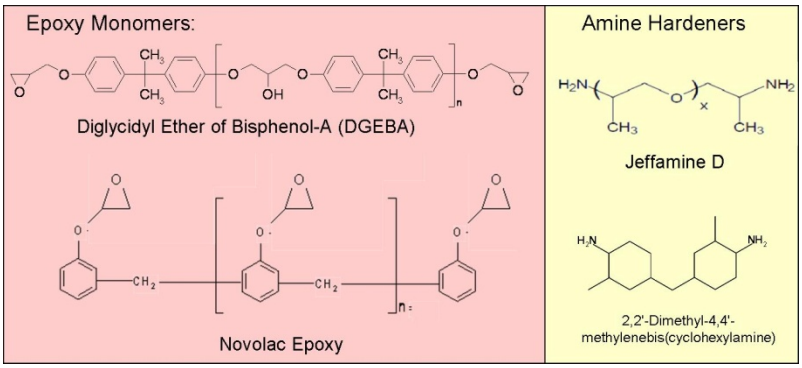

Fig. 4 Epoxy monomers and amine hardeners used in typical commercial epoxy formulations

UPE resins and VE resins are also commonly used matrix resins (Fig. 5). VE monomers are simply methacrylated epoxies. UPEs are short-chain polymers of diols, such as ethylene glycol, and diacids/anhydrides, such as maleic acid and terephthalic acid.[21] The rigidity of UPEs increases as the length of the diol is reduced, the amount of aromatic acids is increased, and the amount of polymerizable unsaturation character from the maleic acid is increased.[21] UPEs and VE resins cross-link upon addition of small amounts of peroxide initiators (1–2 wt%) that generate free radicals and cause the free-radical polymerization of the UPE unsaturation sites or vinyl sites on VE. Unfortunately, both resin types use styrene, a hazardous air pollutant (HAP), as a reactive diluent in the amount of 30–60 wt%. Commercial VEs typically have viscosities of 100–1,000 cP, T_g's of approximately 100 °C (toughened VEs), 120–150 °C (standard diglycidyl ether of bisphenol A [BPA] VE) and approximately 180 °C (Novolac VE). VEs are currently derived from 100% petroleum-based products.[22,23] Commercial UPE resins have a large variety of properties because of their low cost and general-purpose nature. However, UPE resins for DOD applications typically have viscosities of 500–5,000 cP, T_g's of approximately 100 °C, strengths of 50–100

MPa, moduli of 2–3 GPa, and elongation to failure of 2%–4%.[21] UPEs currently can be derived partially from biobased sources, as maleic anhydride (MA) and diethylene glycol are currently manufactured in biological processes. However, both UPE and VE resins use styrene as a reactive diluent, which is a HAP and volatile organic compound (VOC) and its use in composites manufacturing is regulated.[24]

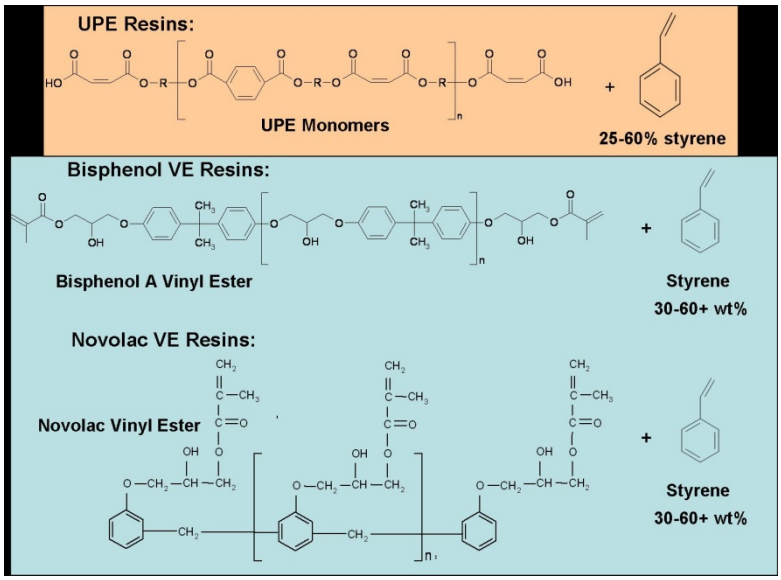

Fig. 5 Chemical structure of the major components of UPE and VE resins

Fatty acid VE resins have viscosities less than 1,000 cP, T_g's greater than 100 °C, and strength over 100 MPa, but they only use 10–25 wt% renewable component. Higher renewable components result in viscosities over 1,000 cP and T_g's below 100 °C.[1,3] Maleinized triglycerides have achieved T_g's of 140 °C,[2] but the moduli and heat distortion temperatures of these resins were very low. This occurred because high cross-linking prevented complete thermal softening at temperatures below 140 °C, but the aliphatic character of these resins enabled various motions of these polymeric chains causing significant softening at temperatures as low as 50 °C.

3. Materials and Methods

Figure 6 shows the general concept of this project. Several natural resources are currently used to produce biobased chemicals, including lignin, carbohydrates, cellulose, hemicellulose, chitin, and plant oils. This work focused on developing high-T_g biobased resins by selecting or preparing cyclic and aromatic derivatives of lignin, carbohydrates, cellulose, hemicellulose, chitin, and hybrid monomers based on multiple renewable sources. Biobased fibers were prepared from lignin-

based oligomers. The biobased resins and fibers were combined to make high-performance biobased composites for DOD applications.

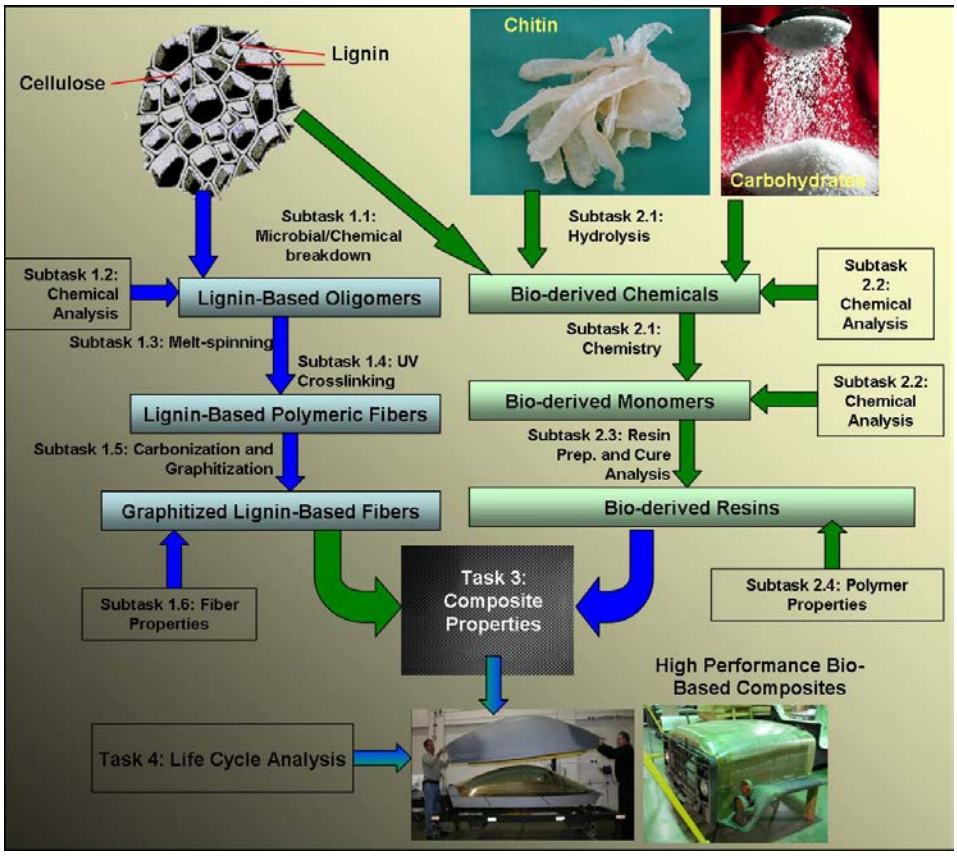

Fig. 6 Overall structure of this project whereby natural resources were used to make high-performance fibers, resins, and composites. (The tasks and subtasks are labeled according to the accepted WP-1758 proposal, not the sections of this report.)

In the following sections, a general listing of the methods used to develop biobased resins and fibers is presented. However, specific methodologies performed are listed at times throughout this text. Because these methods were not generally performed, it does not make sense to specifically call out these methodologies in this section.

3.1 Task 1: Lignin-Based Carbon Fibers

Task 1 entails using lignin to make high-performance carbon fibers. Among biobased alternatives, lignin is an aromatic encrusting material found in vascular plants, which confers rigidity and strength to wood. Lignin is abundantly available; over 3×10^{11} ton of lignin exist in the biosphere with approximately 2×10^{10} ton generated annually.[25] Because of the aromatic nature of the compound, lignin may be used to generate a valuable source of aromatic precursors for melt processing

into fibers. However, because of its 3-D aromatic structure, lignin is intractable in its unmodified state and must be broken down into lower-molecular-weight aromatic fragments largely involving the basic repeat units trans-conipheryl, trans-sinapyl, and trans-coumaryl. Thus, this project focused on ways to degrade lignin into a tractable form so that carbon fibers can be produced as outlined in Fig. 7.

Since the 1960s, lignin has been studied as a precursor for carbon fibers. Overall, the properties of lignin-based fibers using these methods are low relative to commercial carbon fibers. Generally, the lignin-based fibers had significant amounts of defects causing low properties.[13,17] In addition, the DOE at Oak Ridge National Laboratory (ORNL) is working to make low-cost, moderate-performance carbon fibers from lignin. These fibers are being developed for automotive applications to enable high automobile fuel economy. Although developments by ORNL are important, the low-performance goals are not sufficient for DOD applications. Thus, it is important that the DOD also work on developing lignin-based carbon fiber. This team performs work that others have not done to make high-performance lignin-based fibers. This includes novel fractionation and decomposition techniques, surface stabilization of fibers, and other controls of the processing to limit defect growth as detailed in the following subsections.

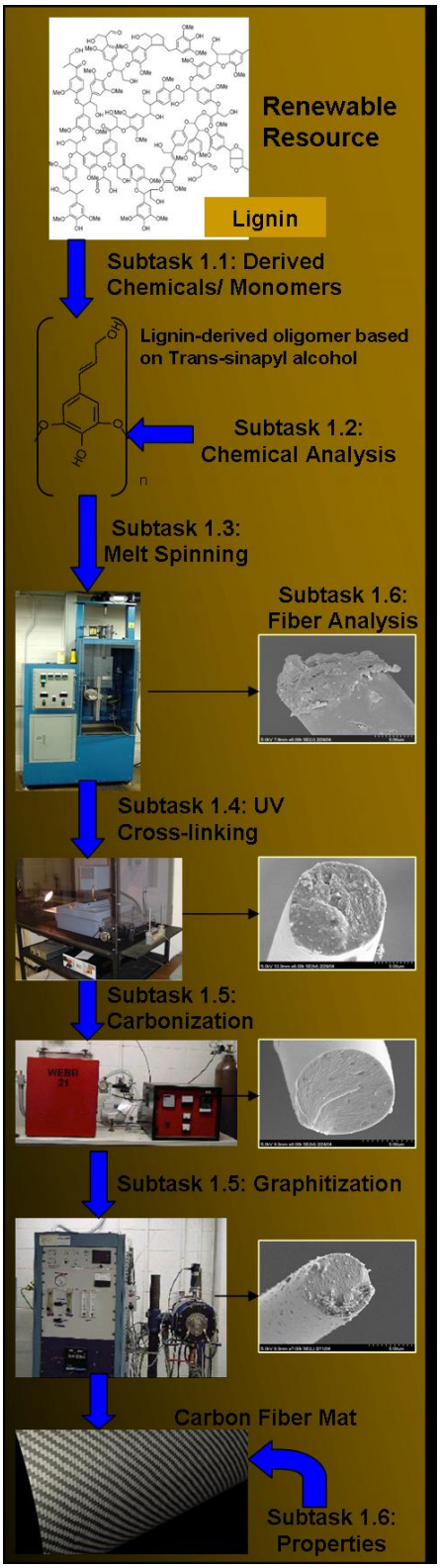

Fig. 7 Process for making biobased carbon fibers from lignin

3.1.1 Subtask 1.1: Preparation of Lignin-Based Oligomers for Fiber Production

The processes involved in the breakdown of lignin can be broadly identified as chemical or microbial. Chemical processes include high-rate but low-selectivity catalytic cracking and acidification. In contrast, microbial mechanisms produce better selectivity but often lack speed and do not require the use of elevated temperature processes. Therefore, both routes are pursued in this work.

Other researchers have investigated the chemical breakdown of lignin mostly for fuel applications.[26] Fluidized lignin was thermally cracked in a reactor by exposure to elevated temperatures for short durations. Simple thermal cracking using basic or acidic aqueous environments were performed at elevated temperatures (250–450 °C) and pressures (1–20 atm) for durations ranging from 10 s to a few hours.[26] Hydrogen peroxide has been effective in reducing the required temperatures down to 80–160 °C for cracking.[27] We examined other methodologies, including chemical modification combined with extractions to obtain desired products.

3.1.1.1 Microbial Decomposition of Lignin for Fiber Production

Microbial lignin degradation using eukaryotic organisms has previously failed because of long incubation times.[28] Fungi, in general, produce more complex digestive enzymes but do so at a much slower rate than bacteria. Therefore, research into bacterial degradation of lignin, investigated by co-investigator Greene, yielded wild-type bacteria capable of degrading lignin.[28] Using an isolation chemostat method with methanol as the sole carbon source, we rapidly screened potential isolates for ligninolytic activity.

Lignin chemistry varies according to the plant it comes from and the process used to recover the cellulosic fibers from that plant. Some have suggested that birch lignin may be better than pine lignin for fiber production.[29] Therefore, we investigated different lignin and different lignin recovery processes.

Full details of experimental methods of the microbial lignin decomposition work can be found in the report titled *Isolation and Characterization of Ligninolytic Bacterial Species* (Appendix A).

3.1.1.2 Material

Three grades of lignin were obtained:

- Softwood Kraft lignin (SKL), Indulin AT, was obtained from Mead-Westvaco, Charleston, South Carolina.[30]

- Soda lignin Protobind 1000 was obtained from GreenValue Enterprises LLC in Media, Pennsylvannia, derived from wheat straw and grass.
- An organosolv hardwood lignin was provided by Energy Research Centre, Netherlands (ECN lignin). The ECN lignin was derived from poplar with an ethanol-organosolv process (<0.1% ash content).

Soil and humus samples were collected aseptically at various locations in Louisiana, Florida, Georgia, South Carolina, North Carolina, Tennessee, Maryland, and Delaware. Samples were transported to the laboratory under refrigeration.

3.1.1.3 Lignolytic Culture Isolation

Since the world population of bacteria is so immense (>10^{30} bacteria and more than 10^5 to 10^7 unique species), searching for a specific organism capable of breaking a specific molecule is a challenge. The traditional method for isolating such an organism involves plating billions and billions of cultures on solid microbial media in Petri dishes. However, this method is time consuming, costly, and often leads to failed results. A method of continuous culture chemostat isolation is a much more efficient preliminary screening method of searching through subsamples of the more than 10^{31} bacteria in the Earth's environment. In a chemostat isolation system, a liquid microbial media is prepared that contains only one carbon source. In seeking a lignolytic organism, the choice for sole carbon source is dependent on the many different linkages found within lignin, factoring in stereochemistry, unique bond strengths, and potential lethality to bacteria. In this study, the goal is to find organisms that can break one or more of the different linkages in lignin.

A bacterium will not produce a particular byproduct if it is lethal to the bacterium because any organism that does so will kill itself. Therefore, noting the structure of lignin and surmising potential breakdown products, we find that the simplest sole carbon source for a chemostat used in the search for a lignolytic organism is methanol. Methanol is toxic to many organisms, but if a culture survives in the presence of methanol, then it is possible the organism may produce methanol as a byproduct of lignin degradation. Other potential carbon sources are those compounds that contain similar linkages or that would be likely breakdown products of lignin degradation. All organisms require carbon for life. When a sole source of carbon is used in the only medium provided to bacteria, those organisms that survive and grow must either be able to use that carbonaceous compound for life-sustaining carbon or derive carbon from atmospheric carbon (carbon dioxide). For this study, the search is for organisms that can use the sole carbon source provided.

In the chemostat (Figs. 8 and 9), a mixed culture of billions to trillions of bacteria is added to the vessel, and liquid media containing the sole carbon source is pumped into the vessel. Temperature and pH are controlled in the vessel. The flow rate of the liquid media is steadily increased. Those organisms capable of growing under the conditions and using the sole carbon source will multiply and increase in population size within the vessel. However, those organisms that are incapable of growing on the sole carbon source medium will not grow, their population will not increase, and they will be gradually washed out with continual dilution by the influx of new media.

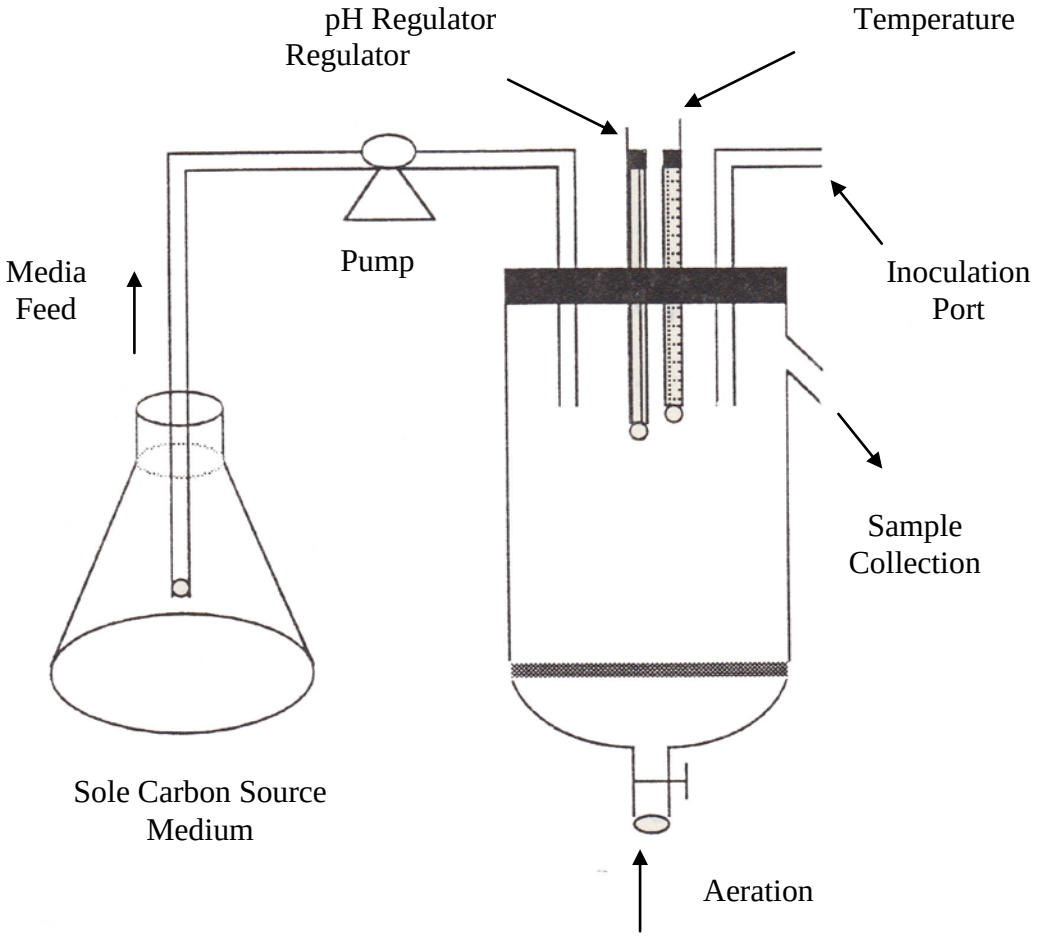

Fig. 8 Schematic of chemostat used for isolation of lignolytic bacteria

Fig. 9 Chemostat assembled for lignolytic microorganism isolation

The best choice of a bacterial population source to seed a chemostat would be from an environment where lignolytic organisms likely live in nature.[28] Bacteria do not expend energy to generate degradative enzymes unless those enzymes are used in survival. Survival to a bacterium is the ability to access food and water. Natural bacterial selection leads to die-off of the species that cannot survive within a particular environment. Therefore, to have such a specialized ability to degrade lignin, the organisms would most likely need to live in an environment where lignin is being degraded or where similar compounds exist, such as in rotting wood and wood products, decomposing bagasse, ruminant/cecal feces, lignin-attacking plant pathogens, oil-soaked soil, creosote posts, swamp soils, crude oil, soils, and decomposing hay.

For this study, a continuous culture isolation chemostat was aseptically assembled with temperature, pH, media infusion rate, and aeration controls. Sole carbon source liquid media were formulated using a 0.5%–3.0% carbon source, a carbon-free vitamin mixture, and stock solutions of mineral salts. For microbial growth, there is a limit to the concentration of solutes that can be presented within an

aqueous microenvironment. At too high a concentration, osmotic pressure restrictions overwhelm microbial capability, prevent growth, and can even be lethal to sensitive organisms. In this experiment, an upper limit of 3% carbon source was chosen, since this typically is a safe concentration for most bacterial species. As the purpose of this phase of the experiment was to isolate as many potential lignolytic organisms from the environment as possible, it was important to maintain practical concentration conditions that would promote microbial growth. At some future date, isolated lignolytic organisms should be tested to determine the optimum lignin concentrations that allow maximum growth and lignin degradation.

Analogs were chosen as carbon source molecules based on similar chemical structure and bonding as in the complex lignin molecule. Analogs used in the chemostat media feed included methanol, vanillin, vanillic acid, guaiacol, veratraldehyde, and 4-hydroxy, 3-methoxy cinnamic acid. Indulin AT lignin also was used. A sterilized solution of 0.1 M sodium hydroxide (NaOH) was used for pH adjustment. Incubation temperature ranges included 21–35 °C and pH ranges included 7.0–9.5. With alterations to pH, temperature, analog, and formulation concentration, over 200 combinations of parameters were conducted using the chemostat. Temperature and pH ranges were selected based on typical growth parameters for bacteria and typical growth conditions that would be expected in the environment. Since it is highly unlikely that an organism would grow in conditions outside those typically encountered in its native conditions, conditions mimicking environmental conditions were selected.

Over 50 soils, rotting wood, creosote, and crude oil samples were collected from the environment in Louisiana, Florida, Georgia, South Carolina, North Carolina, Tennessee, Maryland, and Delaware. The environmental samples were inoculated into the chemostat, one sample at a time, and in mixtures of 5 samples at a time. Each sample was allowed to equilibrate and was then tested through the entire range of temperature, pH, and flow rate conditions through each sole source medium type while maintaining constant atmospheric conditions (aerobic). Since aerobic metabolism generates 19 times more adenosine triphosphate than anaerobic metabolism, it is understood that an aerobic organism would be preferred for rapidly degrading lignin. Therefore, the lignolytic screening study was designed to seek only aerobic organisms. At peak turbidity for each condition and each hour as flow rates were increased incrementally until washout, subsamples were collected for further isolation and study. These subcultures were transferred to fresh broth culture and then subsequently streaked for isolation on a variety of solid agar media containing lignin and lignin analogs as described previously. After more than 100 trials, we determined that a modified version of Dye's medium[31] was the best agar medium for final culture isolation. The development of this modified Dye's

medium using Indulin AT lignin as the sole carbon source proved beneficial for use in the chemostat, and a broth version was used in all subsequent chemostat runs. Samples collected from the chemostat were pre-enriched in 10 mL of modified Dye's broth overnight and then streaked for isolation on modified Dye's agar through at least 2 subculture passages to ensure culture purity (Fig. 10). Isolates were scored for robust growth on the modified Dye's medium (Table 2).

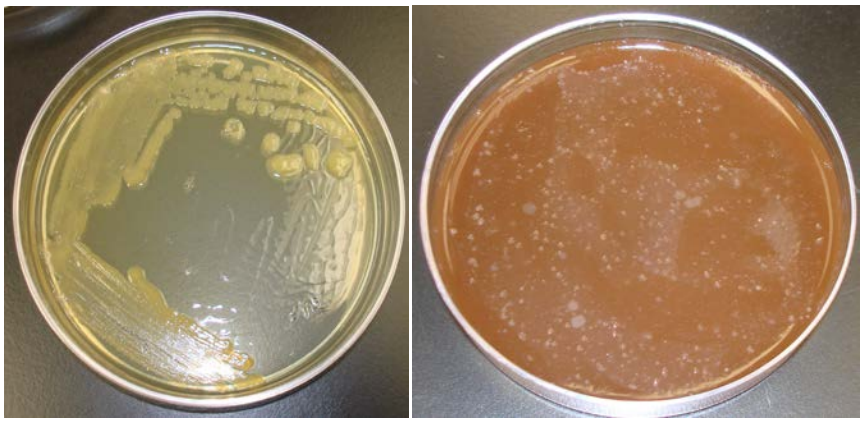

Fig. 10 Bacterial cultures streaked for isolation on modified Dye's agar

Table 2 Modified Dye's medium

Broth
1 g ammonium phosphate
2 g potassium phosphate
2 g potassium chloride
0.2 g magnesium sulfate
1 g yeast extract
0.5 g Indulin AT in 2 mL of 1 M NaOH
1 L distilled, deionized (DI) water
pH adjusted to 7.8 and sterilized by autoclaving
Agar
1 g ammonium phosphate
2 g potassium phosphate
2 g potassium chloride
0.2 g magnesium sulfate
1 g yeast extract
0.5 g Indulin AT in 2 mL of 1 M NaOH
1 L distilled, DI water
15 g agar
pH adjusted to 7.8 and sterilized by autoclaving

3.1.1.4 Isolate Characterization

The following procedure was used to identify the isolated bacterial cultures:

1. Ensure the culture is pure. Streak for isolation on agar, incubate 24–72 h, and examine for pure cultures. If not, repeat.
2. Transfer pure culture to slants (Fig. 11); incubate 24–72 h. Also grow each pure culture in sterile broth (incubate 24–72 h) and freeze using sterile glycerol. Label and record library documentation.
3. Examine colony morphology and color. Gram stain each culture on microscope slide and examine under the microscope. Note Gram reaction and cell morphology. Do wet mount to examine for movement, which would indicate the presence of flagella. Conduct biochemical assays to help narrow to genera.
4. On selected cultures: conduct colony polymerase chain reaction on the isolates from the slants to amplify the 16S rRNA gene from the bacterial isolates using the forward oligonucleotide primer (8F, 5' AGAGTTTGATCMTGGCTCAG 3') and the reverse oligonucleotide primer (1492R, 5' GGYTACCTTGTTACGACTT 3’). Amplified 16S rRNA samples are sequenced and then analyzed using the BLASTn program on the National Center for Bioinformatics website. Bacterial identity is selected from the top 25 BLAST nucleotide database results with max identity greater than 90%.

This work allowed a level of confidence that the isolates were indeed different cultures and not multiple copies of the same organism(s).

Fig. 11 Photograph of agar slant

By using the chemostat prescreening, researchers were able to rapidly screen trillions of bacteria through the continuous flow system. The selective nature of the chemostat system eliminated from consideration greater than 99.999% of the organisms in each sample and allowed only those with greatest potential for lignolytic activity to be selected for further testing. Through this method, more than 300 potential lignolytic cultures were selected out of the trillions of organisms presented in the original environmental samples.

3.1.1.5 Lignolytic Activity Characterization

To examine each of the more than 300 isolated cultures for lignolytic activity, 1 L of modified Dye's broth was prepared and sterilized for each isolate. Each pure culture was inoculated, and the culture was incubated at 25–35 °C with shaking for 24–48 h depending on previous cultural information derived during isolation. The broth was centrifuged (8,000 × g) for 30 min at 4 °C to remove most of the cells. The supernatant was collected and lyophilized for 48–72 h. Uninoculated lignin controls were similarly incubated, centrifuged, and freeze-dried. Culture controls were grown without lignin (using glucose or another carbon source) to ensure bands observed on thin layer chromatography plates were not generated as part of the cell. In cases where a secondary (nonlignin) broth could not be readily identified that would allow growth, cells were grown in modified Dye's broth containing Indulin AT lignin. The cultures were centrifuged to isolate the cells and washed 3 times in a sterile 4 °C phosphate buffer to remove broth components, and the pelleted cells were extracted as the cell control.

3.1.1.6 Extraction and Thin Layer Chromatography (TLC)

Each lyophilized and extracted sample was examined by thin-layer chromatography (TLC) for lignin degradation. TLC is a method of visualizing if lignin was broken into subunits. Dye's medium contains lignin but also a number of inorganic compounds and water. Freeze-drying and subsequent extraction allow separation of lignin breakdown products. However, the choice of extraction solvent can greatly affect if all breakdown products are removed. Therefore, this portion of the study is a trial and error to seek the best extraction solvent for each cultured sample. A few extraction solvents were used including methanol, methylene chloride, acetone, and 50/50 binary mixtures thereof. After extraction, the samples in the solvent are spotted onto TLC plates. These plates are then resolved using a different solvent system that draws up the plate by capillary action. As the resolving solvent moves, it will move components in the mobile phase (Fig. 12). Choice of the resolving solvent can also affect subunit separation. Again, this portion of the study is a trial and error to seek the best resolving solvent for each cultured lignin broth.

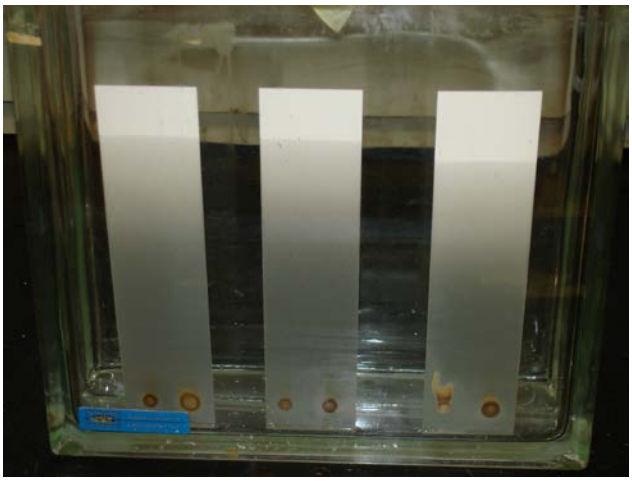

Fig. 12 During TLC, samples are spotted onto a plate and resolved by solvent drawing up the plate by capillary action

Lignin contains numerous aromatic rings. Aromatic rings fluoresce under UV light. If bands are noted on a TLC plate, then it is important to observe the 2 controls. The first control is a lignin (uninoculated control). This control should be extracted using the same extraction solvent as the cultured sample. The uninoculated lignin control will show if there are similar bands in the unmodified lignin. If there are, then the bacteria did not break down the lignin and generate that band. The second control is a culture control. In this case, it is important to ensure the culture does not produce an aromatic compound such as a pigment, which can be mistaken for a lignin breakdown product. Therefore, if a band appears or disappears on a cultured lignin in comparison with the control lignin and culture control, then it is surmised that the culture modified the lignin.

To achieve optimum separation on TLC, various mixtures of solvents (more than 20) were tested for extraction and resolving solvents. On average, 6 different combinations were tried per sample to identify the most effective resolution for that particular sample. These solvents generally included ethyl acetate, acetone, methanol, ethanol, water, and combinations thereof. Different combinations were tested until good band resolution was noted on TLC. Both reverse phase and silica gel (TLC) were used to visualize lignin breakdown.

3.1.1.7 Potential for Melt Fiber Formation

Extracted samples that displayed lignin breakdown, as per TLC, were further characterized for potential for melt fiber formation. A sample of the extracted material was placed on a glass microscope slide. A second slide was placed on top of the first, and the slides were heated on a hot plate. Upon obvious melting, the

slides were quickly pulled apart, and any resultant strand formation was examined under a light microscope. Potential for fiber formation was scored for each culture.

3.1.1.8 Lignin Degradation: Coculturing

Because biological systems act on large molecules by use of enzymes, there are cases where coculturing microorganisms can result in enhanced enzymatic degradation. Based on that principle, selected isolated cultures were cocultured, and subsequently, the same extraction, chromatography, and melt fiber assessments were conducted as mentioned previously. Unfortunately, only limited coculturing can be done, as coculturing the 300 isolates as combinations of 2 cultures would yield 45,000 different combinations to be tested. This is obviously beyond the scope of time and cost parameters for this project. However, some of the cocultured samples tested have yielded good results as scored by TLC and melt fiber formation.

3.1.1.9 Chemical Decomposition and Fractionation of Lignin Experimental Methods

Materials

All solvents, anhydrous phosphorus pentoxide (P_2O_5), acetic anhydride, pyridine, sodium chloride, and Whatman no. 1 filter paper were purchased from Fisher Scientific and used as received. Kraft pine lignin (KPL) (Indulin AT; lot no. MA27) was graciously provided by MeadWestvaco (Charleston, SC) and used as received.

Solvent Fractionation

The solvent fractionation method (Fig. 13) developed by Mörck et al.[32] was used. We added 100 g of KPL to methylene chloride (500 mL) and stirred vigorously for half an hour at room temperature using a mechanical stirrer. Using a separation funnel and Whatman no. 1 filter paper, we filtered the mixture with the supernatant collected. The precipitate was added to methylene chloride (500 mL) and stirred for an additional half hour. The mixture was again separated in the same manner with the precipitate subsequently washed with methylene chloride (1 L). The supernatants were collected as one, dried under reduced pressure, and further dried in vaccuo in the presence of P_2O_5. The precipitate was dried and then subjected to 1-propanol. This procedure was repeated for the next solvents, 1-propanol, methanol, and 7:3 methanol-methylene chloride (Fig. 13).

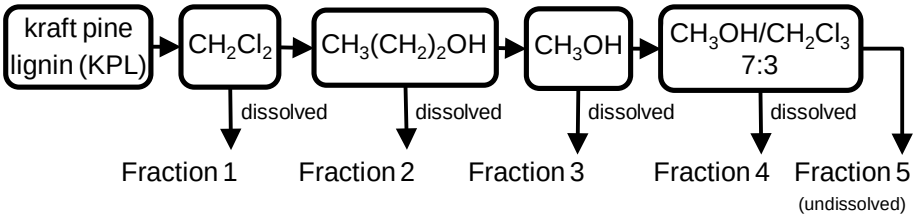

Fig. 13 KPL solvent fractionation technique adapted from Mörck et al.[32]

Gel Permeation Chromatography (GPC)

Size-exclusion chromatography (SEC) was run on the acetylated KPL fractions. A Waters 2695 XE Separations Module was used, operated with Optima-grade tetrahydrofuran (THF) (1 mL/min) as the mobile phase and calibrated with polystyrene standards. Samples were prepared by dissolving 2 mg of lignin in 1 mL of THF. The column eluent was monitored by a Waters 490E multiple wavelength detector operating at 214 and 254 nm (absorbed by phenyl rings) and a Waters 410 refractive index detector.

Acetylation of Kraft Pine Lignin (KPL)

Various acetylation procedures were used to make acetylated SKL (Ace-SKL) (Fig. 14).

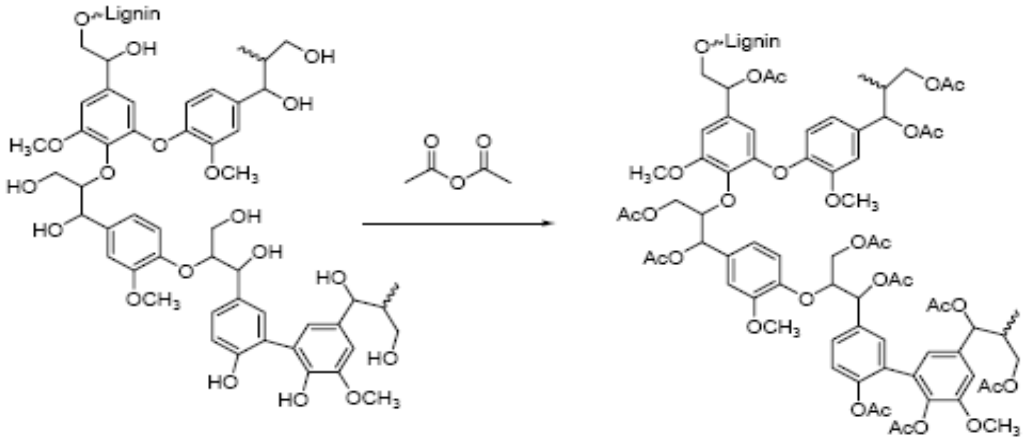

Fig. 14 Acetylation of lignin

The general procedure was the same for all reactions: SKL or soda lignin powder was poured into a 500-mL round-bottomed flask. Acetic anhydride was added to the flask. The flask was connected with a reflux condenser and dipped into a water bath set at around 85–90 °C with continuous stirring. Prior to adding the catalyst pyridine (or alternative catalyst) to the flask, we sealed and subsequently purged the flask with argon gas for a half an hour to remove moisture and oxygen from the

reaction vessel and then placed it in an ice bath. The reaction was allowed to progress as the reaction temperature increased to room temperature for a minimum of 24 h.

After reaction, the solvent present in the SKL reaction mixture was removed directly under reduced pressure to obtain the acetylated lignin (Ace-SKL). The following procedure was used to prepare the Ace-SKL:

1. 10 g of Indulin AT + 150 mL of acetic anhydride, 80 °C, 4-h reaction.
2. Extraction of Ace-SKL:
    - Ace-SKL in procedure 1 was extracted with acetic acid and washed with water until fractionated with 70% aqueous acetic acid, and the dissolved fraction was obtained by evaporating the aqueous acetic acid under reduced pressure. The undissolved fraction was discarded because its unmodified and higher molecular weight makes it intractable.
    - Ace-SKL in procedure 1 was extracted with acetic acid and washed with water until fractionated with 75% aqueous acetic acid, and the dissolved fraction was obtained by evaporating the aqueous acetic acid under reduced pressure. The undissolved fraction was discarded because its unmodified and higher molecular weight makes it intractable.
    - Ace-SKL in procedure 2a was washed with deionized (DI) water 4 times and dried overnight at 80 °C. The fraction that dissolved in the water was discarded.
    - Ace-SKL in procedure 2b was washed with DI water 4 times and dried overnight at 80 °C. The fraction that dissolved in the water was discarded.
3. Perform reaction as described in procedure 1 with the following exceptions:
    - Reduce the amount of acetic anhydride to 2 mL/g SKL to 2, 1.5, 1, and 0.66 mL, with a 15-min reaction.
    - Reduce the amount of acetic anhydride to 1.5 mL/g SKL to 2, 1.5, 1, and 0.66 mL, with a 15-min reaction.
    - Reduce the amount of acetic anhydride to 1 mL/g SKL to 2, 1.5, 1, and 0.66 mL, with a 15-min reaction.
    - Reduce the amount of acetic anhydride to 0.66 mL/g SKL to 2, 1.5, 1, and 0.66 mL, with a 15-min reaction.

Note the stoichiometric amount of acetic anhydride per gram of SKL was calculated using Eq. 1:

$$\frac{7.99\,\text{mmol OH}}{\text{g}} \times 1\,\text{g} \times \frac{102\,\text{g}}{\text{mol}} \times \frac{\text{mL}}{1.082\,\text{g}} = 0.7532\,\text{mL}\,, \qquad (1)$$

where 7.99 mmol OH/g is the hydroxyl number of the lignin as provided by the manufacturer, 102 g/mol is the molecular weight of acetic anhydride, and 1.082 g/mL is the acetic anhydride density.

For soda lignin, the reaction mixture was cooled for about 12 h to allow the precipitation of any insoluble fraction. The insoluble fraction was filtered out, and solvent present in the dissolved fraction was evaporated under reduced pressure to obtain the favored product, acetylated soda lignin (Ace_Soda).

Acetylation of Soda Lignin

Acetylation of soda lignin was very similar to that of KPL—10 g of soda lignin was dissolved in 150 mL of acetic anhydride. The reaction was run at 80 °C for 4 h. The flask was cooled down to room temperature and left to stand to precipitate an undissolved fraction. The undissolved fraction was removed by filtration. Resulting Ace_Soda had a softening point between 130 and 143 °C.

3.1.1.10 Methacrylation of the Methanol KPL Fraction and Unmodified KPL

Meth_KPL_UD

Methacrylation of lignin involved reacting the hydroxyl groups of lignin with methacrylic anhydride as described in Fig. 15.

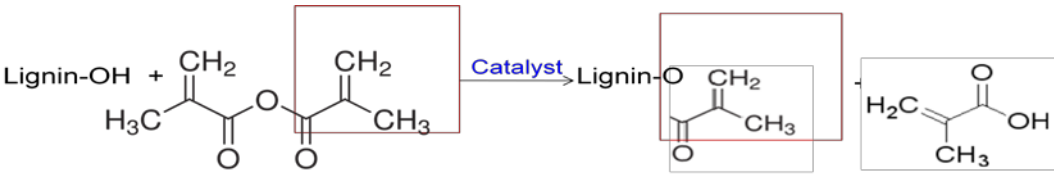

Fig. 15 General reaction scheme to produce methacrylated lignin

Meth_KPL_UD is the University of Delaware-prepared methacrylated KPL. Five methacrylations are currently being investigated to potentially enhance the solubility of KPL and methanol fraction of KPL in traditional and biobased monomers and functionalize the KPL with polymerizable, terminal, carbon–carbon double bonds. The 5 methacrylation techniques are briefly described as follows:

1. Coreactant = methacrylic anhydride; catalyst = 1-methylimidazole (1MIM); solvent = 1,4-dioxane or none; reaction temperature = approximately 50 °C; reaction time = minimum of 24 h; byproduct = methacrylic acid.

2. Coreactant = methacrylic anhydride; catalyst = pyridine in equal mole ratio with methacrylic anhydride; solvent = none; reaction temperature = ice bath to room temperature or greater; reaction time = minimum of 24 h; byproduct = methacrylic acid.

3. Part A: coreactant = acetic anhydride; catalyst = pyridine in equal mole ratio with acetic anhydride; solvent = none; reaction temperature = ice bath to room temperature or greater; reaction time = minimum of 24 h; byproduct = acetic acid. Part B: primary reactant = acetylated KPL; coreactant = methyl methacrylate (MMA); catalyst = p-toluenesulfonic acid; inhibitor = hydroquinone; solvent = none; reaction temperature = 75 °C; reaction time = minimum of 24 h.

4. Coreactant = methacrylic anhydride; catalyst = 4-(N,N-dimethylamino) pyridine as little as 0.2 wt% of methacrylic anhydride; solvent = none; reaction temperauture = room temperature to 60 °C; reaction time = minimum of 8 h; byproduct = methacrylic acid.

5. Coreactant = MMA; catalyst = p-toluenesulfonic acid; solvent = none; reaction temperature = 70 °C or greater; reaction time = to be determined; byproduct = methanol, which is distilled off during the reaction.

Meth_KPL_Clemson

Meth_KPL_Clemson is the Clemson University–prepared methacrylated KPL. The procedure followed was similar to that of the University of Delaware procedure but more closely matched the procedure outlined by Thielemans and Wool[33]— 10 g of indulin AT was dissolved in 40 mL of 1,4-dioxane, and 60 mL of methacrylic anhydride and 1 mL of 1MIM were added to the reactor. The reaction was run at 50 °C for 24 h under a closed nitrogen atmosphere while stirring.

The product was purified by filling the flask with DI water while stirring for hours to allow the decomposition of methacrylic anhydride and the precipitation of solid. The solid was sedimented overnight and filtered. The reaction product was washed 3 times with DI water.

Methacrylated and Acetylated SKL

Methacrylated and acetylated SKL samples were prepared using 3 procedures.

In procedure 1, 10 g of Ace-SKL (1.5 g/mL [1 g/0.66 mL]) was reacted with 60 mL of methacrylic anhydride and 1 mL of 1MIM catalyst. No dioxane was used. The reaction was run for 24 h at 50 °C. The flask was filled with DI water to precipitate MA_Ace_SKL, then the product was washed 3 times with DI water. The solid was dried in a vacuum oven at approximately 55 °C for more than 48 h but was still "soft" at 55 °C (low T_g).

Procedure 2 was the same as procedure 1 except only 25 mL of methacrylic anhydride and 0.5 mL of 1MIM with 10 g of Ace-SKL was used.

In procedure 3, 10 g of Ace-SKL (1.5 g/mL [1 g/0.66 mL]) was reacted with 10 mL of methacrylic anhydride and 0.2 mL of 1MIM catalyst. No dioxane was used. The reaction was run for 16 h at 50 °C. The material was not soft when taken out from the 55 °C vacuum oven. MA_Ace_SKL was dissolved in acetone and coated on aluminum foil.

Olefin Metathesis Decomposition of KPL

So far, olefin metathesis degradation of KPL (Indulin AT; lot no. MA27) has been attempted 3 times. Each time, a first-generation Grubbs catalyst was employed (Table 3). Prior to each experiment, unmodified KPL was dried under reduced pressure at approximately 40 °C for a minimum of 12 h.

Table 3 Experimental conditions of the attempted olefin metathesis degradation reactions of unmodified, dried KPL (Indulin AT)

Reaction conditions	Experiment 1	Experiment 2	Experiment 3
Unmodified, dried KPL (g)	10	10	10
Ethylene glycol (mL)	50	50	100
Catalyst (mg)	100	100	100
Ethylene gas	Desired 200 psi	Desired 200 psi	300
Max reaction temperature (°C)	60	60	85
Reaction time (h)	6	6	5

In experiment 1, after the KPL, ethylene glycol, catalyst, and magnetic stir bar were added, the Parr bomb was cooled down to roughly –110 °C using an ethanol-liquid nitrogen (N_2) cooling bath. Ethylene gas was added to the Parr bomb via the relief valve opening and a long needle at a constant pressure of approximately 15 psi for 10 min. The reactor was then sealed and heated up to the desired reaction temperature while continuously stirring.

In experiment 2, after the KPL, ethylene glycol, catalyst, and magnetic stir bar were added, the Parr bomb was chilled down to roughly liquid N_2 temperature (–196 °C) using a liquid N_2 cooling bath. Ethylene gas was added to the Parr bomb via the relief valve opening and a long needle at a constant pressure of approximately

15 psi for 10 min. The reactor was then sealed and heated up to the desired reaction temperature while continuously stirring.

In experiment 3, after the KPL, ethylene glycol, and catalyst were added, the reactor was sealed. After connecting the Parr bomb (equipped with a pressure gauge and an internal mechanical stirrer) to an electrical motor and an ethylene gas cylinder, we pressurized the reactor with roughly 300 psi of ethylene gas.

To determine whether or not the olefin metathesis degradation reactions of KPL were successful, state-of-the-art chromatography instrumentation with online mass spectroscopy is desired. To limit error, the ideal situation would be to perform chromatography on aliquots of the reaction mixtures as is; separation of the lignin from the polar solvent is not required. It has been reported in the literature that alkaline solutions (0.1–0.5 M NaOH) with the addition of low-concentration salt solutions (0.05 M lithium chloride or 0.1 M sodium nitrate) were deemed necessary to perform aqueous size exclusion chromatography on KPL.[34] Unfortunately, these conditions cannot be achieved at the University of Delaware, at least to our knowledge.

Singlet Oxidation Decomposition of Kraft Pine Lignin (KPL)

Unmodified KPL (Indulin AT; lot no.: MA27) (1.0 g) was added to a 3-neck round-bottom flask equipped with a mechanical stirred 1:1 acetonitrile-ethanol solution (100 mL) with Rose Bengal (a photoinitiator [PI], 5.4×10^{-4} M) and dried. The flask was placed in a 13 ± 0.1 °C water bath that contained a 1% (w/v) solution of sodium amide ($NaNO_{2(aq)}$); $NaNO_{2(aq)}$ solution was used to cut off the irradiation at 400 nm, as described by Bonini et al.[35] Irradiation was performed by using a 100-W tungsten-halogen lamp. Air or high-purity oxygen (O_2) was continuously bubbled through the reaction mixture. Reactions were conducted for 4, 8, 12, and 24 h. Upon evaporation of the solvent, the KPL was acetylated using the procedure previously described.

3.1.2 Subtask 1.2: Chemical Analysis of Lignin Decomposition Products

A number of analytical techniques are being used to assess the chemistry and molecular weight of modified lignin. Fourier transform IR (FTIR) spectroscopy was used to determine the general chemical makeup of the lignin-derived oligomers using known standards (Fig. 16).[36] A Bruker 600-MHz spectrometer with a spectral window of ±2,000 Hz, 16 scans at 293 K, and 90° pulse width was used to run nuclear magnetic resonance (NMR) spectroscopy (Fig. 17). This allowed us to determine the functionality and the approximate chemical makeup of the oligomers using known standards.[37] We used SEC to measure the molecular weight of the lignin-derived oligomers (Fig. 18). Because high-molecular-weight species cannot

diffuse into the packing, they elute first from the column, while lower-molecular-weight species elute later.[34,38] Knowing the molecular weight of the lignin allows us to determine whether addition or decomposition reactions take place and the extent of these reactions.

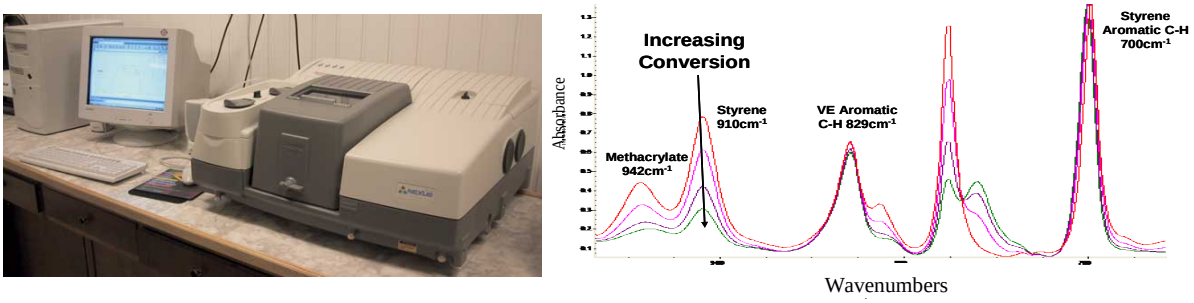

Fig. 16 Thermo Nicolet Nexus 670 FTIR and FTIR spectra of VE as a function of conversion allowed us to measure individual component conversion

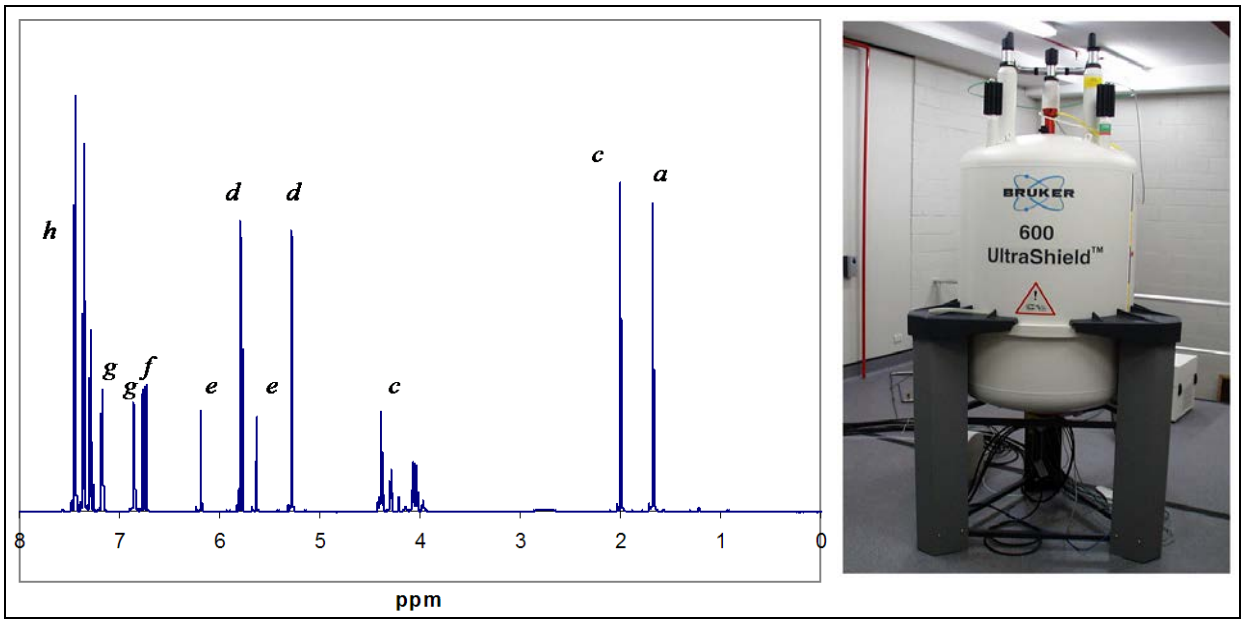

Fig. 17 Bruker 600-MHz NMR and a representative spectrum for VE resins

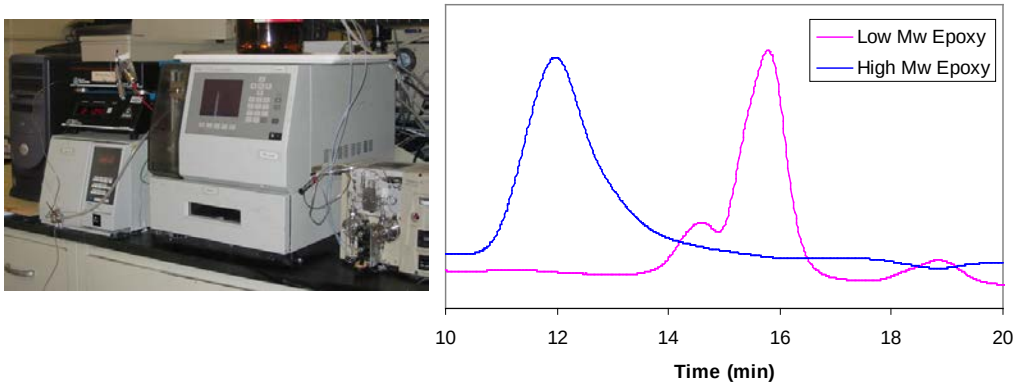

Fig. 18 Waters SEC and SEC chromatographs of low- and high-molecular-weight epoxies

The softening point of lignin samples was measured with a METTLER TOLEDO FP900 Thermosystem using the Mettler Cup and Ball method according to ASTM D3461.[39] The softening point apparatus works by placing a metal weight on top of a charge of sample (Fig. 19). While the sample is solid, the weight is held up by the sample. As the temperature is raised and the sample softens, the weight pushes the sample into the light path to enable the softening point of the material to be measured.

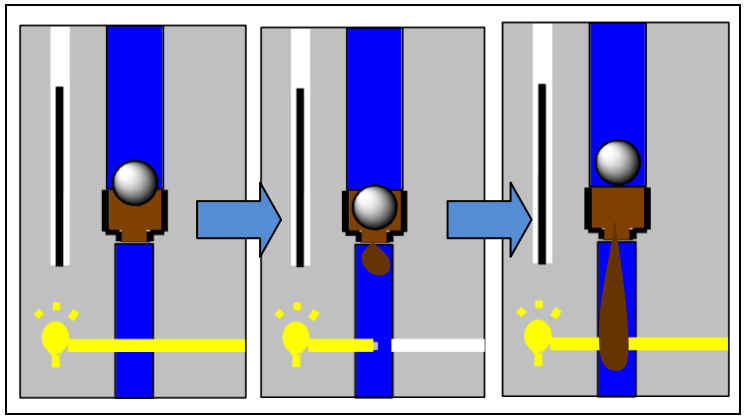

Fig. 19 Depiction of softening point apparatus

Ash content and elemental analysis determination[40] were performed following ASTM D5630 at the Agricultural Service Laboratory, Clemson University. FTIR spectroscopy was performed in the transmission mode with a Nexus spectrophotometer using potassium bromide (KBr) pellets containing 1% samples.

Gel permeation chromatography (GPC) was conducted for Ace-SKL fibers using a Waters Alliance GPCV 2000 model equipped with a Stylegel HT4 column (Waters) and Polargel (Agilent) column. Fibers were ground into powder and dissolved in dimethylformamide solution containing 0.05 M lithium bromide with concentration of 1 mg/mL.

3.1.3 Subtask 1.3: Rheostructural Investigation to Determine Melt Processability

For lignin to be converted into carbon fibers, it must be spun into precursor polymeric fibers. It was first important to assess whether the fibers melt to determine if melt-spinning is even possible. The lignin samples were characterized for their viscosity using a host of rheometers available through the Center for Advanced Engineering Fibers and Films (CAEFF) at Clemson University. Typically, 100 Pa·s of viscosity is needed for fiber spinning, in conjunction with adequate melt strength (i.e., extensional hardening). Prior studies of MP derived from synthetic routes displayed the evolution stress in terms of the texture characterized by the size and orientation of the discotic phase (Fig. 20).

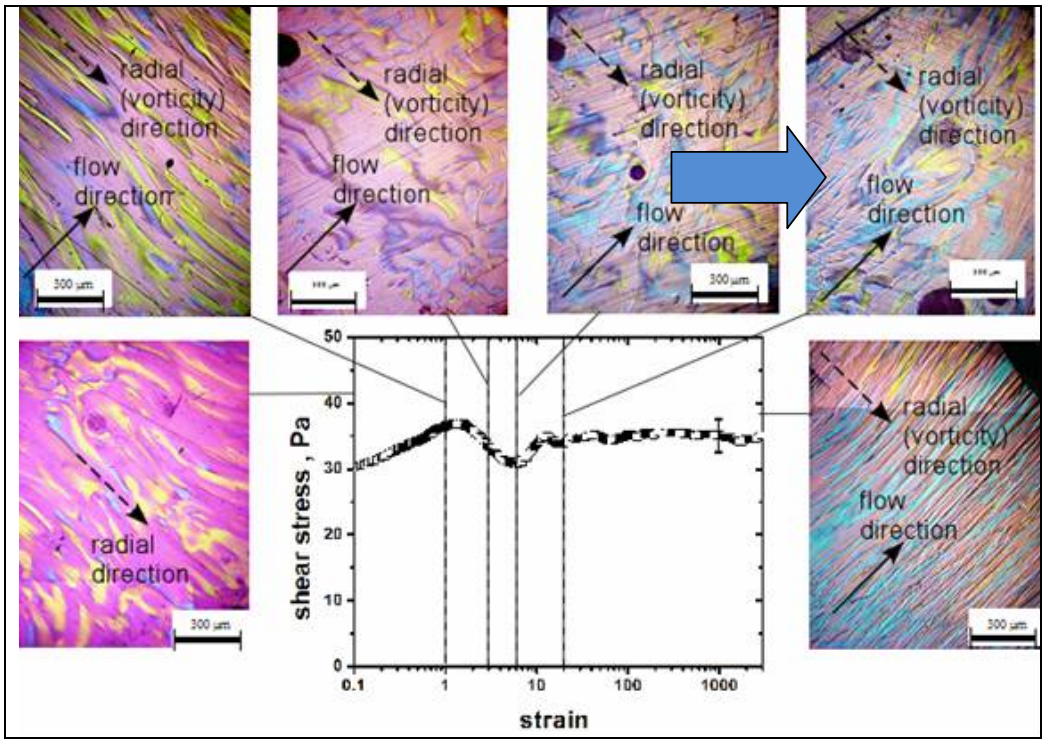

Fig. 20 Rheostructural evolution of MP at a shear rate of 1 s^{-1} and a processing temperature of 297 °C[41]

An important component of rheological studies is the assessment of melt stability of the lignin samples. This step is important for biomass-derived precursors that contain alkoxy side groups that can cross-link or degrade during melting. Typically, precursors must possess thermal stability for approximately 30 min, which is measured by transient experiments. Rheological testing of lignin samples was carried out on an ARES rheometer (TA Instruments) using cone-and-plate fixture under a steady shear rate range of 1 to 10 s^{-1}. Lignin melts were tested at

temperatures above their melting point under a nitrogen flow. The Ace-SKL solution was tested at room temperature without gas flow. We desire 30 min of stable viscosity to process the fibers. However, the material must also increase in viscosity significantly after 30 min, which would indicate that the precursor has some reactivity that is desired during fiber stabilization. After melt processability and fiber-forming characteristics were determined, suitable fractions were processed in batch- and continuous fiber-spinning units (Fig. 21).

Fig. 21 a) Batch-spinning unit for samples up to 100 g and b) continuous fiber-spinning unit for large-scale laboratory production of fibers at rates up to 5 kg/day

Melt-spinning of lignin precursors was performed using an Instron capillary rheometer equipped with a 0.25-mm-diameter die. The maximum take-up speed applied was around 3 m/s. For solution spinning, 50 g of Ace-SKL dry powder was fully dissolved in 100 mL of acetone. The mixture was stirred continuously and solvent evaporated until the solution was concentrated to above 1.8 g solids per milliliter of solvent. The viscous solution was transferred into a spinning barrel equipped with a 12-hole die, with each hole having a 150-µm diameter. Spinning was performed with a batch unit from AJA Inc. (Greenville, SC). Warm air was blown on the extruded fibers in the spinning chamber during spinning to accelerate the evaporation rate of the solvent during the dry-spinning process. In this lab-scale process, the solvent was vented, but in the continuous commercial process, the solvent is routinely condensed and recycled.

3.1.4 Subtask 1.4: UV-Thermal Dual Mechanism Cross-Linking/ Stabilization and Carbonization

Precursor fibers have to be made intractable to avoid meltdown of the fibers during the high-temperature carbonization process. This is the most critical step in the precursor conversion process because molecular structure necessary for turbostratic or graphitic carbon is locked in this step. We also emphasize that typical thermo-oxidative stabilization conditions established for solution-spun PAN fibers cannot be used with melt-spun precursor fibers because such fibers melt while being heated through the "melting region" into the oxidative temperature regime. Thus, irradiation and thermo-oxidative methods were used to stabilize the fibers.

Irradiation studies were conducted in a high-power UV reactor (Fig. 22) to explore UV sensitivity of the fractions. The presence of conjugated bonds in lignin fractions can help in resonance stabilization, but the kinetics can be very slow. Therefore, extrinsic UV-sensitive initiators were added during the fiber-spinning step. Prior studies with acryloyl benzophenone (ABP) as a termonomer in PAN have established its thermal stability during melt-spinning and retention of subsequent UV-sensitivity.[15,17] We note, however, that the reactivity ratio for ABP is not established for lignin fractions and was studied here. After or in place of UV cross-linking, thermo-oxidative reactions were conducted to obtain an intractable, polyaromatic structure. To assist in thermal cross-linking, we have demonstrated in an earlier study that lauroyl peroxide can survive UV-exposure and then be activated by thermal mechanism.[42] A residence time of 50 s at 250–270 °C has led to almost 50% gel content in PAN precursors, but the duration and number of cycles must be determined experimentally for lignin-based fibers. Lignin fiber samples were placed in a programmable air oven and heated from room temperature up to 220 °C with a heating rate ranging from 0.01 to 0.5 °C/min for different batches of samples. Dwell time at a certain temperature was necessary to prevent fibers from melting and sticking.

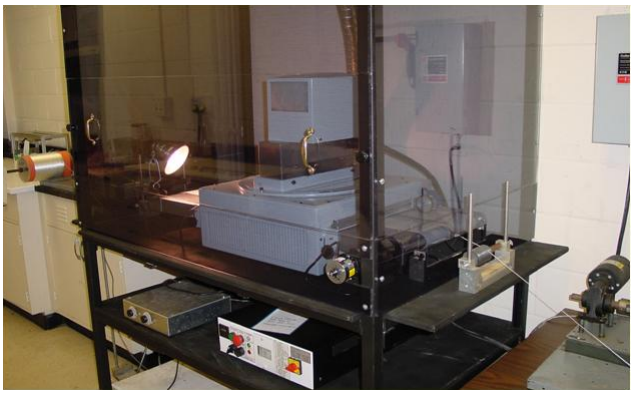

Fig. 22 Custom-built, 5-kW UV irradiation chamber for batch or continuous irradiation of carbon precursor fibers

Differential scanning calorimetry (DSC) was performed on UV irradiated Ace-SKL as-spun fibers and control fibers, with UV irradiation blocked, using a Pyris 1 DSC (Perkin Elmer Instruments). The fibers were ground into powder and the sample pans containing grounded fiber were heated from room temperature to 250 °C under N_2 at a heating rate of 30 °C/min and cooled to room temperature at the same rate. For each sample, the second heating run was used to calculate T_g using the half ΔC_p method.

3.1.5 Subtask 1.5: Carbonization and Graphitization of Lignin-Based Fibers

Carbonization and graphitization of stabilized fibers were conducted using the extensive, ultrahigh temperature capabilities at CAEFF (Fig. 23). These furnaces are capable of treating samples ranging from a few grams to continuous treatment. Residence time and processing temperatures up to 2,400 °C for carbonization were experimentally determined. Graphitization residence time and temperature up to 2,700 °C were experimentally determined. Initially, processing conditions mimicked PAN-based carbon fibers and were adjusted during processing by fiber visual appearance and from batch to batch based on fiber properties.

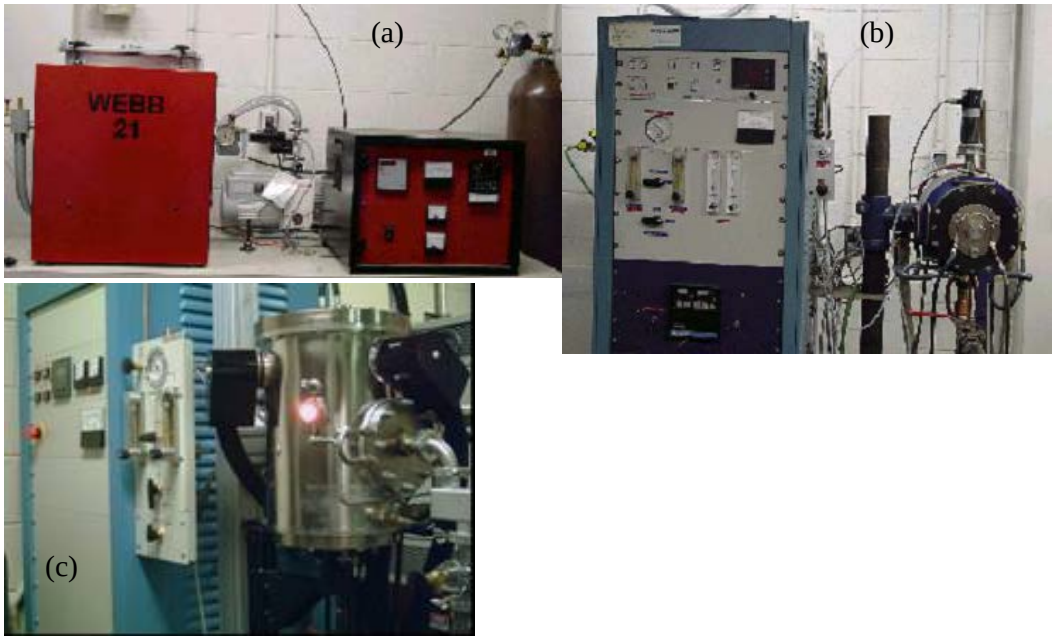

Fig. 23 a) Webb batch carbonization unit for treatment to 2,100 °C; b) ASTRO 1000 batch/continuous unit for carbonization to 2,400 °C; c) ASTRO 1100 ultrahigh-temperature furnace for graphitization to 2,700 °C

After stabilization, the fiber was wrapped in graphite foil and placed into a RED DEVIL furnace. Carbonization was performed by heating at a rate of 4.5 °C/min up to 900 °C in a stream of argon and held at 900 °C for 1 h. Our labs are equipped

with ultrahigh temperature furnaces (2,700 °C), but such temperatures were not used in the present studies because the objective was to obtain higher tensile strength and strain-to-failure properties, which typically decrease at the ultrahigh temperatures.

3.1.6 Subtask 1.6: Testing and Analysis of Biobased Carbon Fibers

Raman spectra were recorded on a Renishaw System (Gloucestershire, UK) using a near-IR (NIR) 780-nm-diode laser. The Raman shift was calibrated with a silicon standard centered at 520 cm^{-1}. Raman spectra were analyzed using WiRE software, v3.2, to integrate the peaks.

To measure 3-D graphitic crystallinity, wide-angle X-ray diffraction (WAXD) studies were conducted. The average unit lattice spacing (d-spacing) for graphite is calculated from a maximum 2θ value in the integrated 2θ profile, which corresponds to (002) lattice plane, using the Bragg equation, $n\lambda = 2d\sin\theta$, where λ = wavelength of the X-ray, n = 1 for first-order scattering, and θ = Bragg angle (half of scattering angle [2θ]). Coherent length along the lattice plane (L_a) and coherent height of stack (L_c) are estimated from the amount of broadening, β, using the Scherrer equation, $L = \frac{K\lambda}{\beta\cos\theta}$, where L is the coherent length, β is the width at half peak height, and K is the Scherrer parameter. β for 002 and 110 plane is used to measure L_c and L_a, respectively. In this case, K is usually taken to be 0.9.

Misorientation of the graphene layers can be calculated from an azimuthal plot of the 002 reflection—either full width at half maxima (Z) in the azimuthal profile for 002 plane or Harman's orientation factor, measured as average squared cosine of the crystal plane orientation $\langle\cos^2\phi_{hkl}\rangle$ to represent misalignment of the planes. As measured by d_{002} spacing of 0.337 nm, the graphitic content can range up to 85%, assuming d-spacing of 0.3354 and 0.3440 nm for perfect graphitic and turbostratic structures, respectively. The density of the fibers, another measure of nanotexture and graphitic content, was measured using standard methods (ASTM C693).[43]

WAXD patterns were obtained from a Rigaku CuKα X-ray source at wavelength of 0.15406 nm, and the X-ray source was operated at 45 kV and 0.65 mA. Fiber bundles were mounted on a paper tab and sprinkled with National Institute of Standards and Technology (NIST)-grade silicon standard powder for accurate identification of 2θ position on integrated azimuthal scan. The exposure time per sample was 1 h. The spacing of (0 0 2) planes (d_{002}) was calculated according to Bragg's law (Eq. 2):

$$d_{002} = \frac{\lambda}{2\sin\theta}, \quad (2)$$

where λ corresponds to the wavelength of the X-ray beam (0.15406 nm), and θ is the angle of incidence of the X-ray beam. The degree of graphitization was calculated (Eq. 3):

$$g(\%) = \frac{0.3440 - d_{002}}{0.3440 - 0.3354} \times 100 \,, \tag{3}$$

where *g* is the degree of graphitization (%).

Scanning electron microscopy (SEM) was used to characterize the fibers before and after testing to examine defect content and the effects on fiber failure (Fig. 24). SEM was used to see defects in the fiber structure, including fractures, cracks, and roughness. The nanoscale graphene layer orientation in the fiber direction leads to fibers with an ultrahigh tensile modulus and thermal conductivity but results in low tensile strength and poor compressive strength. This combination of carbon fiber properties, typically obtained from disc-shaped MP molecules, is not optimum. In contrast, the linear molecular architecture of PAN precursors results in only a turbostratic crystal structure (not truly graphitic) of the carbon, which leads to a high tensile strength and good compressive strength but moderate modulus and low thermal conductivity. A combination of aromatic and aliphatic molecular structures, possible with lignin fractions, presents a unique opportunity to develop an optimum level of nanotexture and graphene orientation in carbon fibers. The spinning process was modified, as needed, to produce this nanotexture resulting in carbon fibers with the optimal combination of thermomechanical properties.

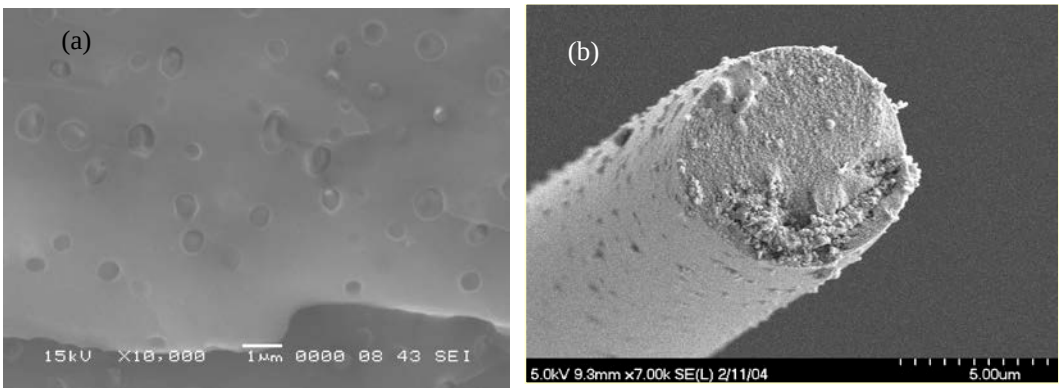

Fig. 24 SEM photographs showing images of a) microphase toughened epoxy and b) graphitized carbon fiber

Tensile testing using an MTI Phoenix instrument was conducted using single-filament testing. The properties of these fibers were compared to that of commercial carbon fibers, such as AS4, IM7, and pitch-based fibers. The effects of reaction conditions on these properties were correlated with the fiber production method to

determine optimum processing conditions. Thus, the role of precursor chemical structure on the properties of the resulting carbon fibers was systematically assessed.

To measure tensile properties, individual fibers were tested in a Phoenix tensile testing device following the ASTM test method D3379-5.[44] The load cell of the MTS apparatus has a maximum capacity of 500 g, and the crosshead speed was set to 0.5 mm/min. Filaments 25 mm in length were mounted in the paper frame. The fiber diameter was measured by using an Olympus BX 60 optical microscope. The individual fibers were placed on the glass slide, and then images were obtained at a magnification of 50×. The diameter was measured with the aid of the image analysis program at 3 different spots on the fiber. Each paper tab was secured in the upper and lower jaws of the MTS. To prevent the accidental breakage of fiber prior to test failure, we used an electric hot wire (instead of scissors) to burn the paper tab.

3.2 Task 2: Biobased Thermosetting Resins

3.2.1 Subtask 2.1: Preparation of Biobased Monomers

Biobased monomers are being prepared from multiple renewable resources, including starch, cellulose, and lignin. Figure 25 shows selected chemical routes to produce monomers from lignin. The cyclic and aromatic structures that can be derived from these renewable resources are ideal for the manufacture of high-performance resins. Derivatives of model lignin components, such as trans-conipheryl, trans-sinapyl, and trans-p-coumaryl alcohols,[33] were used to make aromatic diluents and cross-linkers (Fig. 25).

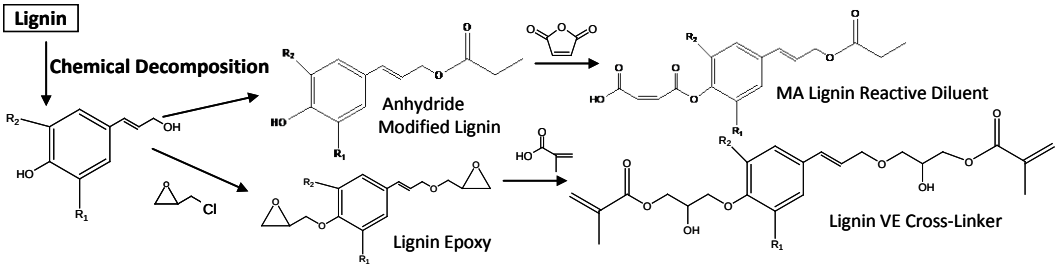

Fig. 25 Selected schemes for preparing lignin-based monomers

The lignin components have one phenyl alcohol and one primary alcohol. As a result, the reactivities of these hydroxyl groups are quite different,[45] allowing the primary alcohol to be functionalized with one chemical group, while the phenyl hydroxyl can be functionalized with another chemical group. In particular, the primary hydroxyl can be converted to an aliphatic ester while leaving the phenyl hydroxyl essentially unreacted using the following 12 methods:

1) Reaction of the hydroxyl group with acetic anhydride at 98 °C for approximately 2 h.[33,45]

Cross-linking monomers based on lignin are more easily prepared in that they simply use the diol lignin-precursor.

The hydroxyl functionality of mono- and di-hydroxyl lignin derivatives were used to produce di-epoxies, VEs, UPE cross-linkers, and monofunctional reactive diluents. This was accomplished by 4 methods:

2) Reaction of the hydroxyl groups with a stoichiometric amount of epichlorohydrin at 70 °C, using acid catalysts to yield epoxy functional monomers.[21]

3) Reaction of the epoxy functional monomers with a 3% stoichiometric excess of methacrylic acid at 90 °C for 3–6 h to yield a VE monomer.[21,23] A secondary hydroxyl group was added to the structure for each vinyl group added.

4) Reaction of the hydroxyl groups with a stoichiometric amount of methacryloyl chloride at 40 °C for 1 h to yield a vinyl functional monomer with no added hydroxyl groups.[33] Alternatively, methacrylic anhydride was used for this reaction.

5) Reaction of the hydroxyl groups with MA at approximately 80 °C for 3–4 h to yield maleate half-esters/UPEs.[46]

Method 2 was used to prepare di-epoxides, which will be the basis of biobased epoxy resins. Di-vinyl cross-linker species were produced from di-epoxides using method 3. The use of methacryloyl chloride to produce vinyl monomers (method 4) has advantages and drawbacks relative to the methacrylation of epoxy method (method 3). Method 4 allows for a higher renewable content and is accomplished in 1 reaction step instead of 2. However, methacryloyl chloride and methacrylic anhydride are more expensive than epichlorohydrin and methacrylic acid.

UPEs generally do not perform as well as VE resins because they contain a distribution of unsaturation, with many molecules containing only one or even zero unsaturation sites, resulting in lower thermal and mechanical properties.[23] These lignin-based UPE monomers, on the other hand, have either 1 unsaturation site per molecule and are potential reactive diluents or have 2 unsaturation sites per monomer and are cross-linkers. This could result in excellent properties relative to commercial UPE resins. The renewable content of the UPE monomers are extremely high, as MA is commercially produced from biological sources.

Lignin-derived chemicals from the chemical/thermal cracking process were used to make aromatic monomers. This process is similar to the chemical/thermal process described previsously, but the target molecules are much smaller in size.

Monomers were prepared from carbohydrates, cellulose, and hemicellulose. One requirement is that the monomer must possess a cyclic structure to provide stiffness to the resulting polymer backbone. For hexoses, we are using 2 major base molecules. The first is isosorbide, which is derived from sorbitol that is in turn derived from glucose.[47] The second is 5-hydroxymethylfurfural (HMF) obtained from a variety of hexoses from starch and cellulose.[47] Isosorbide has a bicyclic 5-member ring structure with 2 hydroxyl groups, and HMF has a single 5-member ring structure with a primary alcohol and an aldehyde group. For pentoses, the major platform molecule that is being used is furfural, which contains an aldehyde group and is produced from cellulose and starch. Furfuryl alcohol, furfuryl amine, and furoic acid are derived from furfural and are commercially available.

Figure 26 shows selected schemes for producing biobased monomers from hexoses and pentoses. Reaction methods 2–5 were used to produce monomers from these starting biobased chemicals. Isosorbide is being used to produce di-epoxides, vinyl cross-linkers, and di-unsaturated polyesters. An additional means of producing di-epoxides and methacrylates can be realized with isosorbide and are described in the following methods:

6) Elimination of water from isosorbide with sulfuric acid at elevated temperatures above 120 °C to yield secondary unsaturations.[45]

7) Epoxidation of the unsaturation sites using peracetic acid or performic acid at 50 °C for 12 h to yield difunctional secondary epoxides.[48]

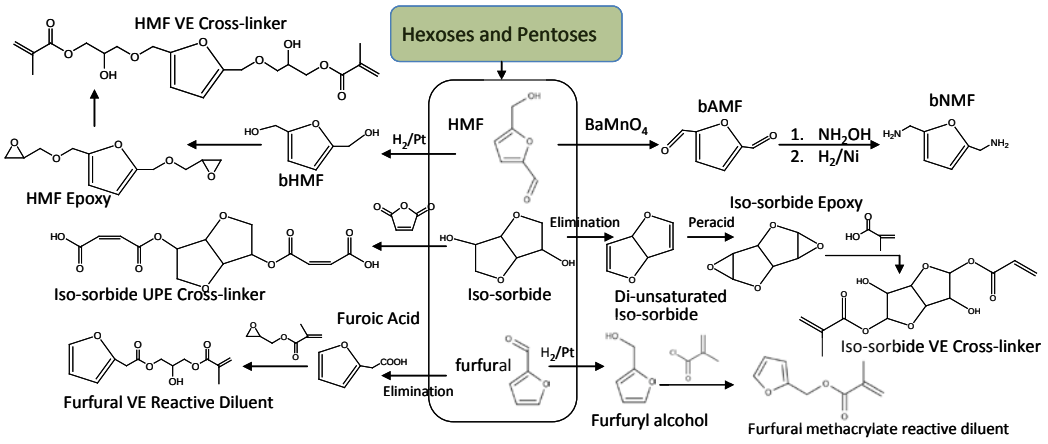

Fig. 26 Schemes for preparing biobased monomers from hexoses and pentoses

The unsaturation sites resulting from water elimination from isosorbide may readily polymerize as a result of the destabilizing effect of the oxygen atoms within the ring structure, and thus this molecule could potentially be used as a cross-linker. The secondary epoxides produced by reaction with a per-acid have low reactivity and thus may not produce good epoxy resins. However, the epoxy groups can be converted to VE groups using method 3.

The use of HMF and furfural were examined to produce monomers. To do this, these chemicals are first converted to other precursors using the following reaction methods:

8) Hydrogenation of the aldehyde over platinum catalyst to yield a hydroxyl group[45] converts HMF to 2,5-bis(hydroxymethyl)furan (bHMF) and furfural to furfuryl alcohol.

9) Conversion of the hydroxyl group to an aldehyde using barium manganate converts HMF to 2,5-bis(aldehydyemethyl)furan (bAMF).[45]

10) Conversion of the aldehyde group to an amine by reaction with ammonium hydroxide followed by hydrogenation over nickel catalyst[45] converts bAMF to 2,5-bis(aminomethyl)furan (bNMF) and furfural to furfuryl amine.

11) Conversion of the aldehyde group to a carboxylic acid by oxidation of bAMF using silver oxide, and NaOH[45] converts bAMF to 2,5-furandicarboxylic acid and furfural to furoic acid.

bHMF was converted to di-epoxides (method 2), difunctional VEs (method 3), dimethacrylates (DMs) (method 4), and UPEs (method 5). bNMF should act as a stiff hardener for epoxy resins because it contains 2 primary amines and a rigid cyclic core.

Carboxylic acid functionality was converted to monomers using the following method:

12) Addition of a carboxylic acid to the epoxide of glycidyl methacrylate at 50 °C for 16 h using AMC-2 catalyst to produce a VE functional monomer.[1]

Using method 12 should convert 2,5-furandicarboxylic acid to a divinyl cross-linker.

Reactive diluents were produced using the same reaction schemes as listed here, but with judicious choice of the biologically derived starting chemical. Furfuryl alcohol was converted to the reactive diluents furfuryl VE (methods 2 and 3), furfuryl methacrylate (method 4), and furfuryl maleate (method 5). Furfuryl amine would act as chain extender in epoxy resins. Furoic acid can be converted to a vinyl

reactive diluent using method 12. HMF can also be used to prepare reactive diluents, as the aldehyde functionality will remain intact during the formation of a monofunctional VE (methods 2 and 3), methacrylate (method 4), and maleate (method 5). In addition, methods 11 and 12 can be used to prepare a distinct monofunctional VE reactive diluent.

Chitin (Fig. 27) is a linear biopolymer whose commercial source is primarily crustacean shells and insect exoskeletons. In nature, chitin is second only to cellulose in abundance but trails cellulose in commercial products by a wide margin.[49] The amine groups on chitosan, the deacetylated form of chitin, make it a candidate to be used as a biobased amine hardener. Since chitin's and chitosan's molecular weights can reach 10^6 g/mol,[49] selective hydrolysis will be required to reduce the molecular weight of the chitosan while retaining the desirable amine functionality. Hydrolysis of chitosan can occur in concentrated acids, often hydrochloric.[50] The exact conditions and duration necessary will depend on the initial and targeted molecular weight. Remaining hydroxyl groups will likely need to be end-capped by reaction with short-chain anhydrides to reduce water uptake. To simplify things initially, a single repeat unit of chitosan, a dimer of glucosamine, will be used as a model compound for preparation of biobased hardeners for epoxies. The glucosamine dimer is very similar in structure and chemical functionality to commercial amine hardeners, such as Amicure PACM or 2,2′-dimethyl-4,4′-methylenebis(cyclohexylamine). Despite this potential for chitin, we did no work with chitin as other research areas were deemed to have higher potential.

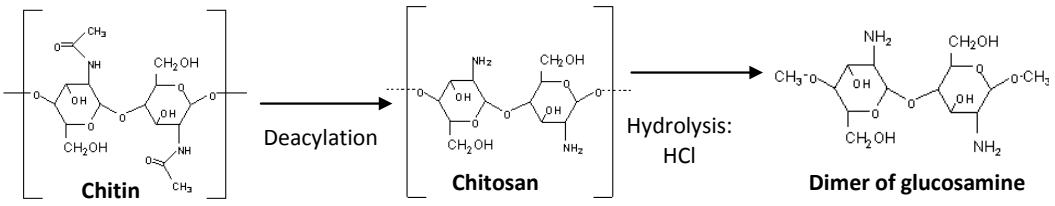

Fig. 27 Preparation of dimers from chitin-based hardeners for epoxy resins

Hybrid molecules containing multiple renewable resources could also be used. For example, alcoholysis of triglycerides with the hydroxyl groups on sucrose, isosorbide, or the lignin-derived structures (e.g., trans-conipheryl) will yield carbohydrate/lipid or lignin/lipid hybrids. The unsaturation sites on the fatty acid can then be methacrylated to yield vinyl functional monomers.[2]

3.2.2 Subtask 2.2: Chemical Analysis of Biobased Chemicals

FTIR (Fig. 16) was used to determine the structure of the resulting biobased chemicals that are prepared synthetically. Functional groups, such as furanyl, phenyl, and epoxy, were identified using a Thermo Nicolet Nexus 870 FTIR in absorbance mode. Spectra were recorded with 32 scans at an 8-cm^{-1} resolution at room temperature with a deuterated tryglycine sulfate detector in 4,000- to 8,000-cm^{-1} range for NIR spectra and 650–4,000 cm^{-1} for mid-IR spectra. During the reaction of epichlorohydrin with hydroxyl functional molecules, the disappearance of hydroxyl groups and appearance of epoxy groups can be tracked by monitoring the peaks at approximately 3,500 and 910 cm^{-1}, respectively.[36] Methacrylation of epoxy functionality was measured by tracking the disappearance of epoxy functionality and monitoring the appearance of methacrylate functionality at 942 cm^{-1}. Reaction of glycidyl methacrylate with carboxylic acid functionality was monitored through disappearance of the epoxy group, and the reaction of MA with hydroxyl functional groups was monitored by the disappearance of the anhydride ring structure at 1,850 cm^{-1}.[36]

NMR was used to determine the molar content of functionality and the chemical content of any side-products. Proton and carbon NMR (^{1}H NMR and ^{13}C NMR) measurements were used to confirm chemical structures of 2,5-bis[(2-oxiranylmethoxy)-methyl]-furan (BOF) and 2,5-bis[(2-oxiranylmeth oxy)methyl]-benzene (BOB). Both ^{1}H NMR and ^{13}C NMR were obtained using a Varian Unity Inova NMR (500 MHz) or Bruker 600-MHz instrument with spectral window of ±2,000 Hz, 32 scans for ^{1}H NMR, and 5,000 scans for ^{13}C NMR at 293 K and 90° pulse width. Epoxy groups typically appear at 2.8–3.5 ppm.[37] Vinyl groups typically appear at 5.0–6.5 ppm, maleate groups at 6.3 and 6.8 ppm, while unreacted MA appears at 7.1 ppm.[37]

SEC was used to measure the molecular weight of the biobased monomers. Knowledge of the molecular weight of the monomers allowed us to determine whether addition or decomposition reactions took place. Addition reactions, such as the reaction of epichlorohydrin and furfuryl alcohol, result in higher-molecular-weight species, while decomposition of lignin and chitin can be observed by measuring the molecular weights and distribution of molecular weights. SEC was used to evaluate the resulting reaction mixtures from the methacrylation reactions to determine the quality of the product and to establish to what degree, if any, epoxy polymerization or other molecular weight building side reactions had taken place. Samples were processed using a Waters 515 GPC with two 30 cm × 7.5 mm columns packed with 5-μm (poly)styrene-divinyl benzene in succession. The columns were equilibrated at 45 °C before elution with THF at a rate of 1.0 mL/min. The eluent was monitored using a Waters 2487 dual channel absorbance detector

at 270 and 254 nm at 25 °C. Samples were prepared by dissolving 3 mg product in 1 mL of THF.

Acid number (AN) titration was performed on various chemicals to determine the percentage of acid remaining in the sample.[51] This method was usually performed during the course of a reaction to produce a desired chemical or after extraction to determine quality of the extraction. Aliquots (0.25–0.80 g) of the reaction mixture were taken at regular intervals and titrated to monitor the progression of the reaction. The AN for each sample was determined by dissolving each aliquot in 10 mL of 2-propanol and titrated using an aqueous 0.1 potassium hydroxide solution (standardized with potassium hydrogen phthalate) in the presence of phenolphthalein as an indicator to calculate the corresponding AN.

$$AN = V_t M \frac{56.1}{W_s}, \tag{4}$$

where V_t is the volume of titrant, M is the molarity of the titrant, and W_s is the mass of the sample being titrated.

Epoxy titration was performed following ASTM D 1652-90, Procedure B,[52] to determine the epoxy equivalent weight (EEW) of synthesized epoxy samples and commercially available epoxy compounds. For example, a mixture was prepared with BOF (0.4 g), methylene chloride (10 mL), tetraethylammonium bromide solution (10 mL, 0.25 g/mL), and 8 drops of 0.1% solution of crystal violet indicator in glacial acetic acid. Titration was conducted using 0.1-N perchloric acid reagent. The mixture displayed a sharp color change from blue to green, and the volume of perchloric acid agent used was recorded. Multiple titrations were conducted.

3.2.3 Subtask 2.3: Resin Preparation and Cure Analysis

Biobased monomers were mixed with other monomers to form biobased resins. Epoxy resins contain di-epoxides and diamine curing agents. Biobased epoxy monomers were mixed with one-half the stoichiometric amount of a commercial diamine (Amicure PACM) and the biobased diamines. Biobased diamines were blended with twice the stoichiometric amount of commercial epoxy monomers, such as Epon 828, diglycidyl ether of BPA. Vinyl resins contain a cross-linker and reactive diluent. Vinyl resins were prepared by blending biobased cross-linkers with styrene and biobased reactive diluents. Biobased reactive diluents were blended with methacrylated Epon 828 VE monomers. Commercial petroleum-derived components were used to determine benefits and problems associated with individual monomer components. However, the ultimate goal of this work was to

develop completely biobased resins, where all components are derived from biobased chemicals.

In situ FTIR was used to determine the extent of cure (Fig. 16). Our setup allows us to heat samples while taking FTIR spectra as a function of time.[53] This is important because resins with low extents of cure tend to be weak and have low ultimate properties. Our previous work has shown that we are able to track the extent of cure of individual components at various cure temperatures.[1,22,23] Furthermore, FTIR was used to determine reactivity ratios to determine the composition of the curing polymer and aspects of the microstructure, such as the presence and size of microgels.[22]

Monomer viscosity and rheology were measured using a rheometer to determine whether flow is Newtonian (shear thinning) and determine the Newtonian viscosity (Fig. 28). Low-viscosity Newtonian resins are desired for most composite applications. Simple steady-state shear flow experiments at room temperature (with temperature stabilization) were used to measure component and resin rheology.[3] Biobased component rheology did not need to match the monomer component it is targeted to replace. However, the biobased resin viscosity should be within 10% of the targeted replacement resin. In addition, the effect of chemical functionality and chemical structure on the rheology of biobased monomers was determined.

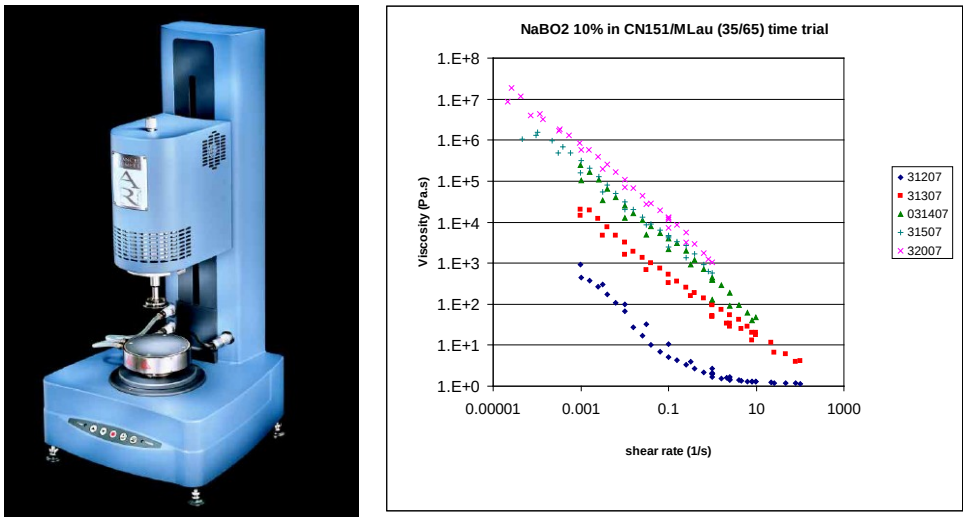

Fig. 28 AR2000 rheometer and viscosity data as a function of shear rate for resins and shear thinning fluids

3.2.4 Subtask 2.4: Polymer Properties

Dynamic mechanical analysis (DMA) using a TA Instruments Q800 was used to determine thermomechanical properties of the resulting polymers (Fig. 29). Polymer samples were prepared with nominal dimensions of 3 × 10 × 60 mm. T_g, modulus,

and cross-link density as a function of temperature was measured from the viscoelastic response of the material at a strain of 7.5 μm, at 1 Hz, from room temperature to 200 °C at 2 °C/min. This was a screening tool allowing us to determine whether the biobased resins produce T_g over 120 °C and moduli over 2 GPa. Cross-link density was measured from the rubbery modulus and Rubber Elasticity Theory.[54,55] Knowledge of the cross-link density allowed us to determine whether an efficient cure has occurred, or if highly cyclized structures have been produced.

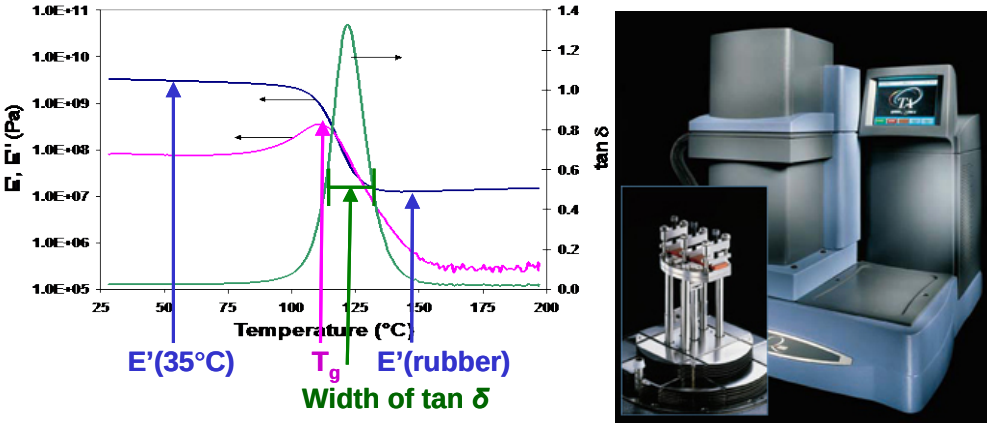

Fig. 29 Q800 DMA and representative results showing storage modulus, loss modulus, and tan delta as a function of temperature and how T_g, glass transition width, glassy modulus, and rubber modulus are determined

Instron mechanical testing was used to assess the ultimate polymer properties. Mechanical testing was performed according to ASTM standards. Flexural strength, modulus, and strain were being measured according to ASTM D790[56] by testing samples with approximate dimensions of 3 × 25 × 80 mm. Fracture toughness was measured according to ASTM D5045[57] using single-edge notch bend specimens. Good polymer samples have strength, modulus, and toughness of greater than 100 MPa, greater than 2 GPa, and greater than 100 J/m^2, respectively.

SEM was used to examine the morphology of fracture surfaces to correlate this with fracture behavior. It is possible that some biobased monomers form microphases during cure because of a thermodynamic tendency to segregate. Microphases typically result in toughening by disrupting crack growth. Larger macroscale segregation, which would also be visible with SEM, could cause a reduction in fracture properties because of poor component compatibility and connectivity.

3.3 Task 3: Testing and Analysis of Biobased Composites

Composites were prepared using the biobased monomers and biobased carbon fibers. Vacuum-assisted resin transfer molding was used to prepare the composites. Initially, unidirectional AS4 or IM7 carbon fibers were infused with biobased

resins. These composites were compared to composites prepared using the same fibers with commercially available resins. Biobased carbon fibers were prepared into unidirectional mats. These mats were infused with commercially available epoxy resin. Again, these were compared to composites prepared using commercial AS4 and IM7 fibers. Composites containing both bioderived carbon fiber reinforcement and bioderived resins were prepared. Mechanical properties of these composites, including strength, modulus, and short beam shear strength, were tested according to ASTM standards. SEM was then used to examine failure and compare the biobased composites to the standard composites. The quality of fiber-matrix adhesion can be simply viewed using SEM, and the observed energy fracture mechanisms, like fiber-pullout rather than simple fiber cleavage, was used to understand the composite fracture strength and toughness.

3.4 Task 4: Environmental and Life Cycle Analysis

The environmental impact from this program was determined by the reduction in HAP emissions and in the carbon footprint. Reactive diluents to replace styrene in VE and UPE resins could eliminate the production of HAPs in DOD composite manufacture. VOC/HAP reductions should reduce costs by eliminating the need for add-on devices to capture fugitive emissions from the fabrication process. The percentage of biobased components used in each resin formulation eliminates a proportional amount of carbon dioxide emissions and hence reduces the carbon footprint.

An estimate of the costs of the biobased fibers relative to the current process was determined. In addition, per-pound cost of the biobased resins was compared to that of analogous commercial resins. Cost savings associated with environmental benefits were factored into the life cycle analysis. Along with leveraged resources, we calculated the environmental and cost savings of switching to candidate environmentally friendly systems. The cost of materials and waste stream management was examined to determine cost savings.

3.5 Project Team

We have assembled a cooperative team, as shown in Table 4, with extensive experience in resin formulation, fiber preparation, mechanical testing, and composite manufacture. The US Army Research Laboratory (ARL) team has exceptional experience with composite materials and reducing environmental hazards associated with military coatings (SERDP PP-1056 and Environmental Security Technology Certification Program [ESTCP] 200024) and resins (SERDP PP-1109, PP-1271, and ESTCP WP-0617 along with Drexel University). John J La Scala, Chief, Coatings,

Corrosion, and Engineered Polymers Branch at ARL, is the principal investigator (PI) for this project. He received a PhD in chemical engineering from the University of Delaware and has over 10 years' experience in composite materials and materials from renewable sources. He was the PI for ESTCP WP-0617, which was awarded the ESTCP WP 2010 Project of the Year. He was lead scientist for SERDP WP-1271, which was also awarded SERDP WP Project of the Year. Dr Joshua Sadler is a postdoctoral researcher at ARL with a PhD in synthetic organic chemistry. Using that expertise, he is the lead synthetic chemist in this project. Ms Phuong Lam is a contractor at ARL and an MS student in chemical and biological engineering at Drexel University. Her role is to formulate and test VE resins. Ms F Toulan has an associate's degree in chemistry and years of experience in formulating adhesives. Her current role in this project is to formulate and test UPE resins.

Table 4 Biobased resins and fibers team

Organization	Team Members	Activities
ARL	Dr JJ La Scala Dr J Sadler Ms P Lam (MS student) Ms FR Toulan Mr Christopher Annunziato (BS)	Biobased monomer preparation and chemical analysis, monomer and resin viscosity, polymer properties, composite properties, environmental and cost assessment
Clemson University	Dr A Ogale (co-PI) Ms M Zhang (PhD student) Ms J Jin (MS student) Dr A Greene Dr A Bodine Mr Steven Chambers	Lignin microbial breakdown, oligomer chemical and rheological analysis, melt spinning, UV stabilization, carbonization, graphitization, fiber mechanical properties, fiber characterization, composite properties
Drexel University	Dr GR Palmese (co-PI) Mr Fengshuo Hu (PhD student) Dr D Koo	Hexoses and pentoses biobased monomer preparation and chemical analysis, monomer and resin viscosity, polymer properties, composite properties
University of Delaware	Dr RP Wool (co-PI) Mr J Stanzione (PhD student) Ms Kaleigh Reno (PhD student)	Lignin chemical/thermal decomposition, lignin-based monomers preparation and chemical analysis, monomer and resin viscosity, polymer properties, composite properties
Rowan University	Dr J Stanzione[a] Mr Eric Hernandez (MS student) Mr Alex Bassett (undergraduate student)	Lignin-based epoxies and VE cross-linkers

[a]J Stanzione began work on this project as a graduate student at the University of Delaware. Upon graduation, he took a position at Rowan University where we continued to collaborate on this research topic.

The Drexel team also has extensive experience with polymeric resins and composite materials and was corecipient for the ESTCP and SERDP Project of the Year awards. Giuseppe Palmese is the department head of the Chemical and Biological Engineering Department at Drexel University and has 20 years' experience in composite materials and over 10 years' experience in materials from renewable sources. Dr Donghun Koo is a postdoctoral researcher in chemical and

biological engineering and is responsible for preparing isosorbide-based UPEs and furan-based epoxies.

Richard Wool is a professor of chemical engineering and a member of the Center for Composite Materials at the University of Delaware. He runs the Affordable Composites from Renewable Sources group, which has been at the forefront of developing biobased composite materials over the past 14 years. Mr Joseph Stanzione is a PhD student in chemical engineering and is responsible for chemical modification of lignin and lignin-based thermosetting resins.

At Clemson University, Amod Ogale (professor, chemical engineering) serves as the deputy director for the CAEFF, the only National Science Foundation Engineering Research Center on fibers. He has over 20 years of research experience with advanced composites and leads CAEFF's effort on high-performance carbon fibers derived from alternative precursors. Ms M Zhang, a PhD student in chemical engineering, is responsible for developing lignin-based carbon fibers. Annel Greene (professor, animal and veterinary sciences) serves as the director of Animal Coproducts Research Center, dedicated to the ecofriendly use of biobased coproducts. She is responsible for the microbial degradation of lignin.

Rowan University was added to the team in 2014 as Dr Stanzione transitioned from PhD student to Assistant Professor at Rowan. His work on the project as a graduate student was exceptional, and his ideas and ability seemed to be of high potential. ARL used its mission funds to pay for its partnership with Rowan, but the focus of this partnership is highly relevant to the SERDP projects.

3.6 Programmatics

The Gantt chart (Table 5) shows the originally proposed schedule as well as the actual schedule. The project schedule had to be adjusted as a result of sequestration, which reduced the project funding in FY13 resulting in extension of the project for an additional year. In the end, the project has achieved all of its goals.

Table 5 Gantt chart showing originally proposed and completed schedule

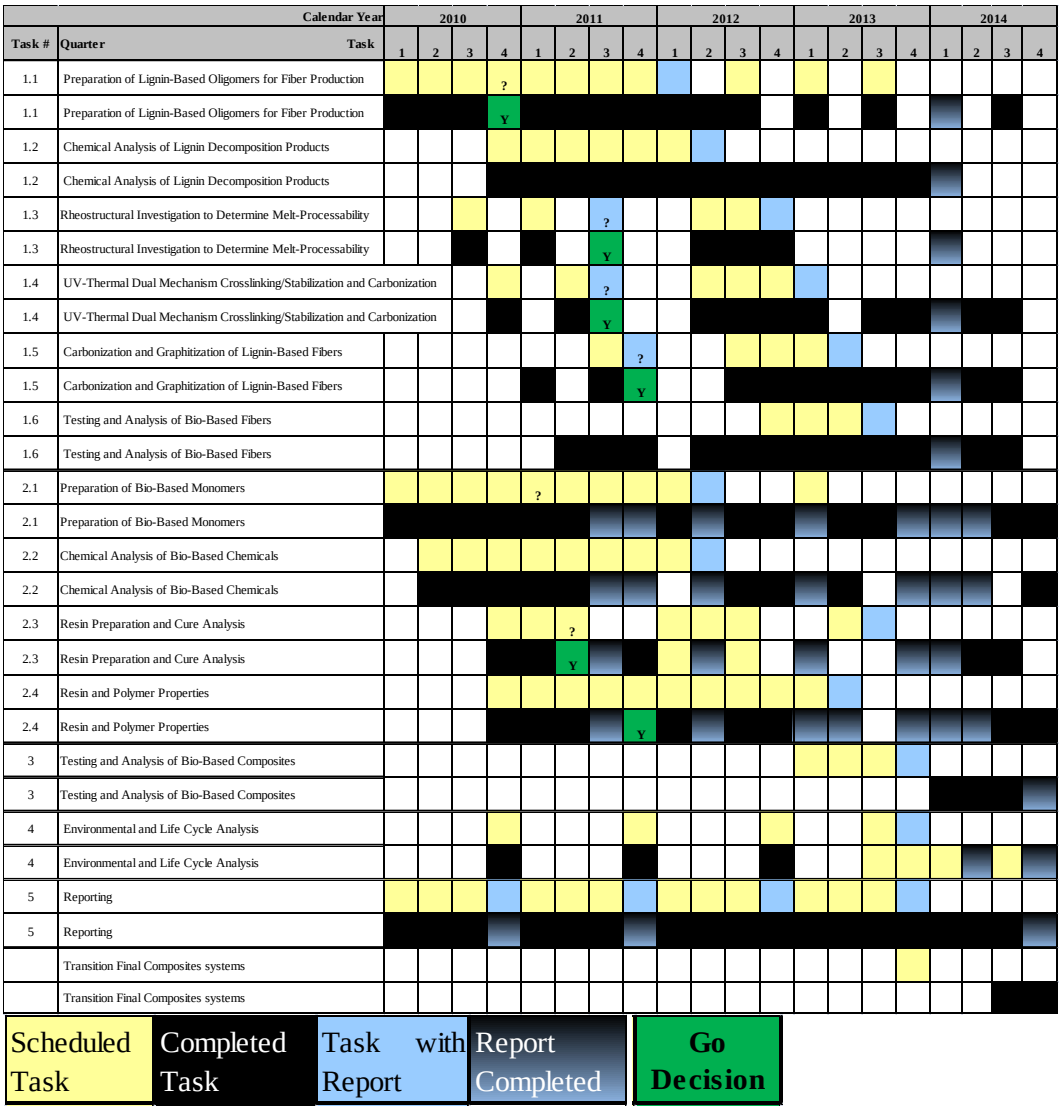

We have encountered a number of "go/no-go" decisions and have proceeded forward as a "go" for all of the following:

- Preparation of lignin-based oligomers for fiber production.
- Demonstration that lignin-based materials have proper rheological characteristics for fiber production.
- Demonstration that UV cross-linking and thermo-oxidative stabilization can successfully stabilize lignin-based carbon fibers.
- Lignin-based polymers can be successfully carbonized into fibers.
- Carbohydrate derivatives have potential for producing high-performance resins.

The following "no-go" decisions were made as subsets of the tasks that are not explicitly listed:

- Feasibility of microbial degradation of lignin. Although this was initially classified as a "go", it became apparent that the skills for the Clemson team were not sufficient to scale up this technology, nor was it looking feasible to scale up this technology to make useful amounts of carbon fiber. As a result, we cancelled this aspect of the project in June 2013.
- Singlet oxidation decomposition of lignin.
- Water washing of lignin to reduce ash content.
- Isosorbide-based unsaturated polyesters.

4. Results and Discussion

4.1 Microbial Decomposition of Lignin: Seeking New Bacterial Species to Selectively Break Lignin Bonds for Making Advanced Carbon Fibers*

4.1.1 Introduction

Lignin, the polyaromatic encrusting material in plants, is the second most abundant organic compound on Earth after cellulose. This complex aromatic biopolymer has properties that make it attractive for use in manufacture of carbon fibers. However, it is important to break the large molecule into smaller subunits for carbon fiber formation. Chemical methods of breaking lignin lack specificity, which can lead to a wide variety of breakdown products. Use of a more specified method of lignin breakdown, such as is available by the microbial world, could yield improved carbon fiber manufacture. However, isolating and culturing microorganisms capable of degrading lignin are difficult challenges.

4.1.2 Background

Lignin consists of 3 primary building blocks: *p*-coumaryl alcohol (*p*-hydroxyphenyl propanol), coniferyl alcohol (guaiacyl propanol), and sinapyl alcohol (syringyl propanol) (Fig. 30).

* Portions of this section were originally published in the ARL report: La Scala et al. Biobased carbon fibers and high-performance thermosetting resins for use in us department of defense applications. Aberdeen Proving Ground (MD): Army Research Laboratory (US); 2012 June. Report No.: ARL-SR-245.)

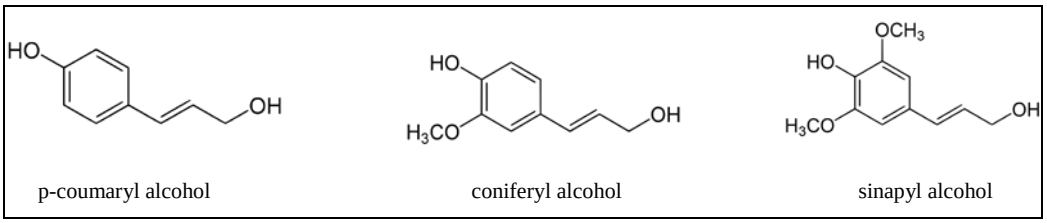

p-coumaryl alcohol coniferyl alcohol sinapyl alcohol

Fig. 30 The primary building blocks of lignin: *p*-coumaryl alcohol, coniferyl alcohol, and sinapyl alcohol

The compositions of lignins vary according to plant species with coniferyl alcohol being the primary subunit in softwood lignin. Similar chemical linkages are found in all species of lignin. In softwood, β-aryl ether linkages account for approximately 40% of the linkages within the lignin. Other linkages such as esterification of terminal hydroxyl groups of propyl side chains with *p*-coumaric acid constitute approximately 5% to 10% of lignin bonds (Fig. 31).[58,59]

Because of the unique structural configuration of lignin, which is impossible to chemically synthesize, material scientists seek to study lignin as a starting material for developing green technology carbon fibers. However, because of numerous linkages found within lignin, many of which would be susceptible during applied chemical attack, chemical degradation of the complex polymer could lead to a wide variety of breakdown products and/or could break the lignin into such small subunits that it would lose the chemical qualities that make it good for carbon fiber formation. Ideally, we desire a method of breaking the complex lignin matrix using a more targeted approach. Microbial degradation offers advantages of specificity. However, although microbial degradation of lignin has been long-studied, only a few species of bacteria that can degrade lignin have been identified.

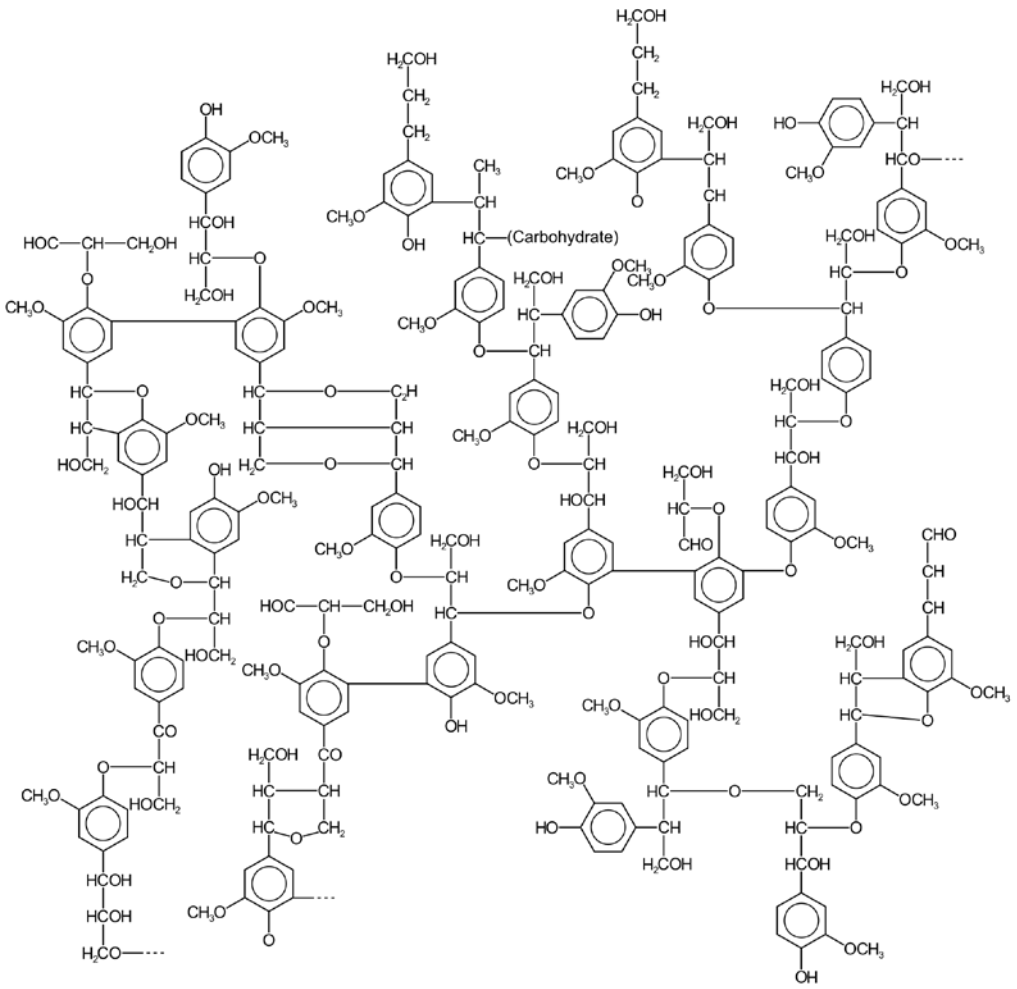

Fig. 31 Typical softwood lignin molecule

Reprinted from Karol Glab via Wikimedia Commons under GFDL Free Documentation License; see http://en.wikipedia.org/wiki/GNU_Free_Documentation_License for details [2015 May 7]. http://commons.wikimedia.org/wiki/File:Lignin_structure.svg.

Lignolytic organisms use the chemicals in lignin for nutrition by breaking the large complex into smaller subunits. For many years, it was thought this task was relegated to only the fungi, but in the past few decades a limited number of lignolytic bacteria have been isolated. Since fungal degradation rates for lignin were slow, microbiologists hypothesized that more rapidly growing bacteria probably account for a significant to major amount of the lignin breakdown that occurs in nature. However, microbiology is a relatively young science, with modern microbiology beginning in earnest with Louis Pasteur's 1862 experiments to disprove spontaneous generation. Although a few bacterial species that are capable of breaking lignin have been identified, it is believed that microbiologists have only just begun to understand the variety of species and capabilities of lignolytic bacteria. It has been estimated that there may be more than 4×10^{30} bacterial cells

on Earth, and those prokaryotic organisms are believed to represent greater than 10^5 to 10^7 unique species.[60] In 1990, Torsvik et al.[61] determined that there were more than 4,000 distinct species of bacteria in a single gram of soil. In 2002, Bach et al.[62] revised this to 10,000 distinct species of bacteria per gram of soil.

A saying often heard in the microbiological research community goes, "There is a bacterial species in the environment capable of breaking any compound". Each year thousands of new bacterial species are identified, but, as Sharma et al.[63] reported, more than 99% of all environmental samples contain bacteria that are "unculturable" simply because the proper conditions for their growth in the laboratory have not yet been deduced. Sharma et al.[63] also reported that these potentially valuable bacterial species remain "unexploited for biotechnical applications". The annual production of lignin from commercial separation (pulping) is estimated to be more than 50 million metric tons, and at least 500,000 metric tons (dry basis) of lignin products are generated annually.[64,65] However, in nature there are many billions of metric tons of wood and wood products that are naturally degraded by the microbial world. With this huge volume of lignin deposited into bacteria-laden soils and similar environments, with the vast bacterial diversity on Earth, and with the extensive ability of those bacteria to mutate to opportunistically take advantage of unique food sources, it is believed that there are potentially hundreds to thousands of unidentified bacterial species that can degrade lignin. Each unique species could have their own unique set of enzymes that could break the complex lignin molecule at specific linkages.

The purpose of this study is to investigate known bacterial species and to isolate new species of bacteria from the environment capable of degrading lignin. Researchers have spent the past many decades using traditional methods to isolate a few lignolytic bacterial species and then study each organism in detail. As such, only 10 lignolytic bacterial species have been reported (Table 6).

Table 6 Reported lignolytic bacteria

ATCC® Number	Description	Designation	
39115	*Streptomyces viridosporus* Pridham et al.	T7A	Low incubation temps/slow growth
39116	*Amycolatopsis* sp. deposited as *Streptomyces setonii* (Millard and Burr) Waksman	75iv2	
39117	*Streptomyces badius* (Kudrina) Pridham et al.	252	
49036	*Pseudomonas fluorescens* Migula	A1 [IFO 15839]	
700072	*Microbulbifer hydrolyticus* Gonzalez et al.	IRE-31	Requires seawater for growth
700073	*Sagittula stellata* Gonzalez et al.	E-37 [CIP 105237]	
700074	*Marinobacterium georgiense* Gonzalez et al. emend. Satomi et al.	KW-40	
BAA-396	*Sinorhizobium* sp. deposited as *Sinorhizobium termitidis*	M3A [DSM 10169]	Not much info on this organism
BAA-1142	*Sulfitobacter* sp.	EE-36	Requires seawater for growth
BAA-1142D-5	*Sulfitobacter* sp.	genomic DNA from strain EE-36 (ATCC BAA-1142)	

There are a number of problems with these reported lignolytic bacteria. The first 3 in Table 6 have slow growths and require low incubation temperatures. *Pseudomonas fluorescens* has potential and is used in this work to decompose lignin for carbon fiber formation. The next 3 and the last 2 require seawater for growth, which is rarely used in commercial industry because of the corrosivity and other issues. The one shown in green is not well characterized but does represent a possibility if a sample of the bacterial culture can be obtained.

This study is directed toward a broader approach of screening as many samples as possible for lignolytic organisms and then learning if these organisms can break lignin in different ways to assist in carbon fiber formation. This study uses a little-known and unique rapid screening method known as the chemostat isolation method. A lignolytic chemostat isolation method was developed by Dr VR Srinivasan at Louisiana State University in the mid-1980s. The method allows rapid selection of organisms possessing certain attributes (such as lignin degradation) out of trillions of bacteria in an environmental sample. The chemostat isolation method is unique, and only a few of those students who studied in Dr Srinivasan's laboratory are familiar with this unpublished technique. Currently, chemostat methodologies are most often used for generating large volumes of biomass, but only rarely are chemostat isolation methods used. As most microbiologists are now involved in molecular manipulation, there is little work being done in chemostat

screening microorganisms for new isolates. Microbial continuous culture methods and kinetics, which provide the basis for understanding the chemostat isolation method, are now rarely taught, yet this information is of great value for rapidly screening populations of bacteria for specific traits.

This study is concentrated on isolating a library of new lignolytic organisms using the chemostat isolation method to separate potential strains from the trillions of bacterial species in environmental samples. After isolating potential bacterial species, we screen and characterize these organisms for lignolytic ability using TLC to reveal the number of lignin subunits generated upon culturing under specific conditions. After characterization, we further screen lignolytic bacterial candidates to determine potential for carbon fiber formation from degraded lignin in the quest to find bacterial species that break lignin at the optimum site for best carbon fiber production. Once screening is completed, the best bacterial candidates will be used in scale-up studies for manufacturing carbon fibers.

Full details of results and discussion can be found in the report titled *Isolation and Characterization of Lignolytic Bacterial Species* (Appendix A).

4.1.3 Lignolytic Culture Isolation

The chemostat method using lignin analog compounds as sole carbon sources in microbial media was not as successful as anticipated. However, by using modified Dye's medium, which contained Indulin AT lignin as the sole carbon source, more than 300 cultures were isolated. It is hypothesized that although the chemostat media using lignin analogs contained linkages indicative of the bonding within lignin or which should have occurred during degradation of lignin, apparently one or more crucial growth factors were missing. More than 40 sole carbon source media formulations were tested using the various lignin analogs. However, during these trials with the chemostat, very few potential lignolytic organisms were collected. Researchers devised a modification of Dye's medium using Indulin AT lignin as the sole carbon source. This medium was highly successful and suggests that it contained an adequate combination of nutrients and/or trace cofactor(s) that were missing in the other sole carbon source media used previously. Upon using this modified Dye's medium in the chemostat, we were able to collect large numbers of potential lignolytic organisms (Fig. 32). Therefore, the chemostat procedure was repeated with Dye's medium for screening all collected environmental samples. Interestingly, the majority of the potentially lignolytic isolates selected were derived from samples collected from Louisiana, and very few isolates were derived from samples from Florida, Georgia, South Carolina, North Carolina, Tennessee, Maryland, and Delaware.

4.1.4 Characterization of Isolated Bacteria

The bacterial colonies were characterized using a number of techniques. First, a visual observation of the cultures was performed to characterize the various differences (and similarities) among the isolates, as illustrated in Fig. 32. Gram staining of the bacteria was performed, as shown in Fig. 33. These identification methods were cataloged for over 300 cultures. Approximately 25 bacterial cultures were submitted for 16S rRNA analysis to more specifically identify the bacteria cultures. Currently, the results are being compiled to determine trends and the range of properties. However, we have putatively identified a number of bacterial cultures that decompose lignin as *Pseudomonas, Klebsiella, Erwinia, Streptomyces, Bacillus badius, Petrobacter, Tepidophilus*, as well as unknown and potentially new bacterial species. The characterization of 2 representative lignolytic bacterial cultures is shown in Figs. 34 and 35.

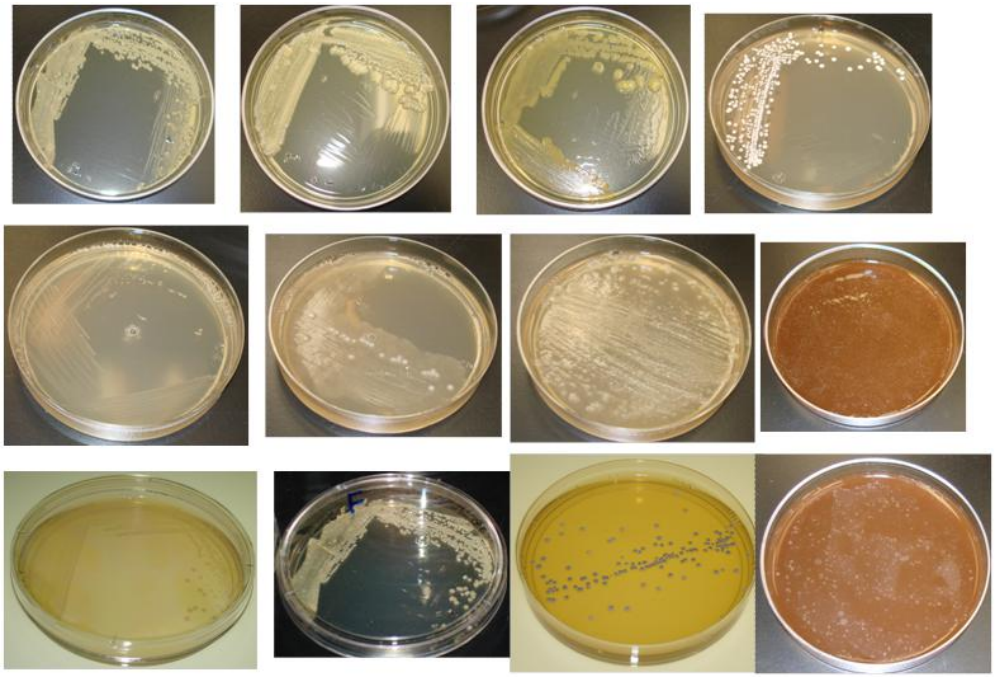

Fig. 32 Selection of isolated bacterial cultures that successfully decompose lignin

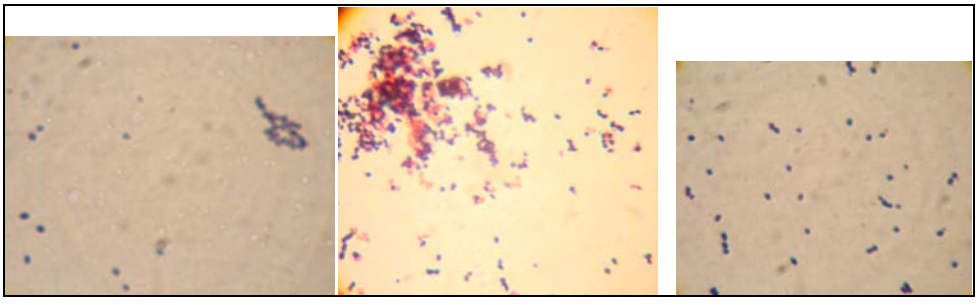

Fig. 33 Micrographs of 3 selected Gram-stained bacteria showing positive (purple) and negative Gram (red) staining

SERDP Project Data Sheet

Sample ID:	LA-SiCr-49
Sample Source:	Mount Hermon, Louisiana (Washington Parish)
Sample Characteristics:	Rotted Cresote Fence Post
Date/Time Collected:	12/29/10 2:23 pm
Prelim. Isolation Method:	Chemostat with Modified Dye's broth pH 7-7.2 30°C 3 hours prior to washout
Sub-culture:	Streaked for isolation – modified Dye's agar – 48 hr incubation at 30°C - appears to be mixed culture Re-streaked for isolation – modified Dye's agar – 48+ hr incubation at 30°C - pure culture achieved
Colony Color:	Grey/Lavender
Colony Morphology:	Round, raised, stone-like, fibrous on agar Stone-like adhesions in broth – adheres to flask walls
Growth Characteristics:	Requires at least 48 hours for any observable growth; afterward exhibits robust growth
Gram Reaction:	Gram variable
Cell Morphology:	Filamentous
Comments:	Potentially a *Streptomyces*? Better growth at lower temps
Lignin Breakdown?	Yes - as noted by TLC – one distinctive extra band in cultured
Best Extracting Solvent:	1:1 v/v ethyl acetate/methanol
Best Resolving Solvent:	10:1:1:0.5 Ethyl Acetate:Methanol:Acetone: H_2O
Melt Fiber Formation?	Yes – as noted microscopically
Melt Fiber Score?	9 out of 10 due to long fiber formation/uniform fibers

a

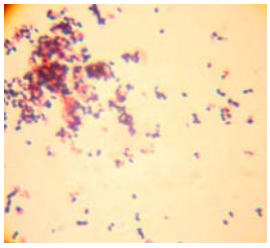

b

c

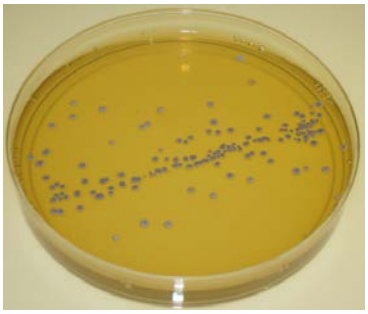

a) LA-SiCr-49 – Gram variable
b) LA-SiCr-49 culture in Modified Dye's broth; 49 hr incubation at 30°C (adhesions)
c) LA-SiCr-49 culture in Modified Dye's agar; 49 hr incubation at 30°C

Fig. 34 Sample data sheet example for LA-SiCr-49

SERDP Project Data Sheet

Sample ID: LA-SiCr-49
Sample Source: Mount Hermon, Louisiana (Washington Parish)

TLC:
Extracting Solvent: 1:1 v/v ethyl acetate/methanol
Resolving Solvent: 10:1:1:0.5 Ethyl Acetate:Methanol:Acetone: H_2O
Visualization: 280 nm ultraviolet – (banding more distinct on greyscale photo) – additional band noted on cultured lignin

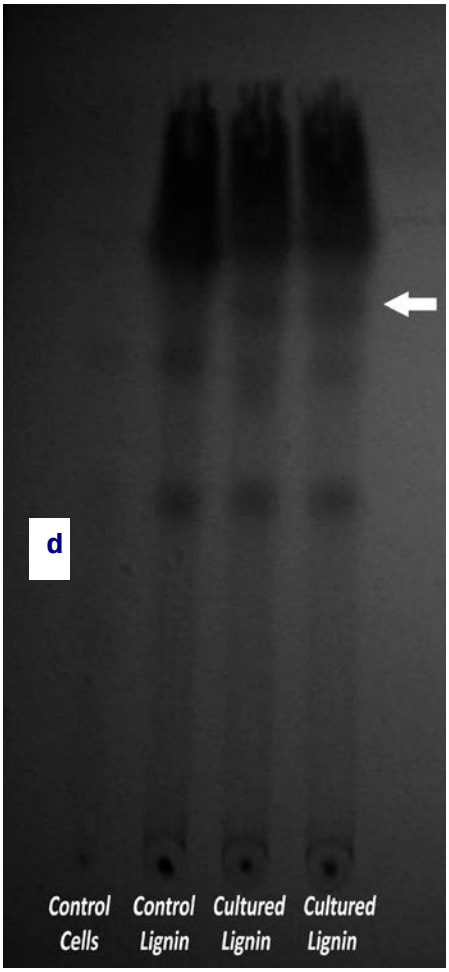

Fig. 34 Sample data sheet example for LA-SiCr-49 (continued)

SERDP Project Data Sheet

Sample ID: LA-SiCr-49
Sample Source: Mount Hermon, Louisiana (Washington Parish)

Melt Fiber Formation Comments:

1:1 v/v ethyl acetate/methanol extracted
100X magnification – microscope slide
Long fiber formation – fibers fairly uniform in thickness along entire length

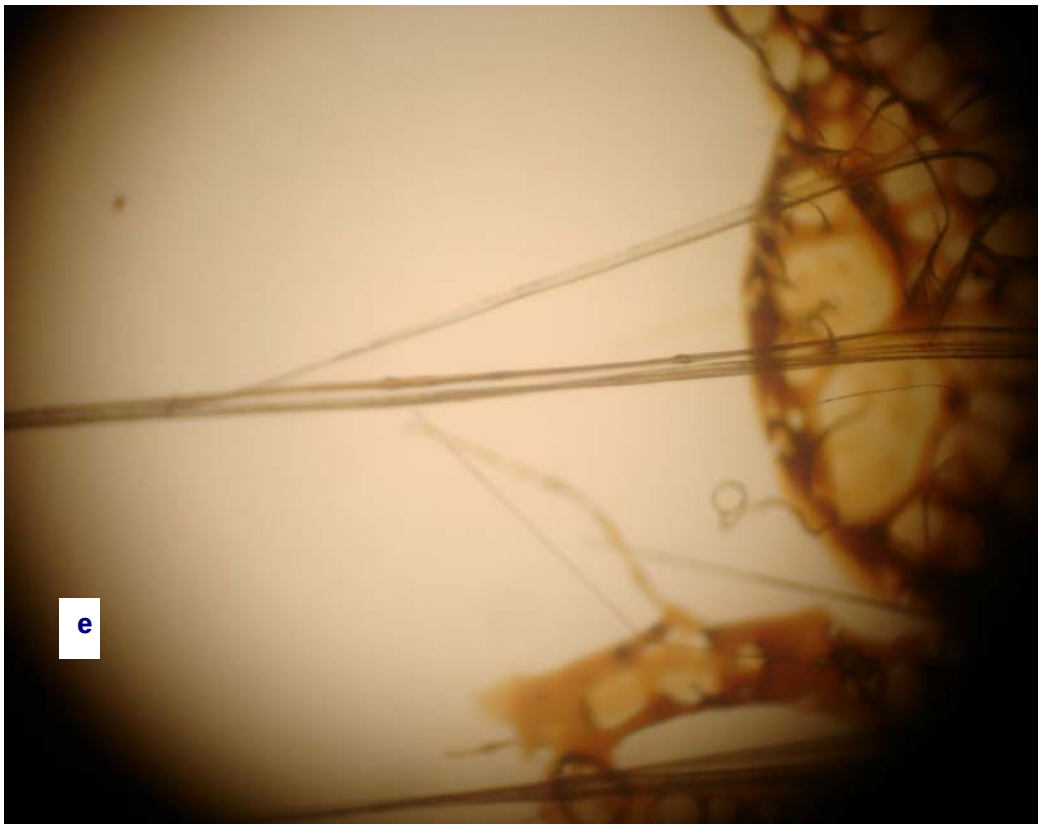

Fig. 34 Sample data sheet example for LA-SiCr-49 (continued)

SERDP Project Data Sheet

Sample ID: LA-SiCr-14
Sample Source: Mount Hermon, Louisiana (Washington Parish)
Sample Characteristics: Upland swamp soil sample
Date/Time Collected: 12/29/10 3:15 pm
Prelim. Isolation Method: Chemostat with Modified Dye's broth
pH 7.3
30°C
5 hours prior to washout
Sub-culture: Streaked for isolation – modified Dye's agar – 48 hr incubation at 30°C - appears to be mixed culture
Re-streaked for isolation – modified Dye's agar – 48+ hr incubation at 30°C - appears to be mixed culture
Re-streaked for isolation – modified Dye's agar – 48+ hr incubation at 30°C - pure culture achieved
Colony Color: Cream
Colony Morphology: Moist, flat colonies
Growth Characteristics: Requires at least 24 hours for any observable growth; afterward exhibits robust growth
Gram Reaction: Gram negative
Cell Morphology: Short rod – possibly peritrichous flagella
Comments: Better growth at lower temps
Lignin Breakdown? Yes - as noted by TLC – one distinctive extra band and lost one band in cultured
Best Extracting Solvent: H_2O-saturated n-butanol
Best Resolving Solvent: 8:1:1 toluene/ethanol/1 M ammonium hydroxide
Melt Fiber Formation? Yes – as noted microscopically
Melt Fiber Score? 7 out of 10 – MANY fibers – but all are short – therefore
may be easy to form but can they provide length?

a

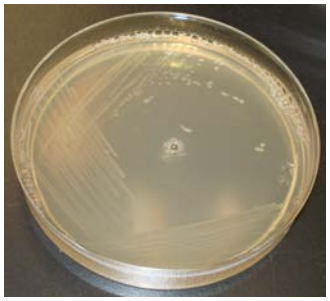

a) LA-SiCr-14 culture in Modified Dye's agar; 24 hr incubation at 32°C

Fig. 35 Sample data sheet example for LA-SiCr-14

SERDP Project Data Sheet

Sample ID: LA-SiCr-14
Sample Source: Mount Hermon, Louisiana (Washington Parish)

TLC: Silica gel
Extracting Solvent: H_2O-saturated n-butanol
Resolving Solvent: 8:1:1 toluene/ethanol/1 M ammonium hydroxide
Visualization: 280 nm ultraviolet
Notes: Control and sample broth were incubated at 30°C for 48 hr - one distinctive extra band and lost one band in cultured

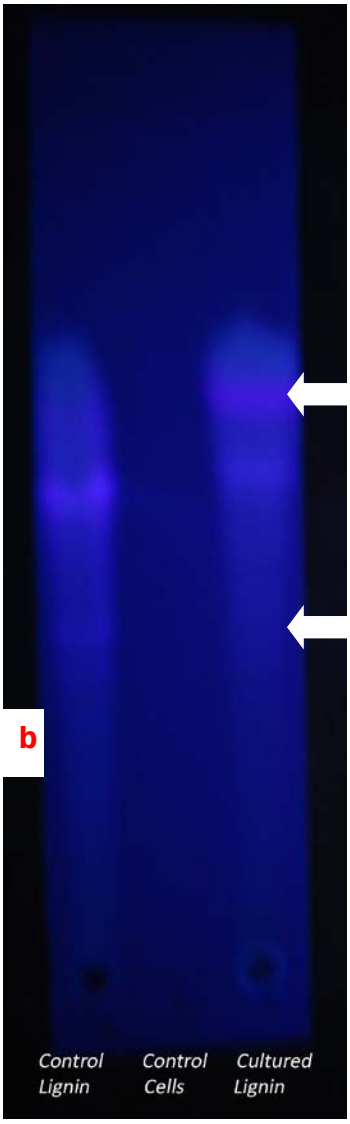

Fig. 35 Sample data sheet example for LA-SiCr-14 (continued)

SERDP Project Data Sheet

Sample ID: LA-SiCr-14
Sample Source: Mount Hermon, Louisiana (Washington Parish)

Melt Fiber Formation Comments:

1:1 v/v ethyl acetate/methanol extracted
100X magnification – microscope slide
Short fiber formation – but high number of fibers formed per unit area

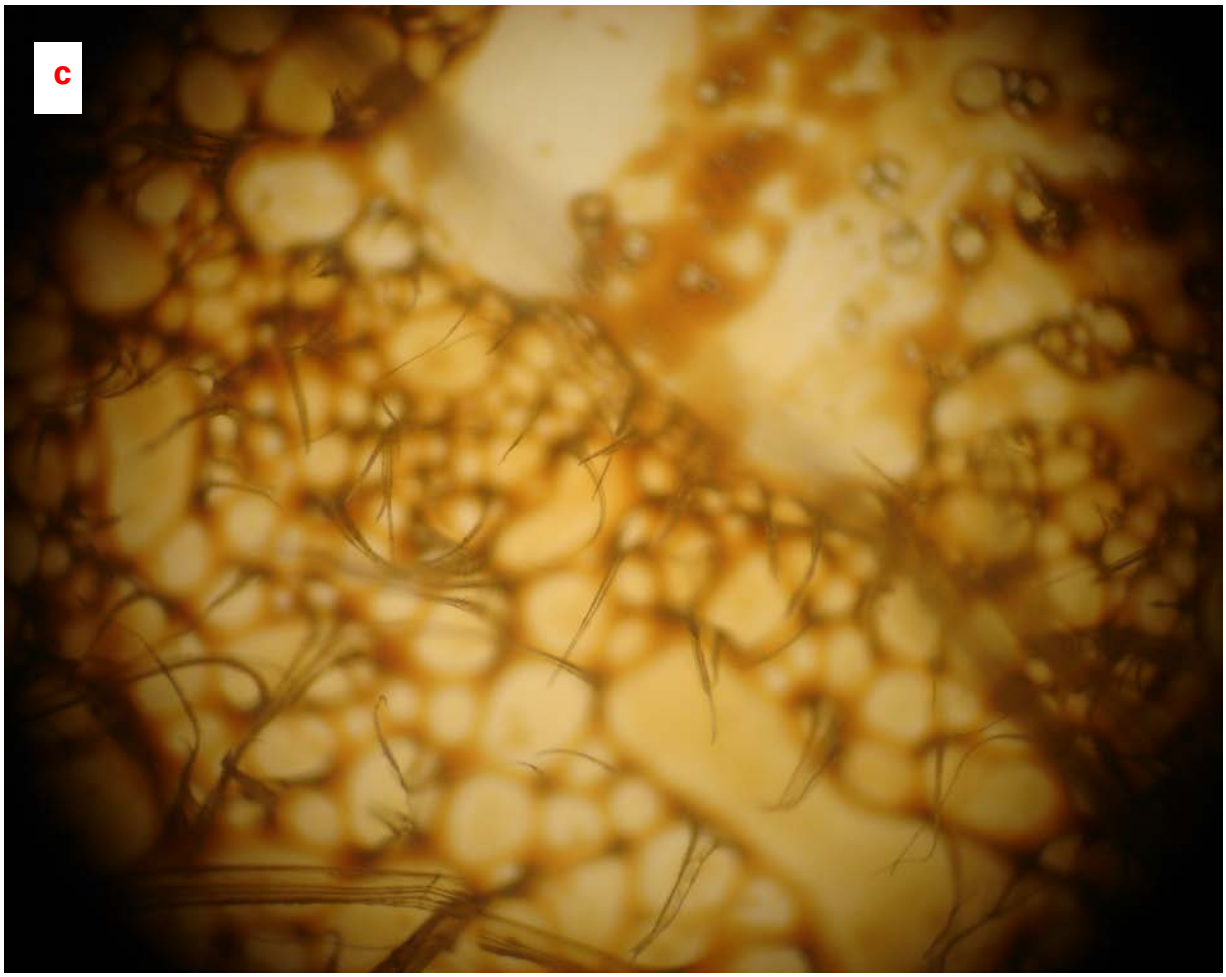

Fig. 35 Sample data sheet example for LA-SiCr-14 (continued)

4.1.5 Verification of Lignolytic Activity

The cultures isolated from the chemostat broth were streaked isolated on modified Dye's agar through at least 2 subcultures (Fig. 34c). Isolated cultures were stored on agar slants for further testing, and broth cultures were frozen (–40 °C) in modified Dye's broth with 30% sterile glycerol for long-term storage. The individual cultures in this library are now being examined to score each culture for degree of robust growth, lignolytic activity, and potential of breakdown products for melt fiber formation. A data sheet is kept on each organism, and additional information is added as derived. Samples of data sheets shown in Figs. 34 and 35 indicate scoring of 2 of the 300+ lignolytic cultures.

So long as the growth of the organism occurs within a few days, the speed with which the bacteria cause the modification to lignin is not as important at this stage as the actual modification. High-volume fermentation methods are commonplace for microbial modifications and could be used in commercial modification if the organism(s) prove capable of modifying lignin for carbon fiber manufacture.

Samples are first evaluated for growth ability in the presence of lignin as a sole carbon source. Cultural characteristics including colony morphology, cell morphology, and Gram reaction were examined. After lyophilization, extraction, and TLC on cultured broth, those cultures that exhibit good separation and distinctive bands were noted on data sheets (Figs. 34d and 35b). The TLC results do indicate significant differences between the control and bacteria-modified lignin, with bands missing and new bands present. However, the TLC results show that much of the lignin solute is being carried across the entire TLC plate, and thus a better eluent would be preferred to better detail the results. A characterization of the differences, especially after improved solvent choice, was compiled and is listed in the full report attached in Appendix A.

4.1.6 Fiber Formation from Microbially Decomposed Lignin

We created a scoring system using the test system of heating extracted samples between 2 microscope slides and analyzing them under the microscope (Fig. 36). Criteria for scoring include whether any fibers are formed, relative ease of fiber formation, length of formed fibers, evenness of fiber thickness, whether any breakage or variation in uniformity of fibers is apparent, and relative number of fibers formed.

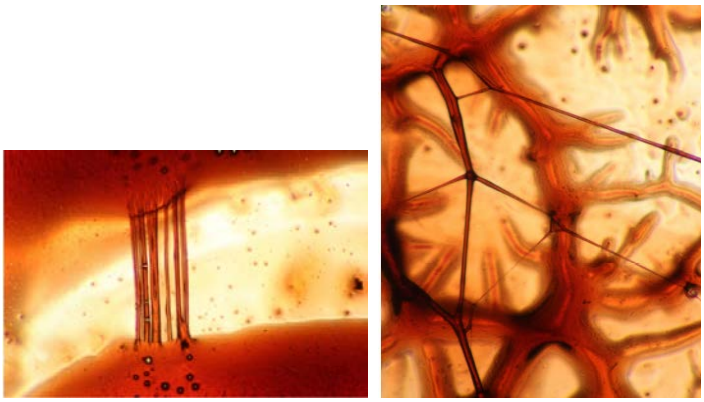

Fig. 36 Fiber generated in crude microscope test from extract of MHLA-01

Fifty-one of the isolates demonstrated some fiber formation upon extraction and testing via the microscope slide technique. Nine cultures were scored as 6 or higher on the text scale. These were identified as LA-SiCr-14, LA-SiCr-49, LA-SiCr-91, LA-SiCr-118, LA-Br-23, MHLA-01, MHLA-07, SC-BG-E, and ATCC 39117 *Streptomyces badius*. MHLA-01 and MHLA-07 produced superior results in the preliminary fiber testing procedures (Figs. 37 and 38).

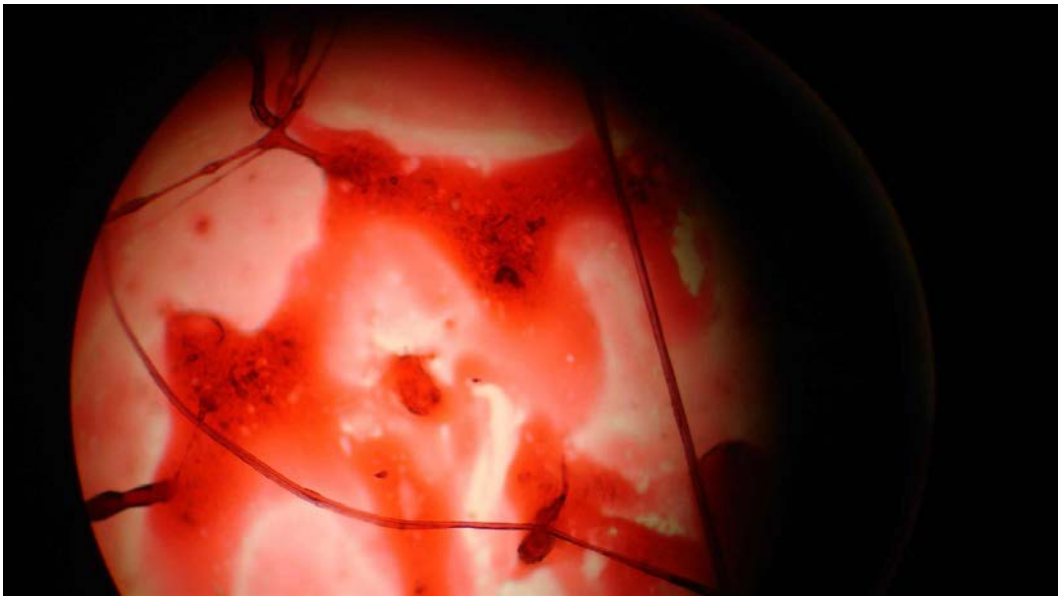

Fig. 37 MHLA-01 fiber former at 100×

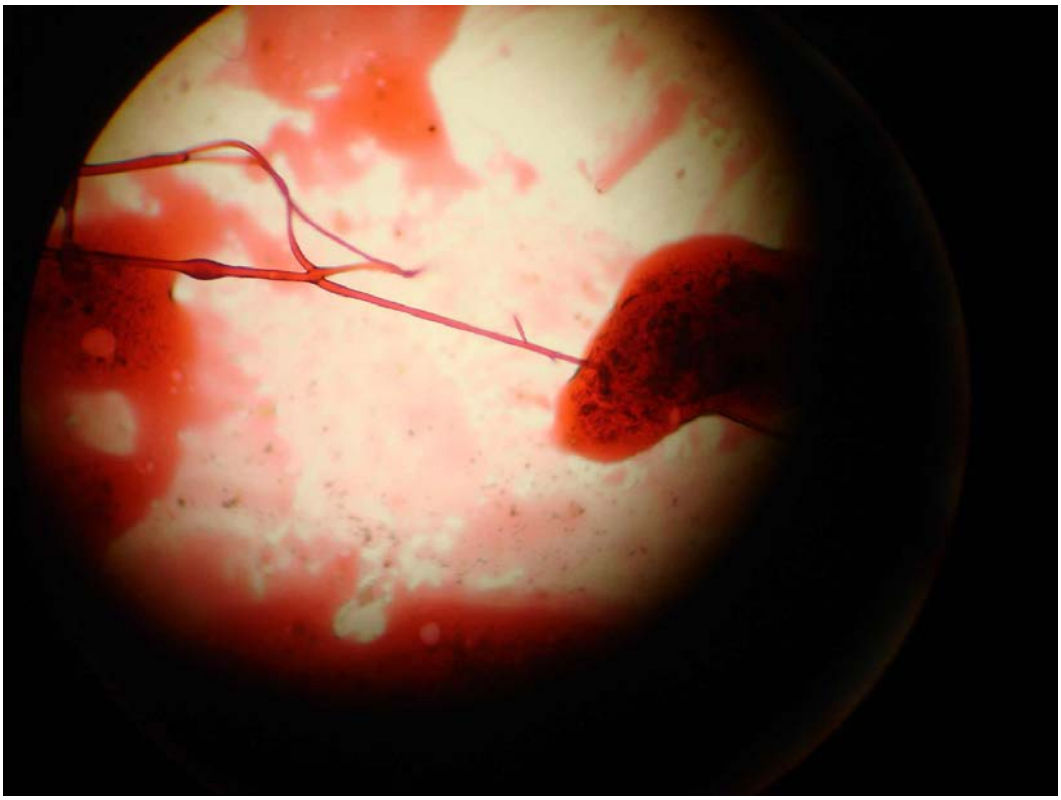

Fig. 38 MHLA-07 fiber former at 100×

Various other conclusions were made from this work based on the results:

- Polymer appears to be linked to pigment production.
- Growth above 35–37 °C results in no pigment production; a similar phenomenon is noted with prodigiosin production in *Serratia marcescens* indicating this pigment may be prodigiosin or may be related to prodigiosin.
- Without pigment production, the polymer is not evident in extracts (4:1 ethyl acetate/methanol); therefore, we believe the polymer may be the pigment. If this is true, we hypothesize that the polymer may be prodigiosin or a variation of prodigiosin.
- Purchased *Serratia marcescens* cultures did not produce polymer as screened by current testing protocol (solvent evaporation/melting on microscope slides).

4.1.7 Fiber Formation from Scaled-Up Microbially Decomposed Lignin

Fiber formation was tested using the scaled-up modified lignin derived from the lignolytic *Pseudomonas* strand identified by Clemson researchers. The samples were picked up using tweezers, and the tweezers were opened and closed to place

a stretching force on the material. As shown in Fig. 39, fibril formation was induced in some cultures, indicating an ability of these decomposed lignin samples to form melt-spun fibers.

Fig. 39 Tweezer stretching experiment of scaled-up *Pseudomonas* decomposed lignin sample

4.1.8 Lignolytic Bacteria Identification

The identification of the bacteria that caused good film formers is discussed in the detail in the report contained within Appendix A. In particular, the work identified these bacteria as genus *Serratia* and likely a new species as there was no rRNA match greater than 97%.

4.1.9 Reconfirmation that MHLA-01 and MHLA-07 Can Use Lignin as Sole Carbon Source

This work is documented in full in the report contained within Appendix A. In summary, the results showed that these organisms can use lignin as a sole carbon source for growth and do break these down into useful oligomeric species that again produce good fibers under the microscope slide test (Fig. 36).

4.1.10 Lignolytic Bacteria Scale-Up to Produce Polymer for Carbon Fiber Preparation

This work is documented in full in the report contained within Appendix A. In summary, the researchers took weeks to scale up production (Fig. 40) to produce approximately 5 g of low concentrated lignin oligomers (Fig. 41). The concentration of solution was too low to produce enough useful material to perform any test for fiber-forming evaluation at the scale Dr Ogale's group needed. As a result, although this technology is promising, at this point, we decided to end the work on lignin microbial decomposition in June 2013 and focus only on chemical methodologies, which were working and are scalable.

Fig. 40 Scale-up of MHLA-01 and MHLA-07 and the decomposed lignin they produce

Fig. 41 A 5-g solution of lignin oligomers from MHLA extract in solvent

4.1.11 Microbial Decomposition of Lignin Summary and Conclusions

The ultimate goal of this work was to determine the best lignolytic organisms to use for scale-up to produce sufficient material for carbon fiber spinning. The first aspect of this work was successful: identifying a number of potential organisms and a few particularly promising species for lignin decomposition. The resulting decomposed lignin appeared to have the desired film-forming properties. However, the ability to scale up this product was not feasible within this project, and thus we discontinued this aspect of the project in June 2013.

Recorded lignin research reveals that very few lignolytic bacteria have been previously isolated and characterized. A search of the American Type Culture Collection bacterial database for the keywords “lignin” and “lignolytic” reveal only 10 bacterial species. In fact, this laboratory has purchased the 3 aerobic species that, the literature reports, have significant lignolytic activity against lignin. These cultures have been included in the study. One of these purchased cultures is showing good promise for carbon fiber formation. Yet, the results of this work indicate that 2 unknown species of *Serratia* bacteria are the most effective at decomposing lignin. As a side aspect of this project, we thus have identified 2 unknown species of bacteria that happen to have good ligninolytic behavior.

The results are profound. This study has yielded more than 300 putative lignolytic organisms. Using 16s RNA identification methods, we have tentatively identified the first of these isolated cultures as species of *Pseudomonas, Klebsiella, Erwinia, Streptomyces, Bacillus badius, Petrobacter,* and *Tepidophilus.* Most of the species were unidentifiable by 16s RNA sequencing, indicating they may be new, previously unknown species. Many of the isolates may be duplicates, but colony morphology and Gram stain results indicate that there are many different species in this collection. Results of this study will provide considerable new knowledge for not only carbon fiber formation from lignin but also new lignolytic species of bacteria.

4.2 Chemical Decomposition and Fractionation of Lignin*

4.2.1 Introduction

Nondegraded and chemically modified lignins have been successfully incorporated into various materials, including polymeric materials.[66–71] Additionally, much research has been conducted in selectively breaking down all types of lignin and multiphenolic lignin model compounds (LMCs) to develop new chemicals and renewable sources of predominantly petroleum-derived chemicals (Fig. 42).[68,69,72–80] Recently, a modest yield of vanillin from Kraft lignin has been obtained using aqueous polyoxometalates in the presence of alcohols to oxidatively degrade lignin.[72] Additionally, vanillin production via Kraft lignin oxidation using a NaOH alkaline medium has been reported.[77] Moreover, a 70% yield of guaiacol has been achieved from common β-O-4 LMCs, guaiacylglycerol-β-guaiacyl, and veratrylglycerol-β-guaiacyl ether under catalytic hydrolysis using an acidic ionic liquid.[75] In 2011, Zakzeski and Weckhuysen[73] reported 22.2% and 12% yields of guaiacol from aqueous phase reforming of a β-O-4 linked and a 5-5′ carbon-carbon linked biphenyl model compounds, respectively, using a platinum (Pt)/aluminum oxide (Al_2O_3) catalyst. Sergeev and Hartwig[80] have reported yields as high as 99% of guaiacol from hydrogenolysis reactions of representative biphenyl LMCs.

The ultimate goal of this research is the employment of KPL and LMCs—compounds that could come from the strategic breakdown of lignin—in the development of high T_g biobased resins by preparing derivatives thereof. KPL has been chosen as the primary lignin source in this study because of its supply dominance and cost-efficiency in industry compared to other forms of lignin, such as steam exploded, organosolv, soda, and sulfonated lignins. If the goal of this

*This section was originally published in La Scala et al. Biobased carbon fibers and high-performance thermosetting resins for use in U.S. Department of Defense applications. Aberdeen Proving Ground (MD): Army Research Laboratory (US); 2012 June. Report No.: ARL-SR-245.

research comes to fruition, the use of modified KPL and functionalized LMCs in biobased composites could be both economical and environmentally friendly.

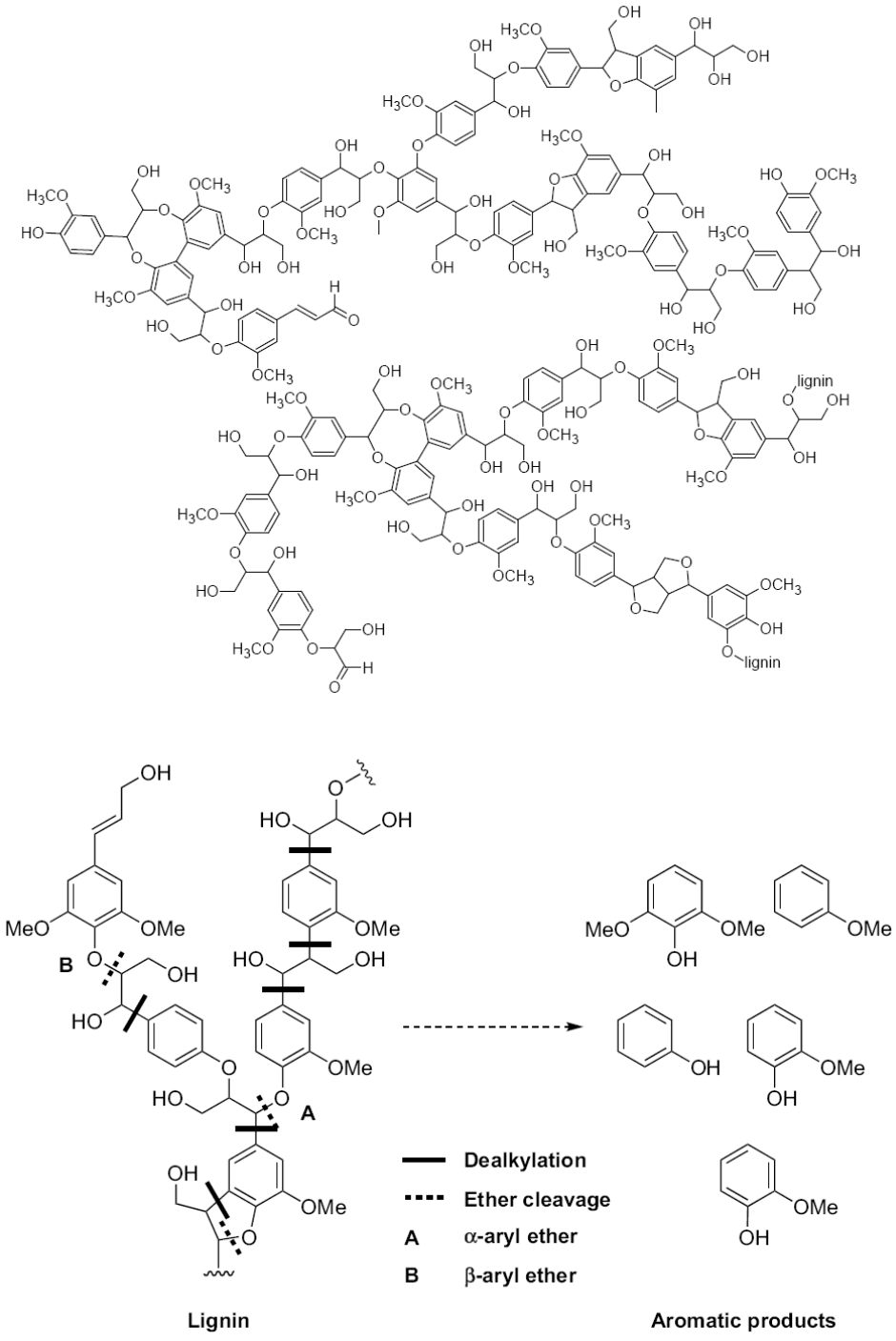

Fig. 42 General chemical structure of lignin (top) with a schematic for its conversion into single aromatic chemicals (bottom).[74,75] (Reprinted with permission from John Wiley and Sons [top] and Elsevier [bottom].)

To test our hypothesis and achieve our ultimate goal, we are currently following the strategy illustrated in Fig. 43. Specifically, KPL is being directly functionalized with free radically polymerizable groups. Lignin is also being fractionated into different fractions based on molecular weight and solubility in different organic solvents. Simultaneously, we are currently investigating the degradation of KPL via an olefin metathesis technique. A proposed model structure of KPL, shown in Fig. 44, includes aliphatic carbon–carbon double bonds.[66,81] It is hypothesized that KPL can be chemically broken down via an olefin metathesis reaction of the aliphatic carbon–carbon double bonds using ethylene as the co-reactant and a ruthenium-based catalyst (Fig. 44) for highlighted, representative aliphatic carbon–carbon double bonds that may be present in KPL. Schrodi et al.[82] demonstrated that ethenolyses of methyl oleate, a natural seed oil derivative, to produce useful terminal olefins could be achieved in dichloromethane under low-pressure (150 psi) conditions using various ruthenium-based catalysts. In addition, Ferré-Filmon et al.[83] have shown that phenolics do not interfere or hinder the olefin metathesis reactions that used first- or second-generation Grubbs catalysts, or modified versions thereof. Moreover, the high activity and chemically tolerant nature of the ruthenium-based catalysts, particularly the first- and second-generation Grubbs catalysts, are well known, even in aqueous solutions.[82,84,85] Therefore, it is proposed that KPL dissolved in either water or a polar solvent, such as ethylene glycol, can be chemically degraded via an ethenolysis reaction using a catalytic amount of ruthenium-based catalyst under moderate pressures at elevated temperatures in less than 6 h. Even though this degradation technique may not produce a high yield of very-low-molecular-weight, single or multiphenolic compounds, it has the potential to lower the statistical molecular weight of the KPL, drastically reduce its polydispersity index (PDI), and chemically incorporate free radical polymerizable groups onto lignin structure. This is all contingent upon the presence, number, and availability of aliphatic carbon–carbon double bonds of KPL.

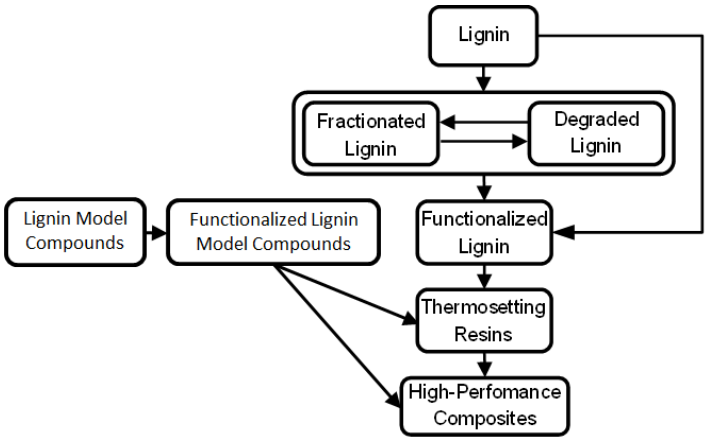

Fig. 43 Lignin project block flow diagram

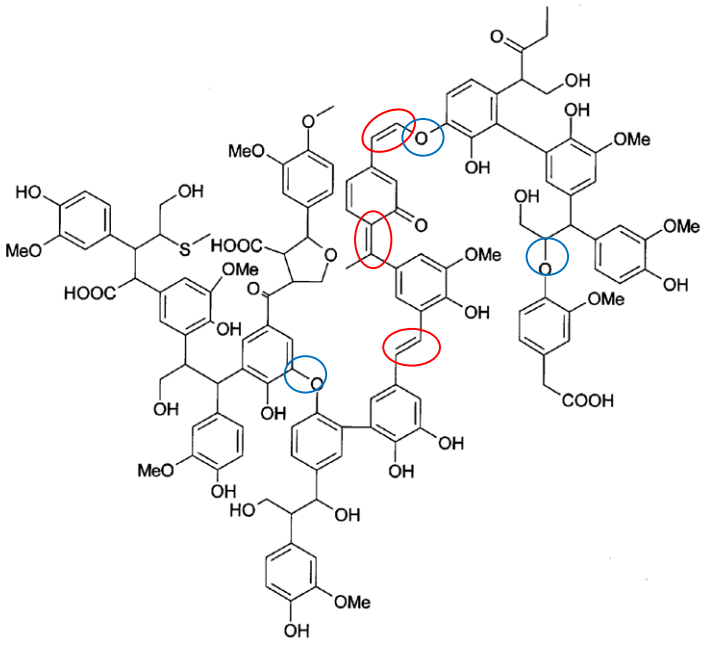

Fig. 44 Proposed model structure of KPL.[66,81] Aliphatic carbon–carbon double bonds present in the proposed model structure of KPL are highlighted by red circles, while ether linkages are highlighted by blue circles.

Additionally, we are investigating the degradation of KPL via a singlet oxygen mediated degradation technique. The proposed model structure of KPL by Marton, shown in Fig. 44, includes alkyl–aryl and alkyl–alkyl ether linkages.[66,81] It is hypothesized that KPL can be chemically broken down via a singlet oxygen (sensitized by Rose Bengal) reaction of the ether linkages; see Fig. 44 for highlighted representative ether linkages that may be present in KPL. In the presence of both oxygen and Rose Bengal, Bonini et al.[86,87] demonstrated that singlet oxygen mediated degradation of steam-exploded pine lignin and steam-exploded beech lignin has the potential to yield single aromatic products. Additionally, as reviewed by Lanzalunga and Bietti,[88] much research has been conducted on the photochemical-induced degradation of LMCs. Similar to the olefin metathesis degradation of KPL, this degradation technique may not produce a high yield of very low molecular weight, single or multiphenolic compounds. However, it has the potential to lower the statistical molecular weight of the KPL and reduce its PDI. This is all contingent upon the presence, number, and availability of residual ether linkages in the KPL.

Moreover, and as can be seen in Fig. 43, fractionated KPL, specifically a fraction that was soluble in methanol, is being directly functionalized with free radically polymerizable groups. Additionally, LMCs—namely, vanillin, guaiacol, and eugenol—are being methacrylated, with methacrylated versions of guaiacol and

eugenol being investigated as biobased reactive diluents as potential styrene replacements. Methacrylated vanillin (MV), a solid at room temperature, is currently being studied in a thermosetting "green" resin. As a side note, the first synthesis of vanillin used eugenol from clove oil. Vanillin was commercially produced from eugenol until the 1920s when it was later discovered that vanillin could be obtained from the by-product of the sulfite process for making wood. Vanillin production from lignosulfonates started in 1937, and by 1981, a single pulp and paper mill in Ontario, Canada, supplied 60% of the world market for synthetic vanillin.[70] However, because of growing public awareness on environmental issues—namely, the hazards associated with waste effluents—as well as cheaper synthesis routes—namely, petroleum-derived synthetic vanillin—mills began to close. Currently, synthetic vanillin is synthesized in a 2-step process from petroleum-derived guaiacol (derived from phenol) and glyoxylic acid.[70] Today and since 1993, the only vanillin producer from lignosulfonate that exists is the Norwegian company Borreegaard.[70,89] It is with great hope that vanillin, and similar chemicals, will be produced from lignin at a much higher volume with the development of sustainable biorefineries that are capable of completely mitigating waste streams or have the ability to drastically reduce the hazards and toxicities of such streams.

4.2.2 Kraft Pine Lignin (KPL) Solvent Fractionation

The yields of KPL in each fraction can be seen in Fig. 45. The average KPL recovery was 93.5% ± 1.2%. As can be seen in Fig. 45, roughly 40% of the KPL dissolved in methanol while over 50% was insoluble in any of the used solvents. Methanol has a solubility parameter of 14.5 $(cal/cm^3)^{1/2}$. KPL has been reported in the literature to have a solubility parameter greater than 12.03 $(cal/cm^3)^{1/2}$.[68] Thus, 40% of the KPL has a solubility parameter close to 14.5. Upon fractionation, the KPL fractions were acetylated to enhance their solubility in THF for GPC analysis. The GPC results can be seen in Fig. 46 where the average molecular weight and polydispersity index are plotted as a function of fraction number. Figure 46 shows a clear trend of increasing number average molecular weight and polydispersity with increasing fraction number, with the undissolved KPL (fraction 5) possessing a relatively high M_N and PDI. Fractions 1–3 possess molecular weights and PDIs that are sought for the use of lignin in biobased composite materials, most especially, fractions 1 and 2. Unfortunately, these fractions totaled less than 1 g of the starting material. However, fraction 3, the methanol fraction, is of considerable yield and possesses a molecular weight and PDI that are potentially workable.

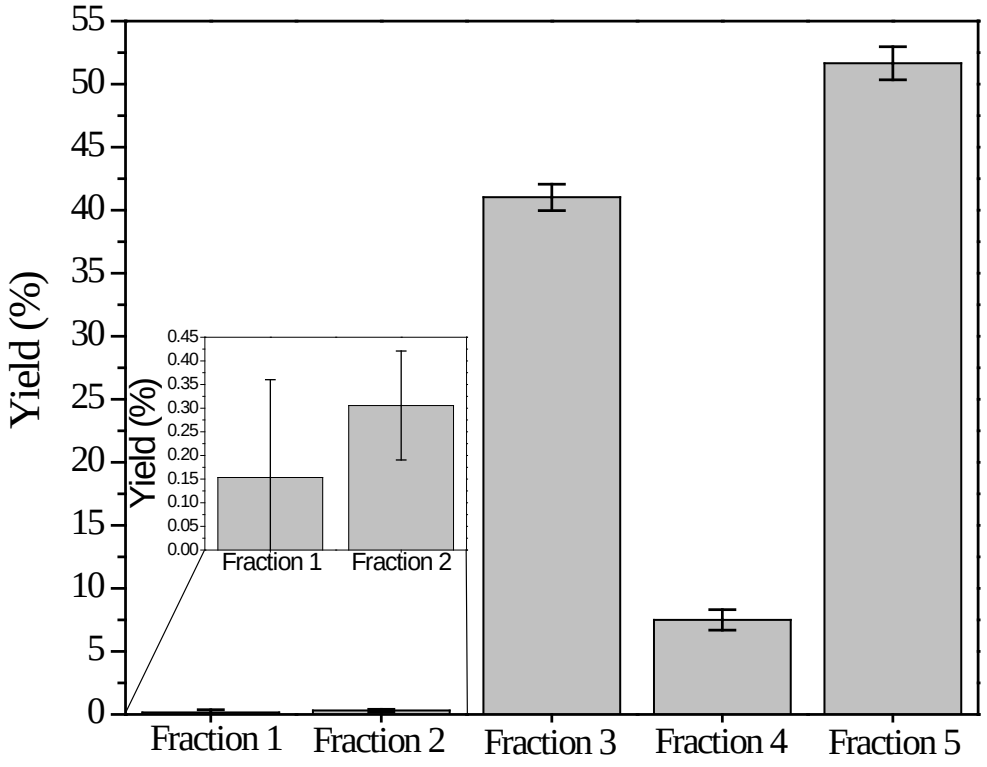

Fig. 45 KPL yields as a function of solvent fraction

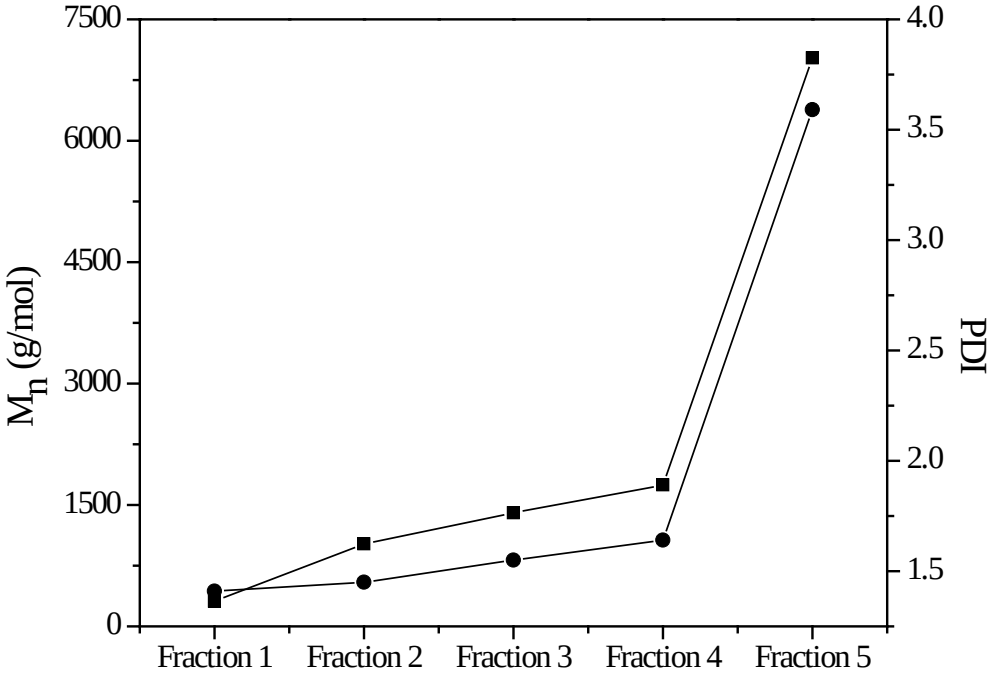

Fig. 46 Number of average molecular weights (M_n) and PDI of acetylated KPL that was fractionated into 5 fractions

4.2.3 Singlet Oxygen Mediated Decomposition of KPL

After each singlet oxygen mediated degradation reaction, the collected, potentially degraded, solid KPL contained a maroon color indicative of the presence of Rose Bengal. Upon acetylation and subsequent work-up, the maroon color vanished with collected acetylated KPL part exhibiting brown hues. Based primarily on quantitative yields of aceylated degraded products (Fig. 47), the KPL was not significantly degraded into smaller molecular weight products. This degradation technique was successful when a considerable amount of β-aryl ether bonds exist in the lignin. The results from this study suggest that KPL is not appreciatively degraded via singlet oxygen. The results are also a testimony to the Kraft delignification process success administered by MeadWestVaco since the Kraft pulping process primarily attacks α-aryl and β-aryl ether bonds to aid in separating lignin from cellulose and hemicelluloses. This study was no longer pursued as a result of these disappointing results.

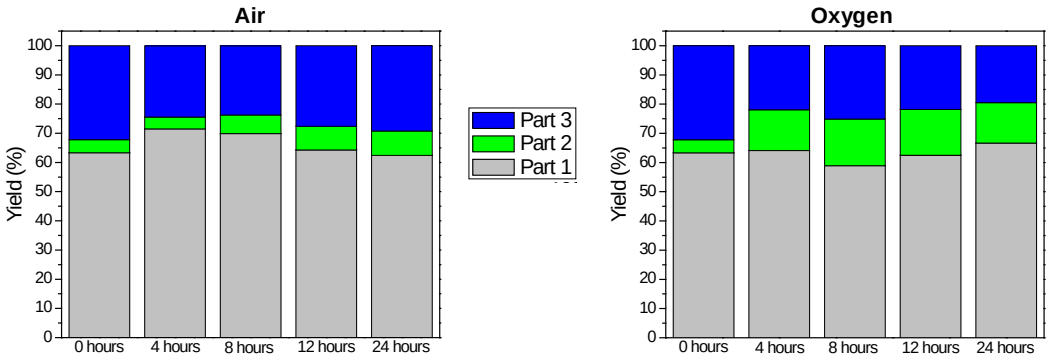

Fig. 47 Yields (*y*-axis) of high-molecular-weight solid (Part 1), medium-molecular-weight solid (Part 2), and low-molecular-weight liquid (Part 3) of acetylated KPL that was potentially degraded via a singlet oxygen mediated degradation in air (left) or O_2 (right) for desired reaction times (*x*-axis)

4.2.4 Acetylation of SKL and Soda Lignin

To modify SKL into a fusible material, acetylation was performed by reacting SKL with acetic anhydride to convert the highly reactive hydroxyl group into an acetyl group. FTIR spectra in Fig. 48 showed a broad band between 3,300 and 3,500 cm^{-1} attributed to the hydroxyl groups in phenolic and aliphatic structures before acetylation. After acetylation, the OH group absorption band decreased significantly, as shown in Fig. 10b, for procedure 1. Also, a strong peak around 1,750 cm^{-1} appeared due to C=O stretching of acetyl group. Note, similar results were found for acetylation of soda lignin and methacrylation of lignin.

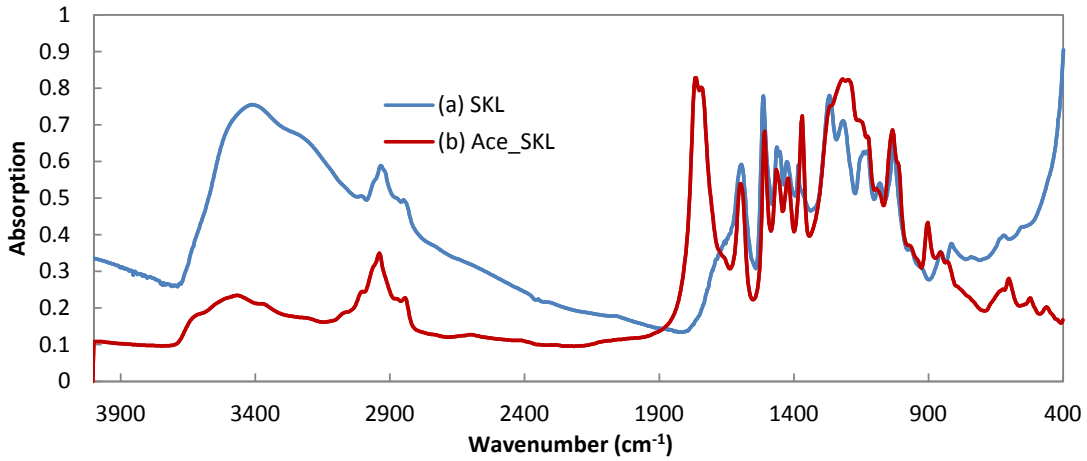

Fig. 48 FTIR spectra of (a) as-received SKL and (b) Ace-SKL

Figure 49 shows the effect of reduced concentrations of acetic anhydride used to produce Ace-SKL. All of the FTIR spectra were normalized with peaks at 856 cm^{-1} (C-H bending on benzene rings). The absorption of the hydroxyl group increased as the amount of acetic anhydride per gram of SKL decreased. A higher content of the hydroxyl group is favorable for thermostabilization but not amenable to melt spinning.

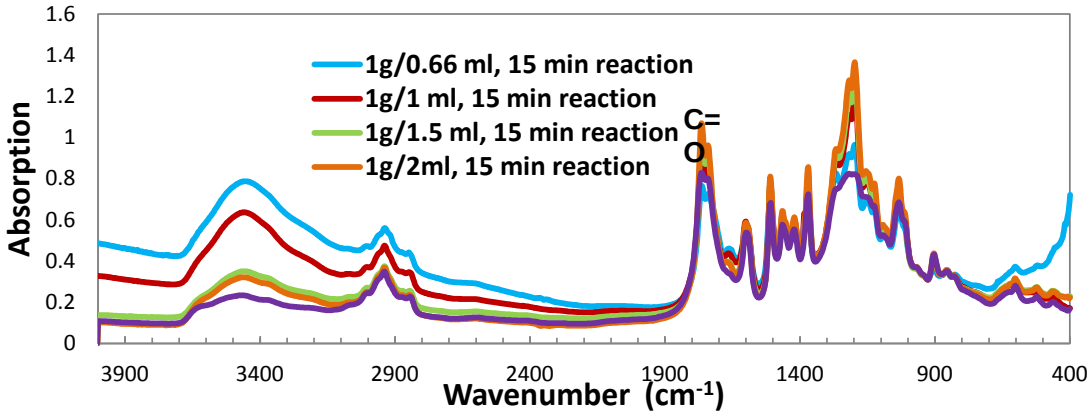

Fig. 49 FTIR spectra of Ace-SKL as a function of the amount of acetic anhydride used

4.2.5 Conclusions

This work shows that there are chemical methods to both effectively fractionate and modify lignin. These modifications can reduce the molecular weight of the lignin, enabling the production of resins or melt-spinnable lignin polymer for fiber production. In particular, metathesis, methacrylation of lignin, and solvent fractionation have effectively improved the processability of lignin for these applications. On the other hand, singlet oxygen decomposition of lignin has not aided in lignin processability and will likely be abandoned in this work.

Future work will focus on improving the metathesis of lignin and using combinations of fractionation, metathesis, and methacrylation to obtain optimum products for resin and carbon fiber production.

Various other lignin chemical decompositions are discussed in the PhD dissertation of Joseph Stanzione.[90]

4.3 Development of Lignin-Based Carbon Fibers*

4.3.1 Introduction

High-strength carbon fibers used in structural composite applications are almost exclusively derived from wet spinning of PAN precursor fibers.[11,12] This wet-spinning process suffers from 2 inherent limitations:

- Chemical conversion of PAN into carbon proceeds via generation of HCN and other toxic gases during the thermal stabilization and carbonization steps.
- Wet-spinning process necessitates use of hazardous solvents.

Therefore, additional studies are needed to investigate the replacement of PAN by an environmentally sustainable precursor such as lignin, which is an abundant biorenewable hydrocarbon source.[13–15] Numerous hydrocarbons can be converted to carbon, but very few have been actually converted to structural carbon fibers. Besides PAN, MP and rayon are the only other precursors that have produced carbon fibers. MP produces highly graphitic carbon fibers with high modulus and high thermal conductivity, but low strength. Rayon, on the other hand, uses naturally occurring cellulose, but its conversion to carbon is mechanistically limited to carbon fibers with poor strength and low thermal conductivity. Therefore, rayon-based carbon fibers cannot be used in primary reinforcement applications.

Among biobased alternatives, the aromatic encrusting material around cellulosic wood fibers is lignin, which confers rigidity and strength to wood. Lignin is abundantly available: over 3×10^{11} tons of lignin exist in the biosphere with approximately 2×10^{10} tons generated annually.[25] Because of the aromatic nature of the compound, lignin may be used to generate a valuable source of aromatic precursors for processing into carbon fibers. However, because of its 3-D aromatic structure, lignin is intractable in its unmodified state and must be suitably modified into components or products that can be converted into fibers.

*Portions of this section were originally published in La Scala et al. Biobased carbon fibers and high-performance thermosetting resins for use in U.S. Department of Defense applications. Aberdeen Proving Ground (MD): Army Research Laboratory (US); 2012 June. Report No.: ARL-SR-245.

The processes involved in modifying lignin can be broadly identified as chemical and microbial. In general, chemical processes are typically not very selective in terms of the reaction products but may be accomplished at commercially viable (fast) reaction rates by adjusting reaction conditions and catalysts. In contrast, microbial mechanisms produce better selectivity, but such biological reactions may proceed at slow rates. Therefore, the project was designed to simultaneously investigate both chemical and biological mechanisms for obtaining suitable precursors to ultimately produce structural carbon fibers.

4.3.2 Literature Review

Since the 1960s, lignin has been studied as a precursor for carbon fiber. In 1969, Otani patented a lignin-based carbon fiber produced by dry spinning from an alkaline solution of lignin with polyvinyl alcohol added as a plasticizer.[91] More recently, researchers have focused on producing carbon fiber from different types of lignin by melt-spinning. Sudo and Shimizu[92] modified a steam-exploded birch wood lignin by hydrogenolysis and followed up with extraction. Uraki et al.[93] converted a lignin obtained from aqueous acetic acid pulping of hardwood into carbon fiber. The acetic acid pulping process partially acetylated the hydroxyl groups in the material and prevented condensation between hydroxyl groups. The resulting organosolv lignin has good melt-spinnability. Kubo et al.[94] applied atmospheric acetic acid pulping on softwood and removed a large molecular weight fraction from it by fractionation with aqueous acetic acid to obtain a fusible material for melt spinning. Kadla et al.[95] produced carbon fiber directly from hardwood Kraft lignin and Alcell organosolv lignin. Poly(ethylene oxide) was also added into hardwood Kraft lignin to increase its processability. Indulin AT SKL from MeadWestvaco was studied as well, but it was not able to be melt spun since it had a highly cross-linked structure and low thermal mobility. ORNL researchers studied a series of lignin from different sources as carbon fiber precursors. They found that a hardwood Kraft lignin from MeadWestvaco was melt-spinnable.[96] They also showed that SKL cannot be melt-spun without proper modification or plasticization. A SKL from Kruger Wayagamack (Quebec, Canada) was successfully melt spun by adding a certain percent of hardwood Kraft lignin as plasticizer, and this SKL had a softening point of 190 °C.[97]

Eckert and Abdullah patented a SKL-derived carbon fiber by acetylation of the hydroxyl group with acetic anhydride.[98] A SKL modified with or without catalyst resulted in 16%–22% acetyl content by weight and became fusible. In their example, a relatively small batch of acetylated lignin (200 mg) was subject to melt-spinning.

Table 7 is a summary of tensile properties of carbon fibers obtained from different precursors from these studies. However, all the listed lignin-derived carbon fibers have relatively poor mechanical properties compared with pitch- or PAN-based carbon fiber.

Table 7 A summary of tensile properties of carbon fibers obtained from different precursors in prior studies

Precursor Type	Diameter (μm)	Elongation (%)	Modulus (GPa)	Tensile strength (MPa)	Electrical resistivity (μΩ·m)	Reference
Steam exploded hardwood	7.6 ± 2.7	1.63 ± 0.19	40.7 ± 6.3	660 ± 230	NA	Sudo et al. 1992[92]
Organosolv hardwood	14–35	0.64–1.12	2.17–39.1	13.3–355	NA	Uraki et al. 1995[93]
Organosolv softwood	84 ± 15	0.74 ± 0.14	3.59 ± 0.43	26.4 ± 3.1	NA	Kubo et al. 1998[94]
Kraft hardwood	46 ± 8	1.12 ± 0.22	40 ± 11	422 ± 80	NA	Kadla et al. 2002[95]
Kraft softwood, acetylated	5–100	NA	NA	NA	NA	Eckert and Abdullah 2008[98]
Rayon-based carbon fiber	5–25	…	172–690	117–3,950	…	Various
PAN-based carbon fiber	5–15	2	100–500	3,000–7,000	…	Various
MP–based carbon fiber	5–15	0.6	200–800	1,000–3,000	1–15	Various

NA = not available

The majority of these studies attempted to obtain low-cost carbon fibers, so performance was not necessarily emphasized. However, in the present study, we plan to investigate strategies to enhance the mechanical performance since the ultimate objective is to obtain structural carbon fibers.

These studies also establish that spinning lignin precursor into thin fibers remains a technical barrier. Consequently, properties of the resulting carbon fibers from such lignin precursors have been rather low. Therefore, the goal of this research project is to produce carbon fiber from lignin precursors such as Indulin AT SKL with enhanced properties such as those suitable for structural composites. The specific research objectives for this component of the project are as follows:

- Chemical modification of lignin to enable fiber spinning
- UV-thermal dual mechanism cross-linking/stabilization
- High-temperature thermal treatment

- Characterization of carbon fiber properties

4.3.3 Unmodified Lignin

As-received SKL showed no softening behavior during the entire heating procedure even when the temperature reached up to 300 °C (Fig. 50). The ball did not fall into the cup. Instead, degradation was observed, and the residue after heating was a foamed state, indicating the generation of volatiles during heating. These results are in agreement with those reported in previous literature studies in which softwood lignin has been shown to possess lower thermal mobility because it has a higher cross-linked structure than does hardwood lignin. The high content of hydroxyl groups results in dehydration reaction between molecules; thus, SKL cannot be melt-spun without appropriate modification.

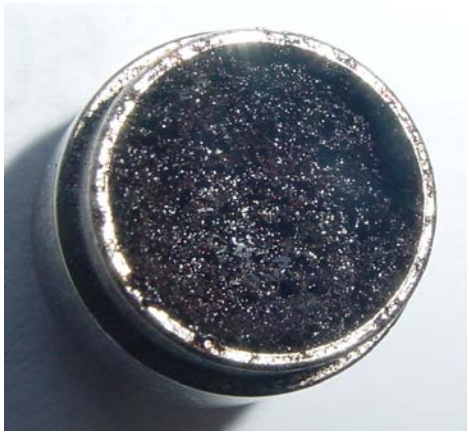

Fig. 50 Unmelted, foamy residue resulting from softening point test of pure SKL (ball removed)

The ash content of unmodified SKL and Protobind was measured as shown in Table 8. A target ash content to make high-performing carbon fibers is less than 0.1 wt%.[15] Indulin AT SKL has a higher ash content at 2.85%, and sulfur and sodium were the primary impurities in SKL. Protobind also has a high ash content at 1.66% with, again, sulfur and sodium as the largest concentration of impurities.

Table 8 Metal analysis and ash content of Indulin AT SKL and Protobind 1000 soda lignin

Sample	K (%)	Ca (%)	Mg (%)	S (%)	Na (%)	Al (%)	Ash (%)
Indulin AT	0.1032	0.0154	0.0167	1.1371	0.7057	0.0142	2.85 ± 0.04
Protobind 1000	0.2094	0.0193	0.0086	1.2303	0.2832	0.005	1.66 ± 0.03

4.3.4 Purification of SKL

To reduce the ash content in lignin, different washing methods were used (Table 9). SKL was washed in boiling water first. The filtered solution was brown because a certain amount of SKL was dissolved in boiled water, which resulted in a yield of 61 wt%. The solubility of SKL in room temperature DI water was lower but also resulted in a higher ash content. Washing with acidified water (using hydrochloric acid [HCl]) with a pH of 2 at room temperature is the most typical method in literature to purify Kraft lignin. When SKL was washed repeatedly up to 28 times, the ash content was reduced to 0.19%. In future studies, boiled water and acidified water will be combined to reduce labor and the amount of water consumed. It was assumed that washing with boiled water could lead to a larger average molecular weight, since small molecular weight fractions will be dissolved in the boiled water together with salts.

Table 9 Washing purification of SKL

Washing liquid	Ash content (%)	Yield (%)
Boiled DI water, 1 time	0.72	61
Room-temperature DI water, 1 time	1.42	85
Acidified water, 5 times	0.75	90
Acidified water, 11 times	0.30	64
Acidified water, 17 times	0.20	Not weighed
Acidified water, 28 times	0.19	62

The ash content of carbon precursors can play a significant role in creating defects, which can lead to weakening of the resulting carbon fibers. To optimize the purification conditions, different combinations of mixing time, liquid-to-solid ratio, and washing solution pH value were studied to find a suitable protocol for washing. SKL was washed once with acidified DI water under different conditions, and ash contents thus obtained are listed in Table 10. The results indicate that a larger liquid-to-solid ratio, pH value of 2, and mixing time of 15 min are favorable to efficiently reduce the ash content. It was also found that using 10 mL of acidified DI water (pH = 2) per gram of SKL and 15 min of mixing time for each wash resulted in ash content of around 0.15% after 20 washes. After 10 more washes, there was no substantial reduction of ash content. Finally, 10 mL of acidified DI water (pH = 2) per gram of SKL, 15 min of mixing time, and 25 washing cycles were established as standard protocol for each batch of SKL purification. After washing under these conditions, the ash content was reduced to 0.15%. A comparison of the main metal impurities is listed in Table 11.

Table 10 Ash content resulting after different washing conditions

Milliliters liquid/gram of SKL	pH	Mixing time (min)	Ash (%)
5	2	30	1.73
12.5	2	30	1.56
30	2	30	1.29
60	2	30	1.09
30	2	3	1.59
30	2	15	1.30
30	2	30	1.29
30	1	30	1.33
30	2	30	1.29
30	4	30	1.98

Table 11 Elemental analysis result of SKL before and after wash

Sample	K	Ca	Mg	Fe	S	Na	Al	Si
	wt%	wt%	wt%	wt%	wt%	wt%	wt%	wt%
SKL	0.105	0.014	0.017	0.005	1.219	0.753	0.015	0.023
Washed SKL	0.003	0.008	0.012	0.004	0.684	0.007	0.014	0.018

The softening point of methanol-fractionated SKL was measured. The lignin displayed no softening point. Thus, the reduction in molecular weight, as demonstrated in Section 3, was not sufficient to enable flow of the lignin.

4.3.5 Carbon Fiber from Highly Acetylated SKL

To modify SKL into a fusible material, acetylation was performed. Highly acetylated SKL was prepared by reacting SKL with acetic anhydride as previously described.

4.3.5.1 Rheological Characterization of Modified Lignin Samples

The acetylated SKL showed a softening temperature between 156 and 167 °C (Fig. 51). To evaluate the melt viscosity of the acetylated sample, it was subjected to a shear rheology test at a shear rate of 1 s^{-1} at 170 °C, which is about 5 °C higher than its softening point. The viscosity of melted Ace-SKL increased from around 80 Pa·s to 8,000 Pa·s within 30 min, as shown in Fig. 52, and the test finally ended because the torque transducer was overloaded. Overall, Ace-SKL had an unstable melt viscosity, as the viscosity build with time was too fast.

Fig. 51 A consolidated melt resulting from softening point test on Ace-SKL (ball removed)

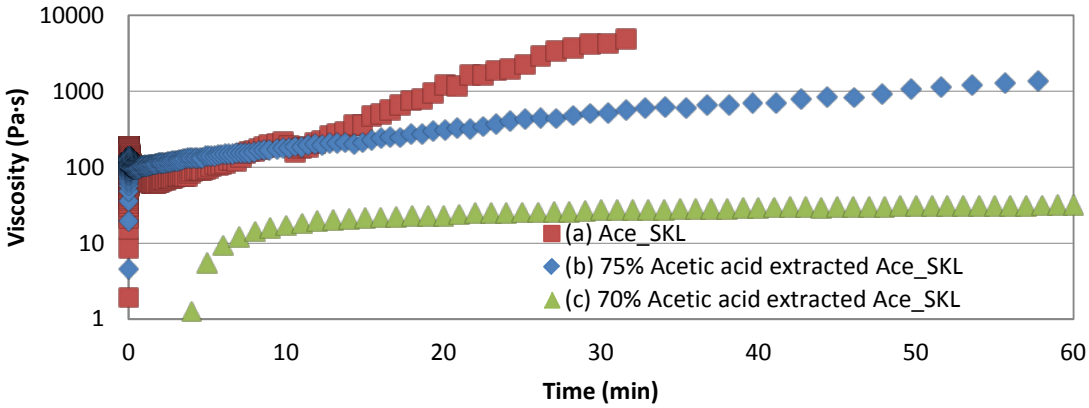

Fig. 52 Transient shear viscosity of Ace-SKL and acetic acid–extracted Ace-SKL

To obtain a material with relatively stable viscosity, Ace-SKL was extracted with 75% acetic acid, and a fraction with relatively large molecular weight was removed in this manner. The fraction soluble in 75% acetic acid had a softening point between 136 and 145 °C and was subject to a rheology test again, as shown in Fig. 52. The viscosity still increased gradually but remained below 100 Pa·s for the first 20 min, which would enable subsequent melt spinning.

Ace-SKL was extracted with 70% aqueous acetic acid first, and the soluble fraction had a softening point of 115–127 °C. When tested at 140 °C, it had a stable melt viscosity of about 70 Pa·s for 1 h (Fig. 52). However, this melt stability also indicates the very stable chemical structure of this composition, which will hinder the thermo-oxidative stabilization step. We then used 75% aqueous acetic acid to extract Ace-SKL.

4.3.5.2 Fiber Spinning and Thermo-Oxidative Stabilization

The Instron capillary rheometer was preheated to 145 °C (for 75% acetic acid extracted Ace-SKL), which was about 5 °C higher than the softening point for each batch of sample. When the temperature reached the target value, sample was loaded into the barrel. The plunger was fitted into the barrel, and the melt was extruded out of the capillary die. A take-up roll was positioned below to draw down the melt into fibers. The total heating time was controlled in this manner to prevent the formation of high-viscosity material before spinning. Both acetylated soda (Ace_Soda) and 75% acetic acid–extracted Ace-SKL were successfully spun into fiber. The lowest fiber diameter was 25 ± 4 μm for 75% acetic acid extracted Ace-SKL fiber, and 22 ± 3 μm for Ace_Soda fiber. Overall, excellent fibers were produced from Ace-SKL, as shown in Fig. 53. The fibers were 29.6 ± 1.6 μm in diameter and were spun continuously for 10 min before they began to break.

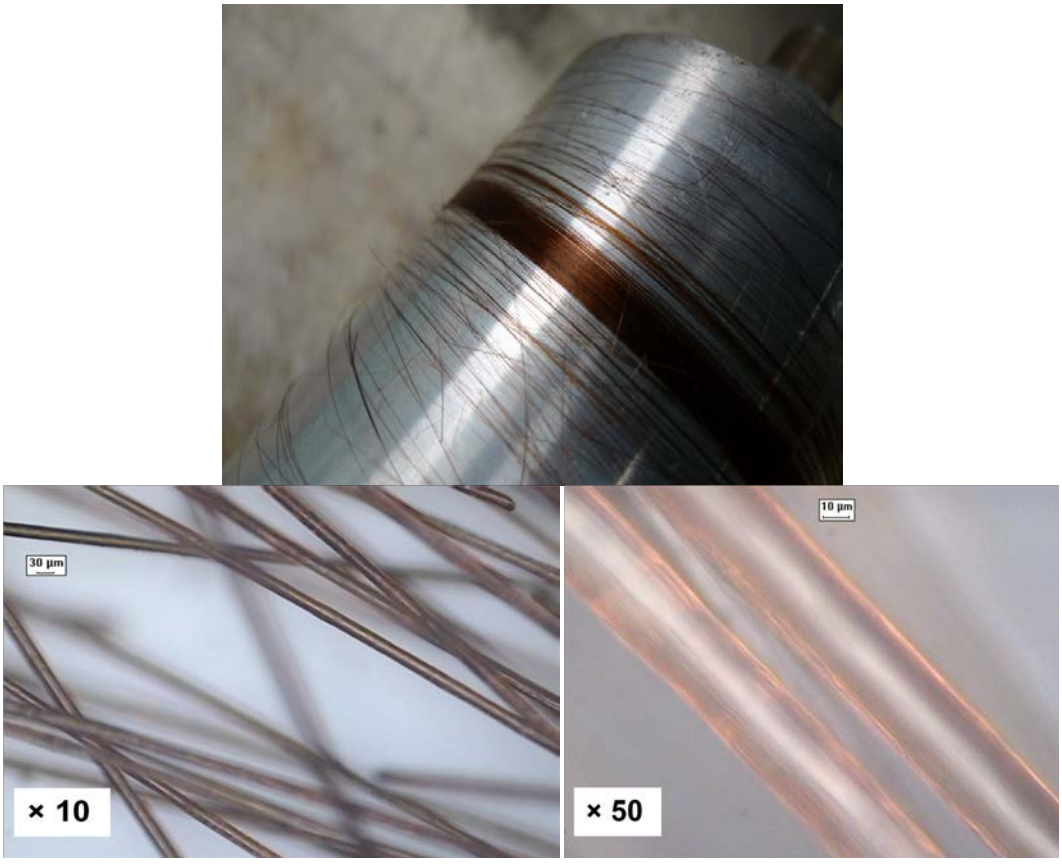

Fig. 53 75% acetic acid–extracted Ace-SKL as-spun fibers on spool (top) and magnified optical microscopy images (bottom)

Although the extracted Ace-SKL fiber was easy to melt-spin, it was virtually impossible to stabilize by thermo-oxidative stabilization. Substitution of hydroxyl groups by the stable acetyl groups prevented any cross-linking and thermal

stabilization of the macromolecules within the precursor fibers. Thus, although we did not attempt fiber formation and stabilization of 70% acetic acid–extracted Ace-SKL, we believe that the resulting material will suffer the same limitations. We emphasize that molecular cross-linking within precursor fibers is an essential step in transforming the fiber into a thermoset before it can be carbonized. Although we applied a ramp program with a heating rate as low as 0.01 °C/min, the fibers could not be maintained in their glassy state and became tacky at around 150 °C. Once the precursor becomes tacky, it is not possible to retain individual precursor fibers; this shows that the composition is not well suited for producing high-performance carbon fibers.

The treated fibers became tacky and stuck to each other, as shown in Fig. 54 (right), during the thermo-oxidative stabilization. Although 1–2 days of dwell time at 140 °C was applied, fibers still became tacky when the temperature was raised above 150 °C. The same situation occurred on Ace_Soda fibers. This indicated that incomplete surface stabilization occurred, and there was not enough reaction occurring at the surface. Thus, another method of surface stabilization of these fibers is needed; otherwise, these fibers will not produce high-performance carbon fibers.

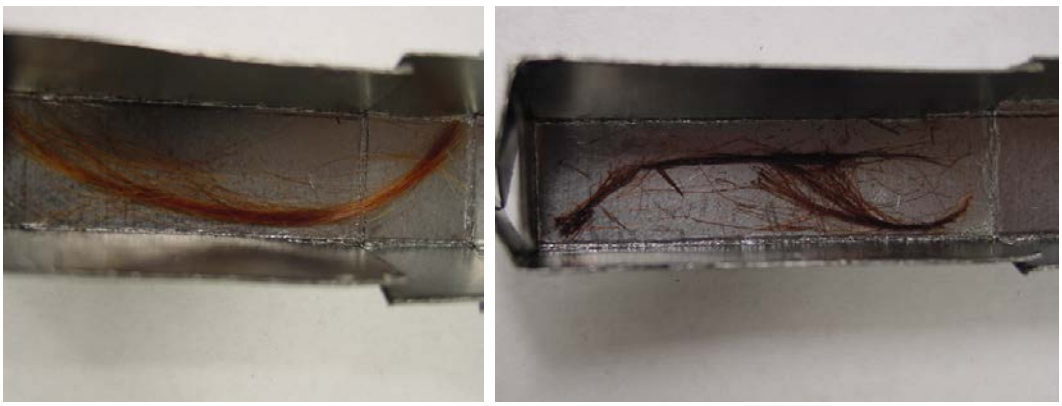

Fig. 54 As-spun Ace-SKL fibers (left) and tacky Ace-SKL fibers after heat treatment (right)

To help the thermostabilization of 75% acetic acid–extracted Ace-SKL fibers, the material was heated in a vacuum oven for different hours to increase its T_g/softening point before spinning (Fig. 55). However, fibers spun with a high softening point (SP) (~200 °C) material still could not be cross-linked.

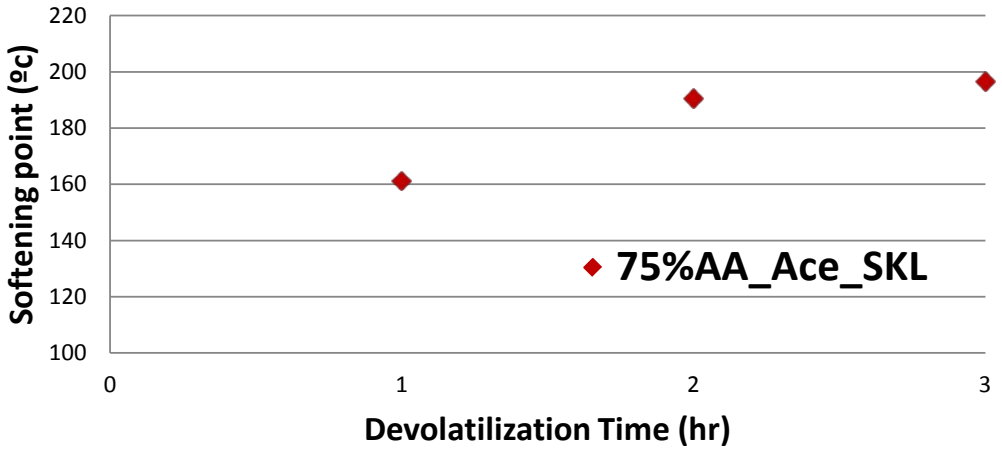

Fig. 55 Softening point of Ace-SKL with different devolatilization time

Although the extracted Ace-SKL fiber was easy to melt-spin, it was virtually impossible to stabilize it by thermo-oxidative stabilization. Substitution of hydroxyl groups by the stable acetyl groups prevented any cross-linking and thermal stabilization of the macromolecules within the precursor fibers. We emphasize that molecular cross-linking within precursor fibers is an essential step in transforming the fiber into a thermoset before it can be carbonized. Although a ramp program with a heating rate as low as 0.01 °C/min was applied, the fibers could not be maintained in their glassy state and became tacky at around 150 °C. Once the precursor becomes tacky, it is not possible to retain individual precursor fibers; this shows that the composition is not well suited for producing high-performance carbon fibers. Thus, reduced acetylation or methacrylation of SKL may be useful in making a thermostabilized carbon fiber. In addition, a different type of lignin may result in improved properties. All of these methodologies are discussed in the following sections.

4.3.6 Carbon Fibers from Soda Lignin

Soda lignin is produced in a distinctly different process than Kraft lignin, as illustrated in Fig. 56. As a result, soda lignin is expected to have a different molecular structure and functionalization that can lead to enhanced properties for melt-spinning and carbon fiber formation.

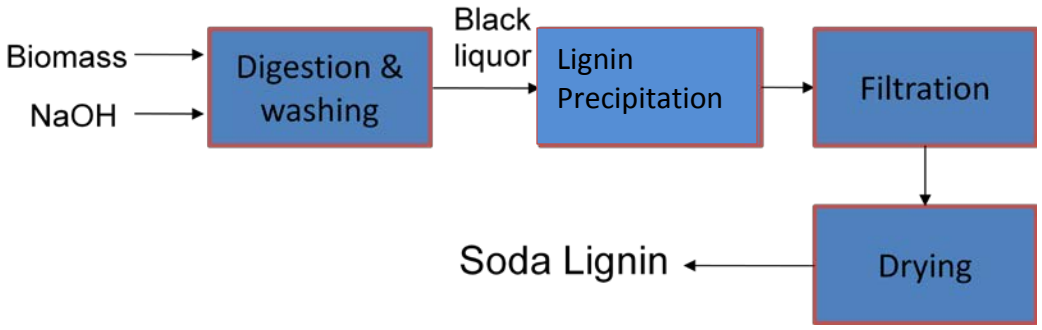

Fig. 56 Soda pulping precipitation process

The soda lignin Protobind 1000 showed a softening point of 245 °C. However, because of degradation, the residue was a foam (Fig. 57). According to a thermogravimetric analysis (TGA), it began to degrade at 200 °C (Fig. 58). Thus, melt spinning of soda lignin is unlikely to be successful because degradation will occur before and as the sample softens enough for spinning. As a result, it is necessary to decrease the softening point below 200 °C. Alternatively, solution spinning can be used to make lignin-based fibers.

Fig. 57 Foamed soda lignin after heating to 250 °C

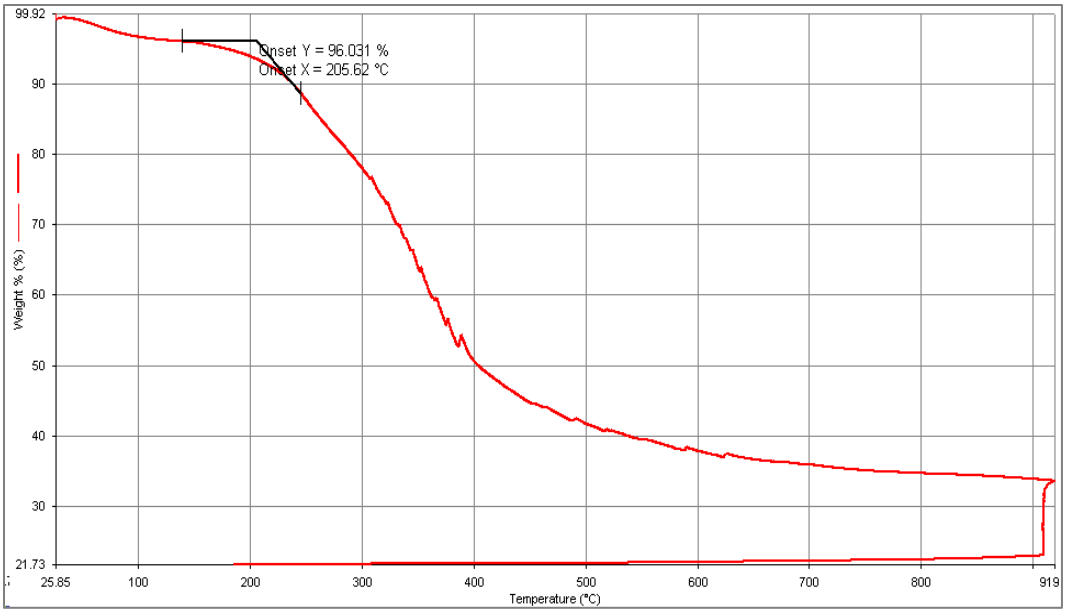

Fig. 58 TGA of soda lignin

Acetylation was carried out to enhance the flow characteristics of soda lignin as previously detailed. Unlike SKL, a fraction of soda lignin spontaneously precipitated from the reaction mixture after cooling. This fraction was regarded as a large molecular composition and removed. The recovered soluble fraction, referred to as Ace_Soda, had an softening point between 130 and 142 °C and a relatively stable melt viscosity when tested at 148 °C—again about 5 °C higher than the softening point (Fig. 59).

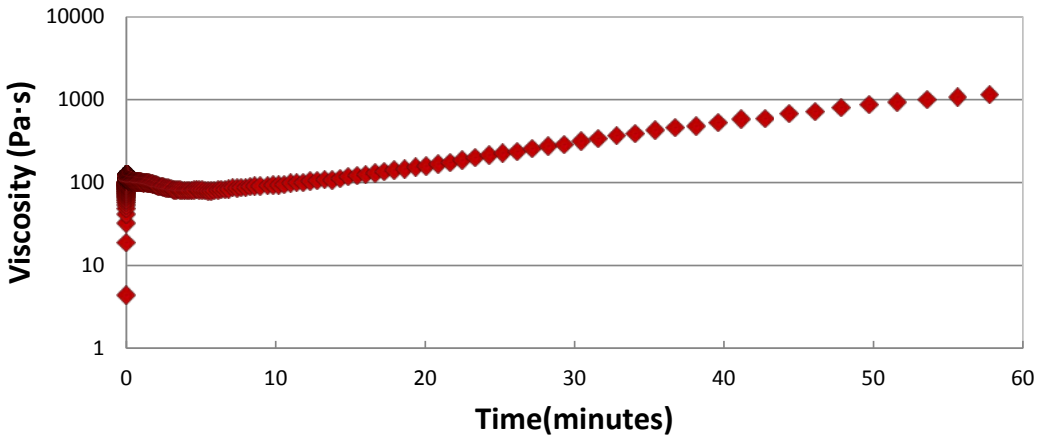

Fig. 59 Transient shear viscosity of Ace_Soda at 148 °C

The Ace_Soda was then melt-spun into fibers. The Instron capillary rheometer was preheated to 148 °C (i.e., about 5 °C higher than the softening point for each batch of sample). When the temperature reached the target value, the sample was loaded

into the barrel. The plunger was fitted into the barrel, and the melt was extruded out of the capillary die. A take-up roll was positioned below to draw down the melt into fibers. The take-up speed was 180 m/min and the spinneret diameter was 254 µm. The total heating time was controlled in this manner to prevent the formation of high-viscosity material before spinning. The resulting fibers were excellent, as shown in Fig. 60, and had a fiber diameter of 22 ± 3 µm.

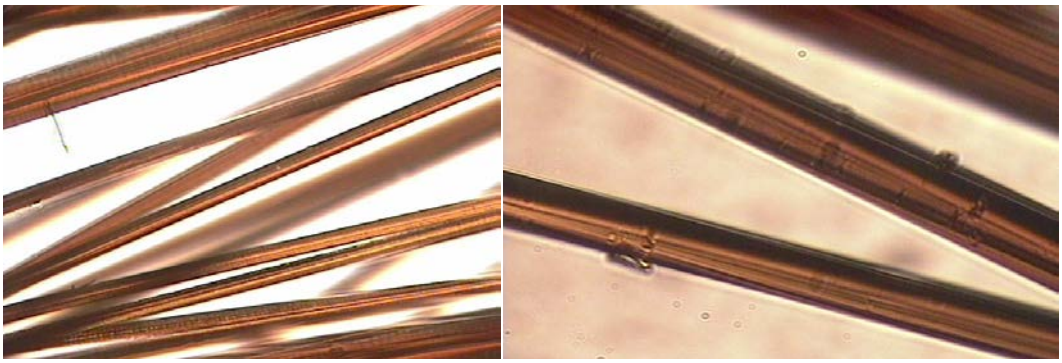

Fig. 60 Polymer fibers of Ace_Soda

These melt-spun Ace_Soda fibers were tacky during thermostabilization even with a heating rate as low as 0.01 °C/min. In retrospect, the stable melt viscosity (see Fig. 59) indicates that little cross-linking of the lignin can occur upon heating, likely as a result of too much acetylation and too little hydroxylation to have enough dehydration cross-linking. To help the thermostabilization, the material was heated in a vacuum oven for different durations to increase its T_g. Softening points of both types of lignin increased from approximately 130 °C to around 190 °C after 2.5 h of devolatilization in a vacuum oven at 160 °C (Fig. 61).

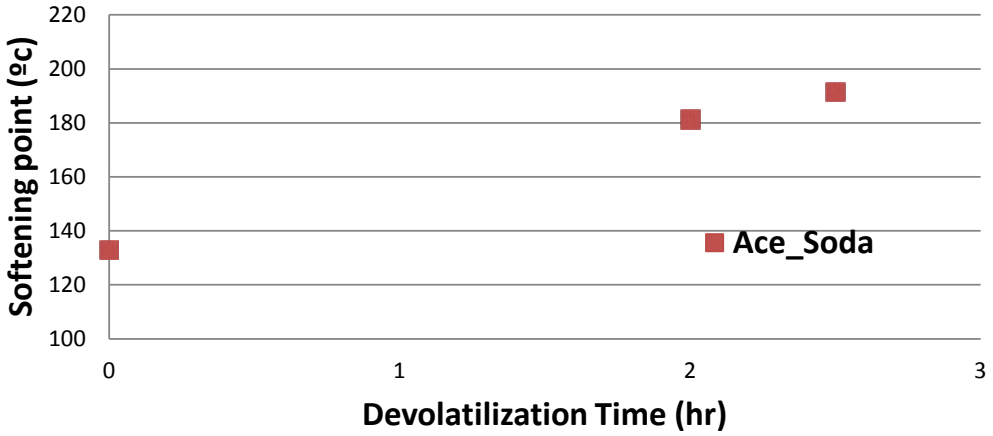

Fig. 61 Softening point change with devolatilization time for Ace_Soda

The viscosity curve of Ace_Soda after different time periods of devolatilization is shown in Fig. 62. The results indicate long periods with a constant viscosity, allowing for significant duration for processing, followed by a significant rise in viscosity, indicating increased thermostabilization with increased devolatilization time. However, fibers spun with the highest softening point (191 °C) material still could not be cross-linked. This is likely due to the lower concentration of alcohol groups on soda lignin, and thus less dehydration can occur.

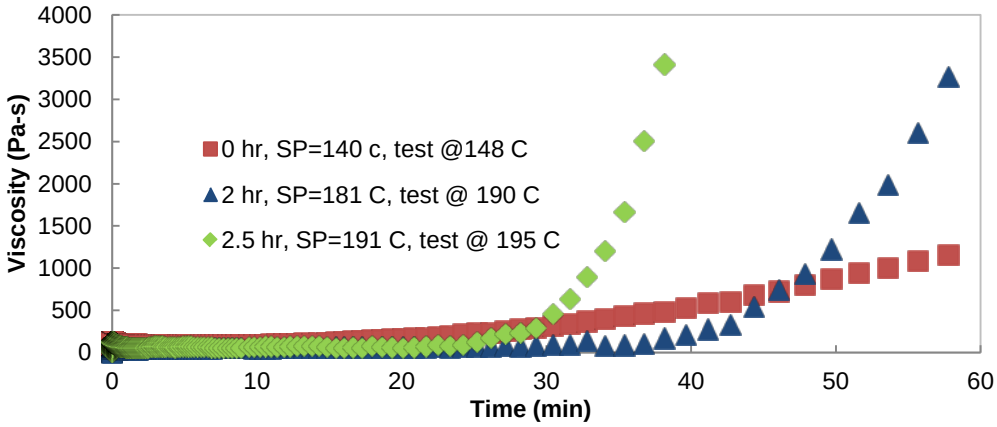

Fig. 62 Transient shear viscosity of Ace_Soda with 0, 2, and 2.5 h of heat treatment

Ace_Soda after heat treatment of 2.5 h and softening point of 190 °C was melt and spun into fibers. However, using the same slow thermostabilization program as Ace-SKL fibers, the Ace_Soda fibers still became tacky at around 145 °C. The main problem of Ace-SKL fiber and Ace_Soda fibers was the difficulty of cross-linking caused by acetylation.

Although the extracted Ace_Soda fiber was easy to melt spin, it was virtually impossible to stabilize by thermo-oxidative stabilization. Substitution of hydroxyl groups by the stable acetyl groups prevented any cross-linking and thermal stabilization of the macromolecules within the precursor fibers. We emphasize that molecular cross-linking within precursor fibers is an essential step in transforming the fiber into a thermoset before it can be carbonized. Although a ramp program with a heating rate as low as 0.01 °C/min was applied, the fibers could not be maintained in their glassy state and became tacky at around 150 °C. Once the precursor becomes tacky, it is not possible to retain individual precursor fibers; this shows that the composition is not well suited for producing high-performance carbon fibers. Thus, methacrylation or reduced acetylation could be used to improve the ability to melt-spin or solution spin these fibers and will be attempted in the future.

4.3.7 Carbon Fibers from ECN Lignin

An organosolv hardwood lignin was provided by Energy Research Centre, Netherlands (ECN lignin). The ECN lignin was derived from poplar with an ethanol-organosolv process (<0.1% ash content).

ECN lignin has a softening point of 155 °C. The transient shear viscosity of ECN lignin tested at 160 °C was shown in Fig. 63. The viscosity increased gradually as time proceeded, but after 1 h, shear viscosity was not higher than 200 Pa·s, which indicates that the material is more thermally stable compared with the lignin materials described in the previous subsections. The result of TGA indicated a decomposition temperature of ECN lignin at around 280 °C.

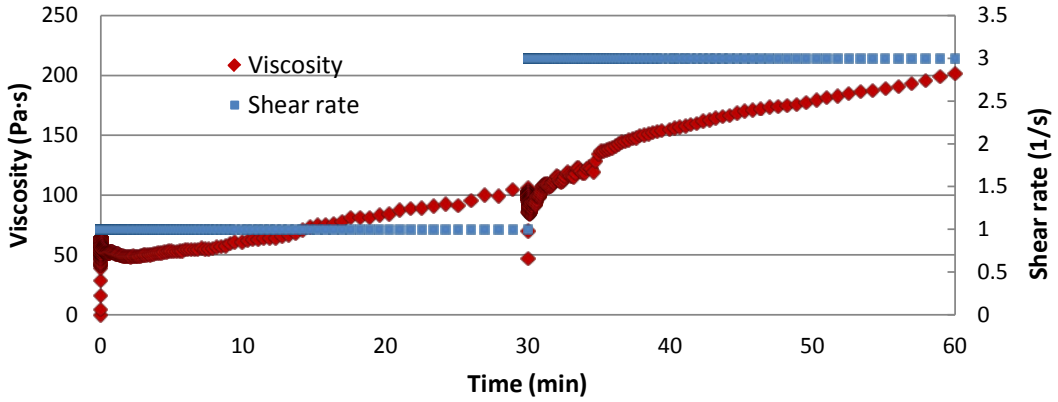

Fig. 63 Transient shear viscosity of ECN lignin at 1 and 3 s^{-1}, 160 °C

Spinning of ECN lignin was also performed on an Instron unit when heated at 160 °C with the winding rate as high as 190 m/min. Fiber was continuously spun on the roll for more than 2 min. The resulting fibers were uniform and defect-free with an average diameter of 29.3 ± 1.1 µm, as seen in Fig. 64.

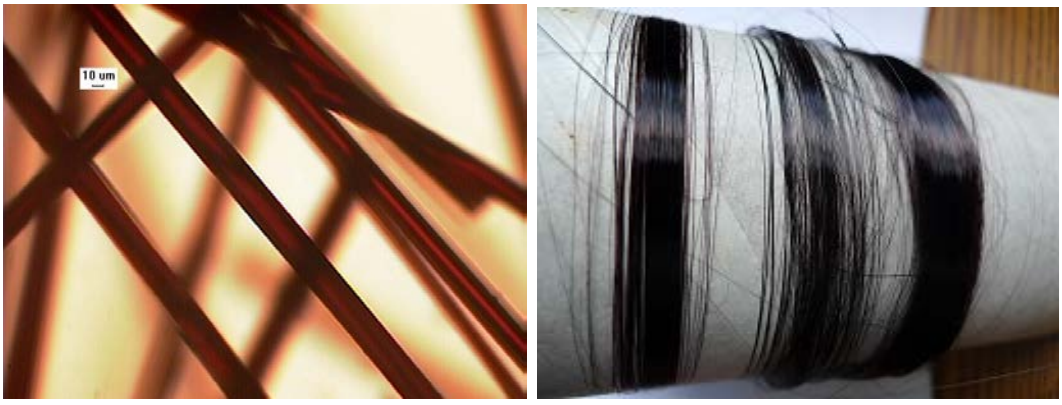

Fig. 64 ECN lignin fibers at magnification (left) and as seen on the take-up wheel (right)

The first stabilization trial was performed with a heating rate of 0.1 °C/min. Fiber became tacky at around 125 °C. The second stabilization trial was performed carefully with a relatively long procedure. The temperature versus time curve is shown in Fig. 65. The fiber survived during stabilization, and the final oxidation temperature was 240 °C. It takes more than 200 h (over 1 week) to stabilize to prevent fibers from being tacky, whereas most commercial processes require about 2 h. The slow oxidation rate was attributed to relatively low hydroxyl content in hardwood organosolv lignin.

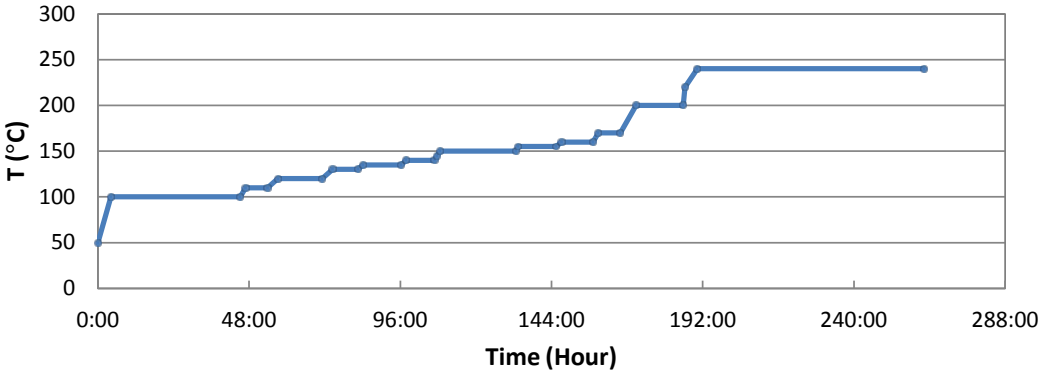

Fig. 65 Thermostabilization of ECN lignin fiber

The average fiber size after oxidation reduced to 23.5 ± 0.5 μm (Fig. 66). After stabilization, the ECN lignin fiber became infusible. The stabilized fibers did not dissolve in acetone, indicating their cross-linked structure after thermo-oxidation.

Fig. 66 Oxidized ECN fiber

The stabilized fibers were carbonized at 1,000 °C. The resulting carbon fibers were nominally 14 ± 1 μm in diameter, as shown in Fig. 67. The results show that the carbon fibers had smooth surfaces and circular cross sections, both of which are good attributes to maintain high mechanical properties. Single fibers were mounted on a paper tap and tested with a Phoenix tensile testing device following the ASTM

test method D-3379-5.[44] The carbonized ECN fibers displayed a tensile modulus, strength, and strain-to-failure values of 34 ± 4 GPa, 450 ± 130 MPa, and 1.4 ± 0.4%, respectively. The electrical resistivity of these fibers was 60 μΩ-m. These results are similar to that of rayon-based fibers. Although not ideal for structural applications, rayon is no longer made in the United States because of the hazards and environmental regulations in processing. Rayon-based carbon fibers are used in missile casings where lightweight and low-thermal conductivity is desired. (The ash content of ECN was not measured and could have played a role in the reduced properties.) Future studies will investigate improvement in properties resulting from reduced ash content of the precursor lignin.

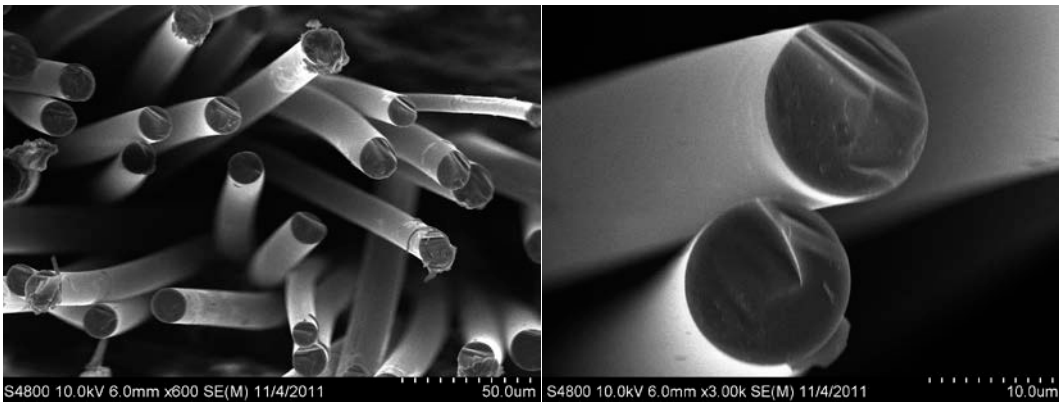

Fig. 67 SEM micrographs of carbonized ECN lignin

4.3.8 Carbon Fibers from Methacrylated SKL

Methacrylated lignin samples could not be melt-spun because of the reactivity of the methacrylate groups. These become unstable at temperatures as low as 90 °C, which is considerably lower than the measured softening points of all lignin samples so far and any expected sample. Thus, only solution spinning is possible when using methacrylated lignin.

Methacrylated SKL was prepared as discussed previously, where the Indulin AT lignin was fractionated using methanol extraction and then methacrylated using methacrylic anhydride. Unfortunately, these samples did not have a measureable softening point. To test the stabilization potential of their methacrylated SKL composition (ethyl ether undissolved fraction), films with thicknesses around 0.5 to 1 mm were made by dissolving the sample in acetone and evaporating the acetone (Fig. 68, left). Heating in an oxidation oven from 50 to 160 °C at 0.2 °C/min resulted in cross-linked material, as the film chips did not dissolve in acetone after heating (Fig. 68, right).

Fig. 68 Left: Film chips made from methacrylated SKL. Right: Film chips of methacrylated SKL tested with acetone.

To test the potential of UV-assisted cross-linking for this sample, we made films with 1% 4,4 bis(dimethylamino)-benzophenone added as a PI. The experimental set included 3 types of films/chips: film 1 had no PI, film 2 had 1% PI, and film 3 had no PI and was shielded by an aluminum sheet on top to block the UV (Fig. 69). The films were processed in a Nordson UV chamber that can deliver up to 5 kW. After 5 min of UV exposure, the films were tested with acetone. A control film without any PI and without UV treatment was also produced. Because of the limited amount of samples available, the acetone-dissolution test was conducted with only films. Partial solubility of films can be deduced by the color of solution generated. In Fig. 70, film 1 and film 2 solutions had a very light color, indicating that only a tiny amount of treated film sample dissolved in acetone. Film 3 underwent the same thermal history as films 1 and 2 but was not exposed to any UV dissolved in acetone, as shown by the yellow color of the resulting solution. Control film without any PI or UV exposure also dissolved easily in acetone. Further, the chips of films 1 and 2 were fairly rigid and kept their shape well when exposed to acetone, but film 3 and the control samples decomposed into small particles after shaking the flask. The acetone tests indicated that both methacrylated samples, with or without PI, were capable of polymerizing in the UV chamber. Since film 1 had no PI, it can be inferred that it self-polymerized when exposed to UV radiation.

Fig. 69 From left to right: film 1 had no PI, film 2 had 1% PI, and film 3 had no PI and was shielded by an aluminum sheet

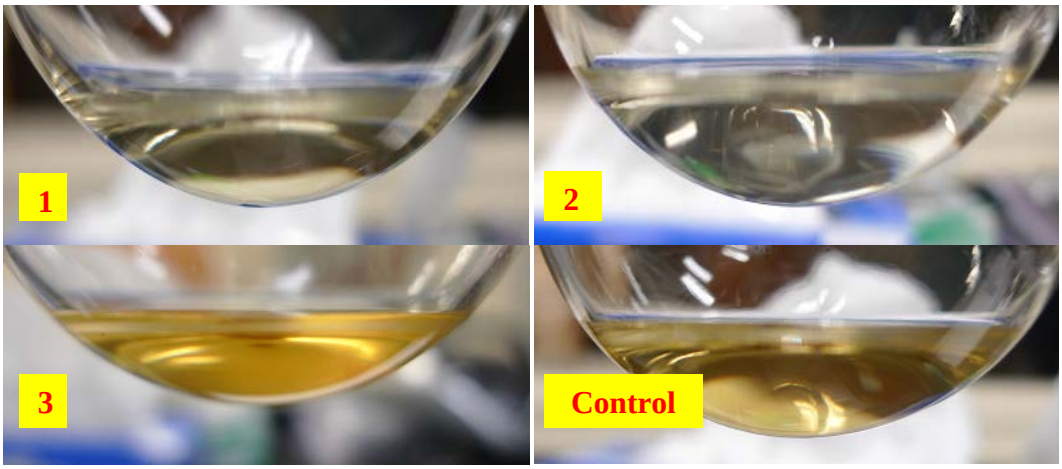

Fig. 70 Acetone tests of film chips after UV exposure

Although methacrylated SKL (ethyl ether undissolved fraction) could be dissolved in acetone, the concentrated solution did not have adequate elasticity to be stretched into filaments. In addition, methacrylated SKL displayed no softening point and thus could not be melt spun. Nonetheless, although 100% methacrylation of lignin is not useful for making fibers, partial methacrylation will enable UV stabilization of the fibers. Thus, partial methacrylation of acetylated SKL is assessed in the following section.

4.3.9 Methacrylated and Acetylated SKL

Methacrylated and acetylated SKL (MA_Ace _SKL) were prepared as discussed previously. Procedure 1 showed that 10 g/60 mL of MA_Ace_SKL can be fully

dissolved in acetone. The concentrated solution can be drawn into short filaments with uneven thicknesses (Fig. 71). The short filaments were soft and tacky during thermostabilization. Thus, this particular sample and procedure were not ideal for carbon fiber formation.

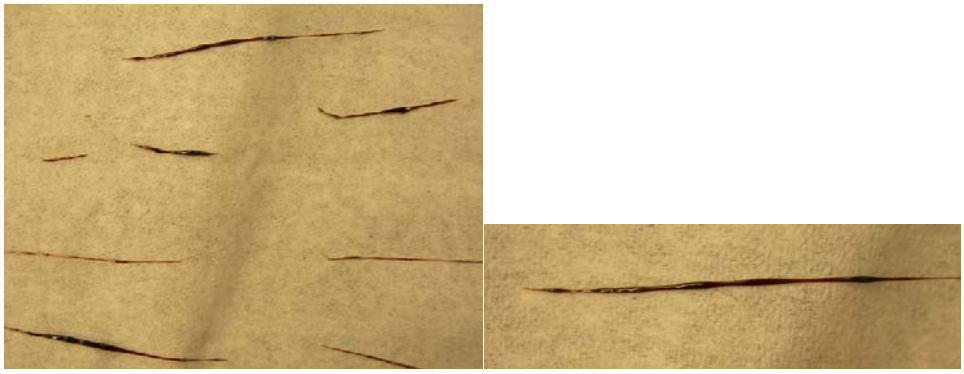

Fig. 71 MA_Ace_SKL (procedure 1) filaments

As previsouly described, 10 g of Ace-SKL + 25 mL of methacrylic anhydride + 0.5 mL of 1MIM was prepared and used to make fibers. The resulting product was still soft when separated from the evaporation dish. The material can be dissolved into acetone and drawn into long filaments (Fig. 72), but the filaments were tacky. The filaments were dried for about 12 h at room temperature. Filaments melted and were tacky after thermostabilization; such filaments are not suitable for carbon fiber formation.

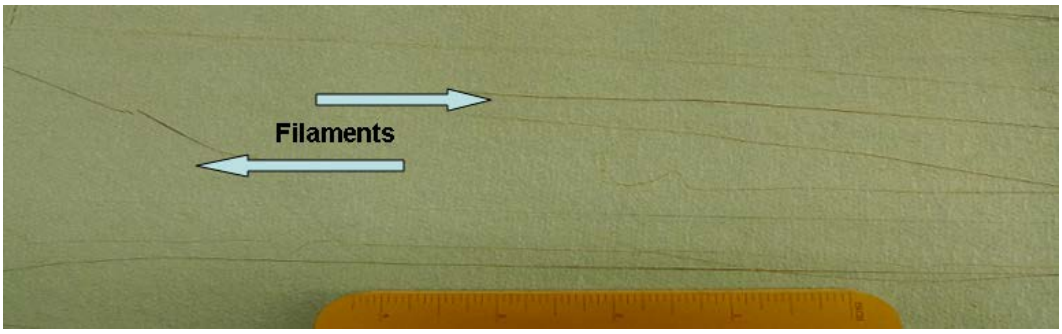

Fig. 72 MA_Ace_SKL (procedure 2) filaments

The 10 g/25 mL of MA_Ace_SKL was made into film chips to assess their ability to be UV stabilized (Fig. 73). After a 20-min UV (48–54 °C) treatment, some chips stuck to the surface of quartz or the aluminum sheet, indicating low T_g. UV-exposed film chips did not dissolve into acetone, but UV-blocked film chips dissolved. These results indicate that the MA groups are sensitive to UV stabilization and should help enable carbon fiber formation.

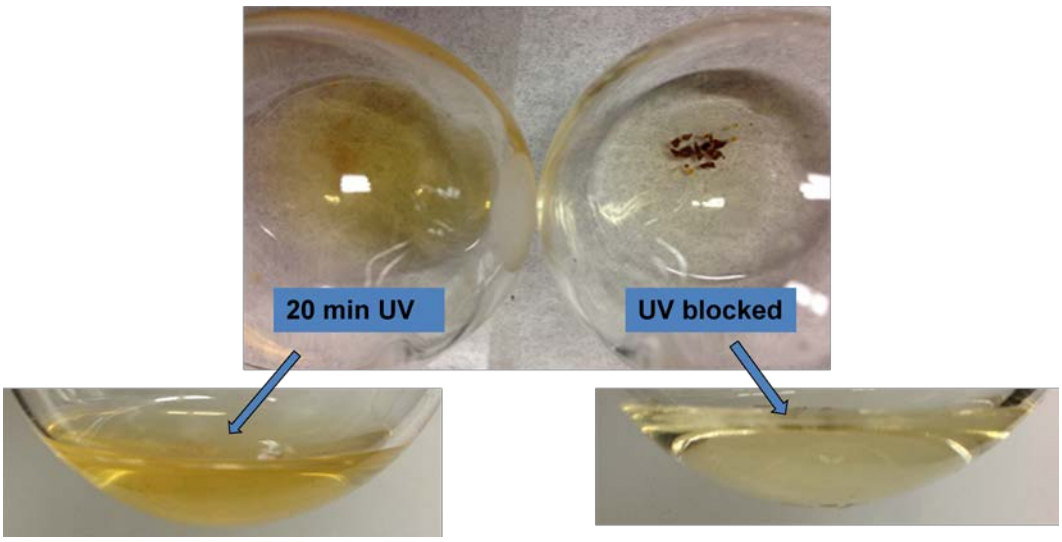

Fig. 73 Photographs indicating UV stabilization of 10 g/25 mL MA_Ace_SKL

As per procedure 3, 10 g/10 mL of MA_Ace_SKL was prepared and tested for UV stabilization (Fig. 74). As before, small pieces of the MA_Ace_SKL film were prepared. The film samples were either UV stabilized or not stabilized. The films samples were placed in a flask and acetone was added. The flask was shaken to help dissolve any sol components of the film. After 20 min, the UV-treated film partially dissolved and had a significant gel fraction, while the UV-blocked film fully dissolved in acetone (Fig. 75). Again, this indicates that UV stabilization can be an effective way to stabilize MA-modified lignin samples.

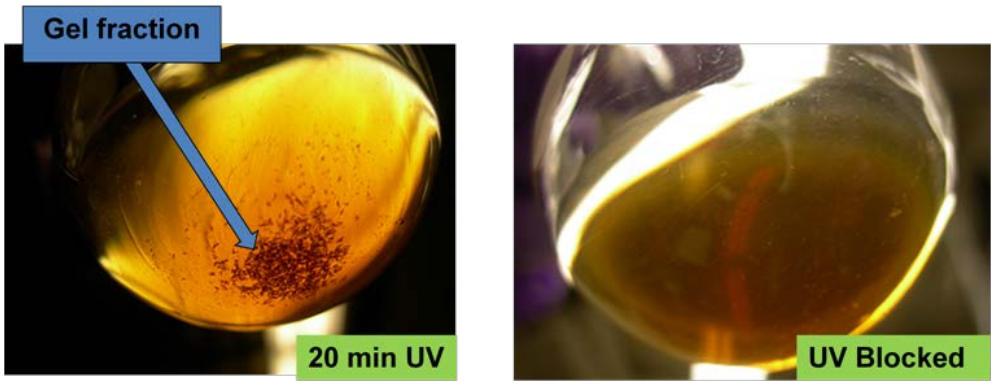

Fig. 74 Photographs indicating UV stabilization of 10 g/10 mL MA_Ace_SKL

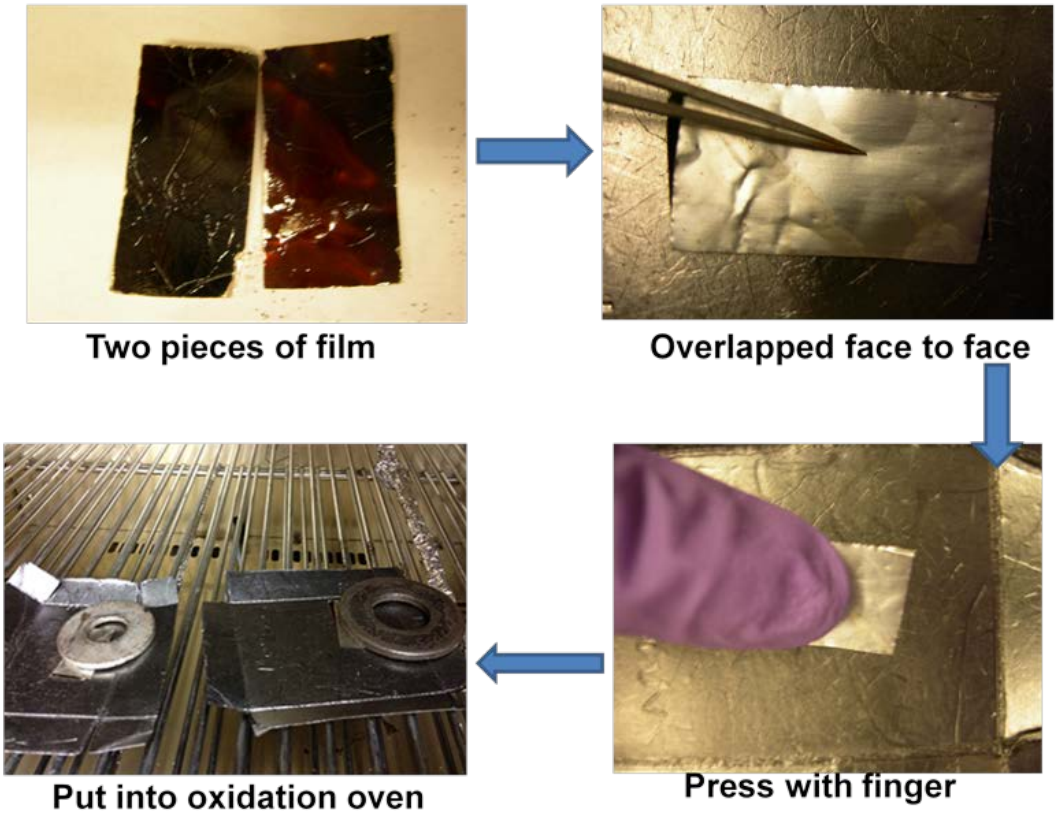

Fig. 75 Thermostabilization test on the UV-treated 10 g/10 mL MA_Ace_SKL

To further test the stabilization, 2 pieces of film were placed face-to-face and pressed together (Fig. 76). The samples were then placed in an oxidation oven and heated from 40 to 150 °C at 0.2 °C/min. Both pairs of films (UV 20 min and UV blocked) can be separated without sticking. Since we were able to separate the UV-blocked samples, we are not sure if the films were close enough. Thus, filaments were prepared with MA_Ace_SKL (10 g/10 mL) and placed into an oxidation oven (40 to 150 °C, 0.2 °C/min). The non-UV-stabilized samples had some tackiness to them.

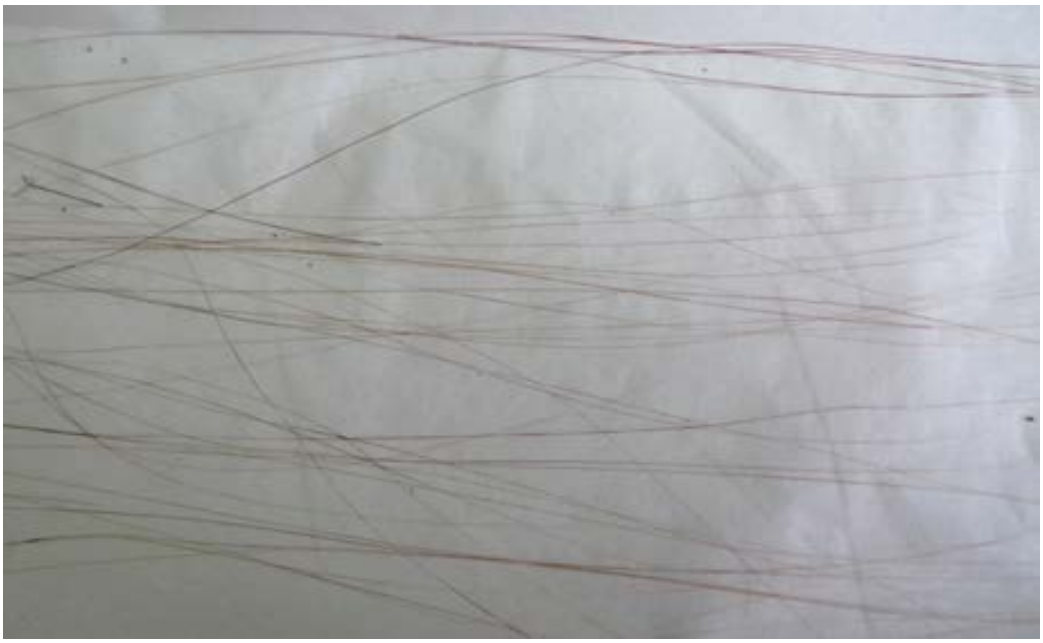

Fig. 76 Solution-spun Ace-SKL fibers

4.3.10 Carbon Fibers from Solution Spinning of Ace-SKL

4.3.10.1 Solution Spinning of Highly Acetylated Ace-SKL

The Ace-SKL from the reaction of 10 g of SKL with 150 mL of acetic anhydride can be fully dissolved in acetone and manually drawn into filaments with minimum diameters as small as 20 μm, indicating its solution-spinning potential. Filaments had a diameter range from 20 to 70 μm (Fig. 76). The filaments kept their shape at around 145 °C while being tacky.

4.3.10.2 Thermo-Oxidative Stabilization of Highly Acetylated Ace-SKL

Thermo-oxidation was attempted to stabilize the fibers. The following general heating procedure was used to thermo-oxidatively stabilize the fiber:

- Heating from 25 to 140 °C, with a heating rate of 0.1 °C/min
- Hold at 140 °C for 10 h
- Heating from 140 to 160 °C, with a heating rate of 0.05 °C/min
- Hold at 160 °C for 20 h

However, these filaments could not be thermo-oxidized even with the heating rate as low as 0.01 °C/min. The resulting filaments were still tacky (Fig. 77) after the process, indicating no ability to thermo-oxidatively stabilize due to the low amounts of hydroxyl groups remaining.

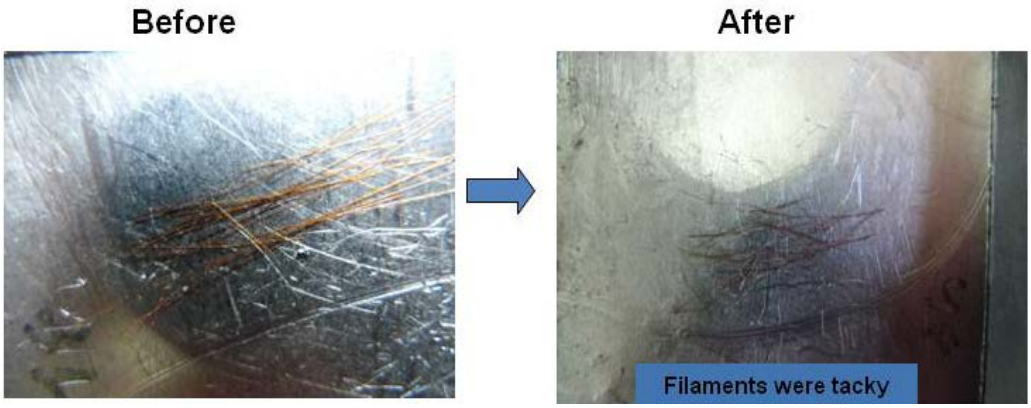

Fig. 77 Thermostabilization of Ace-SKL solution-spun fibers produced tacky filaments

4.3.10.3 Solution Spinning of Ace-SKL with Low Concentration of Acetate Groups

To reduce the degree of substitution, lower amounts of acetic anhydride were applied to preserve more hydroxyl groups in SKL as detailed in the alternative procedures. A higher content of hydroxyl groups is favorable for thermostabilization but is not amenable to melt-spinning.

Since acetic anhydride less than 0.6 mL/g SKL was difficult to mix completely with SKL dry powder, a reaction product of 0.66 mL acetic anhydride per gram SKL reacted for 15 min was chosen as a precursor for the following solution spinning.

Ace-SKL (0.66 mL of acetic anhydride per gram SKL) was predissolved in excess acetone to obtain a homogeneous solution, which was later evaporated. A high concentration of solution was critical for spinning, since proper viscosity and elasticity were needed for the extension of filaments, and fast evaporation of acetone was necessary to prevent the filaments from becoming sticky when winding onto the take-up unit (Fig. 78). We found that when the concentration was between 1.70 and 1.90 g/mL, continuous filaments could be manually drawn out of the viscous solution. The viscosity of a 1.75 g/mL solution was measured at 1,250 Pa·s.

Fig. 78 Photograph showing sticking of Ace-SKL to the roll surface due to insufficient evaporation of acetone

4.3.10.4 Modified Procedures to Solution Spin Lignin-Based Carbon Fibers

To reduce the degree of substitution, lower amounts of acetic anhydride were used to preserve more hydroxyl groups in SKL as detailed in the alternative procedures. A higher content of hydroxyl groups is favorable for thermostabilization but is not amenable to melt spinning. Dry spinning was used to process the fiber, which does not require a stable melt viscosity.

Since acetic anhydride less than 0.6 mL/g SKL was difficult to mix completely with SKL dry powder, a reaction product of 0.66-mL acetic anhydride per gram SKL react for 15 min was chosen as a precursor for the solution spinning. Ace-SKL (0.66 mL of acetic anhydride per gram SKL) was predissolved in excess acetone to obtain a homogeneous solution, which was later evaporated.

4.3.10.5 Rheology of Ace-SKL Solutions

To perform a successful dry spinning with Ace-SKL solutions, proper viscosity and elasticity were needed for the extension of filaments, and fast evaporation of acetone was necessary to prevent the filaments from becoming sticky when winding onto the take-up unit. Then the rheology of Ace-SKL spinning solution was studied.

To measure the solution viscosity at high shear rates, capillary rheology measurements were performed using different concentrations of Ace-SKL acetone solution at room temperature and 45 °C. A die with diameter of 1 mm and length/diameter of 10 was used, and the results are displayed in Fig. 79, which confirm that as the concentration of spinning solution increased, the viscosity increased. Also, increasing the temperature to 45 °C reduces the viscosity for easier processing.

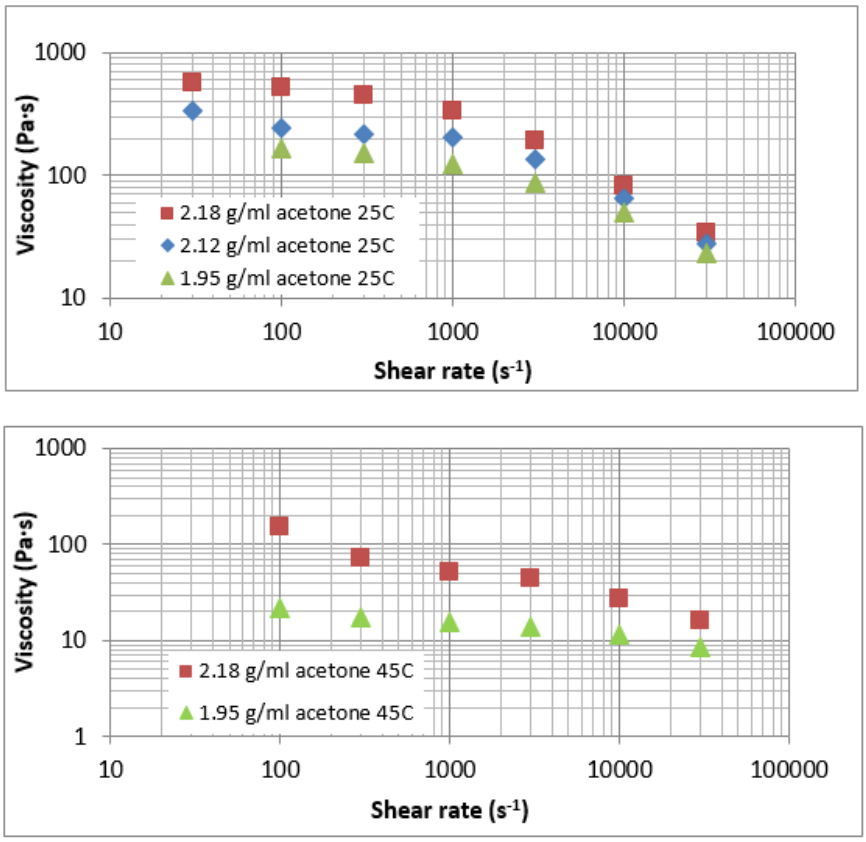

Fig. 79 Viscosity of different concentrations of Ace-SKL solutions at 25 and 45 °C

Ace-SKL solutions at 2.21, 2.08, and 1.93 g/mL acetone concentration were tested using cone and plate rheometer. A thin layer of Vaseline was applied to the outside edge of the sample between the cone and plate to prevent evaporation of acetone. Figure 80 shows that that a thin layer of Vaseline led to a negligible effect on the measured fluid viscosity.

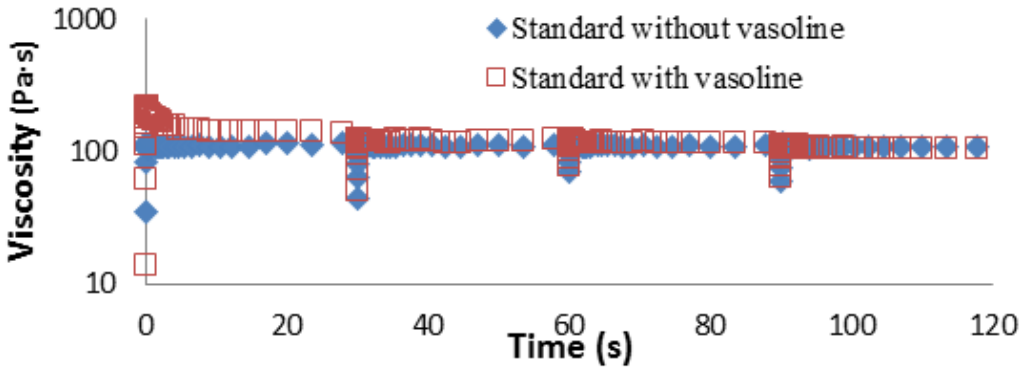

Fig. 80 Standard viscosity test run with and without Vaseline

Strain sweep under 20 rad/s was run for all 3 concentrations to find the linear regime, and 0.3% strain was set for frequency sweep. The G′ and G′ of the strain sweep and frequency sweep are plotted in Figs. 81 and 82, respectively.

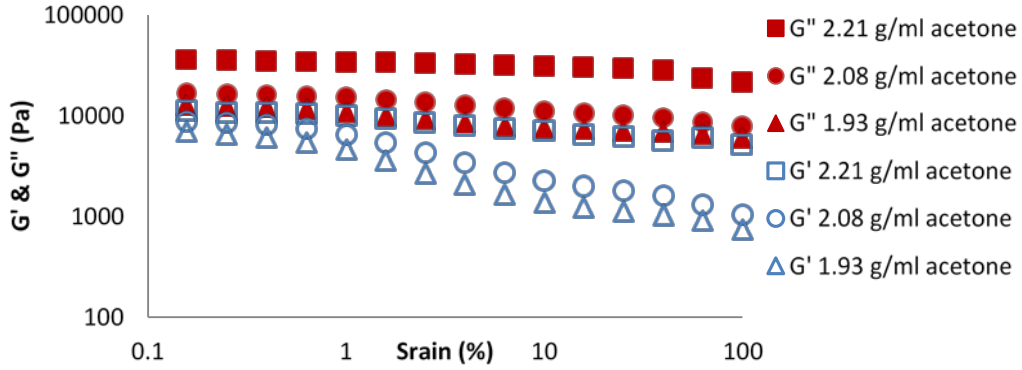

Fig. 81 Strain sweep of Ace-SKL/acetone solutions

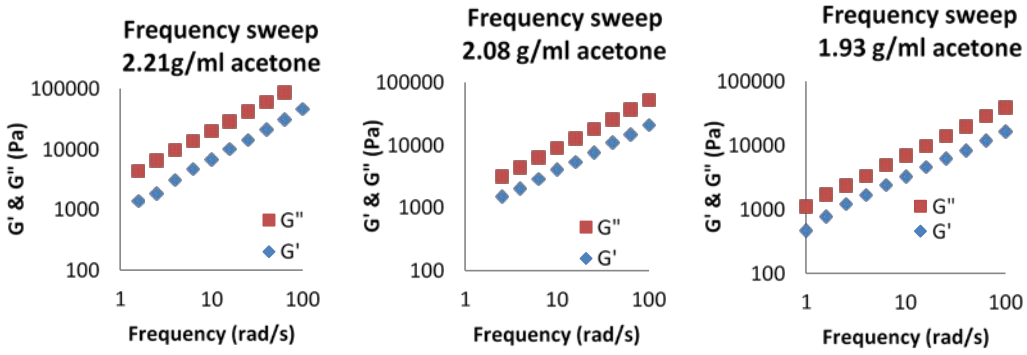

Fig. 82 Frequency sweep of Ace-SKL/acetone solutions

4.3.10.6 Ace-SKL-Derived Carbon Fibers from Dry Spinning

The first spinning trial used a solution with a concentration around 1.85 g/mL, without heating of the spinning barrel. Warm air in the spinning chamber assisted the evaporation of acetone in the filaments. The second trial had a solution concentration above 1.90 g/mL, and the spinning barrel was heated to 40 °C to increase the fluidity of solution. The drawdown was stable for take-up speeds up to about 50 m/min. The spinning temperature was 25 or 40 °C, and the spinneret diameter was 150 µm (8 holes). At higher speeds, the fibers broke during drawing down. Fibers obtained from the 2 different batches had average diameters ranging from 32 to 45 µm, for an average of 39 ± 4 µm (Fig. 83, left). Figure 83 (right) shows dry and wet fibers while being spun onto the take-up roll. The inner part of the take-up wheel shows dry fibers. The outer part shows wet fibers without full evaporation of the acetone. This is not a significant issue and can be resolved by adjusting spinning parameters.

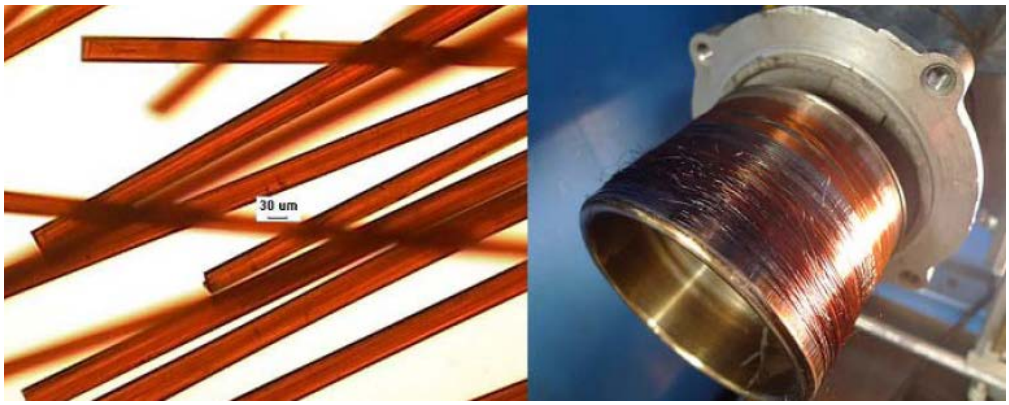

Fig. 83 Solution-spun fibers of Ace-SKL fiber on the take-up roll (right) and micrographs of as-spun fibers (left)

The Ace-SKL fibers were thermo-oxidatively cross-linked with the following heating ramp: heating from 50 to 140 °C at 0.25 °C/min, holding at 140 °C for 10 h, heating from 140 to 155 °C at 0.1 °C/min, holding at 155 °C for 10 h, heating from 155 to 220 °C at 0.1 °C/min, and holding at 220 °C for 24 h. The whole procedure took less than 72 h. Fibers could be stabilized and turned black after oxidative stabilization (Fig. 84).

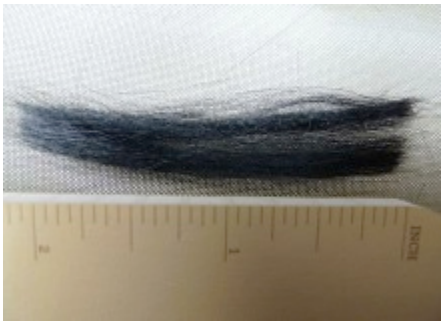

Fig. 84 Oxidized, solution-spun Ace-SKL with low concentration of acetate groups

The oxidized fibers were successfully carbonized. The fibers were heated to 1,000 °C at 4.5 °C/min and held at 1,000 °C for 1 h in a furnace in a stream of argon. After carbonization, the fiber size reduced to 31.7 ± 1.2 μm. The Ace-SKL carbon fibers had a rough surface and noncircular shape due to evaporation of the acetone (Fig. 85).

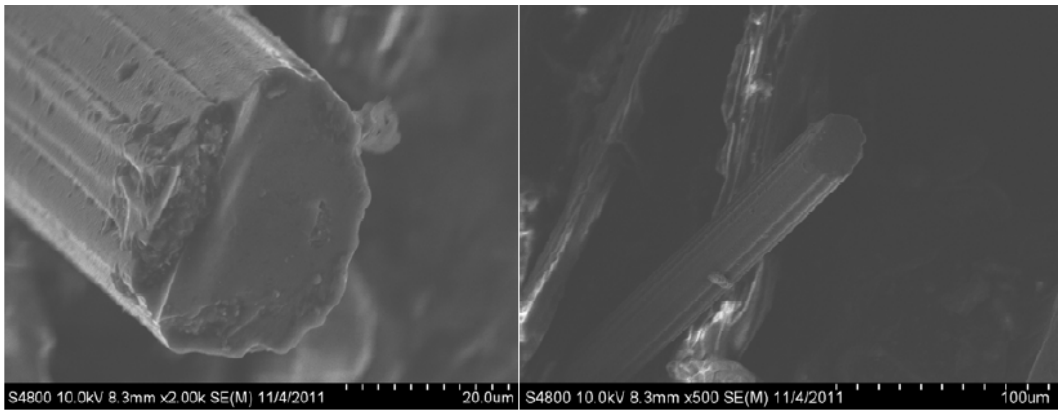

Fig. 85 Carbonized, solution-spun Ace-SKL with low concentrations of acetate groups

A series of density floats was used to prepare cesium formate solutions with specific densities (Fig. 86). Ace-SKL-derived carbon fibers were immersed into these solutions. The fibers floated on the surface of solutions with density greater than 1.75 g/mL and sank to the bottom of solutions with density less than 1.70 g/mL. Thus, the density of Ace-SKL carbon fibers could be bracketed between 1.70 and 1.75 g/cm^3.

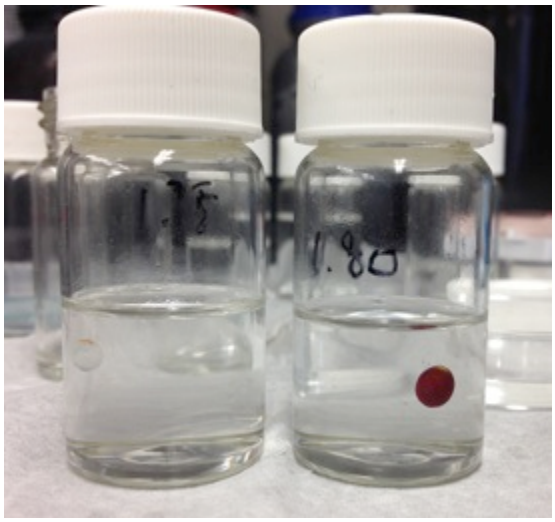

Fig. 86 Cesium formate solution prepared with density floats

These carbon fibers displayed tensile modulus, strength, and strain-to-failure values of 27 ± 3 GPa, 230 ± 30 MPa, and 0.9 ± 0.1%, respectively. The electrical resistivity was quite low, 14 μΩ-m, indicating a high graphitic content in these fibers. Thus, optimizing the processing of these fibers is important to achieving increased carbon fiber properties. Furthermore, these batches of carbon fibers were produced from as-received SKL that had an ash content about 2.85%. It was reduced to improve properties of resulting carbon fibers.

4.3.10.7 Process Optimization: Stabilization and Carbonization under Tension

To increase the mechanical properties of obtained carbon fibers, purified lignin with ash content around 0.15% was used as starting material. Tension was applied during thermostabilization to provide an enhanced degree of molecular orientation within the fibers. As-spun fibers were first stabilized in an oven at constant length. Fibers were mounted with epoxy glue on a graphite frame (Fig. 87). Bending of the frame during stabilization was observed, indicating relaxation during heat treatment. Then another set of as-spun fibers (around 5 cm long) was glued at both ends with hooks inserted. The fibers were suspended in the oven with weight loaded at the bottom. Under tension, of the order of 0.01 g/denier, the fiber tows resulted in an extension of up to 800% as shown in Fig. 88.

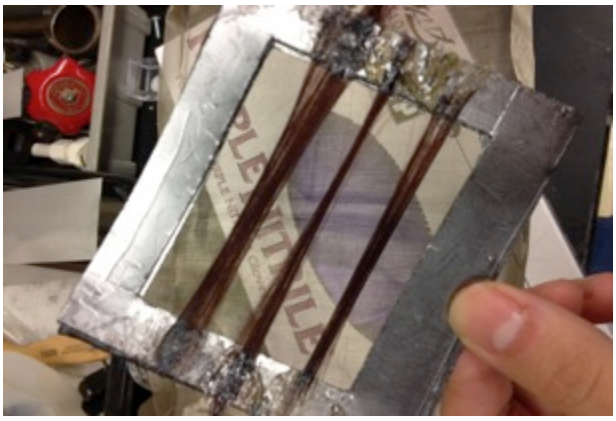

Fig. 87 Mounted fibers on graphite frame

Fig. 88 Fibers stabilized with constant load displayed extension during stabilization

Carbonization was also performed under tension using a customized graphite rack, as illustrated in Fig. 89. A tungsten weight was loaded at the bottom of the fiber tow to provide tension during carbonization. It was observed that when carbonization was conducted under tension, an extension of up to 25% could be achieved with adequate tensile stress. Figure 90 displays the modulus and strength of various carbon fibers as a function of fiber extension-during-carbonization (EDC). As expected, carbon fibers with larger EDC displayed better tensile properties due to higher molecular orientation within the fibers.

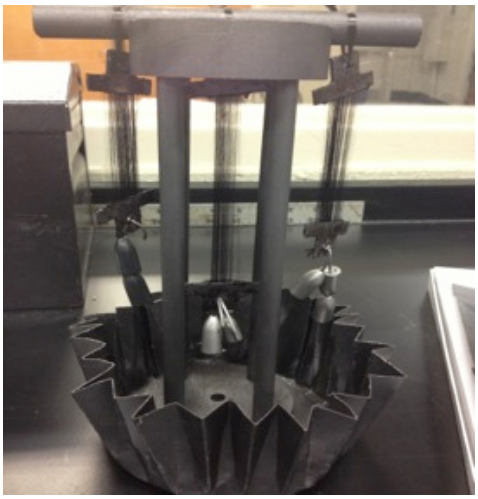

Fig. 89 Fiber tow suspended on a customized graphite rack and tungsten weight loaded at the bottom

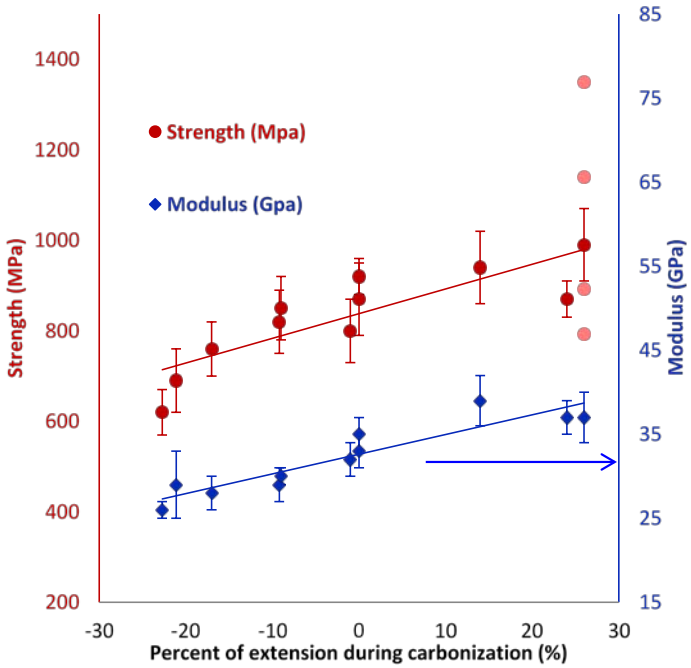

Fig. 90 Tensile strength and modulus of Ace-SKL carbon fibers produced from various levels of tension during carbonization

Table 12 lists the tensile properties of Ace-SKL-derived carbon fiber from different batches stabilized and carbonized with or without tension; the values are before compliance correction. With applied tension, fibers with thinner diameter and better tensile properties were obtained. Fibers processed without any tension during both stabilization and carbonization displayed only half of the tensile strength when compared with fibers processed with tension during both steps. After compliance correction for modulus (using gauge lengths of 5, 10, and 25 mm per ASTM D-3379-5[44]), carbon fibers that underwent significant EDC displayed tensile modulus, strength, and strain-to-failure values of 52 ± 2 GPa, 1.06 ± 0.07 GPa, and 2.0 ± 0.2%, respectively. These strength values are amongst the highest ones reported in literature for lignin-based carbon fibers. The largest individual filament tensile strength was 1.3 GPa.

Table 12 Ace-SKL carbon fiber properties of fiber processed with and without tension

Ace-SKL carbon fiber	Diameter (μm)	Strength (MPa)	Apparent modulus (GPa)	Apparent strain to failure (%)
Stabilized and carbonized without tension	22.5 ± 0.4	510 ± 50	30 ± 2	1.7 ± 0.1
Stabilized with tension, carbonized without tension	8.6 ± 0.2	700 ± 30	28 ± 1	2.5 ± 0.1
Stabilized and carbonized with tension	5.9 ± 0.2	1,050 ± 70	35 ± 3	3.0 ± 0.2

An Ace-SKL batch was processed similarly with the same amount of EDC but with only 0.3 wt% additional ash content, the Ace-SKL batch having a higher ash content resulted in a much lower tensile strength of only 0.6 GPa for the resulting carbon fibers. This clearly indicates that low ash content, in addition to the tension, is also critical for attaining higher performance of the resulting carbon fibers.

4.3.10.8 Process Optimization: Solution Spinning of Ace-SKL under Different Conditions

To optimize the dry-spinning condition, spinning at different temperature with different solution concentration was performed. Then solution spinning with more concentrated Ace-SKL solution was conducted.

First, solution spinning was conducted at 25 °C using 2.15-g Ace-SKL/mL acetone. As shown in Fig. 91, the resulting as-spun fibers had a flat oval shape and relatively smooth surface. The tensile strength obtained from this batch of spinning is no more than 800 MPa due to fiber breakage during carbonization that caused insufficient tension. Under this condition, dry spinning was difficult, as the extrudate had low elasticity and the highly viscous solution resulted in high processing pressure

(1,500–2,000 psi). The spinneret capillaries tend to be blocked at later stage of spinning. Thus, the processing condition of 25 °C and 2.1-g Ace-SKL/mL acetone was not regarded as a good combination for spinning.

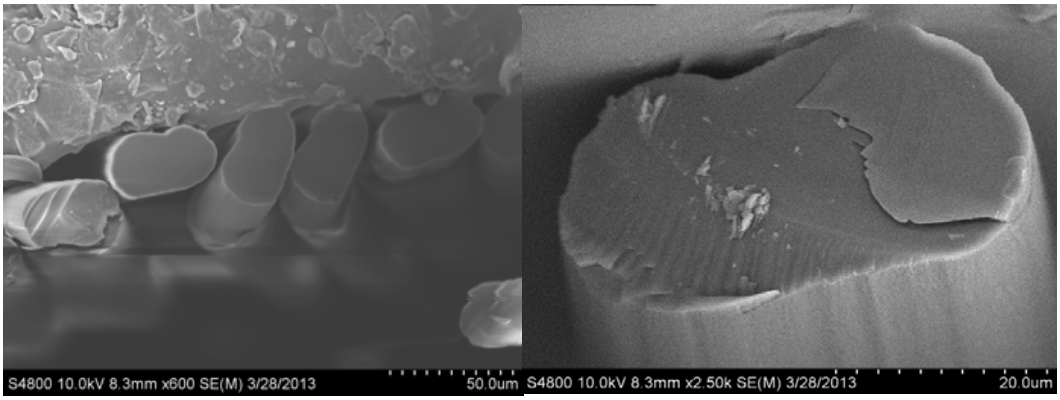

Fig. 91 As-spun fibers obtained from dry spinning with 2.0-g Ace-SKL/mL acetone at 25 °C

Next, solution spinning was conducted using about 2.05-g Ace-SKL/mL acetone solution at room temperature and 2.25-g Ace-SKL/mL acetone solution at 40–45 °C. The SEM images of as-spun fibers are shown in Fig. 92. Compared with as-spun fibers obtained at elevated temperature (left), the room temperature as-spun fibers (Fig. 93, top) displayed less crenulation and smoother surface. SEM images of the resulting carbon fibers are shown in Fig. 93 (bottom), and the geometric features of as-spun fibers are listed in Table 13.

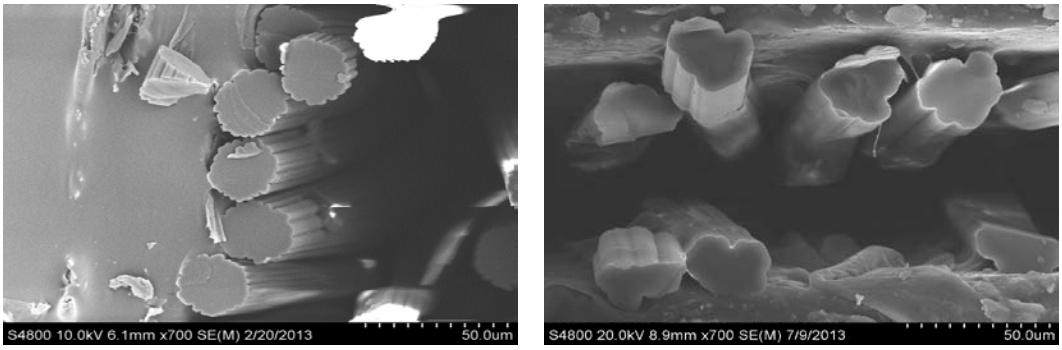

Fig. 92 Ace-SKL as-spun fibers from 2.24-g Ace-SKL/mL acetone (left) and 2.05-g Ace-SKL/mL acetone solution (right)

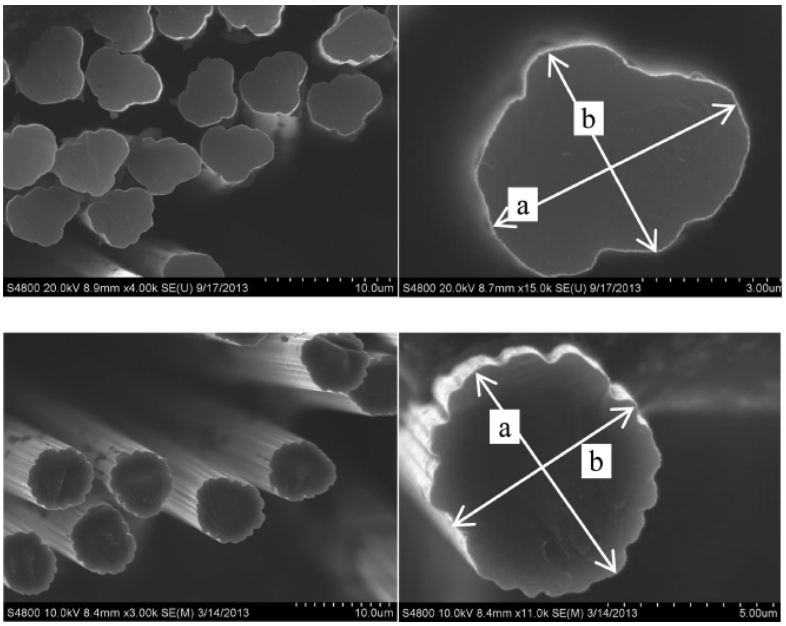

Fig. 93 Ace-SKL carbon 25 °C spinning (top) and 45 °C spinning (bottom)

Table 13 Analysis of the SEM images obtained from different batches of as-spun fibers. P/Pe is the ratio of perimeter over equivalent perimeter for circular fiber.

Spinning conditions	No. of crenulation	No. of cren./perimeter	Aspect ratio (a/b)	P/Pe
2.2 g/mL, 45 °C spinning	20 ± 1	0.19 ± 0.01	1.10 ± 0.03	1.38 ± 0.03
2.0 g/mL, 25 °C spinning	10 ± 0.5	0.09 ± 0.01	1.32 ± 0.04	1.26 ± 0.01

From a comparison of cross-sectional shapes of as-spun fiber (shown earlier in Fig. 92) and carbon fibers, it is evident that the cross-sectional pattern was preserved after carbonization. Fibers spun at a higher temperature undergo a rapid out-diffusion of solvent that can be achieved by a larger number of finer crenulations, which has 38% larger surface area as compared with equivalent circular fiber (same cross-sectional area) that are typically obtained by melt spinning. Fibers spun at a lower temperature of 25 °C undergo a slower out-diffusion of solvent and result in fewer, but larger, crenulations that result in about 26% larger surface area (as compared with their circular equivalents). The average tensile strengths from single filament tests were measured at 1.05 ± 0.07 and 1.06 ± 0.07 GPa for 45 and 25 °C spinning temperatures, respectively; these values are statistically not different. However, the fibers resulting from spinning at 45 °C result in larger interfacial area, and this could ultimately lead to enhanced fiber-matrix interfacial bonding in composites.

4.3.10.9 Crystallinity Characterization of Ace-SKL-Derived Carbon Fibers

To study the graphitic crystallinity development during carbonization, one group of Ace-SKL carbon fibers was further heat treated to 2,400 °C. After this high-temperature carbonization, the tensile strength dropped to 210 ± 30 MPa. This is consistent with other precursors (such as PAN), where out-diffusion of noncarboneous elements leaves behind voids and defects. Representative Raman spectra for Ace-SKL carbon fibers carbonized at 1,000 and 2,400 °C are displayed in Fig. 94. The ratio of integrated intensity value of disordered (D) to graphitic (G) peaks (I_D/I_G) was measured to be about 2.88 and 1.02 for 1,000 and 2,400 °C treated fibers, respectively. Both values indicate a low degree of graphitic crystallinity development within the carbon fibers. This is consistent with the nonhomogeneous chemical structure of the lignin precursor, which is not as conducive to formation of the hexagonal carbon form as is MP. (A higher graphitic crystallinity enhances lattice-dominated properties such as the modulus and thermal conductivity but adversely affects the tensile strength.)

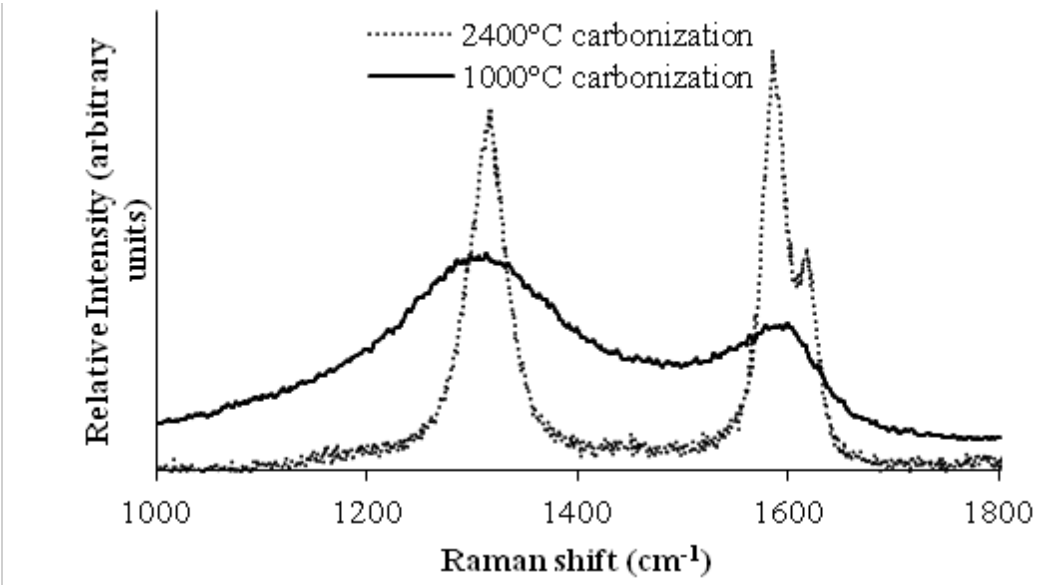

Fig. 94 Raman spectra of Ace-SKL carbon fibers carbonized at 2,400 and 1,000 °C. Intensity values on the ordinate scale are in arbitrary units.

For 1,000 °C carbonized fibers, the integrated azimuthal profiles from WAXD for fibers carbonized with and without tension are similar, with their (0 0 2) peaks located at 2θ value of approximately 24.3°, as shown in Fig. 95a. The 3 small, sharp peaks (first appearing at 28.4°) are from NIST-grade silicon powder sprinkled on the carbon fiber samples for accurate location of 2θ peak positions. For 2,400 °C carbonized fibers, the (0 0 2) peak was located at 26.0°, with d_{002} spacing calculated as 0.3424 nm, and the corresponding degree of graphitization at 18%. These

WAXD results are consistent with those obtained from Raman spectroscopy. Further, the azimuthal profile of the (0 0 2) peak, Fig. 95b, showed virtually no molecular orientation in fibers carbonized without tension. The Herman's orientation factor (fa = [3<cos2ϕ>–1]/2) was measured at about 0.1. In contrast, for fibers carbonized under tension, the peak at ϕ approximately 0° indicates an observable extent of molecular orientation with a significantly higher Herman's orientation factor of about 0.3. The 2,400 °C carbonized fiber also preserved the orientation with Herman's orientation factor still at 0.3.

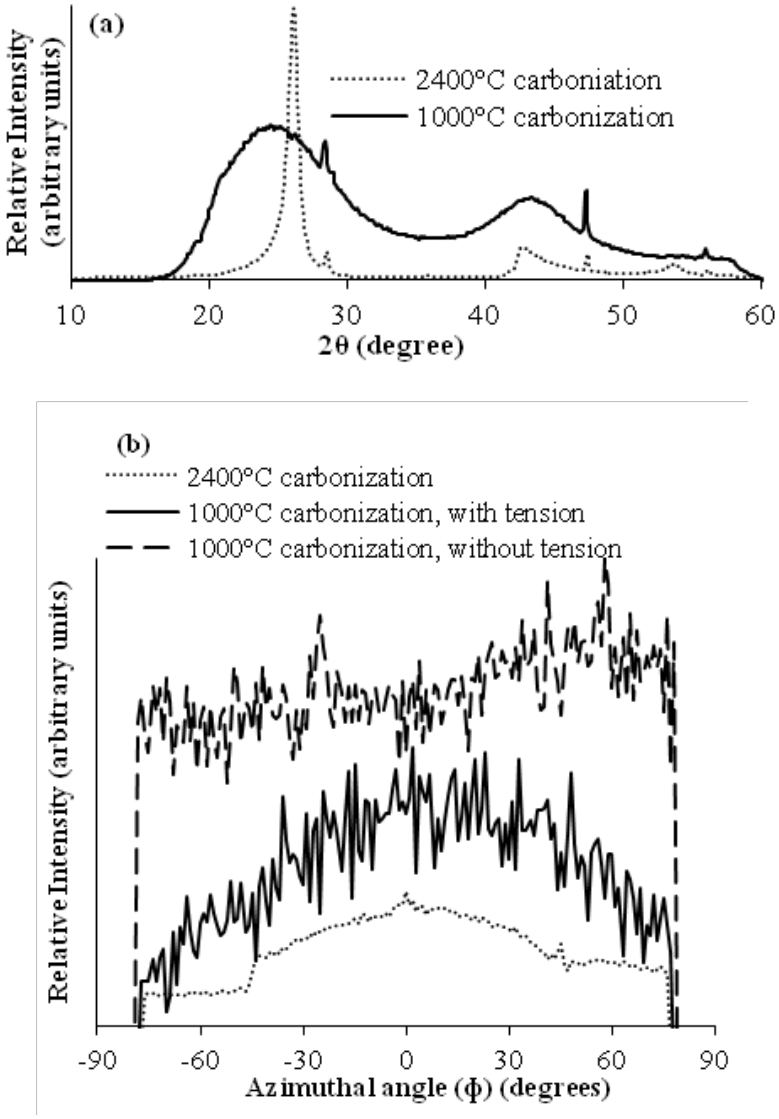

Fig. 95 WAXD of Ace-SKL carbon fibers. Intensity values on the ordinate scale are in arbitrary units. Azimuthal scans have been shifted vertically for visual clarity.

4.3.11 Future Directions

Based on the encouraging results obtained on carbon fibers derived from dry spinning of partially acetylated lignin (Ace-lignin), the following 2 directions are worth pursuing in future studies:

- Dual UV-thermal stabilization of precursor fibers to shorten the carbon fiber production time
- Improve properties of carbon fibers by using a combination of multiple precursors

Initial experiments for these routes have been performed, and the preliminary experiments are summarized in the following section.

4.3.11.1 Dual UV/Thermal Dual Stabilization

Studies using photosensitive precursors on UV-assisted stabilization on PAN precursor fibers to accelerate stabilization process have been previously reported.[13–15] However, the assistance of UV for stabilization of lignin precursor fibers has not been studied yet. Many studies focused on reducing photo-yellowing effect, which was caused by light-induced deterioration of wood surfaces.[99–102] In our study, the positive effect of UV on accelerating the stabilization of Ace-SKL precursor is studied.

A given tow of Ace-SKL fibers was divided into 2 parts and placed in the sample holder with one-half blocked against UV radiation by aluminum foil (control sample) and the other half irradiated with UV for 5 cycles, with 3-min exposure time/cycle. UV-treated fibers had a slightly darker color compared with the control sample.

UV-treated fibers and control fibers were placed in a thermal-oxidation oven for stabilization, using a heating rate of 0.4 °C/min without any dwell time, which was a faster heating program than used previously. Ace-SKL as-spun fibers without any treatment were also placed in the oven. When temperature increased to 165 °C, both the control fibers and as-spun fibers became tacky, but the UV-treated fibers survived during the stabilization up to 220 °C. As shown in Fig. 96, UV-treated Ace-SKL fibers can be separated after stabilization, whereas the control and as-spun fibers fused together. When the heating rate was increased up to 1.2 °C/min, the UV-treated fibers still retained the fiber form, whereas the control fibers melted in the container. These observations clearly prove that UV can help the stabilization of Ace-SKL fibers, and the total stabilization time can be reduced from 38 h to 3 h.

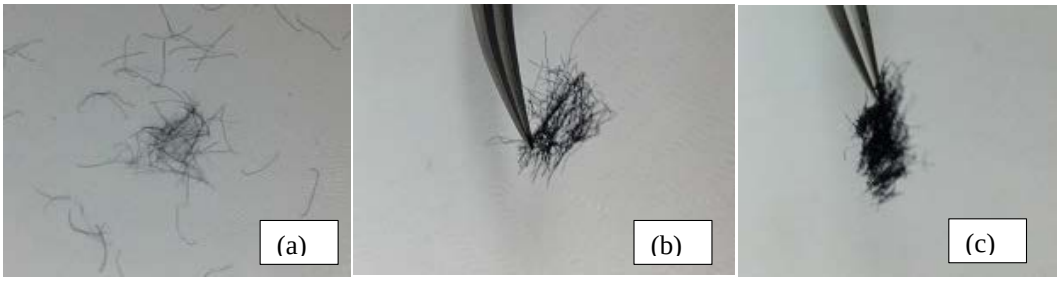

Fig. 96 After thermal-oxidation up to 220 °C at a heating rate of 0.4 °C/min: a) with prior UV treatment of fibers; b) control fibers; c) as-spun fibers

Ace-SKL powder was dissolved in acetone to prepare a 0.03 g/mL solution. Pure KBr was pressed into a pellet and coated with Ace-SKL solution on the surface by evaporation of acetone. The Ace-SKL-coated KBr pellet was irradiated with UV and taken out of UV chamber for FTIR study after 3, 10, and 15 min, respectively. At the same time, an Ace-SKL-coated control pellet was wrapped in aluminum foil to block the UV rays. There was no significant change in the FTIR spectra of control pellet before and after each UV exposure. For the UV-irradiated pellet, the spectra shown in Fig. 97 were normalized with the intensity of 1,033 cm^{-1} peak, which is attributed to aromatic C–H in-plane deformation. As the FTIR spectra show, intensity of the 1,740, 1,597, and 1,265 cm^{-1} peaks increased significantly, indicating the formation of carbonyl groups.

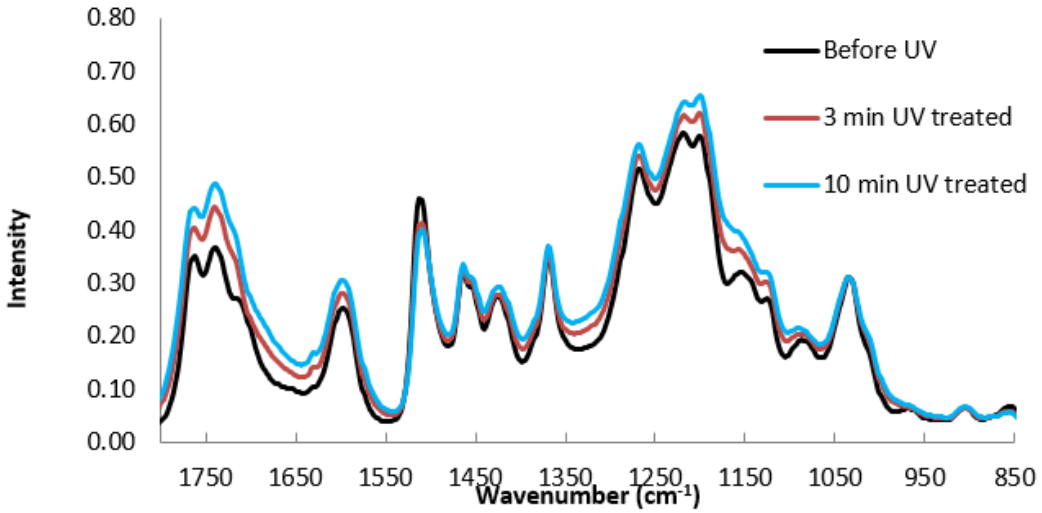

Fig. 97 FTIR spectra of Ace-SKL at different UV treatment times

A 15-min UV-treated fiber tow and a control fiber tow (without any UV exposure) were thermo-oxidatively stabilized at 1.2 °C/min heating rate. A portion of fibers was taken out of the oven at 100, 130, 190, and 220 °C, respectively, for DSC tests. The DSC scan results are shown in Fig. 98. T_g for both groups of fibers increased

gradually as the thermo-oxidation proceeded. It was observed that the control fibers fully melted into a liquid form after heat treatment. In contrast, the UV-treated fibers preserved their shape without becoming tacky during the entire stabilization up to 250 °C due to the stabilized surface resulting from UV.

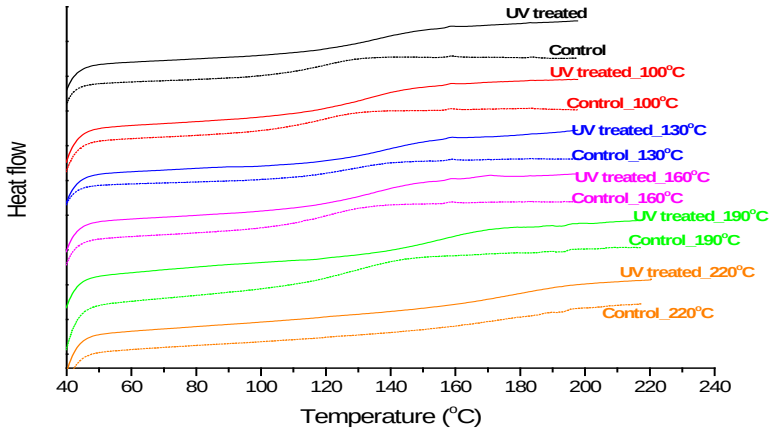

Fig. 98 DSC shift of UV-treated and control fibers during thermostabilization

Ace-SKL fibers underwent various treatments (heat-treated for 15 min, 3 min, and a control group) and were studied using GPC. The weight and number average molecular weights are listed in Table 14. As shown in Fig. 99, the molecular weight of Ace-SKL fibers after UV treatment was slightly higher compared with that of the control fibers, and 15-min treated fibers had a larger molecular weight than 3-min treated fibers. Although the difference was small, the resulting molecular weight was obtained from the whole fiber, including UV-treated surface and untreated fiber core. Broadened peaks for fibers with 15-min UV treatment indicate that a small portion of larger molecular weight fraction was formed.

Table 14 GPC results for different Ace-SKL fiber samples

Molecular weight characteristic	UV-treated 15 min	UV-treated 3 min	Control
M_n	10,636	8756	7,790
M_w	87,613	72,797	63,209
M_w/M_n	8.24	8.31	8.11

M_n = number average molecular weight; M_w = weight average molecular weight

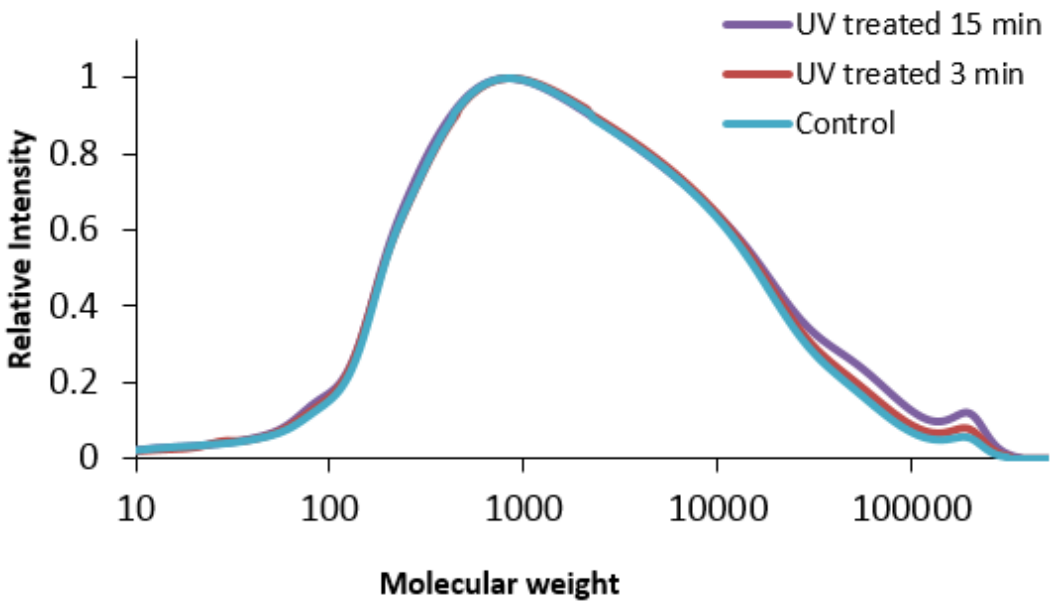

Fig. 99 GPC of Ace-SKL fiber samples with different of UV treatment time

To exert tension during UV treatment, as-spun Ace-SKL fibers were mounted with graphite end tabs on both ends. Also, predrawing was done to obtain thinner fibers and provide even tensions to all fibers in the same tow. The fiber tow was fixed at one end on a fixture, and the free end was loaded to maintain tension during UV treatment, as displayed in Fig. 100. Fibers survived and slightly stretched after UV stabilization (1%–3%). Next, the UV-treated tow was put into an oxidation oven using a 1.2 °C/min heating rate up to 220 °C for thermo-oxidation. The fiber tows survived this heating program and were subsequently subjected to carbonization under tension at 1,000 °C. Because of inadequate load during carbonization, fibers shrunk 14%–20% during carbonization. The carbon fibers with even 14% shrinkage displayed tensile modulus, strength, and strain-to-failure values of 31 ± 2 GPa, 860 ± 80 MPa, and 2.8 ± 0.3%, respectively. Future studies will focus on carbonization under adequate tension such that the fibers will stretch during heat treatment (not shrink), which will further aid in the enhancement of properties while reducing the processing time.

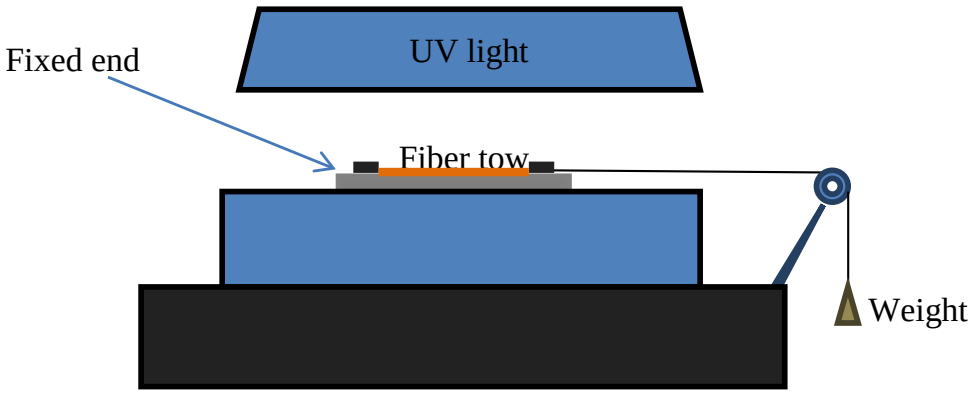

Fig. 100 Schematic of UV irradiation setup for fiber tow with weight loaded at end

4.3.11.2 Carbon Fibers Derived from PAN/Lignin Blended Precursors

PAN-based carbon fibers possess excellent strength, but such commercial carbon fibers derived from PAN are relatively expensive. The introduction of lignin into the PAN precursor to produce carbon fiber could dramatically reduce the material's cost.

Mixtures of lignin/PAN solutions with different ratios were prepared, and the viscosities of such blends were tested using a capillary rheometer. All the solutions displayed shear-thinning behavior as shown in Fig. 101.

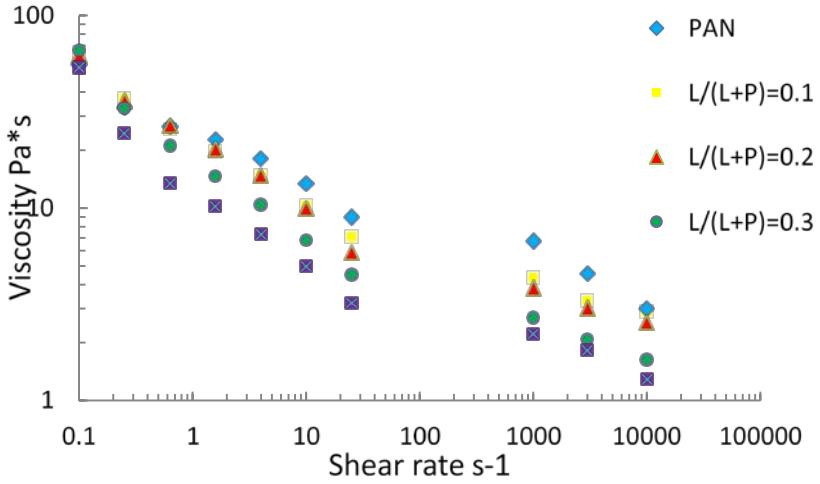

Fig. 101 Viscosity versus shear rate results for PAN and lignin/PAN blend solutions with different lignin content

4.3.11.3 Wet Spinning of Lignin/PAN Polymer Blends

SKL/PAN (0.35/0.65 by weight) polymer blend was used for wet spinning, and SKL was dissolved in dimethyl sulfoxide (DMSO) to make 22 wt% spinning

solution. As-spun fibers had an average diameter of 34.5 μm. The diameter was reduced to 21 μm after stretching in a hot water bath at 80 °C (Fig. 102).

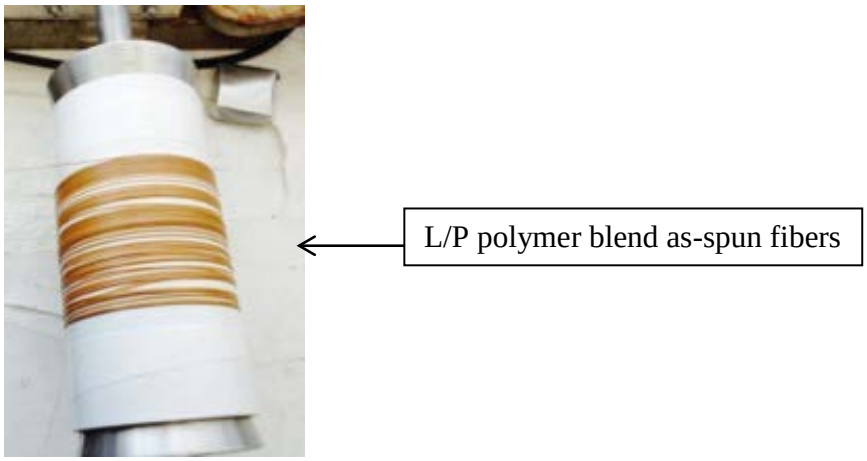

Fig. 102 As-spun fibers wet spun from lignin/PAN blend as seen on the take-up roll

As-spun fibers were stabilized in air at 220 °C at a heating rate of 1 °C/min first, then heated up to 300 °C at a rate of 2 °C/min. Step heating was used because lignin has lower stabilization temperature than PAN. Carbonization was achieved at 1,200 °C at a heating rate of 7.5 °C/min.

The resulting carbon fibers had a tensile strength of 255.35 ± 64.57 MPa and tensile modulus of 41 ± 7 GPa. As shown in SEM micrographs (Fig. 103), the carbon fibers contained a significant number of macro-voids. Thus, the lignin/PAN blends were not successful in these initial experiments for conversion to high-performance carbon fibers.

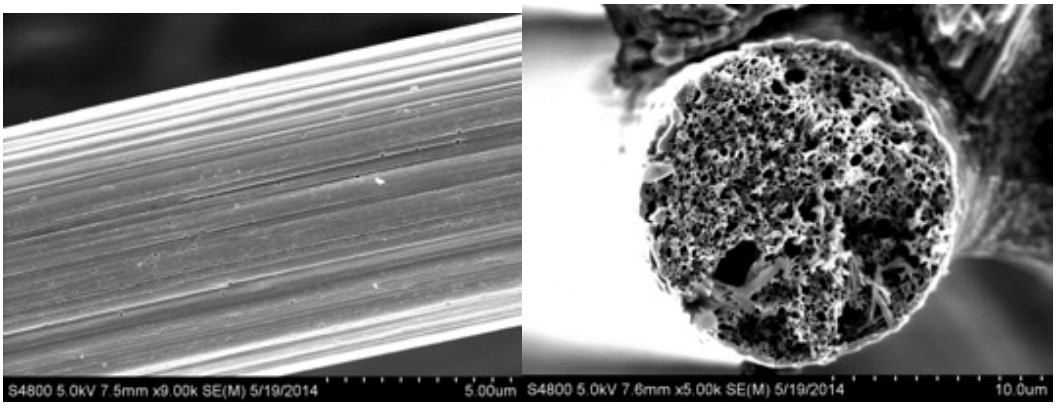

Fig. 103 SEM images of carbon fibers derived from lignin/PAN blend: (left) longitudinal surface and (right) cross-sectional area

Next, we investigated the production of lignin-PAN/PAN b-component precursor fibers. A 0.1/0.9 ratio of lignin/PAN polymer blend was used, and the blend was dissolved in DMSO to make 20 wt% spinning solution. Pure PAN with a molecular weight of 150,000 g/mol was dissolved in DMSO to make a 16 wt% solution. Both lignin-PAN and PAN spinning solutions were coextruded through a spinneret with a shell-core structure. Specifically, PAN was extruded through the core and L/P blend extruded through the shell. As-spun fibers were successfully produced in a coagulation bath containing 60 wt% of DMSO, as displayed in Fig. 104.

Fig. 104 Bi-component wet spinning

The as-spun fiber was stretched in a hot water bath at 80 °C that resulted in a stretched fiber with a diameter of approximate 215 μm. As-spun fibers were stabilized in air at 300 °C with heating rate of 3 °C/min, and held at 300 °C for 30 min. Carbonization was achieved at 1,000 °C with a rate of 7.5 °C/min.

The resulting carbon fibers have very low tensile properties because the macro-pores in the cross section caused defects and made carbon fibers very weak. SEM images (Fig. 105) of stabilized fibers and carbon fibers derived from lignin-PAN/PAN bicomponent precursor display a porous microstructure, which leads to low tensile properties of these fibers. Further stretching of as-spun fiber in 0.01 M HCl bath reduced the diameter of final resulting carbon fibers and the pore size as well. However, the fibers produced in these initial experiments are still very thick at about 100 μm, when considerably thinner fibers of 10-μm diameter are ultimately needed for high strength. Spinnerettes with smaller die size will be used to reduce the fiber size in future studies.

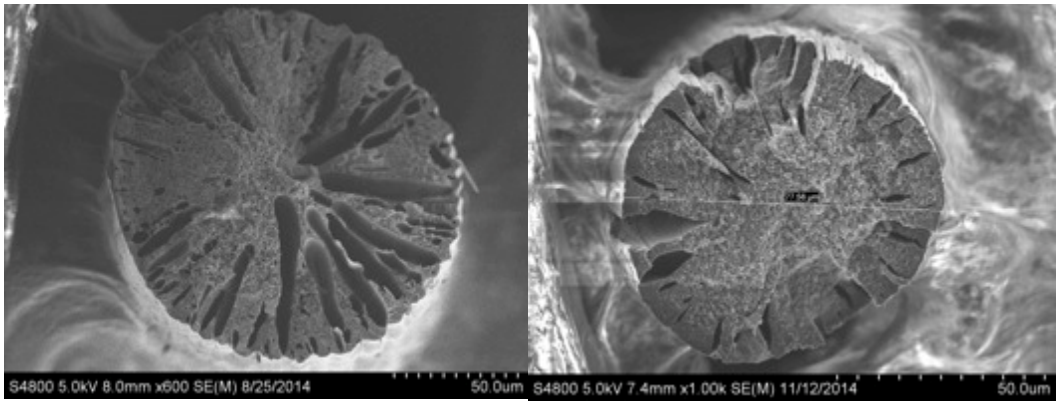

Fig. 105 SEM images: a) carbon fiber from hot water stretched as-spun fiber and b) carbon fiber from 0.01 mol/L HCl acid stretched as-spun fiber

4.3.12 Feasibility Study of Fiber Spinning of ARL-Synthesized Perfluoroalkoxy Alkane (PFA) Samples

4.3.12.1 PFA Resin Samples

1. Four samples were received from ARL (ca. April 2013). All samples were synthesized at 100 °C through oligomerization of furfuryl alcohol.
2. Samples 1, 2, 3, and 4 were produced from reactions times of 45, 90, 120, and 165 min (2.75 h), respectively.
3. Samples 1, 2, and 3 were soft and slightly tacky at room temperature, clearly establishing that fibers generated from such compositions are incapable of being further stabilized and carbonized. Precursor fibers should be solid and nontacky not only at room temperature but also at stabilization temperature.
4. Sample 4 was solid at room temperature and was further tested.

4.3.12.2 Processing of Sample 4

1. 8.7 g of PFA sample 4 (2.75 h reacted) was chopped into particles, stirred with 125 mL of acetone, and heated to approximately 55 °C to increase its solubility.
2. Sample dissolved only partially.
3. Liquid phase was filtered, and acetone evaporated to obtain a gel content of about 65%.
4. The original filtered solution was not able to form filaments.

5. Concentrated solution was spread on a glass surface but still could not form filaments, likely due to its low molecular weight. After drying, the filtered polymer remained tacky.
6. Sample 4 was added to DMSO. It dissolved partially in DMSO with a concentration of only 0.0734 g/mL.
7. Filtrate was a dark solution that could not form fibers.

4.3.12.3 Coagulation Characteristics

1. One drop of solution was spread on a piece of glass, and 2 mL of DMSO coagulant (70 wt% DMSO) was added.
2. Only small particles precipitated (i.e., no thin film was formed).
3. For the purpose of comparison, an equally dilute PAN-DMSO solution (~7 wt% PAN) was tested and found to form thin film after coagulation (Fig. 106).

Fig. 106 Comparison of dilute PFA and PAN solution after coagulation

4.3.12.4 Concentrated Sample 4 Coagulation Testing

1. Evaporated above solution to approximately 25 wt% solids in DMSO.
2. Concentrated PFA sample 4-DMSO solution still does not coagulate to form a film.
3. Only a coating remained, such as that generally observed from low-molecular-weight resins that do not form fibers or films.

4.3.13 Summary and Conclusions

Table 15 summarizes the results observed for lignin-based fibers and carbon fibers. Overall, unmodified lignin is not ideal for preparing carbon fibers. Even ECN organosolv lignin, which we could convert to carbon fiber, had low properties and

poor processing characteristics. In fact, one type of surface functionality—be it hydroxyls, acetates, or methacrylates—is not good for preparing carbon fibers. The results indicate that balance of these properties is desired. Low hydroxyl content is necessary to enable some oxidative stabilization, but high amounts reduce processing time unacceptably. High acetylation enables melt spinning but prevents efficient oxidative stabilization.

Table 15 Carbon-fiber potential of lignin and modified lignin. Shading provides a general rating of carbon fiber potential: red = poor, yellow = possible, and green = good.

Lignin type	Softening point (SP)	Spinning potential	Stabilization potential	Carbon fiber potential
SKL	No SP	Not spinnable	X	X
Soda lignin	245 °C	Not melt-spinnable, degrades before it melts, solution spinning possible	High potential for thermo-oxidative stabilization	Potential
ECN organosolv lignin	155 °C	Melt-spinnable	Very slow thermo-oxidative stabilization procedure	√ - can be heat treated to carbon fibers, methacrylation of ECN should help stabilization (solution spinning required)
Ace-SKL with high extent of substitution followed by fractionation	115–145 °C	Melt-spinnable	Not able to cross-link	X
Ace-SKL with low extent of substitution followed by fractionation	187 °C	Not melt-spinnable, can be solution spun	Thermo-oxidative stabilized	√ - made carbon fibers; tensile properties are low and need to be optimized
Methacryated SKL	No measurable SP	Not melt-spinnable due to methacrylate reactivity; solution cannot be drawn into filament	Cross-links easily – UV and thermo-oxidative stabilizable	X
Methacrylated and acetylated SKL	No SP, cross-links during heating	Melt-spinning not possible; solution spinnable and high likelihood of proper stabilization	UV and thermo-oxidiative stabilizable	High potential for making carbon fibers
Methacrylated (and MA/Ace) soda lignin	No SP, cross-links during heating	Not melt-spinnable; potentially solution spinnable	UV and thermo-oxidiative stabilizable	Potential
Methacrylated (and MA/Ace) ECN	No SP, cross-links during heating	Not melt-spinnable; potentially solution spinnable	UV and thermo-oxidiative stabilizable	Potential
Bacteria-modified lignin	Not available	Melt-spinnable; solution spinnable	UV and thermo-oxidiative stabilizable	Potential

From the current limited acetylation results, it is evident that suitable modification of lignin composition and spinning conditions has been achieved to obtain precursor fibers that could be thermo-oxidatively stabilized and carbonized. By limited acetylation, Ace-SKL could be dry spun and was capable of stabilization. Tension was applied during thermal treatment and resulted in a tensile strength, modulus and strain-to-failure values of 52 ± 2 GPa, 1.06 ± 0.07 GPa, and 2.0 ± 0.2%, respectively. These mechanical properties are among the highest values reported in the literature for lignin-derived carbon fibers.

Although high electrical conductivity was not the focus of this work, we showed that electrical resistivity for lignin-based carbon fibers can be varied. The relatively low electrical resistivity of 14 μΩ-m found in Ace-SKL-derived carbon fibers (processed at only 900 °C) suggests that these fibers are developing a graphitic texture. Although these carbon fibers had low resistivities, their mechanical performance was poor, consistent with their graphitic structure. The previously summarized lignin-based carbon fibers with good mechanical properties, on the other hand, had higher resistivities with less graphitic structure and more turbostratic structure.

The cross-section shape can be controlled during dry spinning, and crenulated carbon fibers obtained in this study have up to 35% larger surface area as compared with equivalent circular fibers that are typically obtained by melt spinning. Because of the lack of graphitic crystallinity in these lignin-derived carbon fibers, their surface is expected to be more reactive than that of carbon fibers processing from graphitic precursors. The resulting carbon fibers were processed into composites, and the tensile properties were tested. Surface reactivity and larger surface area both likely led to better fiber-matrix interfacial bonding in composites, as seen from composite fracture surfaces.

In future studies, UV irradiation could be employed for stabilization, which could significantly increase the speed of thermostabilization. With just 0.25 h of UV irradiation, the total stabilization time could be reduced by almost 35 h (from 38 to 3 h). Furthermore, novel shell-core morphology of carbon fibers as derived from biocomponent wet spinning will also be further explored. For enhanced carbon fiber performance with reduced precursor costs.

The results of this work have been published in a number of papers and a dissertation.

4.4 Reactive Diluents from Lignin Model Compounds

4.4.1 Introduction

VE resins are used to produce polymer composites for commercial applications because they have relatively high moduli, strength, and glass transition T_g's while maintaining low weight and cost.[21,66] To facilitate the use of liquid molding techniques to fabricate large-scale composite parts, commercial VE resins typically contain high concentrations (>40 wt%) of a reactive diluent, such as styrene. In addition to lowering resin viscosity, styrene acts as a linear chain extender, thus improving the overall polymer performance by allowing for a higher degree of monomeric reactivity by delaying the onset of gelation and reducing diffusion limitations.[22] However, despite its benefits, styrene has been designated a HAP, a VOC, and a suspected carcinogen.[24,103] In 2003, with an amendment in 2005, the EPA introduced legislation to limit styrene emissions from composite manufacturing.[24] More recently, in June 2011, the Department of Health and Human Services through the National Toxicology Program in their 12th edition of the *Report on Carcinogens* has designated styrene as "reasonably anticipated to be a human carcinogen".[103] Moreover, styrene is emitted during metering, mixing, processing, and curing, and studies have shown that up to 40% of styrene can remain unreacted after curing and can continue to be released from composites during the remaining phases of their life cycle.[22,24] With this significant drawback, new resins are required for the continued use of polymer composites. Therefore, the development of nonvolatile reactive diluents with styrene-like performance is gaining interest. Additionally, with the continued volatility of the petroleum industry and crude oil price fluctuations, the cost of styrene will eventually become a factor in the production of future resins if a suitable biobased replacement is not identified. These significant factors give impetus for the discovery and development of renewable biobased reactive diluents that have styrene-like performance with minimal VOC emissions.

Previous work conducted by La Scala et al.,[1,104–107] in conjunction with the Affordable Composites from Renewable Sources program at the University of Delaware, has demonstrated the potential of using methacrylated fatty acids as styrene replacements. These include methacrylated lauric acid (MLau), methacrylated hexanoic acid, and methacrylated octanoic acid as styrene reducers in VE, soybean-based, and castor oil-based polymer matrices. These renewable, naturally occurring methacrylated plant oil derivatives exhibit low volatilities and viscosities (40–80 cP at 30 °C) and have the ability to act as acceptable chain extenders. These functionalized plant oil derivatives also demonstrate the ability to toughen polymer matrices via the flexible, long alkyl side chains. However, while

showing promise, styrene, at a considerably reduced concentration, was still needed to produce biobased resins with comparable thermal and mechanical performance to commercial VE-styrene resins.[1,105] Thus, lower-viscosity, nonvolatile, renewable reactive diluents with styrene-like performance are still being sought; particularly, reactive diluents that have similar T_g's to styrene when polymerized.

Lignin is a renewable biobased alternative rich in aromaticity with the capability to yield single aromatic chemicals when selectively broken down. Lignin is the second most abundant natural raw material, surpassed only by cellulose, with more than 3×10^{11} tons existing in the biosphere and approximately 2×10^{10} tons generated annually.[25,67,72] As of 2004, the pulp and paper industry alone produced roughly 50×10^{6} tons of extracted lignin of which 95% was Kraft lignin.[68,72] The Kraft process, invented in 1879 by Carl F Dahl, treats wood chips with a mixture of NaOH and sodium sulfide, known as white liquor, and separates the lignin from cellulose and hemicelluloses.[68,72] However, only approximately 2% of the available lignin is used commercially, with the remainder used as a low-value fuel to cover internal energy needs of the pulp and paper industry.[73] Because of its very complex 3-D aromatic structure, lignin is largely intractable in its unmodified state and therefore is often sought to be broken down into smaller-molecular-weight aromatic components.

Nondegraded and chemically modified lignins have been successfully incorporated into various materials, including polymeric materials.[67–69,72,73] Additionally, much research has been conducted in selectively breaking down all types of lignin and multiphenolic LMCs to develop new chemicals and renewable sources of predominantly petroleum-derived chemicals. [67,69–71,74–80] Recently, a modest yield of vanillin from Kraft lignin has been obtained using aqueous polyoxometalates in the presence of alcohols to oxidatively degrade lignin.[67] Additionally, vanillin production via Kraft lignin oxidation using an NaOH alkaline medium has been reported.[78] Moreover, a 70% yield of guaiacol has been achieved from common β-O-4 LMCs, guaiacylglycerol-β-guaiacyl and veratrylglycerol-β-guaiacyl ether, under catalytic hydrolysis using an acidic ionic liquid.[71] In 2011, Zakzeski and Weckhuysen[73] reported 22.2% and 12% yields of guaiacol from aqueous phase reforming of a β-O-4 model compound and a 5-5' model compound, respectively, using a Pt/Al_2O_3 catalyst. Sergeev and Hartwig[80] have reported yields as high as 99% of guaiacol from hydrogenolysis reactions of representative biphenyl LMCs.

In this work, vanillin, guaiacol, and eugenol have been selected as representative LMCs for the synthesis of novel reactive diluents as styrene replacements in polymer matrices. Specifically, these LMCs were selected based on extensive studies and the potential to obtain these chemicals in high yields from lignin as well as from clove oil in the case of eugenol.[70,76,108] To chemically incorporate the

selected LMCs into VE resins, polymerizable carbon-carbon double bonds need to be integrated onto the phenolic compounds. Methacrylated analogues of vanillin,[82,83] guaiacol,[84-87] and eugenol[108,109] have been reported in the literature but, to date, have not been studied as styrene replacements in polymer resins. We report the synthesis, relative volatilities, viscosities, and polymer T_g's of the methacrylated lignin model compounds (MLMCs) as well as viscosities and T_g's of a commercial VE resin that contains 50 wt% of an MLMC. The relative volatility of styrene and T_g of the commercial VE resin (bismethacryl glycidyl ether of BPA epoxy, VE828) with 50-wt% styrene are also reported for direct comparison.

4.4.2 Publications

This work was summarized in the following 4 papers:

Stanzione JF, Sadler JM, La Scala JJ, Wool RP. Lignin model compounds as bio-based reactive diluents for liquid molding resins. ChemSusChem. 2012;5:1–8.

Abstract: Lignin is a copious paper and pulping waste product that has the potential to yield valuable, low-molecular weight, single aromatic chemicals when strategically depolymerized. Single aromatic lignin model compounds, vanillin, guaiacol, and eugenol, were methacrylated via esterification with methacrylic anhydride and a catalytic amount of 4-dimethylaminopyridine. Methacrylated guaiacol (MG) and methacrylated eugenol (ME) exhibited low viscosities at room temperature (MG: 17 cP and ME: 28 cP). When used as reactive diluents in VE resins, they produced resin viscosities higher than that of VE-styrene blends because of the lower viscosity of styrene monomer. Under thermogravimetric analysis (TGA) experimental conditions, the relative volatilities of MG (1.05 wt% loss in 18 h) and ME (0.96 wt% loss in 18 h) were much lower than that of styrene (93.7 wt% loss after 3 h) indicating the potential of these chemicals to be environmentally friendly reactive diluents. Bulk polymerization of MG- and ME-generated homopolymers with T_g's of 92 °C and 103 °C, respectively. Blends of a standard VE resin with MG and ME (50-wt% reactive diluent) produced thermosets with T_g's of 127 °C and 153 °C, respectively, that are comparable to a VE-styrene resins demonstrating the ability of MG and ME to completely replace styrene as reactive diluents in liquid molding resins without sacrificing cured resin thermal performance.

Stanzione JF, Sadler JM, La Scala JJ, Reno KH, Wool RP. Vanillin-based resin for use in composite applications. Green Chem. 2012;14:2346.

> Abstract: Lignin is an abundant, renewable material that has the potential to yield valuable, low-molecular-weight, single aromatic chemicals when strategically depolymerized. To generate a highly biobased thermoset for use in polymer composites, a lignin-derived chemical, vanillin, was methacrylated in a 2-step, one-pot synthesis to produce a VE resin (87 cP at 25 °C) with a 1:1 mole ratio of a monofunctional monomer, methacrylated vanillin, to cross-linking agent, glycerol dimethacrylate. The synthesis scheme was solventless and required little catalyst and moderate reaction temperatures while generating no by-products. Upon resin curing, a hard transparent thermoset with a broad glass transition, T_g = 155 °C (based on the tan δ maximum) and a temperature of maximum decomposition rate, T_{max}, of 426 °C was produced. Overall, a potentially 100% biobased thermoset was synthesized possessing comparable thermo-gravimetric and thermo-mechanical properties to commercial VE-based thermosets.

Stanzione JF, Giangiulio PA, Sadler JM, La Scala JJ, Wool RP. Lignin-based bio-oil mimic as biobased resin for composite applications, ACS Sustainable Chem. Eng. 2013;1:419−426.

> Abstract: Lignin is an abundant renewable raw material that has the potential to yield valuable bio-oils consisting of aromatic chemicals when strategically depolymerized. To determine if lignin-based bio-oils can be used in the development of biobased VE resins without the need of extensive and costly separations, a methacrylated lignin-based bio-oil mimic (MBO) was generated and used as a low-viscosity VE resin (30.3 cP at 25 °C) and as a reactive diluent in a standard commercial VE resin. MBO consisted of phenol, guaiacols, and catechols that were methacrylated by esterification with methacrylic anhydride and a catalytic amount of 4-dimethylaminopyridine. Curing the resin produced hard transparent thermosets that had near-complete conversion of free-radical polymerizable groups as per near-infrared spectroscopy. Temperatures of maximum decomposition rate (≥400 °C) and initial decomposition temperatures (≥300°C) were measured by means of TGA. T_g's of ≥115 °C and storage moduli of ≥2.5 GPa at 25 °C were measured by dynamic mechanical analysis (DMA). Overall, high-performance lignin-based thermosets were synthesized having comparable thermo-gravimetric and thermo-mechanical properties to commercial petroleum- and VE-based thermosets.

Bassett AW, Rogers DP, Sadler JM, La Scala JJ, Wool RP, Stanzione JF. The effect of impurities in reactive diluents prepared from lignin model compounds on the properties of vinyl ester resins. J Appl Polym Sci. 2016;133(45). doi: 10.1002/APP.43817.

> Abstract: Vinyl ester resins (VERs) often contain high concentrations of a petroleum-based reactive diluent, such as styrene. Reactive diluents that can be derived from lignin, including phenyl methacrylate (PM), 2-methoxyphenyl methacrylate (MG), and 4-propyl-2-methoxyphenyl methacrylate (M4PG), were synthesized and investigated as potential styrene replacements. A commercial VER was blended with each lignin-derived reactive diluent, and styrene, in 7:3 and 1:1 weight ratios and cured to ≥ 94 %, based on near-IR spectral analysis. The substituents on the aromatic ring of the lignin-derived reactive diluent are shown to have small effects on viscosity, thermogravimetric, and thermomechanical properties of the cured resins, where, in general, the smaller the reactive diluent, the greater the T_g and the lower the viscosity. Increasing purity of the reactive diluents substantially increases the T_g and degradation temperatures of the resins. The results suggest that PM, MG, and M4PG are effective bio-based reactive diluent replacements for styrene.

Additional details on each of these resins systems are discussed in JF Stanzione's PhD dissertation and Daniel Rogers' master's thesis.[90,110]

Tangential research not covered under this SERDP project was published in Holmberg et al.[111]

4.4.3 Highlights

Lignin model compounds can be simply derived from lignin and contain the compounds listed in Fig. 107. These LMCs were methacrylated using methacrylic anhydride to produce useful monomers similar to that of styrene for use in unsaturated polyester and VE resins (Fig. 108).

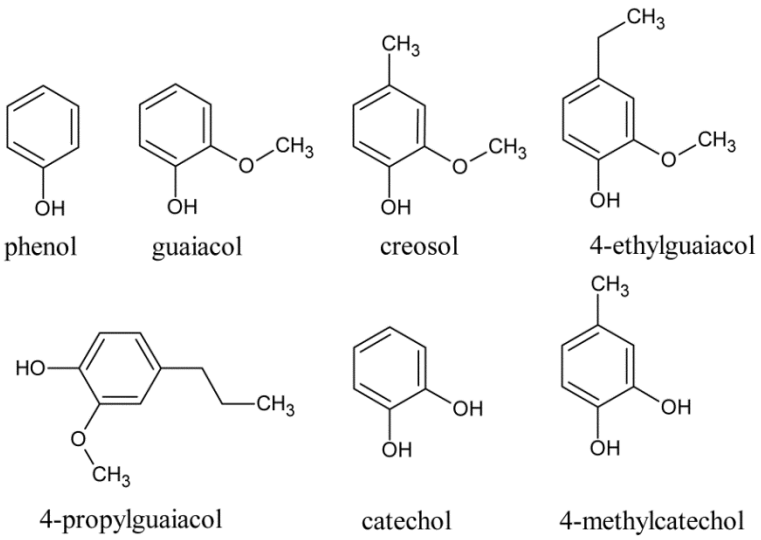

Fig. 107 Chemical structures of the phenolic compounds used in the representative lignin-based MBO. Used with permission from Stanzione.[90]

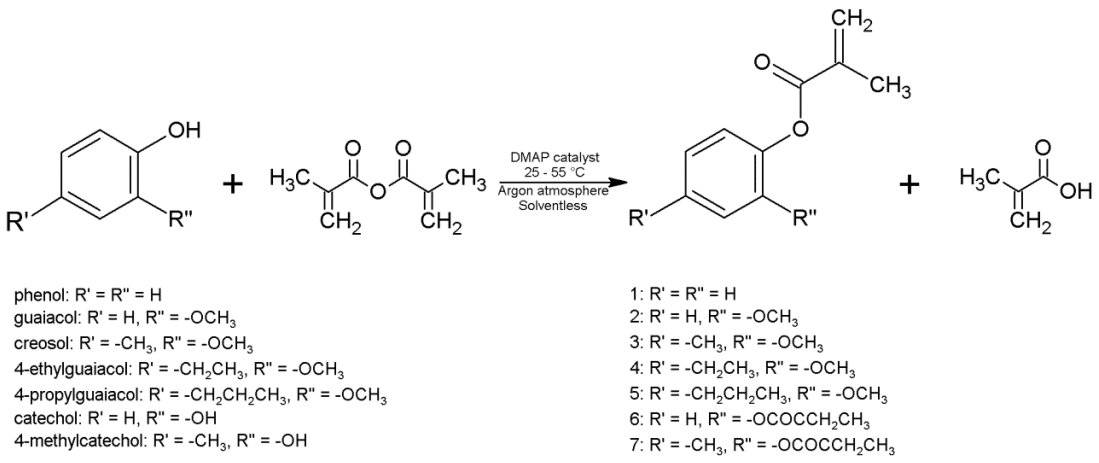

Fig. 108 Esterification reaction used to methacrylate the lignin model compounds that were blended to generate the representative lignin-based MBO. Used with permission from Stanzione et al.[90,112]

TGA results show that these methacrylated LMCs have much lower volatilities relative to that of styrene and thus could not be classified as VOCs (Fig. 109).

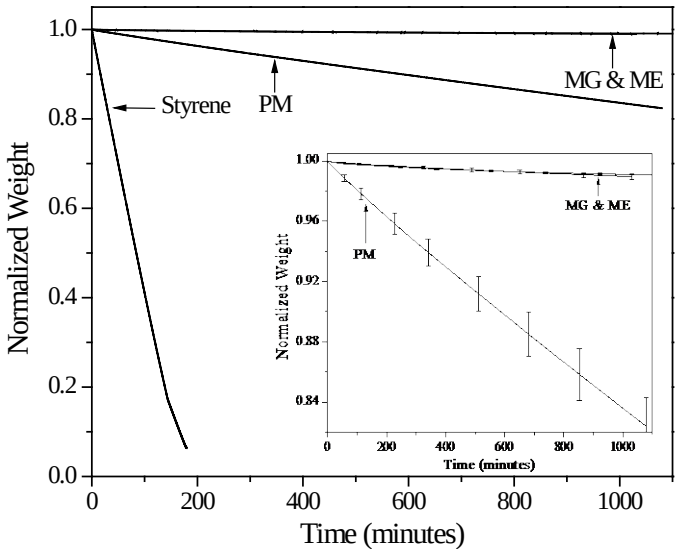

Fig. 109 TGA normalized weight as a function of time for styrene, PM, MG, and ME at 30 °C. See inset for the PM, MG, and ME behavior. The maximum standard deviation among the styrene the experiments was ±0.17.

Resin blends of VE and MLMCs show that these can have viscosities low enough for liquid molding applications (Fig. 110).

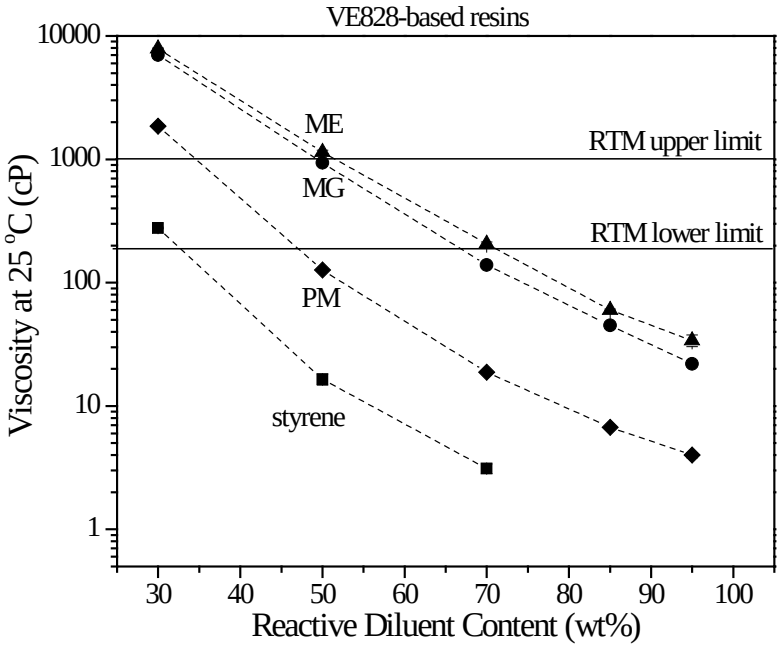

Fig. 110 VE828-based resin viscosities at 25 °C as a function of reactive diluent content. Upper and lower room temperature viscosity limits as required/desired by the composites industry for resin transfer molding techniques. Dashed lines are viewer guidelines.

Thermomechanical properties show that lignin-based resins have similar glass transitions (Fig. 111) and similar modulus (Fig. 111 and Table 16), but lower

strength (Table 16) and fracture toughness (Table 17) as a result of lower extent of cure. Therefore, methods to improve the extent of cure of these resins would be effective in making these resins drop-in replacements for VE/styrene.

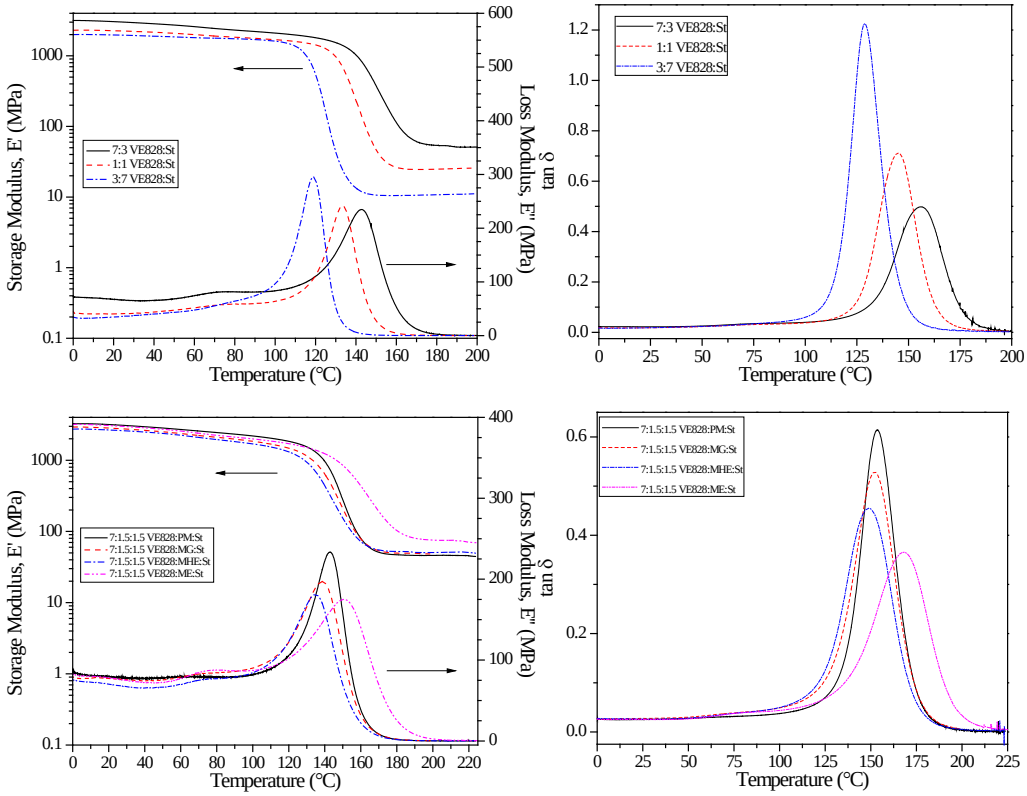

Fig. 111 Storage moduli (*E'*) (left graphs), loss moduli (*E''*) (left graphs) and tan δ (right graphs) as a function of temperature for the VE828-based thermosets that contain styrene; VE828:St (top graphs), 7:1.5:1.5 VE828:MLMC:St (bottom graphs).

Table 16 Flexural properties of the VE828-based thermosets

System (weight ratio)	Flexural Modulus (GPa)	Flexural Strength (MPa)	Elongation to Break (%)
7:3 VE828:St	3.9 ± 0.1	109 ± 19	3.1 ± 0.6
1:1 VE828:St	2.3 ± 0.1	83 ± 14	3.8 ± 0.3
7:3 VE828:PM	3.9 ± 0.4	115 ± 20	3.4 ± 1.2
1:1 VE828:PM	3.8 ± 0.5	90 ± 9	2.7 ± 0.2
7:1.5:1.5 VE828:PM: St	4.5 ± 0.2	99 ± 7	3.3 ± 1.1
7:3 VE828:MG	3.9 ± 0.1	98 ± 31	2.7 ± 0.6
1:1 VE828:MG	4.0 ± 0.1	102 ± 4	2.9 ± 0.3
7:1.5:1.5 VE828:MG: St	4.4 ± 0.3	90 ± 9	2.1 ± 0.4
7:3 VE828:ME	3.6 ± 0.1	41 ± 14	1.2 ± 0.3
1:1 VE828:ME	3.5 ± 0.1	62 ± 12	2.0 ± 0.2
7:1.5:1.5 VE828:ME: St	3.7 ± 0.3	95 ± 12	2.7 ± 0.6

Table 17 Fracture properties of the VE828-based thermosets

System (weight ratio)	K_{1C} (MPa $m^{1/2}$)	G_{1C} (J m^{-2})
7:3 VE828:St	0.95 ± 0.14	281 ± 87
1:1 VE828:St	1.18 ± 0.14	453 ± 101
7:3 VE828:MG	0.70 ± 0.10	133 ± 24
1:1 VE828:MG	0.45 ± 0.07	54 ± 11
7:3 VE828:ME	0.34 ± 0.04	45 ± 9
1:1 VE828:ME	0.30 ± 0.03	39 ±7

Figure 112 shows a novel route to make a largely biobased resin system using vanillin and gylcidyl methacrylate to replace both the VE and styrene component of a resin.

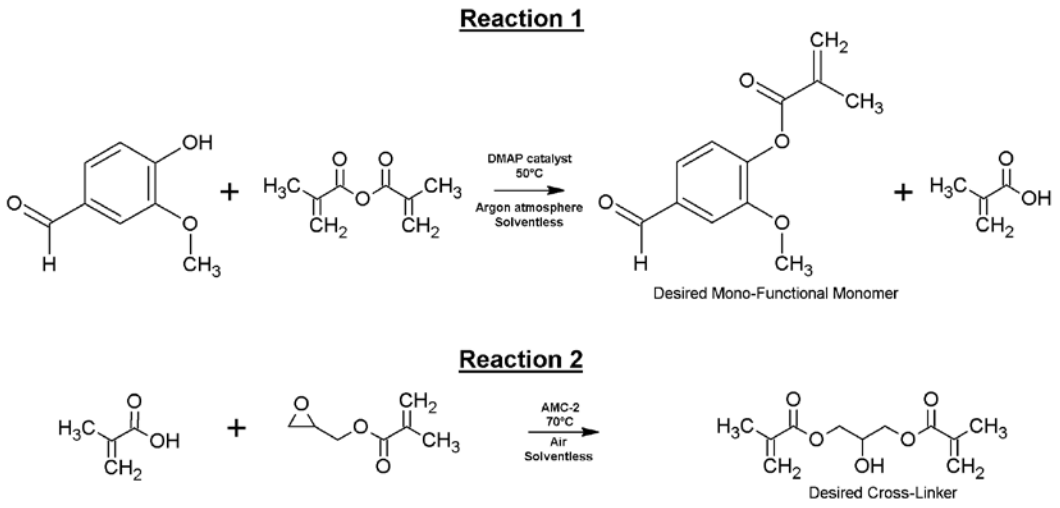

Fig. 112 Two-part reaction scheme to produce a resin that contains a 1:1 mole ratio of MV (desired monofunctional monomer of reaction 1) and glycerol dimethacylate (GDM, desired cross-linker of reaction 2). The methylcrylic acid (MAA) produced in reaction 1 is consumed in reaction 2.

The methacrylated vanillin-glycidyl dimethacrylate (MVGDM) resin had a low extent of cure (~67% vs. ~80% for VE/styrene) (Fig. 113) yet had high thermomechanical properties, with T_g of approximately 155 °C (Fig. 114).

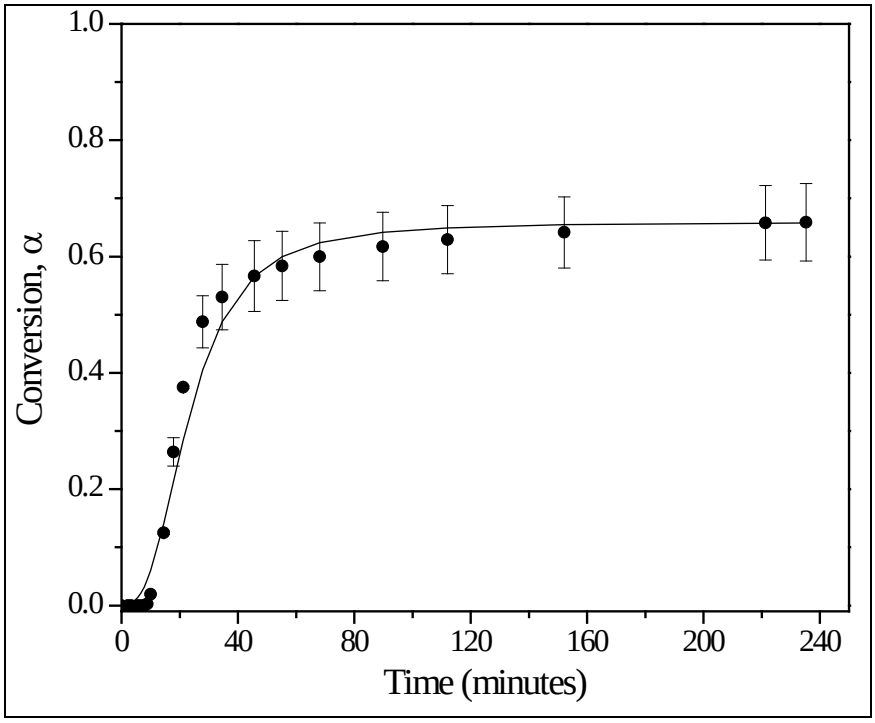

Fig. 113 The conversion as a function of time for the cure of MVGDM resin. Samples were cured at 70 °C for 4 h and then postcured at 130 °C for 2 h. Autocatalytic kinetic model fit is shown as the solid black line.

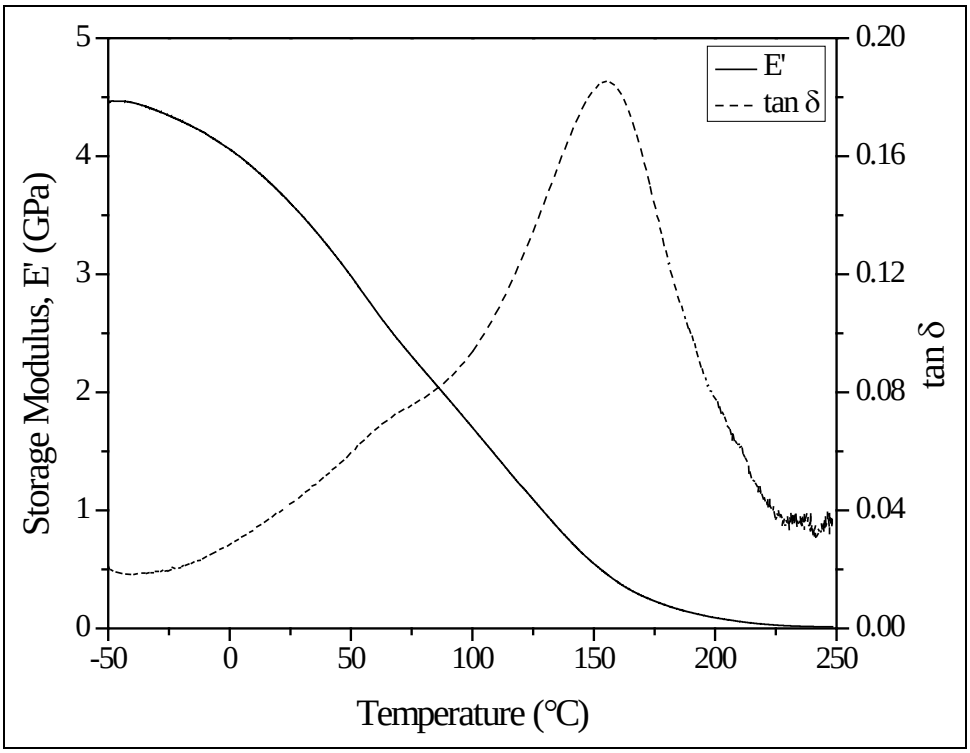

Fig. 114 Storage modulus (E') and tan δ of MVGDM as a function of temperature

Pyrolysis of lignin is likely to be used to derive the LMCs. Rather than using costly separation techniques to separate the individual components, similar hydroxyl-containing compounds can be used, as shown in Fig. 107, to make highly biobased resins. Table 18 shows the high biobased atomic efficiency of these lignin-based resins. Figure 115 shows polymers based on the MBO relative to that of VE/styrene resins. Aside from the different color, the resins are hard and rigid and appear very similar to the touch.

Table 18 Atom economies and environmental (E) factors of the chemical reactions used in our lab to synthesize the MBO, 1:1 VE828:MBO, and 1:1 VE828:St thermosets

Chemical Reaction	Atom Economy (%)	Environmental (E) Factor
Phenol Methacrylation	48.5	56
Guaiacol Methacrylation	52.7	61
Creosol Methacrylation	54.5	65
4-Ethylguaiacol Methacrylation	56.1	69
4-Propylguaiacol Methacrylation	57.6	74
Catechol Methacrylation	41.7	40
4-Methylcatechol Methacrylation	43.0	42
Epon 828 Methacrylation	100	~ 0
MBO Polymerization	100	~ 0
1:1 VE828:MBO Polymerization	100	~ 0
1:1 VE828:St Polymerization	100	~ 0

MBO 1:1 VE828:MBO 1:1 VE828:St

Fig. 115 MBO (left), 1:1 VE828:MBO (middle), and 1:1 VE828:St (right) thermosets

4.4.4 Conclusions

Lignin is a copious paper and pulping waste product that is primarily burned for energy recovery. Despite being considered intractable, novel methods to selectivity that break down lignin into valuable, lower-molecular-weight chemicals, often referred to as LMCs, are being developed. The major highlights of the research to date are as follows:

- LMCs, vanillin, guaiacol, and eugenol have been successfully methacrylated in modest yields (85.5% ± 4.5%).
- MV was a solid at room temperature while MG and ME were low-viscosity liquids (17 and 28 cP, respectively) at room temperature.

- MG and ME were successfully blended with VE828 with the majority of the resin mixtures having room temperature viscosities acceptable for liquid molding applications (<1,000 cP at 25 °C).
- Relative to styrene, the volatilities of MG and ME were shown to be much lower, ultimately showing that they have potential to be environmentally friendly, low-VOC reactive diluents.
- Homopolymerizations of MG and ME produced transparent and hard polymers that have Tg's (92 and 103 °C) that are similar to polystyrene (100 °C) and poly(methyl methacrylate) (104 °C).
- VE828:MG and VE828:ME cured resins were shown to have T_g's (via DSC and DMA) and room temperature storage moduli values comparable to VE828:St cured resins. The molecular weights between cross-links of cured resins containing ME were higher than cured resins that contained MG and St, indicating that ME partially acts as a cross-linker. This was further confirmed via in situ FTIR cure kinetics studies, which showed that a significant percentage of ME allyl groups polymerize during curing.
- TGA studies of the cured VE828 resins showed that the polymers containing MG and ME have comparable thermal resistivity to polymers containing styrene, with VE828:MG polymers exhibiting a slightly lower thermal resistivity than VE828:ME polymers.
- A low-viscosity polymer resin consisting of a 1:1 mole ratio of MV to GDM was synthesized using a 2-step, one-pot reaction scheme. The reaction scheme used the renewable, lignin-derived chemical vanillin and potential biobased reactants methacrylic anhydride and glycidyl methacrylate. Additionally, the reaction scheme generated no byproducts, required small quantities of catalyst and relatively low reaction temperatures, and produced the biocompatible cross-linking agent GDM. Resin curing generated a hard transparent thermoset that had a broad glass transition and T_g = 155 °C (based on the tan δ maximum). An overall fractional conversion of monomer C=C to polymer -C-C- during a cure of 0.78 was elucidated from an FTIR cure study, while TGA revealed a 2-stage thermal decomposition profile with a Tmax occurring at 426 °C. Overall, a potentially 100% biobased resin was synthesized for use in composite applications and, when cured, had thermogravimetric and thermomechanical properties to commercial VE resins. However, optimization of cure and postcure temperatures and durations as well as initiator concentration is recommended to improve overall conversion, thus reducing the concentration of unreacted monomer that could potentially leach into the environment.

- MBO composed of a mixture of various lignin model compounds similar to that derived from lignin pyrolysis has excellent mechanical and thermal properties while having very high bio-efficiency.
- Separation of reaction products to remove unreacted and side-products from the methacrylated lignin compounds results in significantly higher-performing resins

4.5 Synthesis and Characterization of Vanillyl Alcohol (VA)–Based Thermosetting Epoxy Resins

This section has been reported in a master's thesis and has been published in *ACS Sustainable Chem. Eng.* Thus, we refer the reader to these documents for more details although a summary is provided below.

Lignin is a natural and abundant renewable material composed of crosslinked phenylpropenyl units that when strategically depolymerized could potentially yield renewable biobased aromatic building blocks for applications in high-performance resins. Vanillyl alcohol (VA), a lignin derived aromatic diol, is a potential platform chemical for the production of renewable bisphenols and epoxy thermosets. A new biobased bisphenolic analogue, bisguaiacol (BG), was synthesized via electrophilic aromatic condensation of VA and guaiacol, from which diglycidyl ether of BG (DEGBG) was prepared. In addition, 2 biobased diepoxy monomers were synthesized from VA (DGEVA) and gastrodigenin (DGEGD). All biobased epoxies were characterized via ^{1}H NMR, ^{13}C NMR, FTIR, mass spectrometry (MS), and GPC. DMA of DGEBG, DGEVA, and DGEGD, blended with a commercial BPA-based epoxy resin and cured with a diamine, was conducted to determine the effect of the methoxy moiety on polymer properties. The thermomechanical results indicate that the presence of the methoxy lowers the T_g, yet increases the glassy storage modulus at 25 °C in cured epoxy-amine systems.

- Hernandez ED. Synthesis and characterization of vanillyl alcohol based thermosetting epoxy resins [master's thesis]. [Glassboro (NJ)]: Rowan University; 2015 Aug.
- Hernandez ED, Bassett AW, Sadler JM, La Scala JJ, Stanzione JF. Synthesis and characterization of bio-based epoxy resins derived from vanillyl alcohol. ACS Sustainable Chem Eng. 2016;4(8):4328–4339.

4.6 Bisguaiacol Polymers

Results of this work have been published in the following patent applications and in the following thesis:

- Reno K, Stanzione JF, Sadler JM, Hernandez E, La Scala JJ, Wool RP. Bisphenol alternatives derived from renewable substituted phenolics and their industrial application. PCT/US2015/032583, 2015 May 27.
- Reno K, Stanzione J, Sadler J, La Scala J, Wool R. Bisphenol alternatives derived from renewable substituted phenolics and their industrial, application. US Provisional Patent 62,003,115. 2014 May 27.
- Hernandez ED. Synthesis and characterization of vanillyl alcohol based thermosetting epoxy resins [master's thesis]. [Glassboro (NJ)]: Rowan University; 2015 Aug.

4.6.1 Introduction

BPA is a major component in many plastic materials including polycarbonates, plastic bottles, epoxy resins, adhesives, VEs, and various food packaging. The impact of replacing BPA with a nontoxic and biobased alternative would be far-reaching and drastically reduce the dependence on petrochemical reserves and the associated price fluctuations/environmental impacts. At an annual global production rate of approximately 6.5 billion pounds worth $13.1 billion in 2010,[113,114] BPA is used extensively to synthesize high-performance plastics such as epoxy resins, VE resins, and polycarbonates.[114–119] BPA is synthesized industrially through the condensation of acetone with 2 equivalents of phenol. This reaction is catalyzed by cation exchange resins such as Dowex and Amberlyst.[120,121]

BPA is one prominent endocrine disruptor chemical that mimics estrogen in vivo and can interfere with early reproductive development and cause irreversible physical changes. Therefore, designing sustainably sourced, less-toxic BPA alternatives is desirable. In our studies for a search for a BPA replacement, we synthesized bisguaiacol F (BGF) as a potential BPA alternative from 2 lignin model compounds, VA and guaiacol.[118,122] Lignin is a promising feedstock for aromatic monomers, as the paper and pulping industry produces 70 million tons a year as a waste product, and can be depolymerized into useful aromatic compounds.[123–125] Significant improvements in lignin pyrolysis, solvolysis and thermolysis have been made in the past 10 years, and the potential use of lignin as a BPA replacement is now much enhanced.[126] We are interested in using lignin pyrolysis products including the functionalized phenolics, as shown in Fig. 116.[127]

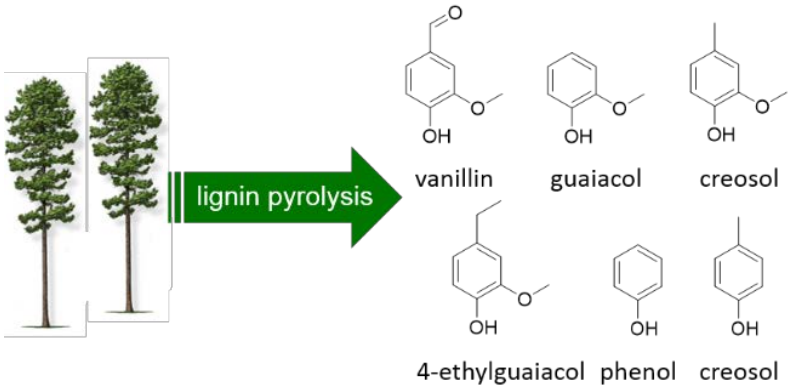

Fig. 116 Kraft lignin pyrolysis products[128]

The food (soup, vegetables) and drink (e.g., Coke, Pepsi, beer cans) industries are rapidly abandoning BPA because of the environmental damage potential and currently do not have a suitable replacement with comparable mechanical and thermal properties. The leading industry (Pittsburgh Plate and Glass Company) in industrial coatings has signed a nondisclosure agreement with the primary investigator in support of this research. The wind energy industry alone would consume 27 billion kilograms of BPA-based composite resins to construct 10^6 wind turbines, which would address about 10% of the global energy needs (15 TW). China, as of 2014, leads the world in wind energy production and has an ambitious plan to address most of its energy needs (~5 TW) with the construction of about 300,000 turbines. Since this future application in renewable energy generation is more than 5 times the global supply of BPA-based VE and epoxy resins, the sustainable replacement of these resins with nontoxic materials from renewable resources with comparable thermal and mechanical properties indeed represents a major intellectual challenge. The high-volume sustainability supply problem is further complicated by the automotive companies' desire to enhance fuel efficiency (50 mpg by 2025) by changing from a metal to a lightweight composite materials platform using extensive new amounts of BPA-based epoxies and thermoplastics.[129]

A novel family of bisguaiacol compounds can be synthesized from functionalized aromatics recovered from lignin (Fig. 116), as shown in Fig. 117. For example, BGF is synthesized from guaiacol and the reduced form of vanillin (VA), through an acid-catalyzed condensation reaction. Guaiacol and VA are environmentally benign and relatively nontoxic, which are desirable attributes in designing green reactions.[130] We use cation resin exchange resins, such as Dowex DR-2030, to catalyze this reaction and increase selectivity of the desirable *p,p*-BGF product (Fig. 117).[120,121,131,132] An example reaction scheme is shown in Fig. 118 for the synthesis

of BGF, and similar reaction conditions will be used to synthesize other bisguaiacols.

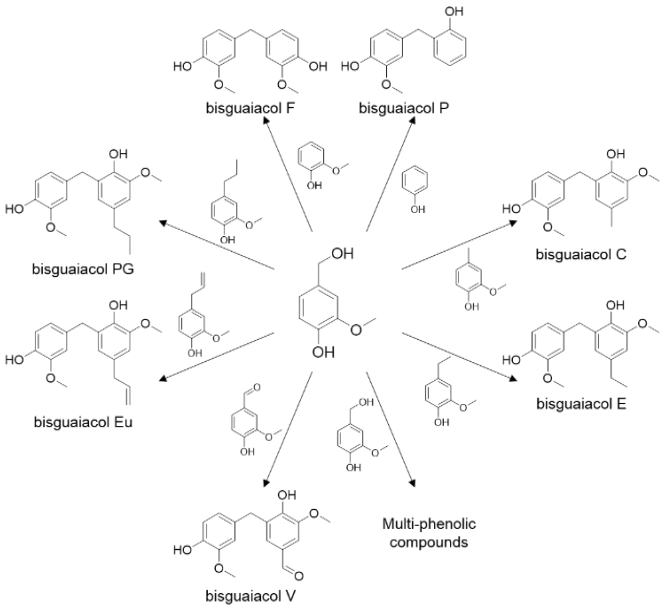

Fig. 117 Bisguaiacol monomers and their reactants. Additional monomers can be synthesized from other renewable functionalized aromatics such as phenol and syringol derivatives.

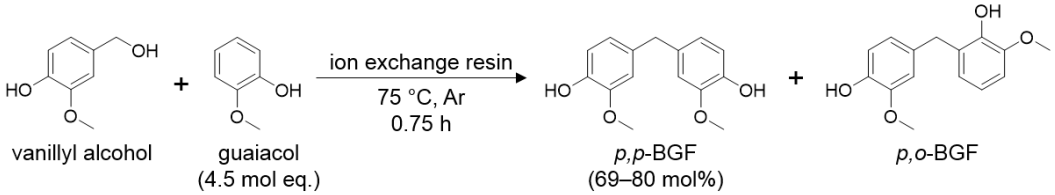

Fig. 118 BGF is synthesized from VA and guaiacol through an acid-catalyzed electrophilic aromatic substitution reaction. This reaction produces 2 regioisomers, *p,p*-BGF and *p,o*-BGF.[133]

4.6.2 Experimental

Exploration into the synthesis of bisguaiacol compounds began with BGF and used reaction conditions similar to the work by Harvey et al. for the synthesis of bisphenol compounds.[132] Mineral acid catalysts in a biphase system under reflux for multiple hours were used. However, these reaction conditions are undesirable for facile industrial synthesis of commodity chemicals. Therefore, we began exploring the use of solid acid catalysts such as those used in the synthesis of BPA with success and began using Dowex DR-2030 hydrogen form (see Table 20 for properties).[122] When these results were first presented at the 247th American Chemical Society national meeting, large amounts of water, energy, time, and

catalyst were required. The reaction was run in a biphase system, under reflux for 6 h, with 2.5 molar equivalence of guaiacol and included catalyst loadings of 70 wt% of VA. Pure BGF was recovered through many serial extractions and recrystallizations from hexanes, resulting in significant loss of product. Overall, this reaction scheme was inefficient and inappropriate for industrial scale applications.

Through reaction condition optimization, we have increased BGF yield and decreased the production of undesired high-molecular-weight, colored byproducts. This has been achieved by performing the reaction in solventless conditions, decreasing the reaction temperature to 75 °C and reaction time to 45 min, and performing the reaction in an inert atmosphere as shown in Fig. 118. To drive the reaction toward production of BGF over high-molecular-weight products, the molar equivalence of guaiacol was increased from 2.5 to 4.5. All of these factors collectively increased product yields to 60 mol%, which we plan to improve considerably in this research. These reaction conditions facilitate the ability to perform these reactions at approximately 100-g batch scales, an indication of ease of scaling from benchtop to pilot plant production at low cost. To promote easier recovery and the reuse of unspent guaiacol, guaiacol is vacuum-distilled from the crude reaction mixture before further purification through recrystallizations from heptane.[118]

Preliminary exploration of other bisguaiacols shown in Fig. 117 show promise of facile synthesis as summarized in Table 19. These reactions were performed with a co-reactant molar equivalence of 6 with a catalyst loading of 20 wt% relative to VA at 75 °C with the exception of bisguaiacol V. The reaction temperature of bisguaiacol V was increased to 85 °C, above the melting point of vanillin, to promote homogenous mixing and increase solubility of VA. As shown, regardless of shorter or longer reaction times, as the functionality of the R_1 group increases in size, the molar percentage yield of the bisguaiacol generally decreases, which may indicate that bulkier functionalities sterically hinder the substitution of VA onto the co-reactant. As expected and similarly to BGF, bisguaiacol P (BGP) has 2 regioisomers due to the strong directing hydroxyl group, *p,p*-BGP and *p,o*-BGP. The molar percentage of VA reacted relative to the overall bisguaiacol yield are not significantly different for the synthesis of bisguaiacol E, bisguaiacol PG, and bisguaiacol V, indicating there are limited side reactions occurring to form unwanted side products. However, bisguaiacol C, BGP, and bisguaiacol Eu appear to have significant side product formation as their molar percentage of VA reacted is greater than the desired product yield. An increase in the amount of co-reactant present compared to VA is likely to reduce the synthesis of side product formation.

Further reaction optimization and pure product characterization is required to determine if these bisguaiacols are feasible BPA alternatives.

Table 19 Reaction conditions, molar percentage of VA reacted, and yields of bisguaiacols as determined by ^{1}H NMR

co-reactant	bisguaiacol	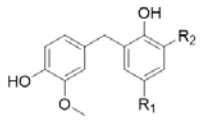	reaction time (h)	mol% VA reacted	bisguaiacol mol% yield
creosol	C	R_1=CH_3, R_2=OCH_3	1.5	100	86
phenol	P	R_1=H, R_2=H	1.5	100	82 (57 mol% *p,p*-BGP)
4-ethylguaiacol	E	R_1=CH_2CH_3, R_2=OCH_3	1.5	36	30
eugenol	Eu	R_1=$CHCHCH_3$, R_2=OCH_3	1.25	66	35
4-propylguaiacol	PG	R_1=$CH_2CH_2CH_3$, R_2=OCH_3	1.25	13	13
vanillin	V	R_1=CHO, R_2=OCH_3	1.25	26	21

The quantity, capacity, and porosity of the catalyst used in the synthesis of bisguaiacols are important to promote high-bisguaiacol yields, minimize energy inputs and reaction times, and reduce side product formation. Reaction conditions for Dowex DR-2030 have been optimized as summarized previously. Amberlyst 15 hydrogen form was used to synthesize BGF on small scales to determine the rage of solid acid catalysts capable of producing bisguaiacols with minimal side reactions. Important catalyst properties of Amberlyst 15 compared with Dowex DR-2030 are summarized in Table 20. While the 2 catalysts have the same sulfonic acid functionalized styrene-divinylbenzene matrix and similar porosities and capacities, the particle size and moisture content differ. A decrease in moisture content should increase *p,p*-BGF selectivity, making Amberlyst 15 preferred over Dowex DR-2030.[121,131]

Table 20 Property comparison of Dowex DR-2030 to Amberlyst 15

	Dowex DR-2030 hydrogen form	Amberlyst 15 hydrogen form
matrix	sytrene-divinylbenzene	sytrene-divinylbenzene
acid group	sulfonic acid	sulfonic acid
particle size (μm)	< 1190	< 300
porosity (cc/g)	0.33	0.4
capacity (meq/g by dry weight)	4.7	4.7
moisture content (%)	< 3	< 1.6

4.6.3 Reaction Conditions

Preliminary, small scale tests of Amberlyst 15 in the synthesis of BGF are shown in Table 21. At low reaction temperatures (<75 °C, A1–A4), there is little to no reaction, as quantified by the molar percentage of VA reacted. VA is less soluble at these temperatures in the co-reactants and readily precipitates out of solution, indicating the lack of reaction could be due to insufficient mixing. While the catalyst decreases the activation energy to promote the formation of BGF, the activation energy may be too large at these temperatures to overcome, even in the presence of a strong catalyst. At a reaction temperature of 75 °C, a catalyst loading of 1.0 wt% relative to the amount of VA (A5 and A6) was insufficient at promoting the reaction, resulting in little to no reaction. The importance of reaction time is shown in reactions A7 and A8, where increasing the reaction time to 1 h, increases the amount of VA reacted by a factor of at least 2.5. However, with Dowex DR-2030, at a catalyst loading of 10 wt% at 75 °C (the reaction conditions of A8), 100% of VA has reacted, indicating that particle size may affect the efficiency of the catalyst. While Amberlyst and Dowex have the same capacity, crowding of the acid cites on the smaller Amberlyst particles may decrease efficiency. To determine efficiency as a function of particle size and to optimize particle size and capacity, further experiments must be performed by systematically varying particle size and capacity.

Table 21 Reaction conditions and molar percentage of VA reacted using the catalyst Amberlyst 15

reaction	cat. (wt%)	temperature (°C)	reaction time (h)	mol% VA reacted
A1	1.0	45	0.5	~0
A2	1.0	50	1.0	~0
A3	10	45	0.5	~0
A4	10	50	1.0	~0
A5	1.0	75	0.5	~0
A6	1.0	75	1.0	~0
A7	10	75	0.5	<5
A8	10	75	1.0	13

4.6.4 Control of BGF Regioisomers and Preliminary Results

The condensation of guaiacol and VA produces 2 regioisomers, *p,p*-BGF and *p,o*-BGF, as shown in Fig. 119. Two regioisomers are present due to the strongly activating hydroxyl group on VA, which directs the substitution of activated VA onto guaiacol in the *ortho*- and *para*- positions, with *para*- being favored. Relatively pure fractions were recovered through differences in crystallization kinetics and flash column chromatography. The 2 regioisomers were confirmed by

2-D heteronuclear single quantum coherence (HSQC) spectroscopy NMR as shown in Fig. 119.

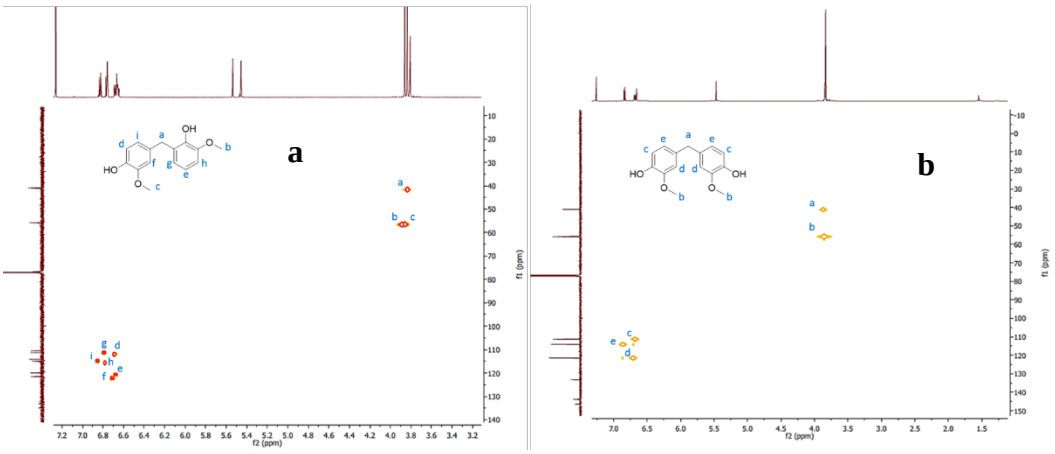

Fig. 119 HSQC 2-D-NMR analysis of a) pure *p,o*-BGF and b) *p,p*-BGF; proton assignments in blue

The relative ratio of the regioisomers influences the molecular symmetry through steric and intermolecular interactions between polymer chains to alter macromolecular properties such as the T_g, thermal stability, chemical resistance, and mechanical properties. Recently work by Liu and Ishida[134] studied the effect of BGF regioisomers on T_g and thermal stability of benzoxazines, in which the ortho-ortho isomer yielded higher-performing polymers than the para-para isomer, indicating that the study of isomer effects of BGF is critical. Similar to the synthesis of BPA, selectivity for the *p,p*-BGF regioisomer over *p,o*-BGF can be tuned by reaction time, temperature, and the amount of water present.[121,131] We will continue investigating these effects through a design of experiments to simultaneously probe multiple dependent variables.

Property differences in the 2 regioisomers are also evident in the melting point depression as shown in the DSC traces in Fig. 120 for 2 samples with different regioisomer ratios, 84- and 95-mol% *p,p*-BGF. The 95-mol% *p,p*-BGF sample has a melting temperature (T_m) of 97 °C and crystallized from the melt upon cooling. By contrast, the 84-mol% *p,p*-BGF sample exhibits a T_m of 91 °C and a cold crystallized exotherm at 47 °C. The thermal transitions in the 90-mol% *p,p*-BGF are a result of the reduced recrystallization kinetics from the melt upon cooling. Also, the co-crystals inhibit uniform crystal packing and, therefore, lowering T_m of the mixture of regioisomers.

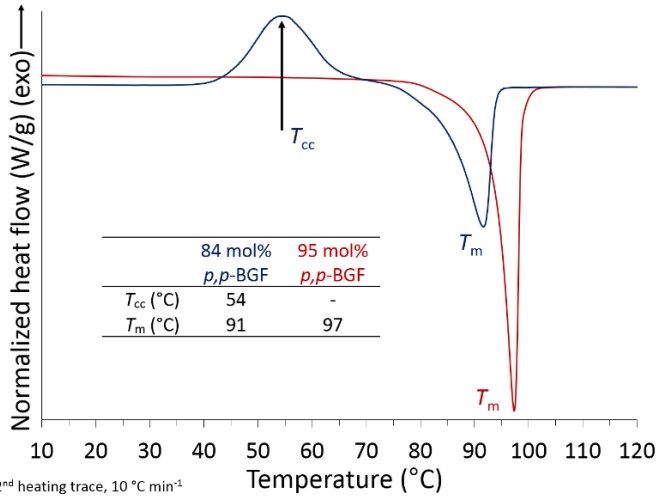

Fig. 120 Second DSC heating traces of BGF samples with different regioisomer molar ratios at a heating rate of 10 °C/min

Patent literature suggests that the amount of water present during the synthesis of BPA considerably affects the regioisomer selectivity. By removing water produced by the condensation of phenol and acetone, *p,p*-BPA selectivity increases.[121,131] Preliminary results indicate that 2 different techniques of removing water during the reaction affect the regioisomer selectivity compared with a reaction where no water was removed, as summarized in Table 22. Under the described reaction conditions, without removing water, 100-mol% VA conversion and a *p,p*-BGF selectivity of 69 mol% was achieved. The addition of sodium sulfate anhydrous in excess resulted in 67-mol% VA conversion and a selectivity of 74-mol% *p,p*-BGF. In comparison, the use of a Dean-Stark apparatus resulted in 8-mol% conversion of VA and a selectivity of 80-mol% *p,p*-BGF. The Dean-Stark appartus was inefficient at removing the majority of water produced during the reaction, but further optimization of the reaction setup will allow controlled increase of water removal and is expected to further increase *p,p*-BGF selectivity. As these preliminary data indicate, the regiosiomer selectivty can be controlled by the amount of water removed, with *p,p*-BGF synthesis favored with the removal of water. However, it appears there is a tradeoff in conversion with greater selectivity. Additional experimentation and exploration will allow these phenomena to be decoulpled and studied independently and dependently, such as drying the catalyst before use.

Table 22 Effect of water removal on regioisomer content and VA conversion

	p,p-BGF mol%	vanillyl alcohol conversion (mol%)
normal reaction conditions	69	100
With Dean-Stark apparatus	80	8
Sodium sulfate anhydrous	74	67

In addition to controlling regioisomer selectivity by tuning the reaction conditions, preliminary experiments suggest that various regioisomers can be separated through recrystallization. Qualitatively, the presence of different crystalline morphologies is evident when the BGF product is recrystallized from hot heptane. Further investigation of the thermal behavior and crystal structures of the regioisomers will allow for greater control over the recovery of the desired *p,p*-BGF and/or *p,o*-BGF product. Overall, the dependence of the thermal behavioral on the relative amount of *p,o*-BGF present provides a chemical handle for tuning the polymer's chemical and thermomechanical properties.

4.6.5 Difunctional Monomers and Polymers from Bisguaiacols

Currently, BPA is used in a variety of diverse polymer applications including thermosets (epoxies and VEs) and thermoplastics (polycarbonates, polyesters). For the BPA alternatives to be industrially relevant, bisguaiacols must be able to partake in the same chemical reactions in a controlled manner. Our research compares physicochemical and thermomechanical properties of bisguaiacol and other bisguaiacol-derived monomers with analogues synthesized from BPA. The functionalization chemistries include amination, esterification with methacrylates, and epoxidations, resulting in diamines, DMs, di-epoxies, diglycidyl ethers of bisguaiacol, and VEs of diglycidyl ether of bisguaiacol, as summarized in Fig. 121. Pure bisguaiacols and mixtures of bisguaiacols derived from bio-oil samples are synthesized and characterized as high-performance and commodity chemicals, respectively. The synthesized monomers a quantitatively compared with BPA and its derivatives through characterization techniques including NMR, DSC, TGA, DMA, tensile testing, and toxicity testing.

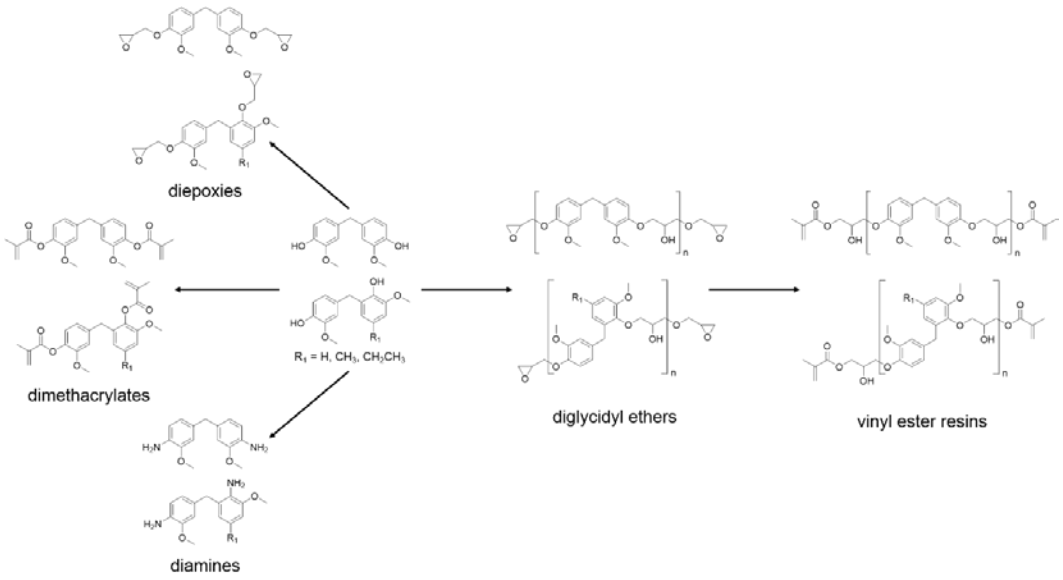

Fig. 121 Simplified reaction scheme summarizing chemistries that will be used to determine application diversity of the new bisguaiacol library

Subsequent polymerization of the synthesized monomers for thermoplastics and thermoset applications as proposed in Fig. 122. VE resins and composites will be synthesized from VEs and bisguaiacol DMs and when reacted with reactive diluents. Historically, styrene is used as a reactive diluent, but is considered a HAP and a human carcinogen. Therefore, we will explore the use of biobased styrene alternatives developed by the Wool lab as reactive diluents as well.[133,135,136] Bisguaiacol diepoxies and diglycidyl ethers of bisguaiacols, when cured with aliphatic and aromatic diamines, yield epoxies and adhesives for applications such as epoxy beverage can linings and adhesive automotive coatings. Curing the epoxy resins with bisguaiacol diamines may provide biobased high-performance epoxies. Approximately 70% of BPA produced is used to synthesize polycarbonates for shatter-resistant applications.[113]

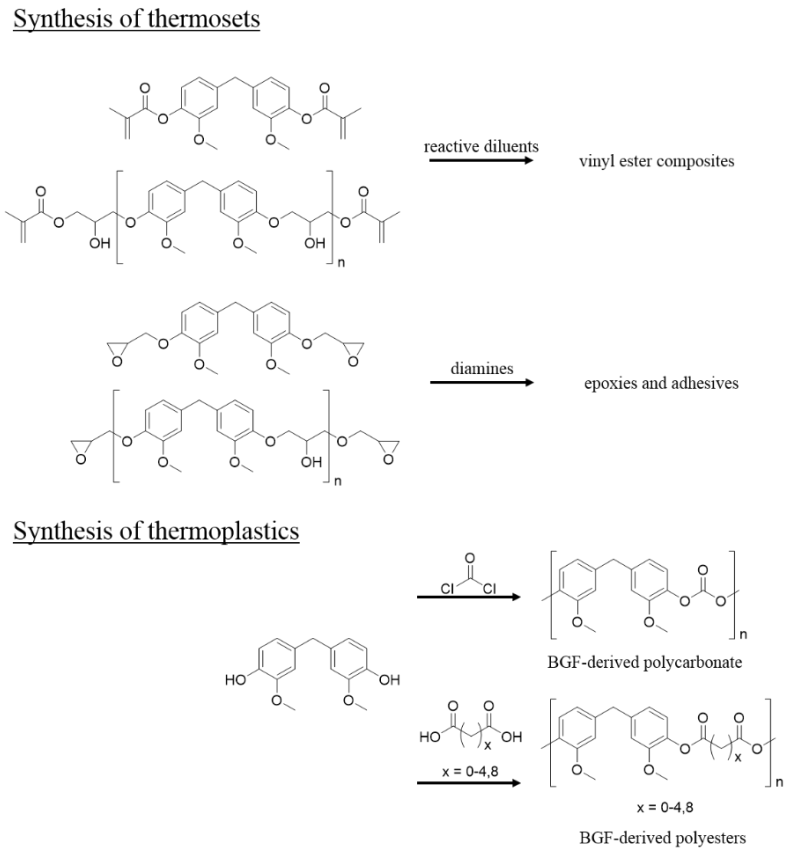

Fig. 122 Proposed thermoplastics and thermosets synthesized from bisguaiacols in which *p,p*-BGF is used as an example

We propose using bisguaiacol monomers to synthesize biobased polycarbonate analogues. However, polycarbonates are synthesized by the polycondensation of BPA and phosgene, a highly toxic, corrosive, and categorized as a schedule 3 controlled gas by the Organization for the Prohibition of Chemical Weapons.[137] "Greener" syntheses of polycarbonate with carbon dioxide or with diphenyl carbonate are under investigation and may prove beneficial for this research.[138,139] Other applications of bisguaiacols include the synthesis of biobased polyesters that will employ diacid comonomers.

Functionalization of BGF began with the synthesis of BGF-DM using established esterification reactions with methacrylic anhydride.[135,136,140] Thermosets were subsequently polymerized by free-radical polymerization with 50-wt% styrene initialized with Trigonox 239 (1.5 wt%) by a 2-step curing cycle in an inert atmosphere: 2 h at 90 °C then 2 h at 120 °C. Vinyl ester 828 (VE 828, Fig. 123), a common BPA-derived industrial VE used in high-performance composites, was used for comparison and cured under identical conditions. TGA (Fig. 123) indicates that maximum degradation temperatures (T_d's) for VE 828 and BGF-DM

thermosets are relatively similar and significantly above normal processing conditions. In contrast, the T_g of BGF-DM thermoset was determined to be 50 °C above that of the VE 828 thermoset from first heating DSC traces, which is expected based on the lack of flexibility in the backbone relative to VE 828. The presence of a curing exotherm in the BGF-DM DSC trace around 120 °C suggests that upon additional heating, further polymerization occurred, indicating that the curing procedure is inappropriate for this system. Optimization of the curing conditions, such as longer curing times at 120 °C or higher curing temperatures, will likely increase T_d and T_g of BGF-DM thermosets. Future synthesis of a BPA DM under the same polymerization conditions will provide a direct comparison of BGF with BPA. Similarly, BGF analogues of VE 828 will be synthesized as another direct comparison of BGF with BPA in methacrylate-based thermosets. Preliminary thermal property results are promising for the application of BGF as a BPA alternative for thermoset applications in composite resins.

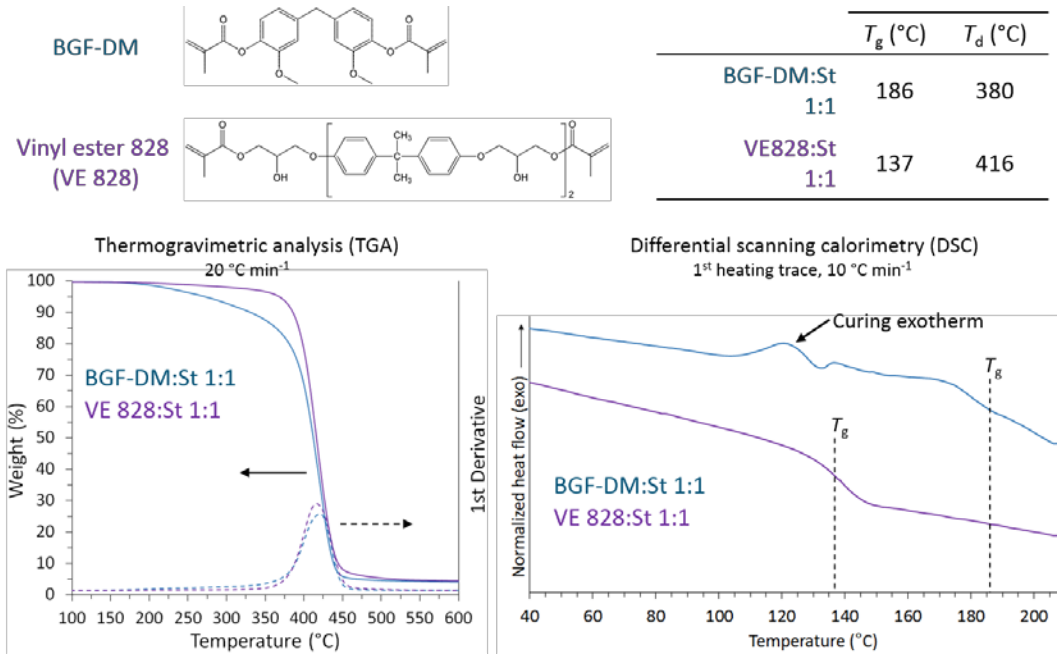

Fig. 123 Thermomechanical characterization of BGF-DM cured with styrene compared with VE 828, an industrially relevant BPA-derived VE

Industrial applications of diglycidyl ethers of BPA and BPA diepoxies include epoxies for food and drink can linings and adhesives. Industrial leaders in epoxy coatings have expressed interest in BGF analogues of these epoxy precursors. Diepoxies and diglycidyl ethers of BGF will be synthesized using established epoxidation reactions for biobased epoxies.[141,142] Upon further esterification reactions, VE resins of BGF will be generated as VE resin alternatives. VE resins are important precursors to high-performance composite materials used to

manufacture products such as lightweight cars and wind turbines. Reactive diluents such as styrene are used to increase the molecular weight between crosslinks and increase fracture toughness. Ultimately, we will incorporate the styrene alternatives developed by the Wool group to provide a mostly renewable, high-performance VE resin system synthesized from lignin. Thermal (DSC [T_g] and TGA [T_d]) and mechanical (DMA and tensile testing) characterization of the thermosets will help to quantify the resulting properties of these BGF-based macromolecular systems compared with their BPA-based counterparts. Success will be determined by obtaining stable high-performance engineering materials with strength on order of 100 MPa, tensile moduli of 2–4 GPa, and T_g values greater than 100 °C.

Common laboratory polyester synthesis techniques will be used to synthesize our BGF macromolecules,[143–147] in which a 2-stage melt polycondensation reaction yield high-molecular-weight polyesters. The length of the aliphatic diacid comonomer provides the ability to tune polymer crystallinity, as percent crystallinity is directly proportional to aliphatic chain length.[148,149] Dicarboxylic acids of interest include oxalic, malonic, glutaric, adipic, and sebacic acids. High-performance polyesters can be synthesized from cyclic and bicyclic diacids including isosorbide, manitol, and 1,4-cyclohexanedimethanol.[117] The copolymerization of aromatic and cyclic monomers with aliphatic diacids or diols (1,3-propandiol) as spacers ultimately may improve fracture toughness and decrease brittleness.

Furthermore, we tune the thermomechanical properties of these novel polymers not only through the use of the different bisguaiacols, but through the manipulation of the BGF regioisomer ratio. The effect of incorporating BGF with various *p,o*-BGF contents will be examined in terms of reaction kinetics, reactivity ratios (functional group reactivity), and resulting macromolecular properties such as T_g, mechanical strength, and fracture toughness. By exploring the effect of *p,o*-BGF content on T_g, we can correlate regioisomer ratios that will optimize monomer purity/yield and macromolecular properties.

4.6.6 Toxicity Evaluation of Monomers and Polymers

4.6.6.1 TiPED Approach and Evaluation of Bisguaiacol

The determination of potential candidates for sustainable BPA alternatives involves a multitiered approach, including environmental, economical, and social considerations. To ensure social sustainability, the PIs consider toxicity and endocrine disruption potential testing of these novel chemicals paramount. The tiered protocol for endocrine disruption (TiPED) approach (Fig. 124) uses a combination of techniques to study endocrine disruption, including both in vitro

and in vivo testing, which has been proposed to guide the development of inherently safer materials by avoiding chemicals likely to disrupt the endocrine system.[150] The complex biology of endocrine disruption means that neither a single assay nor a single approach can be used to identify chemicals with environmentally destructive characteristics. To ensure responsible development and deployment of new chemicals, we will also provide a comprehensive evaluation on the environmental stability, fate, and transport characteristics of the monomers in soil and water media, as recommended by the EPA.

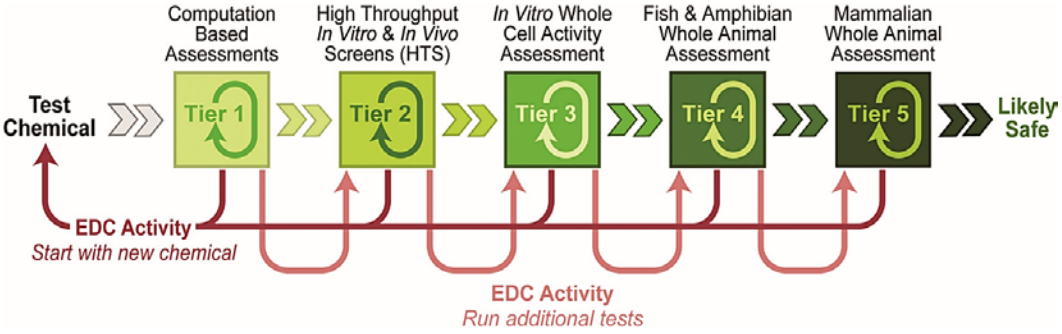

Fig. 124 TiPED approach to endocrine disruption testing, applied to the synthesis of less-hazardous biobased BPA alternatives, systematically increasing complexity[62]

4.6.6.2 Computational Methods: TiPED Tier-1 Methods and Results

The TiPED approach to endocrine disruption uses a computational assessment (Tier-1) to provide a preliminary screening assessment of new chemicals. Approaches to estimating toxicity include chemical reactivity analyses, physicochemical property estimations, quantitative structure-activity relationship analysis, and molecular docking simulations (MDSs). Current computational methods include physicochemical property assessment using Estimation Program Interface (EPI) Suite software and MDSs using a robust, accurate, user-friendly program developed by the Scripps Institute called Autodock Vina.[151] EPI Suite is a program based on group and bond contribution theory as well as structure-property correlations of known chemicals; it is funded by EPA to estimate physicochemical properties and environmental fate of novel chemicals.[152] Estimated properties include boiling point, vapor pressure, octanol-water partition coefficient (log K_{OW}), lethal concentration (LC50), bioaccumulation factors, and effective dose (ED50).

Unknown properties of the reactants used to synthesize bisphenols were estimated and compared to BPA's reactants, phenol and acetone, as shown in Table 23. Known properties were gathered from material safety data sheets provided by Sigma Aldrich and not estimated by EPI Suite. As expected, the boiling point of the substituted phenols is higher than phenol and acetone, with vanillin and VA being solids at room temperature. Similarly, vapor pressures are decreased by at

least a factor of 3 over phenol, a HAP. Lethal doses (LD50s) in rats and ED50s for daphnia over 48 h are reported as well to assess environmental and potential human impacts. EPI Suite does not estimate mammalian toxicity but readily estimates LC50 and ED50 for aquatic life. For mammalian toxicity, vanillin is less toxic by an order of magnitude compared with phenol, whereas creosol and guaiacol have similar LD50s. Reported EC50s and EPI Suite predictions suggest that vanillin, guaiacol, and creosol have similar if not slightly decreased aquatic toxicities than phenol. In contrast, 4-ethylguaiacol is predicted to be more toxic than phenol, and VA is predicted to be significantly less toxic than phenol by 2 orders of magnitude. These results and predictions indicate that the use of 4-ethylguaiacol should be limited in designing sustainable BPA alternatives, exemplifying that biobased does not necessarily mean nontoxic.

Table 23 Physicochemical properties of BPA and bisphenol reactants as reported by Sigma Aldrich Chemical and estimated using EPI Suite

	BPA reactants		Bisguaiacol reactants				
			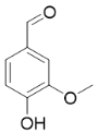	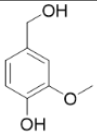		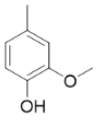	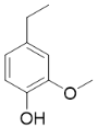
	phenol	acetone	vanillin	vanillyl alcohol	guaiacol	creosol	4-ethylguaiacol
boiling point (°C)	182	56	285	293 [a]	205	221	234
vapor pressure (Pa)	50	24,500	< 1	< 1 [a]	15	8 [a]	3 [a]
LD50 oral rat – (mg/kg)	317	5,800	3,300	-	520	740	-
EC50 – daphnia 48 h (ppm)	56	8,800	88	1,630 [a]	60	150	34 [a]

[a] Property estimated using EPI Suite™

Similarly, EPI Suite was used to estimate properties of BGF compared with BPA and summarized in Table 24. Log K_{OW} is calculated as a chemicals affinity for lipids over its affinity for water. These values may indicate the ability of a chemical to bioaccumulate or biomagnify when values are 2–6 and 3–6, respectively, but must only be used as guidelines.[128] BGF and BPA have similar log K_{OW} values, but BGF is less toxic aquatically by a factor of 10 compared with BPA. Further experimental testing is required to make definitive claims to the toxicity of BGF, but preliminary approximations indicate BGF is less toxic to aquatic life than BPA, and this is very promising for this research.

Table 24 Toxicity parameters for BGF compared with BPA

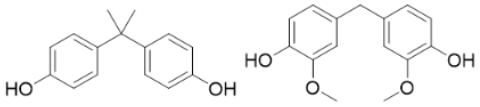

	BPA[a]	BGF[b]
Log K_{OW}	3.32	2.70
EC50 – green algae 96 h (ppm)	3	29
LC50 – fish 96 h (ppm)	5	50

[a] Properties reported by MSDS [b] Property estimated using EPI Suite™

Computational MDSs allow potential BPA alternatives to be screened in silico for the potential for binding to endocrine receptors, such as ERα (estrogenic) and AR (androgenic) by estimating the binding conformations and binding affinities. Models developed for drug screening are now available for studying endocrine disruption for chemicals used in polymer chemistry. Such computational methods allow for high-throughput screening of compounds. We chose to begin molecular docking simulations with AutoDock Vina, which estimates binding conformations and binding affinities through minimizing the chemical potential of the ligand (or chemical of interest) using an empirical scoring function. Preliminary work has been done to predict binding conformations and binding affinities for *p,p*-BGF for the ligand-binding domain of human ERα. The crystalline structure of hERα complexed with 17β-estradiol as reported by Eiler et al.[151] was downloaded from the Protein Database and used for these simulations. BPA and 17β-estradiol were used to optimize the search conditions for AVA, including reducing the search space to the native ligand-binding domain and verify results using the method outlined by Trott and Olson.[153] AutoDock Vina was run with a setting of 20 to find the optimal binding conformation.

The preliminary results of the molecular docking simulation are shown in Fig. 125 and Table 25. At first estimation, the binding affinity for the BGF monomers are substantially lower than BPA, which is an excellent outcome from these simulations and bodes well for the future success of this work.

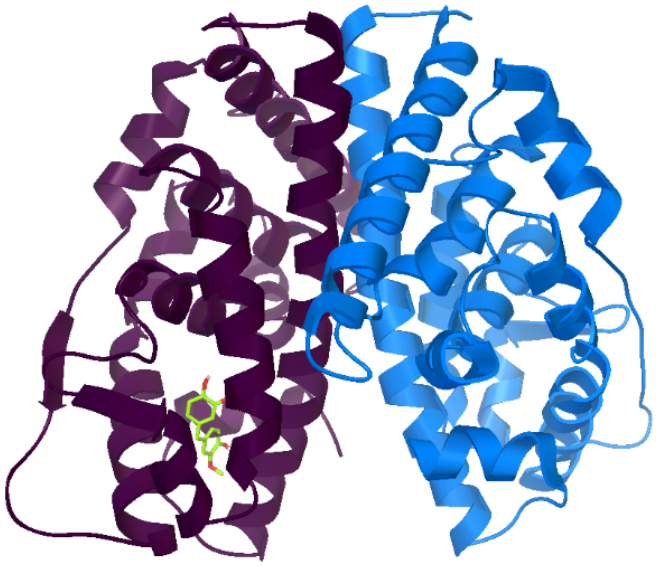

Fig. 125 Predicted binding conformation of BGF to ERα

Table 25 Binding conformations and binding affinities for 17β-estradiol, BPA, and BGF for ERα as simulated using Autodock Vina

	17β-estradiol	BPA	*p,p*-BGF	*p,o*-BGF
binding conformation in LBD	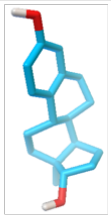	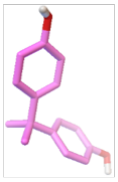	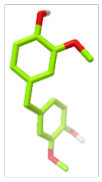	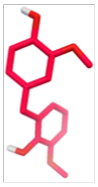
binding affinity (kcal/mol)	42	28	20	22

4.6.7 Summary and Conclusions

This work has resulted in the development of a replacement scaffold/core for BPA that we call BGF. This BGF core has demonstrated high-performance material properties and significantly reduced toxicity relative to BPA. Given the high visibility of BPA toxicity, it was not surprising to see significant interest from the media on these developments and thus the potential for technology transition seems high. As a result we have filed a US Patent Application and PCT Patent Application for this technology as listed in the beginning of this section.

4.7 Summary of Furoic Acid-Glycidyl Methacrylate: Synthesis and Characterization of a Novel Biobased Reactive Diluent as a Styrene Replacement

This work has been published in the following journal paper and only a summary of the work is provided herein:

- Sadler JM, Nguyen AP, Greer SM, Palmese GR, La Scala JJ. Synthesis and characterization of a novel bio-based reactive diluent as a styrene replacement. Journal of BioBased Materials and BioEnergy. 2012;6:86–93. http://www.ingentaconnect.com/content/asp/jbmb/2012/00000006/00000001/art00009?token=004d1c7dc4bd36d5512139412f415d7678255f45514a2f42384259253033294876c47b8945a83.

Recent years have seen a shift toward the use of composite materials in a number of applications because of their improved attributes when compared to traditional building materials. VE and unsaturated polyester resins require the use of reactive diluents, such as styrene and MMA, for liquid molding manufacture of composites. However, these diluents are HAPs and VOCs, and are emitted during every phase of production. This work focuses on the formulation of a novel biobased reactive diluents for VE resins in an effort to reduce emissions while maintaining the properties of styrene-based systems. A novel furanic reactive diluent, furoic acid glycidyl methacrylate (FA-GM), was synthesized from biobased starting materials and then blended with a VE cross-linker in order to study the potential as a styrene replacement. VE resin blends using FA-GM and another furanic reactive diluent were found to have higher viscosities (4-234 cP) and lower T_g's (82–100°C) relative to styrene-based vinyl esters.

The FA-GM was synthesized by reaction of furoic acid, a biobased product, and glycidyl methacrylate (Fig. 126). FA-GM could not be prepared in a manner analogous to methacrylated fatty acids by simple reaction of the fatty acid with glycidyl methacrylate in the presence of AMC-2 catalyst. When performed in this manner, there was significant amounts of starting reactants remaining, and the molecular weight of the resulting product increased significantly (Fig. 127). Instead, the reaction required glycidyl methacrylate with tetra-n-butylammonium bromide (Bu_4NBr) in acetonitrile at reflux for 4 h. The product then had to be separated using solvent extraction. Properly prepared FA-GM was blended with VE resins and had higher viscosities than other reactive diluents (Fig. 128). The polymer properties were lower than that of styrene-based resins but were higher than that of furfuryl methacrylate and methacrylated fatty acid resins (Fig. 129).

In all, this FA-GM molecule is not recommended for use for high-performance composites because of the resulting low polymer properties and high viscosities.

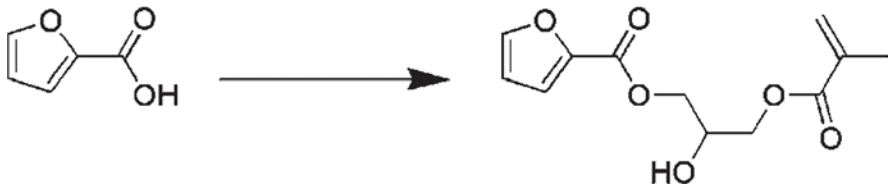

Fig. 126 Synthesis of FA-GM by reaction of furoic acid with glycidyl methacrylate with Bu_4NBr in acetonitrile at reflux for 4 h

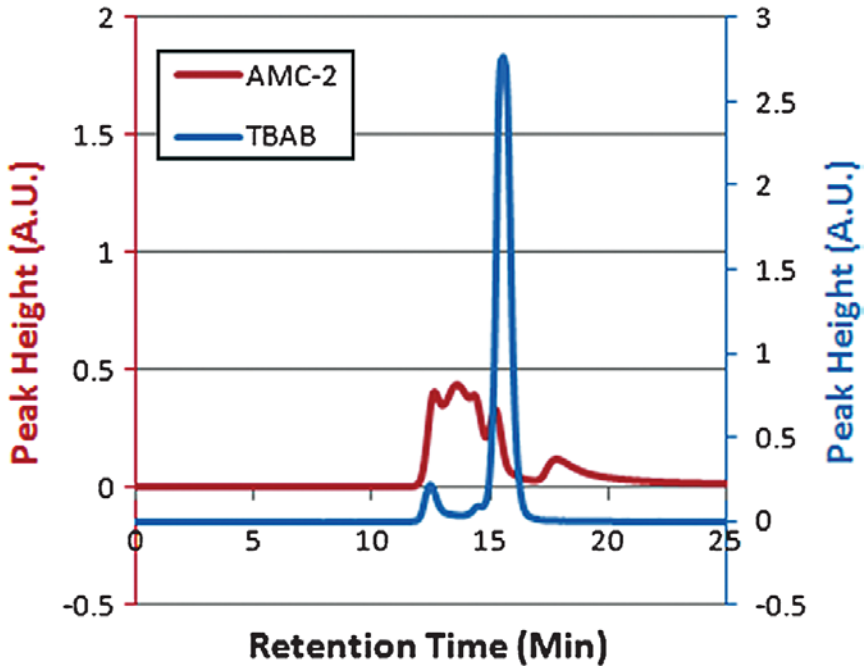

Fig. 127 SEC chromatogram comparison of products via Bu_4NBr catalyzed and AMC-2 catalyzed reactions (axis offset for clarity)

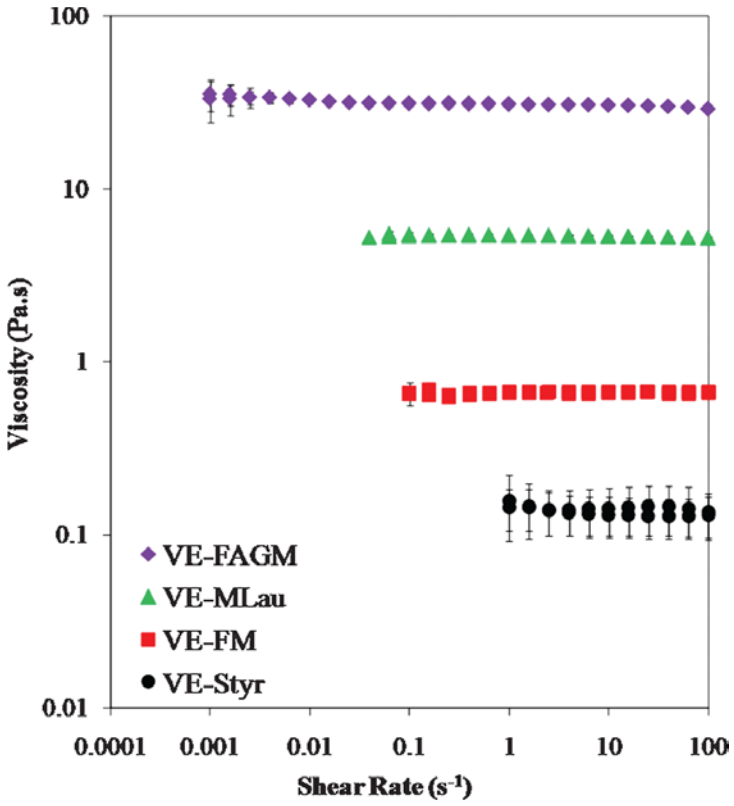

Fig. 128 Viscosities at 25 °C of vinyl resins with 35 wt% reactive diluent as a function of shear rate.

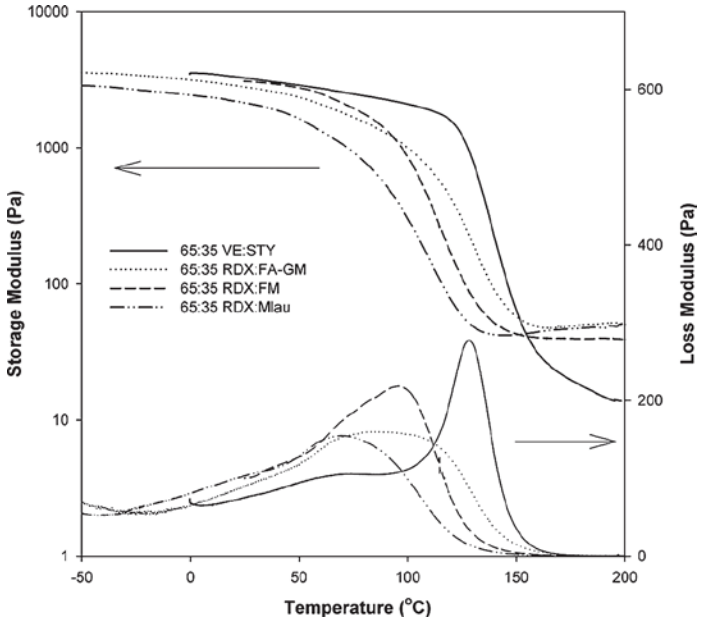

Fig. 129 Storage and loss moduli of vinyl resins with 35 wt% reactive diluent as a function of temperature

4.8 Initial Studies of Furan-Based Epoxy Cross-Linkers*

4.8.1 Introduction

Furan groups are aromatic and represent a potential biobased replacement for phenyl rings that are components of high-performance epoxy resins. This section examines initial methods to prepare furan-based epoxides and begins to develop structure-property relationships.

4.8.2 Experimental Details

4.8.2.1 Synthesis: Furan-Based Epoxy Was Synthesized Via Various Synthetic Routes

bHMF, epichlorohydrin, water (5 mL), and benzyl trimethyl ammonium chloride were put in a flask under nitrogen gas. The reaction was carried out at 100 °C for 5 h. Next, 40 wt% NaOH solution was added dropwise to the mixture while it was stirred at 100 °C for 2 h. The organic phase was extracted with ethyl acetate and washed with DI water several times. Ethyl acetate was evaporated by a rotary evaporator.

Dimethyl Formamide (DMF) Instead of Water. Based on the previous synthetic condition, only one reagent was changed. DMF replaced water to investigate the effects of these components on the synthesis. bHMF (20.5 g), epichlorohydrin (59.2 g), DMF (30 mL), and benzyl trimethyl ammonium chloride (1.18 g) were mixed and heated up to 100 °C. The reaction was conducted for 5 h. Next, 40 wt% NaOH solution (14 g) was added dropwise for 2 h.

Water Control. The control of water is an important factor because water can act as a promoter for this reaction and produce the by-product at the same time. Therefore, the least amount of water to obtain a high yield and minimize the by-product should be determined. bHMF (20.16 g), epichlorohydrin (70 g), water (0.5 mL, the optimal amount), and benzyl trimethyl ammonium chloride (2.9 g) were mixed and heated up to 100 °C. The reaction was performed for 5 h. Then, 40 wt% NaOH (19 g) was added dropwise for 2 h.

Scale-up of Furan-Based Epoxy. bHMF (100 g), epichlorohydrin (216.5 g), water (2.5 mL), and benzyl trimethyl ammonium chloride (14.48 g) were mixed by a mechanical stirrer in a 3-L flask under nitrogen gas. A homemade heating controller and mantle were used for reaction temperature control. The reaction was performed

* This section was originally published in La Scala et al. Biobased carbon fibers and high-performance thermosetting resins for use in U.S. Department of Defense applications. Aberdeen Proving Ground (MD): Army Research Laboratory (US); 2012 June. Report No.: ARL-SR-245.

at 130 °C for 6 h. After the reaction temperature changed from 130 to 90 °C, 40 wt% NaOH solution (93.6 g) was added dropwise for 2 h.

Small-Scale Synthesis of Furan-Based Epoxy without Water (2-Step Reaction). bHMF (12.8 g), epichlorohydrin (55.5 g), and benzyl trimethyl ammonium chloride (1.85 g) were mixed under nitrogen gas. The solution was heated at 100 °C for 18 h. Then, 40 wt% NaOH (4.8 g) was added dropwise for 2 h.

Conventional Synthesis of Furan-Based Epoxy (One-Pot Reaction). bHMF (10 g) and epichlorohydrin (72 g) were mixed in a flask to which a Dean-Stark trap was connected. The solution was heated to 120 °C, and epichlorohydrin was refluxed under nitrogen gas for 1.5 h. Next, 40 wt% NaOH solution (6.24 g, 9.36 mL of water) was added dropwise for 2 h. Water (~10 mL) was trapped in a Dean-Stark tube.

Quantitative Determination of the Epoxy Content of Epoxy Resins. The test method was followed by ASTM D 1652-90.[52]

4.8.2.2 Resin Cure

Furan-based epoxy was mixed with PACM, air products based on mole ratio, and/or the EEW. The mixture was cured at 95 °C for 3 h and postcured at 150 °C for 3 h.

Furan-based epoxy monomer was cured with 1 wt% of diaryliodonium hexafluoroantimonate (DPI, E-beam-induced cationic cure of epoxide) in a DSC hermetic cell.

4.8.2.3 Furan-Based Epoxy Characterization

A 500-MHz Varian Unity Inova NMR was performed in the Department of Chemistry at Drexel University to characterize the chemical structure of the furan-based epoxy monomers. A sample with a concentration of 30 mg/1 mL was prepared with chloroform-d or dimethyl sulfoxide-d6 (DMSO-d_6) as a solvent. NIR spectroscopy (NEXUS 670, Thermo Nicolet) was used to collect NIR spectra of samples operated by OMNIC version 5.2a. The numbers of scans and resolution were 32 and 8, respectively. A kinetic study was also carried out using NIR spectroscopy. An NIR spectrum was collected every 15 min at 95 °C. A DSC measurement was performed using a DSC Q2000 (TA instrument) to obtain the T_g and curing temperature. A temperature ramping function from –60 to 200 °C at a rate of 10 °C/min was selected. The T_g was determined by the middle of the transition. The thermomechanical properties of furan-based epoxy thermosetting resins were measured by using DMA. Rectangular samples with approximate dimensions of 17.5 × 12.0 × 2 mm^3 were tested by using a TA Instruments Q800 in the single cantilever method. The samples were tested at 1 Hz with a deflection of

7.5 µm, and the temperature was ramped from –20 to 150 °C at a rate of 2 °C/min. At the T_g, the storage modulus decreases intensely, and the loss modulus reaches the highest point. In this report, the temperature at which the peak in the loss modulus occurred was selected as the T_g of the cured resin.

4.8.3 Results and Discussion

4.8.3.1 Furan-Based Epoxy Synthesis and Characterization

Furan-based epoxy was synthesized by the reaction between furan derivative and epichlorohydrin. The catalyst, benzyl trimethyl ammonium chloride, was used to prevent potential side reactions. The catalyst was insoluble in the solution of furan derivative and epichlorohydrin. Water was added to improve the miscibility. The yield of the furan-based epoxy was about 85%. In order to reduce the byproduct, DMF was used as a solvent instead of water. However, the yield was very low (below 20 wt%), meaning that the replacement did not work well. The amount of water was decreased to obtain a suitable yield and low byproduct. The solution of epichlorohydrin and catalyst was prepared in advance. Water was added slowly in the solution, and the whole solution was checked to find out the point that it turned clear. The method made it possible to minimize the amount of water. After separation and purification processes, the yield was about 65%.

Large-scale synthesis (~180 g) was tested with the water-controlled method. However, the method failed to synthesize furan-based epoxy because of the leak between the lid and the reactor. Epichlorohydrin was evaporated through the leak during the reaction. The large-scale synthesis will be tested after the leak is fixed by a gasket.

Another synthetic method was tested without water. In this case, furan derivative, epichlorohydrin, and benzyl methyl ammonium chloride were used to prepare a solution. Over 12 h was required to reach about 50% of yield. The last test was a conventional synthetic method. The advantages are a short reaction time (3.5 h) and high yield (70%). This method can be directly compared to the method without water at which a catalyst was used.

4.8.3.2 Furan-Based Epoxy Cured With DPI

The furan-based epoxy monomer obtained from the water-controlled method was used for this cure process. In order to find out a reasonable cure temperature, 1 wt% of DPI was mixed with furan-based epoxy, and a DSC experiment was conducted to confirm the exothermic peak at which the cure process occurs. Figure 130 shows that a shoulder and a peak appeared at 140 and 168 °C, respectively. It was found that the cure temperature for this sample could be near 160 °C. The second scan

was carried out with the sample as shown in Fig. 131. There was no exothermic peak, meaning that the sample was cured completely. However, the T_g was not clear on this DSC thermogram.

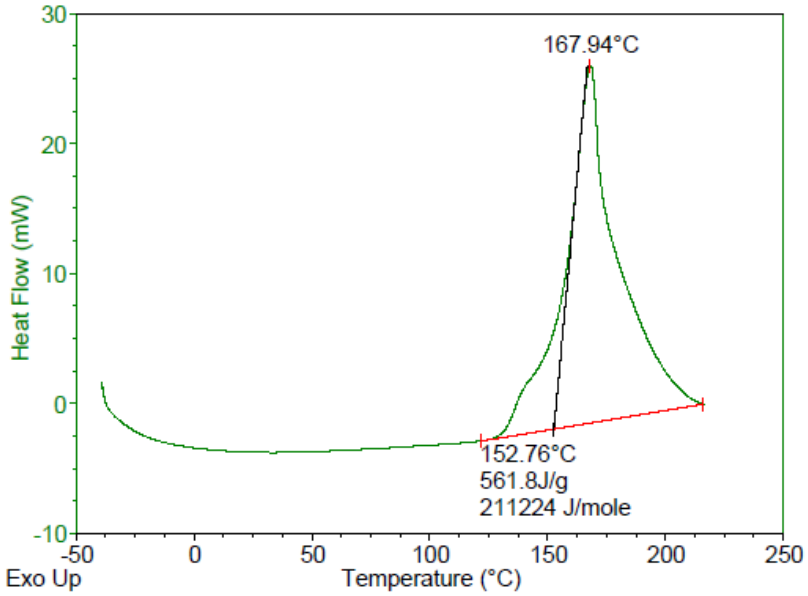

Fig. 130 Furan-based epoxy cured with 1 wt% DPI in DSC hermetic cell

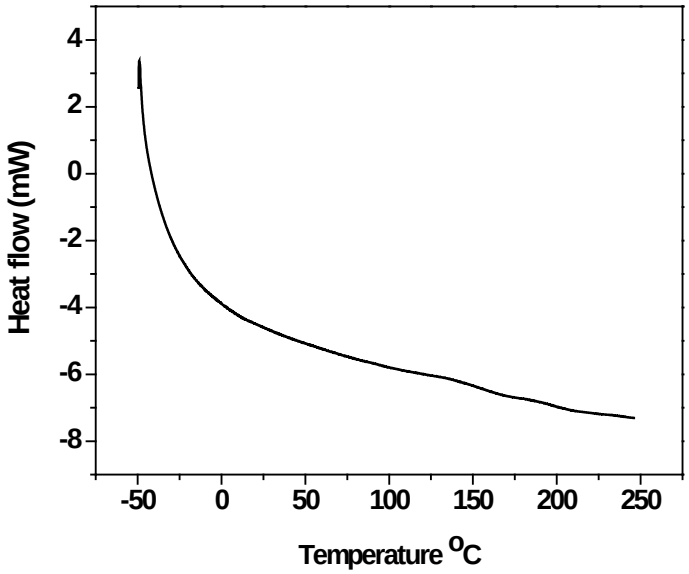

Fig. 131 The second DSC scan of furan-based epoxy cured with 1 wt% DPI

4.8.3.3 Furan-Based Epoxy Cured With PACM

The furan-based epoxy obtained from the water-controlled method was used for the DSC experiment (Fig. 132) to find out the cure temperature. Furan-based epoxy and PACM were mixed by the stoichiometric method. The cure process started at 38 °C, and the peak cure temperature for this system was found at about 100 °C. Figure 133 shows the NIR spectra of the mixture of furan-based epoxy and PACM. The cure process was monitored every 15 min at 95 °C. The initial NIR spectrum (red) exhibits an epoxy peak at 4,500 cm^{-1} and an amine peak at 4,900 cm^{-1}. The next spectrum did not show the peaks, meaning that most of the epoxy and primary amine group reacted in 15 min at 95 °C. DMA was used to obtain the storage modulus (E' at 25 °C) and T_g from the peak of the loss modulus. The mixture of furan-based epoxy was prepared based on the mole ratio. The E' at room temperature was 3.6 GPa and the T_g was 43 °C, as shown in Fig. 134.

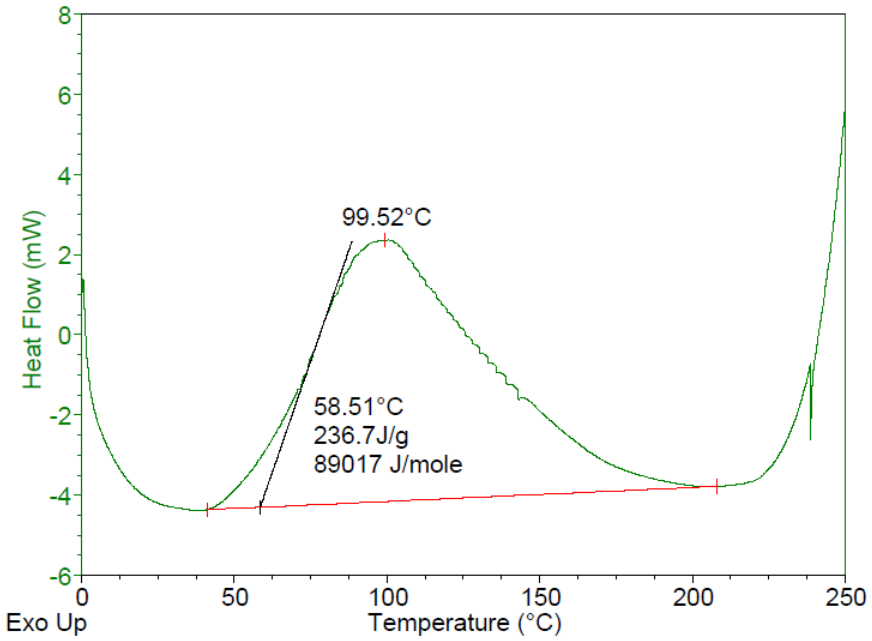

Fig. 132 Furan-based epoxy resin cured with PACM based on EEW

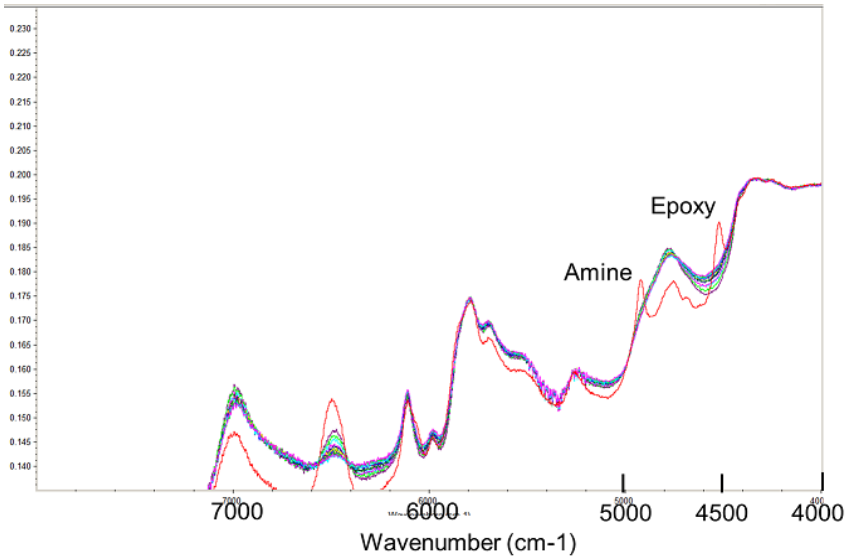

Fig. 133 Cure kinetics of furan-based epoxy and PACM by using NIR at 90 °C for 3 h. All spectra were obtained every 15 min. The red spectrum is an initial one before heating up.

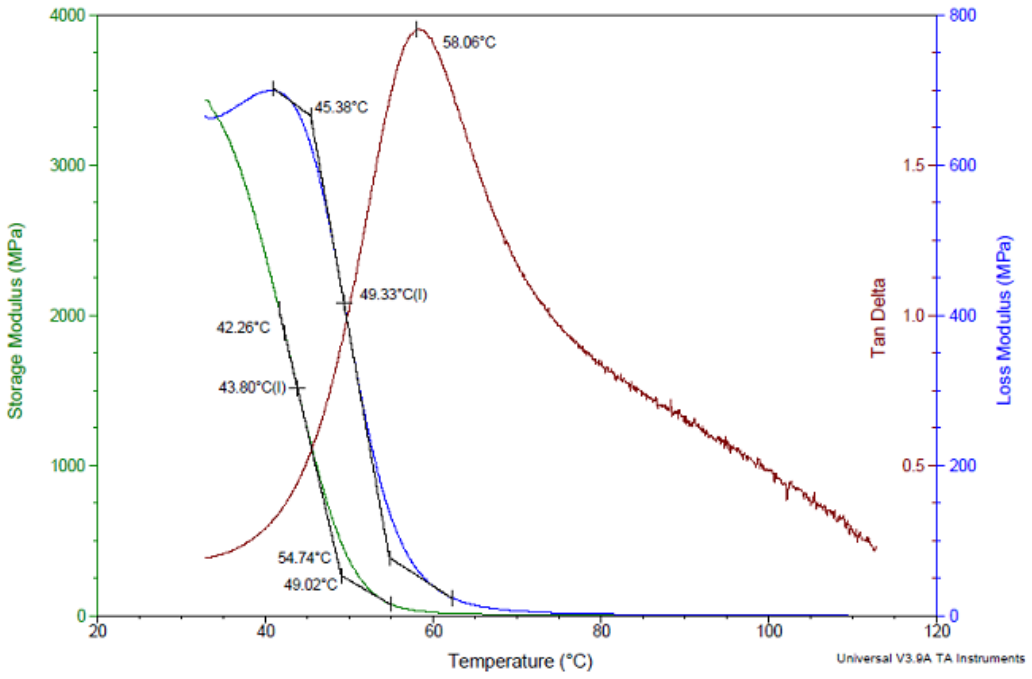

Fig. 134 DMA data of furan-based epoxy and PACM system based on a mole ratio of 2 and 1. The T_g from loss modulus was 43 °C.

Furan-based epoxy monomers synthesized from the conventional method and the method without water were cured with PACM. A DSC experiment was performed to obtain the T_g. It was expected that the furan-based epoxy from the method without water could show higher T_g than that from the conventional method because of the low EEW value. From Figs. 135 and 136, it was confirmed that the hypothesis was correct: the T_g's from the conventional method and the method without water were 7 and 22 °C, respectively. The T_g might increase if a furan-based epoxy having an EEW close to the theoretical EEW value could be prepared.

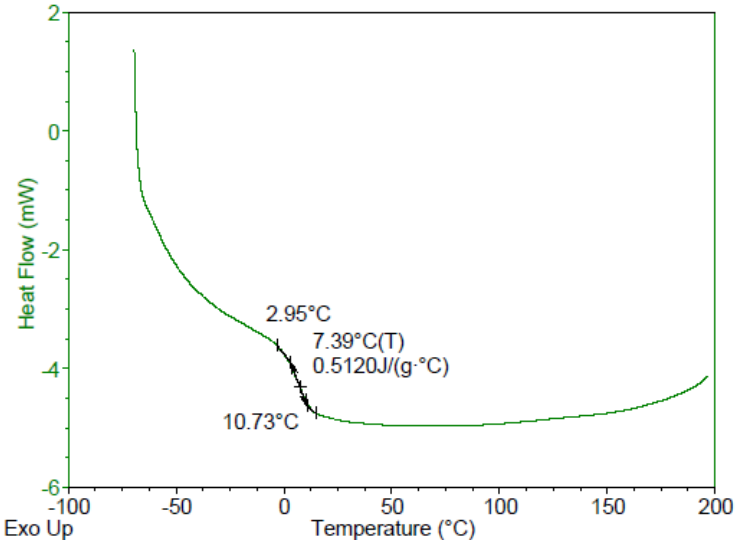

Fig. 135 DSC thermogram of PACM and furan-based epoxy from the conventional method

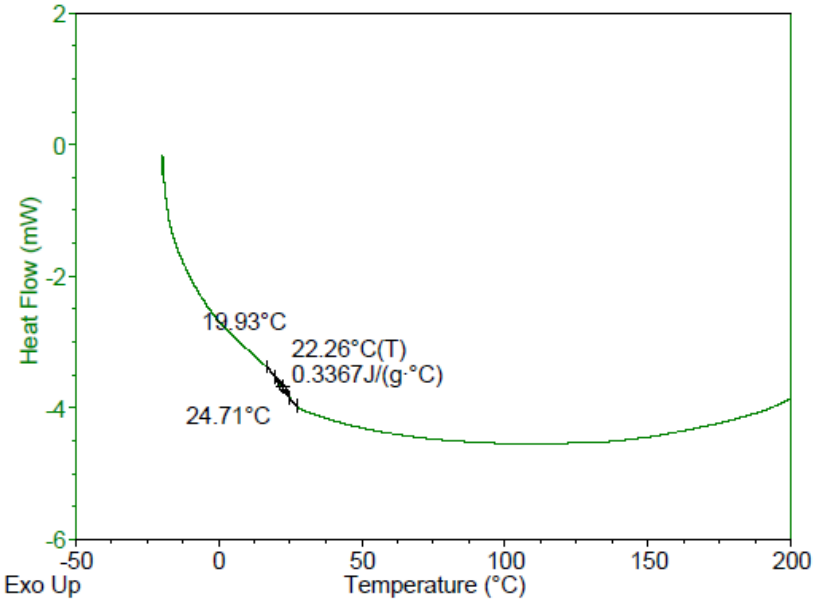

Fig. 136 DSC thermogram of PACM and furan-based epoxy from the method without water

4.8.4 Conclusion

To obtain a high yield and reduce byproduct, furan-based epoxy was synthesized via various synthetic approaches, such as using DMF instead of water and applying the water-controlled method, the method without water, and the conventional method. Furan-based epoxy from the method without water showed the lowest EEW value. However, optimization is needed to obtain furan-based epoxy with a high yield, short reaction time, and reduced side reaction. To increase the T_g of furan-based epoxy resin, the chemical structure is being analyzed by using GPC and MS. In addition, the synthetic strategy will be updated based on the characterization of chemical structures and the properties of thermosetting resins. Besides the furan-based epoxy and PACM system, furan-based epoxy itself was cured with the catalyst, DPI of 1 wt%. The characterization is still being investigated by using modulated DSC and DMA. The next section covers more recent advancements in furan monomers.

4.9 Furan-Based Epoxy Resins

This work has been published in the following journal papers and only a summary of the work is provided herein:

- Hu F, La Scala JJ, Sadler JM, Palmese GR. Synthesis and characterization of thermosetting furan-based epoxy systems. Macromolecules. 2016;49(6): 2408–2408.
- Hu F, La Scala JJ, Sadler JM, Palmese GR. Synthesis and characterization of thermosetting furan-based epoxy systems. Macromolecules. 2014; 47(10):3332–3342.

Renewable alternatives to petroleum-based thermosetting polymers have drawn significant attention due to potential positive economic and ecological impact. New materials should mimic the rigid, phenylic structure of incumbent high-performance thermoset monomers. Furans derived from cellulose and hemicellulose, are promising candidates for phenyl replacement. The synthesis of furan-based di-epoxies is challenging, and direct property comparisons of thermosets prepared using furanyl and phenyl-based epoxy monomer analogs are required. In this work, analog furanyl-based and phenyl-based di-epoxy monomers were synthesized (Fig. 137), and thermosets were prepared using amine curing agents. A structure-property study showed that furan-based polymers possess decreased T_g (Fig. 138) but had improved glassy modulus (Δ = 0.1–0.6 GPa) relative to their phenylic analogs. The furan ring has thus been demonstrated to be a viable building block for renewable high-performance epoxies, with potential for application in other thermosetting polymers.

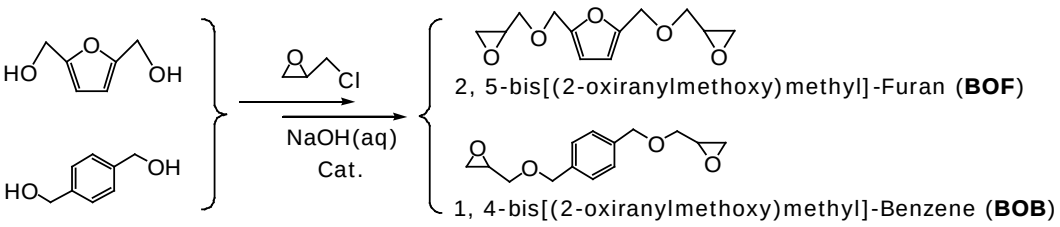

Fig. 137 BOF and BOB chemical structures that were synthesized and compared in this work

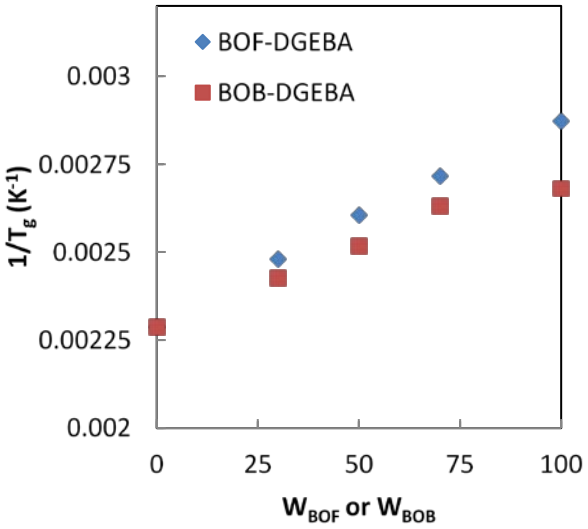

Fig. 138 Glass transition temperature for BOF/DGEBA and BOB/DGEBA cured with PACM as a function of the weight fraction of BOF or BOB in the epoxy component

4.10 Methacrylated Isosorbide Renewable Biobased Monomers as Vinyl Ester (VE) Cross-Linkers

This work has been published in the following patent applications and journal paper and only a summary of the work is provided herein:

- Sadler JM, Lam AP, La Scala JJ, Palmese GR. Renewable bio-based (meth)acrylated monomers as vinyl ester cross-linkers. Provisional Patent Application No. 61//521,981. 2011 Aug.
- Sadler JM, Lam P, Palmese GR, La Scala JJ. Renewable bio-based (meth)acrylated monomers as vinyl ester crosslinkers. PCT Patent Application PCT/US2012/050235. 2012.
- Sadler JM, Nguyen A-PT, Toulan FR, Szabo JP, Palmese GR, Scheck C, Lutgen S, La Scala JJ. Isosorbide-methacrylate as a bio-based low viscosity resin for high performance thermosetting applications. Journal of Materials Chemistry A. 2013;1:12579–12586.

In recent years, the bio-refining industry has developed a number of cyclic molecules with unique attributes derived from renewable carbohydrate feedstocks. Isosorbide is one such compound that has a distinctive fused bicyclic ring system that provides a scaffold for the development of novel biobased resin systems. We synthesized isosorbide-methacrylate (IM) by the direct esterification of isosorbide using highly reactive species such as methacryloyl chloride or methacrylic anhydride and a base catalyst. IM is a low viscosity (157 cP) cross-linking resin that free radically reacts to form a thermoset polymer with extent of cure at 85%. The resulting polymer has a T_g greater than 240 °C and main degradation temperature of 400 °C. Mechanical test results showed that IM had a modulus of 4 GPa and strength of 85 MPa. These thermal and mechanical properties show that IM has a significantly higher temperature operating window than any known VE resin and has similar performance to expensive high-temperature epoxy resins. As such, this material has good potential for use in composite applications where a moderate to high-temperature free radical cured polymer matrix is needed.

4.11 Methacrylated Isosorbide Synthesis

4.11.1 Introduction

Price volatility, environmental impact, and sustainability of petroleum-based resins have led to the need for more renewable and biobased materials.[154] Sugars derived from carbohydrates are a source of renewable materials that can be extracted from the 180 billion tons of biomass generated each year.[155] Structurally unique materials not found in traditional petroleum refining processes show promise for the development of new monomers. Complete dehydration of sorbitol yields isosorbide, a novel biobased building block. Isosorbide is composed of 2 chiral alcohols and a bicyclic ring with ether bridges that has been shown to provide rigidity in polymeric systems.[156,157] Polyurethane, polyester, and epoxy-isosorbide-based resins have been investigated in the past with some success.[158–164] Isosorbide-based VE resins have shown potential as a high-performing thermosetting polymers for use in composite applications. Therefore, finding a new synthetic route to produce isosorbide-based VE resins in high yield, quantities, and purity is of interest.

Isosorbide is a candidate for novel monomer development because of its characteristic V-shaped bicyclic ring system that provides rigidity without sacrificing critical processability characteristics such as viscosity. Other characteristics that make it desirable (e.g., in methacrylated isosorbide) include high glass transition temperature (T_g) of approximately 240 °C, a modulus of approximately 4 GPa, a strength of approximately 85 MPa, and degradation

temperature of approximately 400 °C. It is a unique monomer because it does not have any aromaticity or hydrogen bonding donors once reacted, one of the 2 usually being responsible for good polymer properties. The secondary chiral diols, one endo and the other exo, provide a synthetic barrier; however, once incorporated the asymmetric structure yields a high T_g.

4.11.2 Materials

Isosorbide (98%) was used as the building block for the synthesis of novel VE resins. A comparative secondary alcohol to isosorbide, 2-propanol (99.5%, anhydrous), was used to show how steric hinderance effects the reactivity rate of the substrate. Methacryloyl chloride (97%), methacrylic anhydride (94%), methacrylic acid (99%), and MMA (99%) were used as methacrylating agents. Dichloromethane (99.9%, high-performance liquid chromatography grade), THF (99.9% anhydrous), acetonitrile (99.8%), hexanes (99%), N,N-dimethylformamide (99.8%), and benzene (99.8%) were used as the reaction solvents. 4-dimethylamino pyridine (DMAP, 99%), sodium methoxide (95%), and potassium *tert*-butoxide (98%) were used as Brønsted base catalysts. Triethylamine (99.9%) was used to trap HCl byproduct as triethylammonium chloride. Stearic acid (95%) and lauric acid (98%) were used as a comparative replacement for MMA to show reactivity differences. *p*-toluenesulfonic acid monohydrate (98%), was used as a Brønsted acid catalyst. Titanium (IV) isopropoxide (99.999%), titanium diisopropoxide bis(acetylacetonate) (75 wt% in isopropanol), titanium (IV) (triethanolaminato) isopropoxide solution (80 wt% in isopropanol, Sigma-Aldrich), titanium (IV) bis(ammonium lactate)dihydroxide solution (50 wt% in H_20) and aluminum chloride (99.99%) were used as Lewis acid catalysts. All reagents, all provided by Sigma-Aldrich, were used as received without further purification.

4.11.3 Synthesis

4.11.3.1 Acid Chloride Method

Figure 139 shows the first method investigated for the synthesis of novel VE resins.

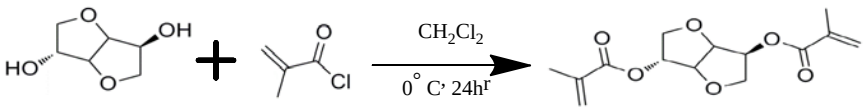

Fig. 139 Acid chloride method

Isosorbide (50 g, 342.13 mmol) was suspended in dichloromethane (DCM, 500 mL) with triethylamine (69.2 g, 718.47 mmol) and cooled to 0 °C before slowly

adding methacryloyl chloride (75.0 g, 684.26 mmol) drop-wise. The reaction mixture was slowly warmed to room temperature and stirred for an additional 16 h. The organic phase was sequentially washed with 1M HCl (3 × 500 mL), saturated sodium bicarbonate ($NaHCO_3$, 4 × 500 mL), DI H_2O (3 × 500 mL), brine (1 × 500 mL), then dried over magnesium sulfate ($MgSO_4$) and concentrated under reduced pressure. The product was a dark brown oil (83.0g, 86.0% yield). IM: ^{1}H-NMR (deuterated chloroform [$CDCl_3$]): δ 6.18 (s,1H), δ 6.12 (s,1H), δ 5.64 (s,1H), δ 5.61 (s,1H), δ 5.31 (s,1H), δ 5.27 (s,1H), δ 5.23 (q,1H), δ 4.93 (t,1H), δ 4.55 (t,1H), δ 4.02 (s,2H), δ 3.99 (d of d,1H), δ 3.92 (d of d,1H), δ 1.98 (s,3H) δ 1.98 (s,3H), δ 1.69 (s,1H), and δ 1.57 (s,1H).

The acid chloride method features the following highlights:

- Employs a highly reactive methacryloyl chloride species to surmount the steric barrier present at the exo and endo secondary alcohols sites in isosorbide.
- Methacrylation takes place without preference for either alcohol.
- Yields are extremely good and pure DM is obtained.
- Reagents can be somewhat expensive, and the use of chlorinated solvents to do biofriendly research is discouraged.
- Workup is extensive and results in approximately 10% loss of product.
- Triethylammonium salt is formed within minutes of reaction starting, so the reaction can be said to proceed rather quickly.

4.11.3.2 Anhydride Method

Figure 140 shows the second method investigated for the synthesis of novel VE resins.

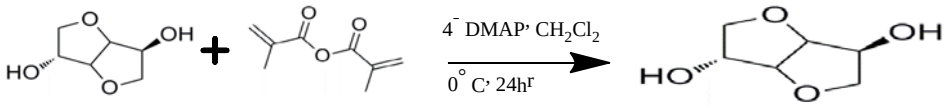

Fig. 140 Anhydride method

Isosorbide (50 g, 342.13 mmol) was suspended in DCM (500 mL) with methacrylic anhydride (158.24 g, 1,026.4 mmol) and cooled to 0 °C before adding 4-DMAP (6.26 g, 51.3 mmol). The reaction mixture was slowly warmed to room temperature and stirred for an additional 24 h. The organic phase was sequentially washed with saturated $NaHCO_3$ (4 × 500 mL) stirring over 8 h and shaken vigorously until the acid was neutralized. Washing continued with DI H_2O (2 × 500 mL), saturated brine

(1 × 500 mL), dried over $MgSO_4$, and concentrated under reduced pressure (62.7 g, 65% yield).

The anhydride method features the following highlights:

- Fair yield, though split product 50% DI and 50% mono, and large amounts of methacrylic acid remain.
- Workup is lengthy and time-consuming.
- Water-sensitive reagent.
- Chlorinated solvents.

4.11.3.3 Brønsted Acid Method

Figure 141 shows the third method investigated for the synthesis of novel VE resins.

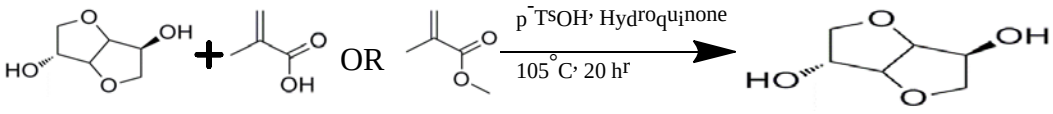

Fig. 141 Brønsted acid method

Isosorbide (10 g, 68.42 mmol) was suspended in methylmethacrylate (17.10 g, 171.06 mmol) and hydroquinone (0.20 g, 1.86 mmol). The reaction mixture was heated to 60 °C to melt the isosorbide before adding *p*-toluenesulfonic acid (0.20 g, 1.07 mmol). The reaction mixture was refluxed at 105 °C with a Dean-Stark trap for 20 h to remove the methanol. The vapor could not make it up the trap, so either higher temperatures or reduced pressure is required to pull the vapor up the arm.

The Brønsted acid method features the following highlights:

- Polymerization occurs, even at mild temperatures.
- Would be feasible without acrylate group present.

4.11.3.4 Brønsted Base Method

Figure 142 shows the fourth method investigated for the synthesis of novel VE resins.

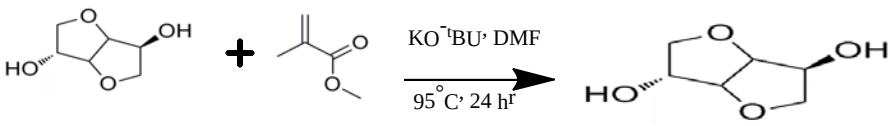

Fig. 142 Brønsted base method

Isosorbide (3.00 g, 20.52 mmol) and potassium *tert*-butoxide (0.115 g, 1.026 mmol) were brought to a melt at 65 °C. Methylmethacrylate (20.54 g, 205.2 mmol) dissolved in dimethyl formamide (5 mL) with phenothiazine (0.081g, 0.410 mmol) was added to the reaction mixture, which was heated to 100 °C for 3 h. Polymerization occurred predominantly by anionic means. However, a split product between di-methacrylated isosorbide and mono-methacrylated isosorbide was observed.

The Brønsted base method features the following highlights:

- Converts rather well; however, split product and polymerization are issues.
- Minor differences in base strength (i.e., methoxide and isopropoxide do not decrease the amount of polymerization).

4.11.3.5 Neutral Brønsted Base Method

Figure 143 shows the fifth method investigated for the synthesis of novel VE resins.

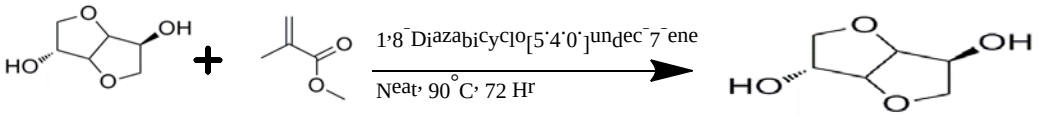

Fig. 143 Neutral Brønsted base method

Isosorbide (20 g, 136.85 mmol) was suspended in methylmethacrylate (191.81 g, 1915.9 mmol) and 1,8 diazobicylco[5.4.0]undec-7-ene (10.55 g, 68.42 mmol). Hexanes (50 mL) were added to try and azeotrope off the methanol with a soxhelet extractor but were completely burned off during the course of the reaction. The reaction mixture was heated to reflux at 90 °C for 4.25 days. An aliquot (1.57 g) of the organic phase was evaporated to remove the MMA and sequentially washed with 1M HCl (1 × 40 mL), saturated $NaHCO_3$ (2 × 40 mL), DI H_2O (1 × 40 mL), brine (1 × 40 mL), dried over $MgSO_4$, and concentrated under reduced pressure. The product was a light yellow oil (0.5 g, 33.2% yield).

The neutral Brønsted base method features the following highlights:

- Homogenous clear brown reaction solution.

- Yields need to be improved, but possibility for being a methacryloyl chloride replacement under increased pressure.
- Solventless.
- Stable even for days after; polymerization will not spontaneously occur.
- Workup may be able to be avoided if higher pressure reduces catalyst loading.
- Negligible polymerization during the course of the reaction due to neutral nature of base.
- Potential to be cost effective.

4.11.3.6 Lewis Acid Method

Figure 144 shows the sixth method investigated for the synthesis of novel VE resins.

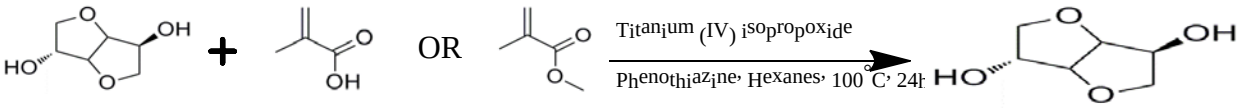

Fig. 144 Lewis acid method

Isosorbide (10 g, 68.42 mmol) was suspended in THF (30 mL) with methylmethacrylate (13.70 g, 136.08 mmol) and titanium (IV) isopropoxide (0.972 g, 3.42 mmol). The reaction mixture was heated to reflux at 65 °C for 18 h; no product was observed.

The Lewis acid method features the following highlights:

- Extremely water-sensitive; catalyst is destroyed before reaction can take place.
- Potential for high yields under anhydrous conditions with more activating, but with pricier metals such as lanthanum (III) isopropoxide.
- Sterics of isopropoxide may be inhibiting the reaction; less bulky ligands are probably better.
- Faint product formation when fluidized bed reactor accidently shot up to 300 °C, showing that the reaction will proceed but the steric barrier is too large to overcome.

4.11.4 Structural Effect Studies

4.11.4.1 Stearic Acid Method

Figure 145 shows the seventh method investigated for the synthesis of novel VE resins.

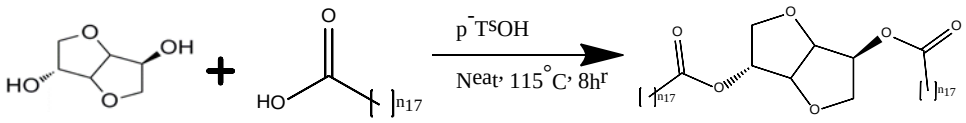

Fig. 145 Stearic acid method

Isosorbide (10 g, 68.42 mmol), stearic acid (38.92 g, 136.84 mmol), and *p*-toluenesulfonic acid (0.130 g, 0.6842 mmol) were added to the reaction mixture, which was heated to 115 °C for 8 h.

The stearic acid method features the following highlights:

- Even though yields were difficult to obtain due to solubility and purification issues, the aliquot used for ^{1}H NMR appeared to be majorly isosorbide-distearate.
- Reaction readily proceeded without issue.
- Reaction proceeds at high temperature overcoming a steric barrier.

4.11.4.2 Lauric Acid Method

Figure 146 shows the eighth method investigated for the synthesis of novel VE resins.

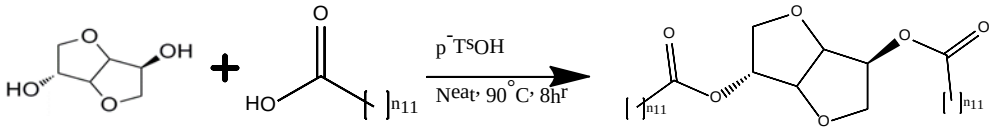

Fig. 146 Lauric acid method

Isosorbide (3 g, 20.52 mmol), lauric acid (8.22 g, 41.04 mmol), and *p*-toluenesulfonic acid (0.039 g, 0.205 mmol) were added to the reaction mixture, which was heated to 90 °C for 8 h.

The lauric acid method features the following highlight:

- Reaction with lauric acid still proceeded readily at lower temperatures, showing that raising the temperature has limited effect on the reaction rate.

4.12.4.3 Isopropyl Alcohol (IPA) Method

Figure 147 shows the eighth method investigated for the synthesis of novel VE resins.

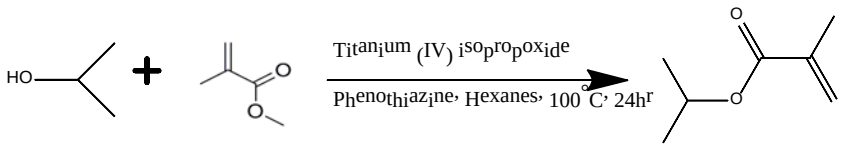

Fig. 147 IPA method

IPA (5 g, 83.33 mmol) and methylmethacrylate (16.66 g, 166.66 mmol), titanium diisopropoxide bis(acetylacetonate (0.303 g, 0.833 mmol), and phenothiazine (0.448g, 2.249 mmol) were added to the reaction mixture, which was heated to 75 °C for 72 h. No reaction occurred.

4.11.5 Summary and Conclusions

We postulated that the reason that IM is difficult to synthesize in one efficient step using the esterification or transesterification methodology is a result of the structural feature of the molecule:

- Isosorbide is composed of a dual ring system with exo and endo secondary alcohols that are sterically hindered by the ring itself.
- The ring system is confomationally locked. This inherent inflexibility, which provides high T_g in polymeric materials, limits the angles of "attack" necessary to undergo the esterification/transesterification mechanism.
- The acrylate functionality readily undergoes anionic, cationic, and radical polymerization, limiting the effective number of reagents and conditions significantly.
- Lewis acid catalysts are highly water-sensitive, and isosorbide innately carries approximately 5%–10% of water at any given time, which can destroy the catalyst before it can convert.
- The acid catalyzed secondary alcohol (IPA) method did not proceed, and the Lauric acid readily proceeded at a reasonable temperature of 90 °C. This shows that not only are sterics an issue for both the isosorbide and the methylmethacrylate separately, but raising the temperature is not an effective method of combating the sterics; removing or lessening the sterics is, and a workaround is proposed. Strikingly IPA failed to react under conditions that isosorbide did, showing that there is still more left to understand about this perplexing system. It seems as though all 3

components, isosorbide, methylmethacrylate, and base for a proton transfer, must line up perfectly, and the crowded nature of the substrates involved makes this task difficult.

There are some possible solutions. Pressure can be used to reduce the amount of catalyst, solvent, and temperature used. It has been demonstrated to be a solution to combating sterically hindered substrates in base-catalyzed reactions. However, typically high pressures in the kilobar range are employed but do not exclude the possibility of less than 1-kbar pressures accelerating the reaction.[165,166] Pressure not only concentrates the solution, but also reduces the destabilizing forces caused by steric interactions, allowing for smoother reaction progress. In high-pressure reactions the mean free path can be affected dramatically. In addition, the effect of pressure on an equilibrium constant follows Le-Chatlelier's principle, inclining one to think this is a good alternative solution.[165]

4.11.6 Supplemental Information: Purified Samples

Figures 148–154 show NMR spectra of purified samples.

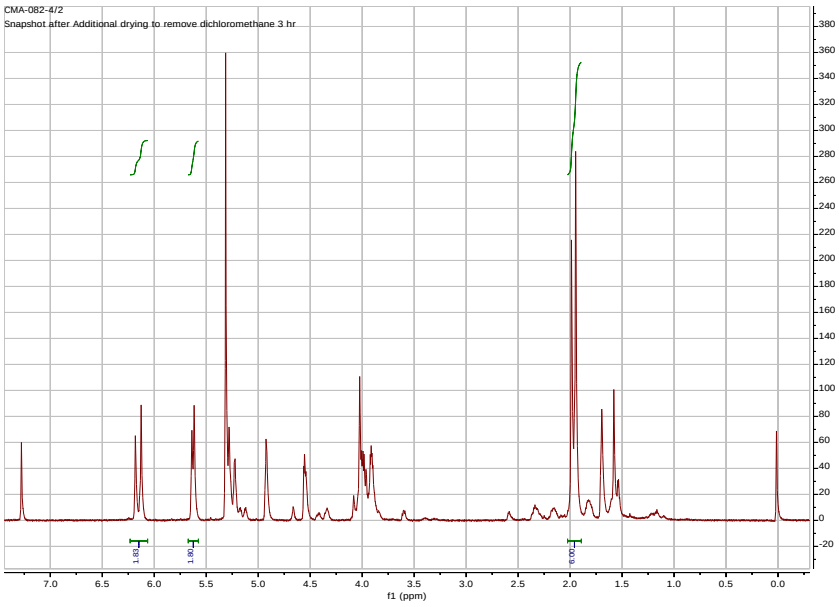

Fig. 148 NMR spectra of methacryloyl chloride method

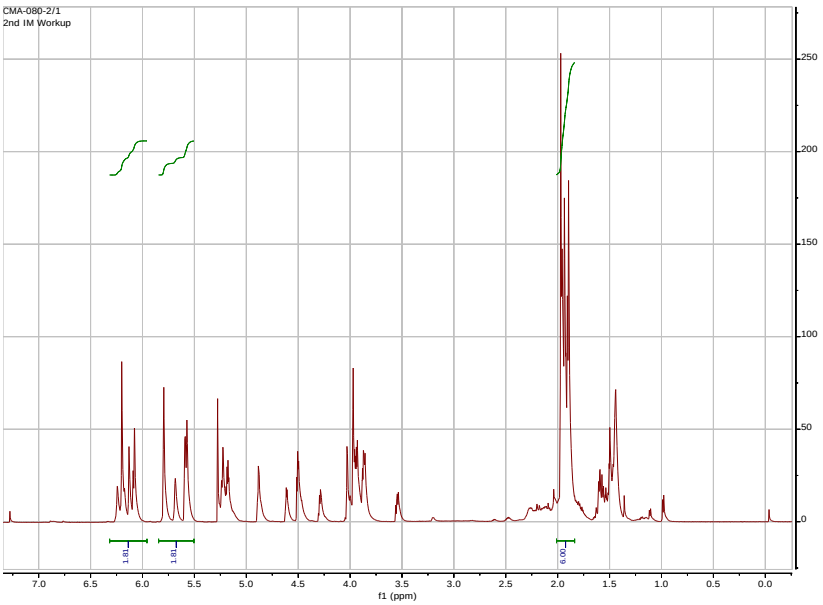

Fig. 149 NMR spectra of anhydride method

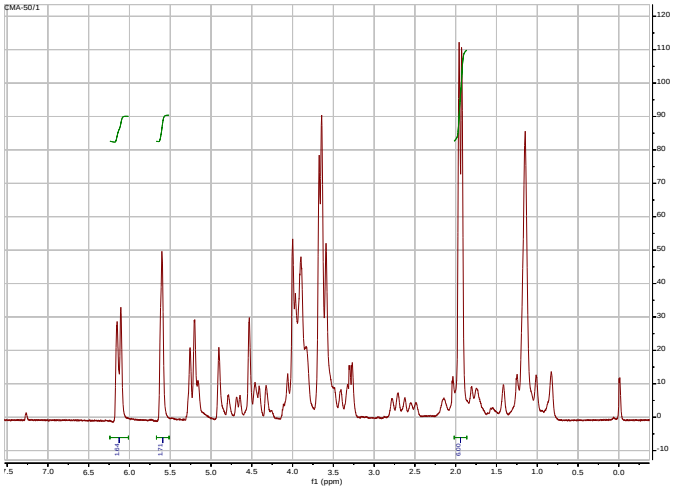

Fig. 150 NMR spectra of Brønsted base method

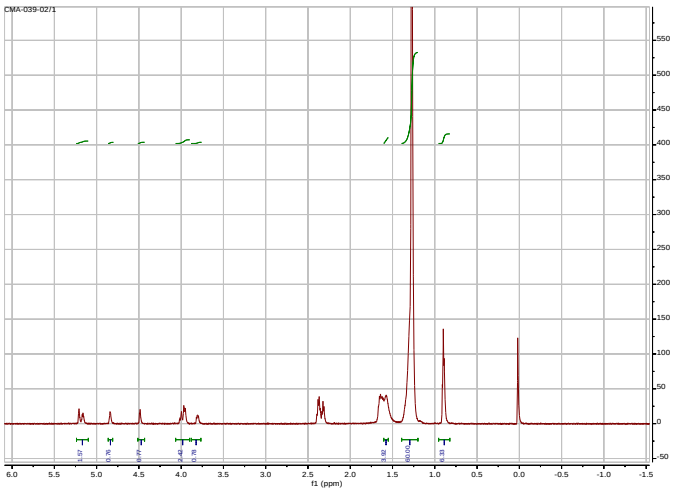

Fig. 151 NMR spectra of stearic acid method

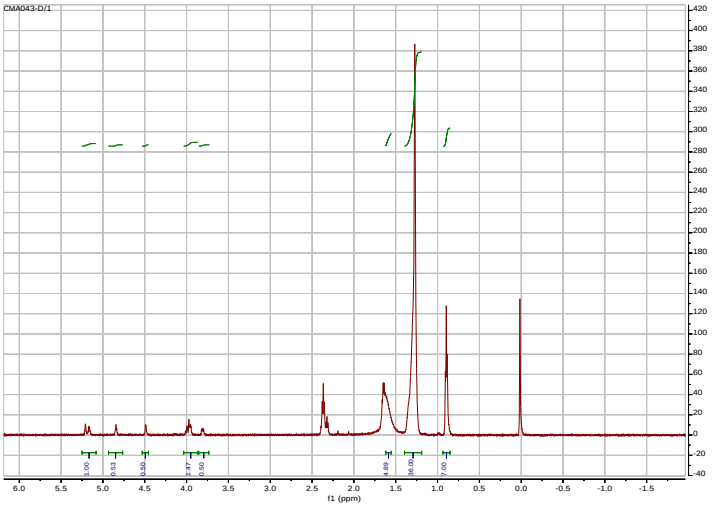

Fig. 152 NMR spectra of lauric acid method

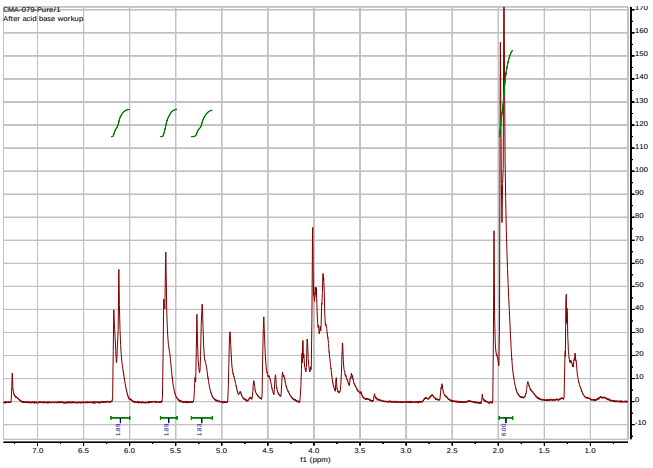

Fig. 153 NMR spectra of neutral base method

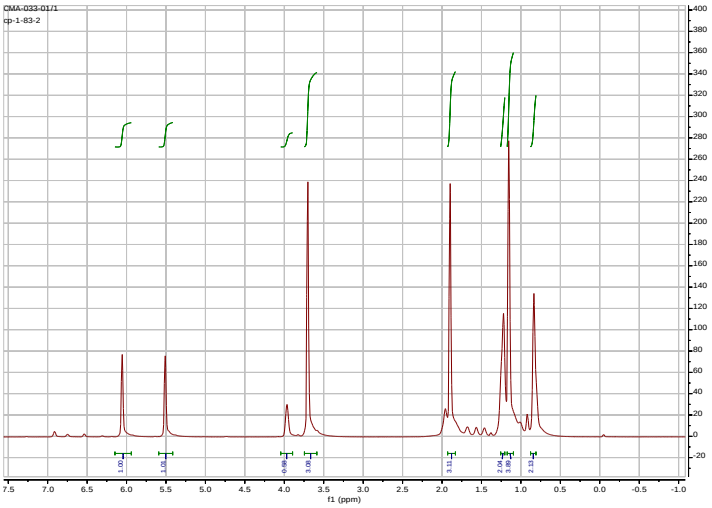

Fig. 154 NMR spectra of secondary alcohol method

4.12 End Group Modification to Enable Development of Isosorbide-Based Unsaturated Polyester Cross-Linkers*

4.12.1 Introduction

Most of the thermosetting resins are produced from petroleum feedstocks. Because of the high prices of fossil fuels and the demand to protect health and the environment, there is a heightened interest in manufacturing polymeric materials from renewable materials with similar or better mechanical and thermal properties

* Portions of this chapter were originally published in La Scala et al. Biobased carbon fibers and high-performance thermosetting resins for use in U.S. Department of Defense applications. Aberdeen Proving Ground (MD): Army Research Laboratory (US); 2012 June. Report No.: ARL-SR-245.

compared to those currently produced from petroleum resources. For a long-term goal, using renewable resources as a feedstock will help to stabilize the cost and supply of polymeric materials. Many different renewable resources such as starch,[167] cellulose,[168,169] and lignin[170] can be used as a feedstock for biobased thermosetting resins.

There are several types of thermosetting resins, such as epoxy, VE, and UPE. UPE resins are widely used as the matrix materials for polymer composites because of the relatively low cost, good balance of properties, and adaptability to many fabrication processes. There are many publications regarding the synthesis, analysis, curing process, and properties of UPE resins. UPE resins are products formed by a condensation reaction between unsaturated and saturated acids/anhydrides and diols. The UPE is mixed with a reactive diluent (typically vinyl monomers such as styrene and MMA) to obtain a liquid mixture with a low viscosity that can be easily cast or molded without high pressures and polymerized at rates faster than the homopolymerization rate of the UPEs by themselves.[171] Unsaturated sites (i.e., carbon–carbon double bonds) react with reactive diluents by radical initiators to form 3-D polymer chain networks. Epoxy thermosetting resins are the class of polymeric materials that contain more than one epoxy group situated terminally, cyclically, or internally on the molecule and will create a cross-linked solid product based on thermosetting reaction.

In UPE, 1,4;3,6-dianhydro-D-glucitol (isosorbide) is an attractive material.[172,173] The polymers derived from isosorbide that have been investigated include polyesters,[174] polycarbonates,[175] polyurethanes,[176–178] and polyamides.[179–181] Isosorbide is a renewable material derived from sorbitol that is obtained from glucose.[182] It consists of 2 combined THF rings with *cis*-arrangement, showing a V-typed molecule and 2 hydroxyl groups. Technically, the precursor containing ring structures is a high-potential candidate for the production of high mechanical and thermal performance resins. Jasinska and Koning[183] reported that the biobased UPEs from isosorbide, MA and succinic acid were polymerized and analyzed. However, the polymers with broad PDI were obtained via a complex synthetic process at a high reaction temperature (~230 °C) where a toxic catalyst (titanium [IV] n-butoxide) was used for the polymerization. MA is manufactured from n-butane as a feedstock. It is also possible to produce MA in biological processes.[184]

In this report, different biobased unsaturated monomer architectures were synthesized with isosorbide and MA under moderate conditions. The end groups on the cross-linkers were modified with hydrophobic groups to improve the solubility with reactive diluents styrene and MMA. These reactive diluents are VOCs and HAPs.[1,2,23] These chemicals risk the health and safety of plant employees and the general public. It is highly desirable that an environmentally friendly

replacement should be found for these materials to reduce or remove this risk. Thus, a biobased reactive diluent was also introduced as a replacement of styrene. We investigated the solubility of these UPE resins in petroleum-derived and biobased reactive diluents. Furthermore, we investigated the thermomechanical properties of these resins.

4.12.2 Experimental

4.12.2.1 Synthesis of Isosorbide-Based Cross-Linkers (UPE1, UPE2, and UPE3)

Isosorbide (0.183 mol, 26.85 g) and MA (0.42 mol, 38.67 g) were put in a 250-mL round flask. A nitrogen gas environment was prepared with a Schlenk line. After toluene (10 mL) was injected, the flask was put in an oil bath at 100 °C, and the reagents were mixed for 30 min. N,N-dimethyl benzyl amine (0.55 mL, 3.66 mmol) was injected into the flask, and the reaction was carried out for 18 h. The cross-linker (UPE1) was put in a vacuum oven to evaporate toluene for 24 h. The obtained cross-linker (UPE1) is a monomer-type shown in Fig. 155. The yield was about 90 wt%.

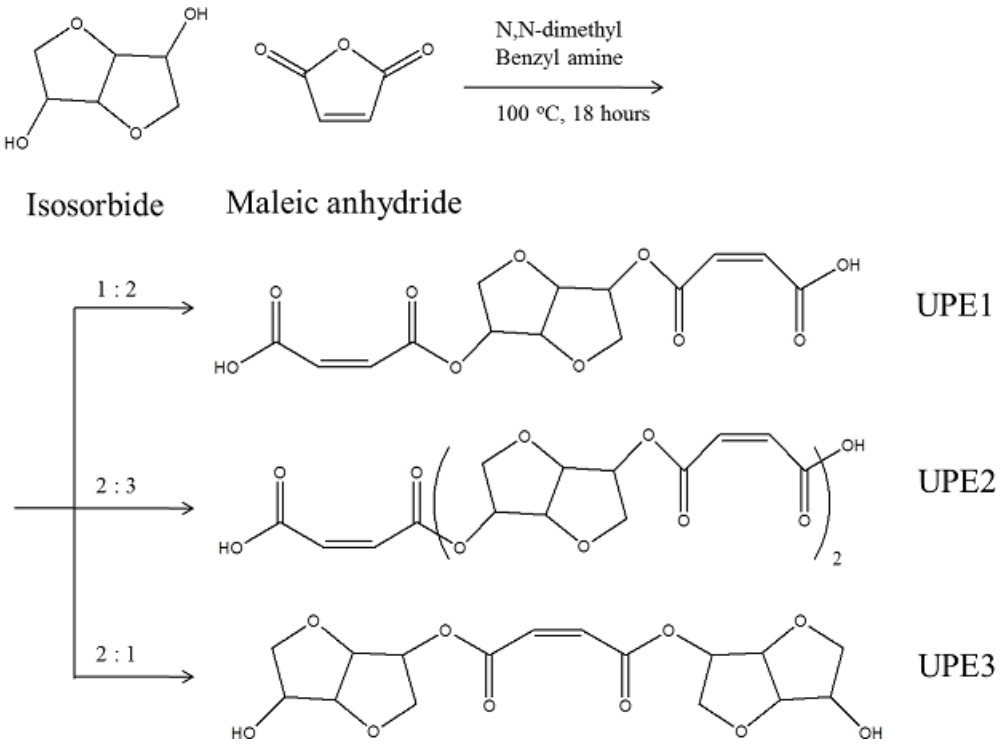

Fig. 155 Synthesis of biobased monomer (UPE1), chain-extended molecule (UPE2), and sequence-inversed monomer (UPE3)

To synthesize the chain-extended molecule (UPE2) shown Fig. 155, the mole ratio of isosorbide and MA was 2 to 3. MA (15 g, 0.154 mol) and isosorbide (15 g, 0.1026 mol) were dissolved in toluene (10 mL) at 100 °C under a nitrogen gas environment. A catalyst, N,N-dimethyl benzyl amine (0.31 mL, 2.05 mmol), was added in the mixture, and the reaction was conducted for 18 h. The yield was about 90 wt%.

The sequence-inversed monomer (UPE3) was also prepared, and the sequence order was isosorbide-maleate-isosorbide (Fig. 155). The mole ratio of isosorbide and MA was 2 to 1. Synthesis condition and termination processes are the same as the processes for UPE1.

4.12.2.2 End Group Modification

The hydroxy end on UPE1 and UPE2 was converted to hydrophobic end, such as hexyl (H) or benzyl (B) groups. One end and 2 ends were modified to investigate the effect of the modification on solubility with reactive diluents. The benzyl-1 end modified UPE2 and hexyl-2 ends modified UPE1 are symbolized as B-UPE2 and H-UPE1-H, respectively.

H-UPE1: The synthetic route of H-UPE1 is shown in Fig. 156. UPE1 (16.1 g) was put in a 250-mL round flask, and toluene (10 mL) was injected in the flask under nitrogen gas. The flask was immersed in an oil bath at 100 °C. A solution of 1-hexanol (5.33 g) and p-toluenesulfonic acid (0.18 g) was mixed in a beaker, and then injected in the flask. The reaction was carried out for 18 h at 100 °C. The final solution was diluted with ethyl acetate and washed with DI water 3 times. The ethyl acetate and unreacted 1-hexanol were evaporated by using a rotary evaporator. The yield was about 70%.

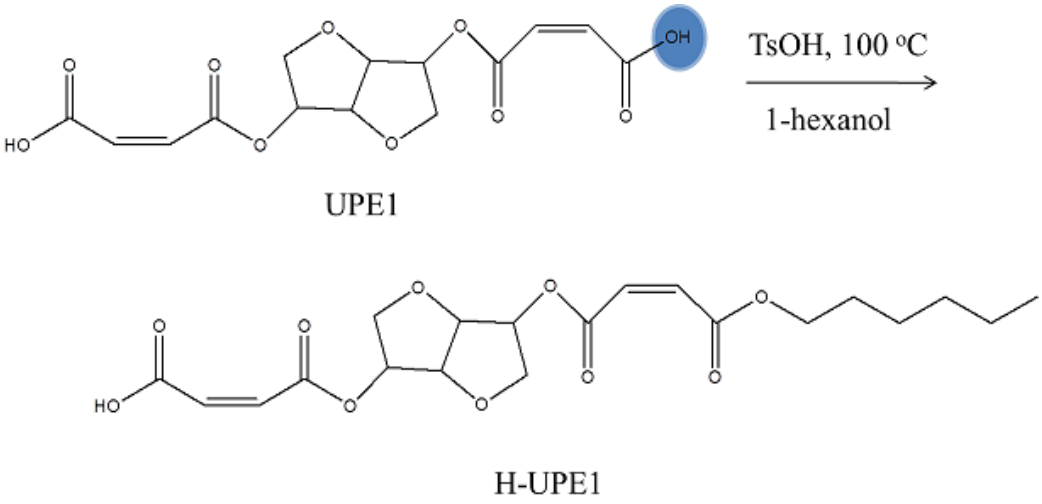

Fig. 156 End group modification of UPE1 from hydroxy to hexyl group

H-UPE1-H: UPE1 (20.82 g) and toluene (10 mL) were mixed in a flask under a nitrogen gas environment at 100 °C. The solution of 1-hexanol (13.72 g) and p-toluenesulfonic acid (0.233 g) was injected in the flask. The yield was about 80%.

H-UPE2: UPE2 (14.4 g) was mixed with toluene (10 mL) at 100 °C under nitrogen gas. The solution of 1-hexanol (2.1 g) and p-toluenesulfonic acid (0.086 g) was injected in the flask, and the reaction was conducted for 20 h. The yield was about 70%.

H-UPE2-H: UPE2 (14.4 g) was blended with toluene (10 mL) at 100 °C under nitrogen gas. The solution of 1-hexanol (5.1 g) and p-toluenesulfonic acid (0.086 g) was added in the flask. The yield was about 80%.

B-UPE1: The synthetic route of B-UPE1 is shown in Fig. 157. UPE1 (27.2 g) was put in a 250-mL round flask, and toluene (10 mL) was injected in the flask under nitrogen gas. The flask was immersed in an oil bath at 100 °C. Benzyl alcohol (8.63 g) and p-toluenesulfonic acid (0.3 g) were mixed in a beaker, and the solution was injected in the flask. The reaction was carried out for 20 h at 100 °C. The final solution was diluted with ethyl acetate and washed with DI water 3 times. The ethyl acetate and unreacted benzyl alcohol were evaporated by using a rotary evaporator. The yield was about 65%.

Fig. 157 End group modification of UPE1 from hydroxy to benzyl group

B-UPE1-B: UPE1 (16.51 g) was added in a flask and prepared in a nitrogen gas environment. Toluene (10 mL) was injected, and the flask was placed at 100 °C. The solution of benzyl alcohol (11.51 g) and p-toluenesulfonic acid (0.184 g) was added in the flask, and the reaction was performed for 20 h. The yield was about 70%.

B-UPE2: UPE2 (20 g) was mixed with toluene (10 mL). The solution, p-toluenesulfonic acid (0.12 g) and benzyl alcohol (4.153 g), was injected in the flask. The yield was about 70%.

B-UPE2-B: UPE2 (18.1 g) was blended with toluene (10 mL), and the solution, p-toluenesulfonic acid (0.1083 g) and benzyl alcohol (6.8 g), was injected in the flask. The yield was about 75%.

4.12.2.3 Preparation of UPE3 Diglycidyl Ether

The reaction shown in Fig. 158 was carried out with a Dean-Stark trap and condenser under a nitrogen gas environment. UPE3 (6.94 g) and epichlorohydrin (6.9 g) were put in a flask. The solution was heated to reflux at 120 °C. NaOH (1.6 g) in water (5 g) was added dropwise to the flask for 2 h. Then, the reaction was left for 1 h to complete. After the solution was cooled to room temperature, the solution was filtered, diluted with ethyl acetate, and washed with water. Solvents were evaporated by a rotary evaporator.

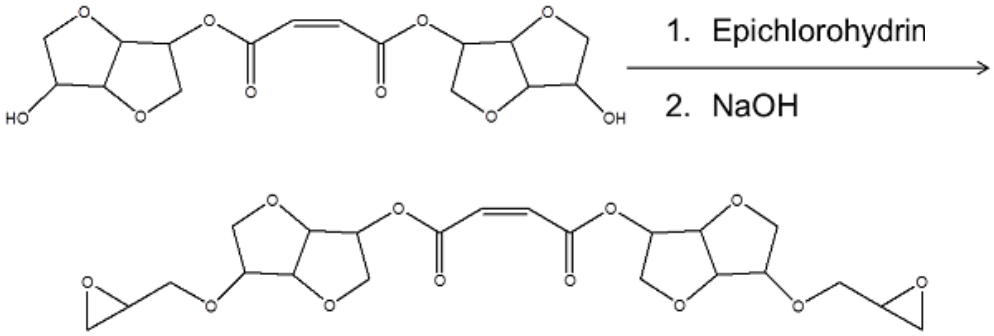

Fig. 158 UPE3 glycidyl ether by the reaction of UPE3 cross-linker and epichlorohydrin

4.12.2.4 Blending of Unmodified Cross-Linker and Reactive Diluent

The initial blending condition of cross-linker and reactive diluent was 70 and 30 wt%. If the cross-linker mixed completely with reactive diluent, the result was 70/30. If the cross-linker did not mix well with reactive diluent, a double layer should be observed (Fig. 159, UPE1/styrene [70/30] mixture). The mass of unmixed reactive diluent layer was measured, and the amount of the reactive diluent mixed with cross-linker was determined by the mass of the unmixed reactive diluent.

Fig. 159 Photograph showing insolubility of UPE1/styrene (70/30)

4.12.2.5 Blending of Modified Cross-Linker and Reactive Diluent

All modified UPE cross-linkers were mixed well with styrene and MMA of 30, 40, and 50 wt%, respectively. All blending was clear, and there was no phase separation.

4.12.2.6 Resin Cure

A modified cross-linker solution containing various amounts of reactive diluents such as styrene, MMA, and MAA was prepared. The mixtures were cured overnight at 70 °C using a Norox MEKP-9, whose mass was 3 wt% of the total cross-linker solution weight, and then postcured at 150 °C for 3 h.

4.12.2.7 Polymer Characterization

The isosorbide-based cross-linkers and their thermosetting resins were analyzed by NMR, GPC, MS, mass differential scanning calorimetry (MDSC), or DMA. The chemical structures of unmodified and modified cross-linkers and the number-average molecular weight (M_n) were determined by ^1H NMR. All samples were dissolved in DMSO-d_6 or $CDCl_3$ solvent for NMR analysis. Spectra were acquired at 25 °C using the 500-MHz Unity Inova Varian NMR instrument operated with VNMR 6.1B software. The pulse sequence was as follows: relaxation delay (0.3 s), pulse (54.6°), acquisition time (3.744 s), width (4,000.00 Hz), number of data points (32,768), and total acquisition time (1 min, 4 s).

Waters AutoSpec Ultima Q triple sector mass spectrometer was carried out with positive ion CI mode (chemical ionization) by using methane as the ionizing gas [CI+ with CH_4]. A solid probe was ramped from 50 to 150 °C at a rate of 25 °C/min.

M_w, M_n, and PDI (M_w/M_n) were determined by a GPC system consisting of a Waters 515 HPLC pump, a Waters RI 2410 detector, first column (Perkin-Elmer, single pore size, effective molecular weight range: up to 2,000), and second column (Perkin-Elmer, mixed pore size, linear molecular weight range: 200–2,000,000 g/mol). GPC was carried out at a flow rate of 1.0 mL/min at 30 °C and eluted with dimethyl

formamide. The sample concentration was 1.0–1.5 mg/mL. A calibration curve was developed with polystyrene standard data and estimated molecular weights.

The thermomechanical properties of UPE thermosetting resins were measured by using DMA. Rectangular samples with approximate dimensions of 17.5 × 12.0 × 2 mm^3 were investigated by using a TA Instruments Q800 in the single cantilever method. The samples were tested at 1 Hz with a deflection of 7.5 μm, and the temperature from –20 to 150 °C was ramped at a rate of 2 °C/min. Two temperature ramp experiments were carried out for each sample. The DMA traces for the first and second ramps were almost identical, meaning that cure and postcure processes were applied properly for this polymer system. At the T_g, the storage modulus decreases intensely, and the loss modulus reaches the highest point. In this report, the temperature at which the peak in the loss modulus occurred was selected as the T_g of the cured resin.

An MDSC measurement was performed using a DSC Q2000 (TA instrument) to obtain T_g from reversible heat flow. The modulation temperature amplitude, modulation, and ramp rate were ±1.0 °C, 60 s, and 3 °C, respectively. The T_g was determined by the middle of the transition.

4.12.3 Results of the Synthesis of Isosorbide-Based Cross-Linkers

The chemical structures of UPE1 and UPE2 were confirmed by ^{1}H-NMR as shown in Fig. 160. The main peaks of the UPE cross-linkers were assigned based on the literature.[183] According to Jasinska and Koning,[183] the chemical structure was confirmed by using 2-D NMRs, such as correlation spectroscopy (COSY), heteronuclear multiple-bond correlation spectra, and heteronuclear single quantum correlation spectra; this allowed them to determine the sequence of specific protons and carbons. As shown in Fig. 160a, the unsaturated part (a,b) was found near 6.4 ppm, and the protons (d,g) attached between isosorbide and maleate appeared near 5.3 ppm. The peak integration ratio of (a,b) and (d,g) was 2 to 1, meaning that the monomer type of the cross-linker consisting of one isosorbide and 2 maleic acid half esters, UPE1, was obtained successfully. Figure 161 shows the mass spectrum of UPE1. The magnified insert contained the target molecular weight, 343 g/mol. However, the MS spectrum provides only qualitative information. Figure 162 shows GPC data of the UPE1 cross-linker, where M_w, M_n, and PDI were 344 g/mol, 324 g/mol, and 1.06, respectively. Those results confirmed that the monomer type of UPE cross-linker, UPE1, was synthesized with a narrow molecular weight distribution.

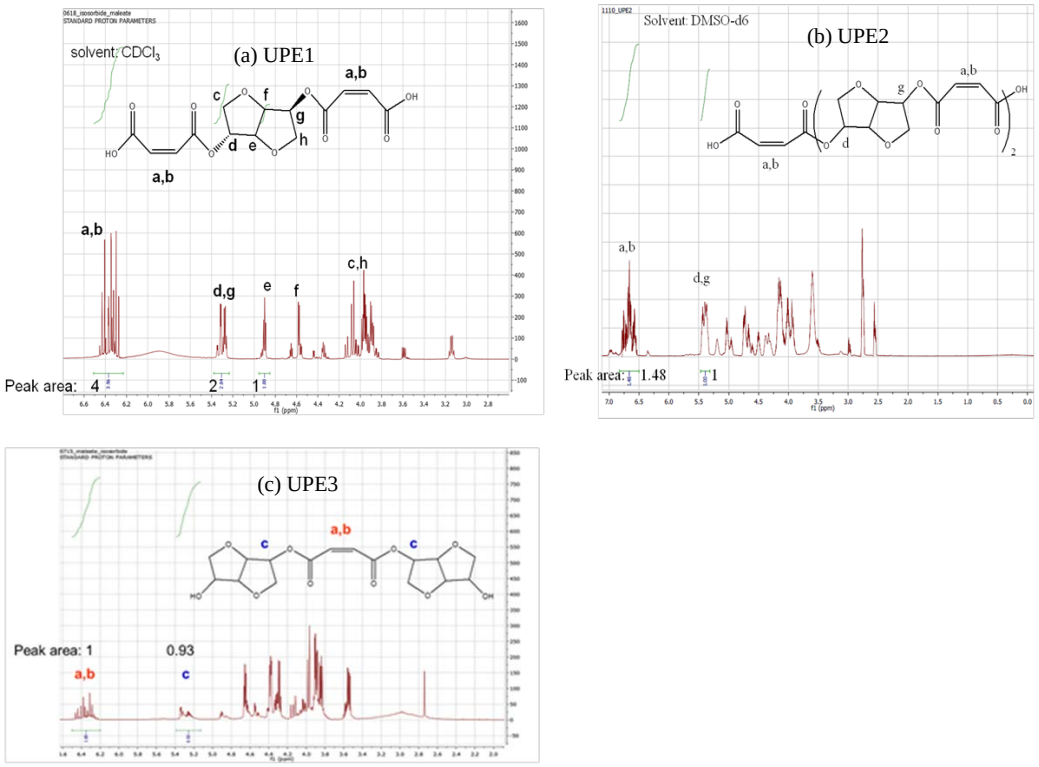

Fig. 160 NMR spectra of isosorbide-based cross-linkers: a) UPE1, b) UPE2, and c) UPE3

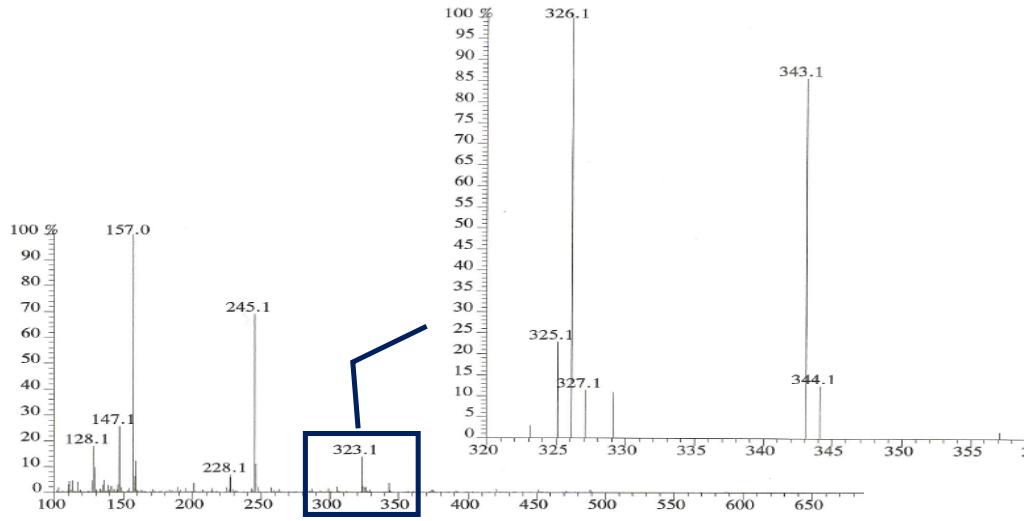

Fig. 161 Mass spectrum of UPE1

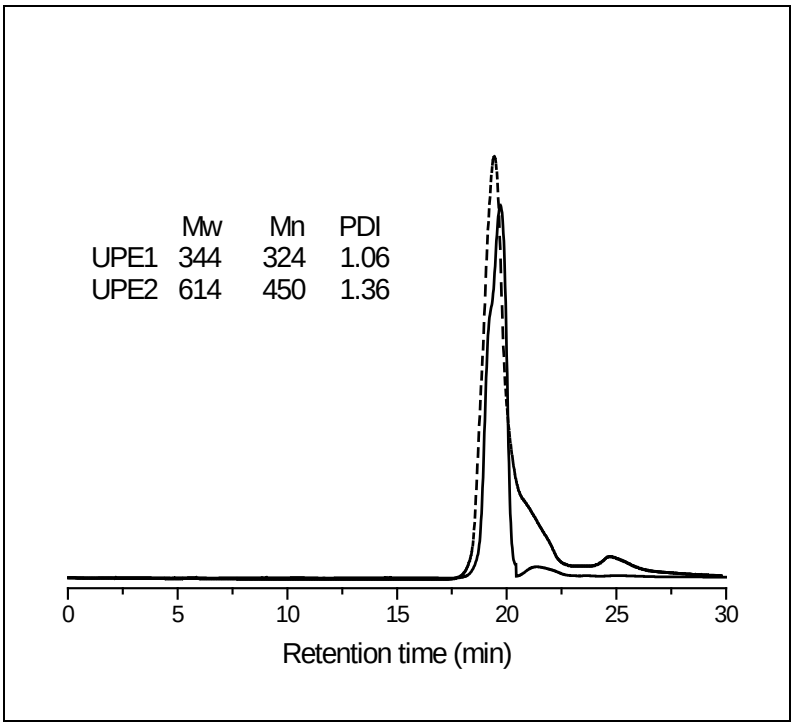

Fig. 162 GPC data of UPE1 (solid line) and UPE2 (dashed line)

The chemical structure of the chain extended type of UPE cross-linker, UPE2, was also confirmed by ^{1}H NMR and GPC. The target molecular weight was 556 g/mol (number average repeating unit [n] = 2). The peak integration of (a,b) and (d,g) was 1.48 to 1, indicating that the number average molecular weight was 574 g/mol (n = 2.08) (Fig. 160b). GPC (Fig. 162) confirmed that M_w, M_n, and PDI were 614 g/mol, 450 g/mol, and 1.36, respectively. UPE3 was also confirmed by NMR. The integration ratio of (a,b) and c was 1:1, meaning that the molecule consists of 2 isosorbides and one maleate.

4.12.3.1 Blending of UPE Cross-Linkers and Reactive Diluents

The synthesized UPE cross-linkers were mixed with various reactive diluents, such as styrene, MMA, and MAA to prepare thermosetting resins. Table 26 summarizes the blending results. However, the cross-linkers showed a poor solubility with reactive diluents (Fig. 159). UPE1 was mixed with styrene of up to 1.5 wt%, while UPE2 was blended with styrene of up to 15 wt%. For UPE thermosetting resins, 25–60 wt% of the reactive diluent is used in general. The solubility of the cross-linker and the reactive diluent became a big problem when preparing thermosetting resin. MMA demonstrated better solubility than styrene. However, UPE1 and UPE2 still showed a poor solubility of up to 10 and 30 wt% with MMA, respectively. MAA was blended completely with UPE cross-linkers.

Table 26 Blending of UPE cross-linkers and reactive diluents. Initial blending condition: cross-linker/reactive diluent (70/30 wt%).

Unsaturated polyester	Styrene	MMA	MAA
UPE1	98.5/1.5	90/10	70/30
UPE2	85/15	70/30	70/30
UPE3	92/8	84/16	70/30

Most of the reactive diluents have hydrophobic properties rather than hydrophilic ones. Based on the chemical structure of the UPE cross-linkers, it was expected that the end group modification of the hydroxy ends on the UPE cross-linkers would be a key point to solve the solubility problem. Two different types of hydrophobic end groups (hexyl and benzyl) were selected to improve blending properties.

4.12.3.2 End Group Modification of Cross-Linkers

The one hydroxy end of UPE1 cross-linker was modified to hexyl group. The modified UPE1 is symbolized as H-UPE1. As one more example, the symbol B-UPE2-B means that 2 hydroxy ends of UPE2 cross-linker were converted to 2 benzyl groups. H-UPE1, B-UPE1, B-UPE1-B, B-UPE2, and B-UPE2-B were prepared, and NMR confirmed their chemical structures as shown in Fig. 163 (NMR for B-UPE2-B is not shown). Fig. 163a shows the chemical structure of H-UPE1. The integration ratio of (a,b) and (d,g) is 2 to 1, and the integration of the methyl group on the hexyl group, $–OCH_2(CH_2)_4CH_3$, is 1.6, indicating that H-UPE1 was prepared successfully. In the case of B-UPE1 (Fig. 163b), the number of protons at the connection between isosorbide and maleate (d,g) at the unsaturated part (a,b) and at benzene (c) are theoretically 2, 4, and 5, respectively. The NMR spectrum (Fig. 163b) proved the chemical structure of B-UPE1. Figure 163c shows that the integration of benzyl (c) is 2 times higher than that of B-UPE1, meaning that B-UPE1-B was obtained. The chemical structure of B-UPE2 was also confirmed as shown in Fig. 163d. The number average repeating unit (n) was 1.8, which was consistent with the previous UPE2 result and therefore proved the reproducibility. The integration of benzyl (c) indicated that B-UPE2 was also synthesized successfully because the number of protons on (d,g) and (c) was 3.56 to 5, respectively, and the integration ratio of (d,g) and (c) was 1 to approximately 1.4.

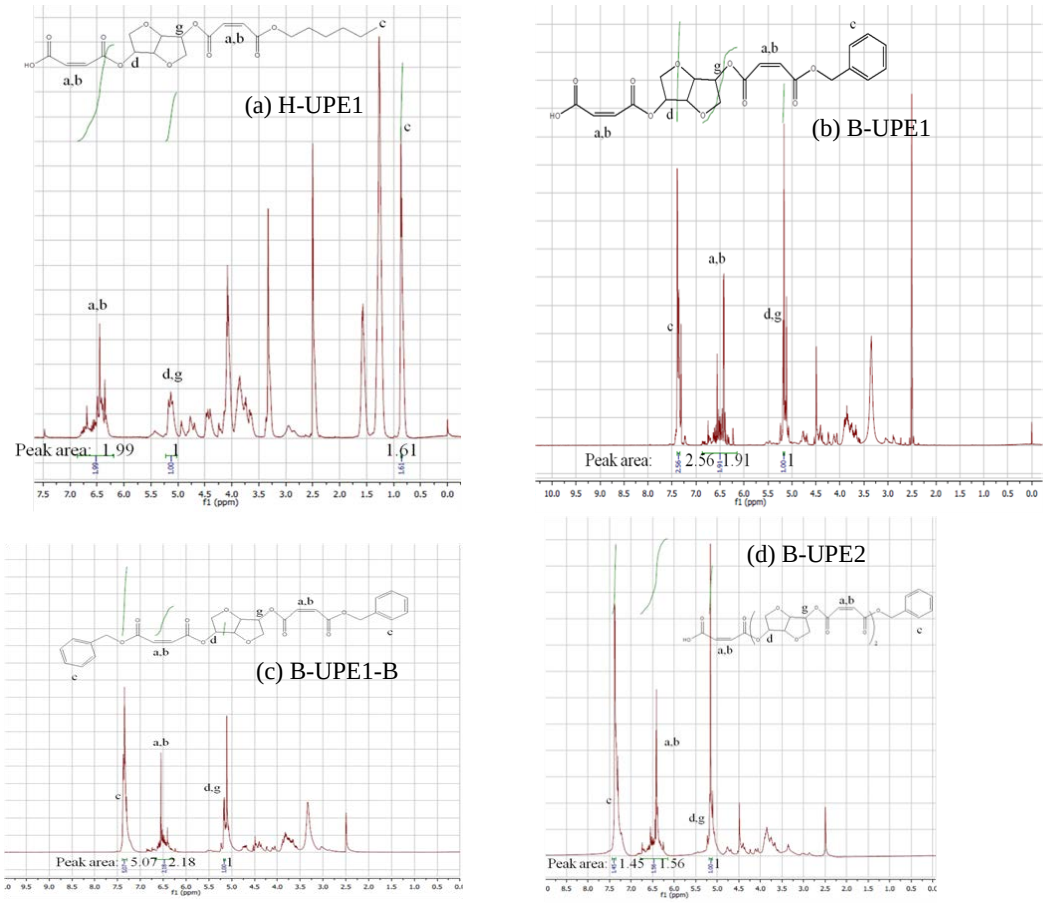

Fig. 163 NMR spectra: a) H-UPE1, b) B-UPE1, c) B-UPE1-B, and d) B-UPE2

4.12.3.3 UPE3 Diglycidyl Ether

Instead of end group modification, UPE3 attempted to obtain epoxy material as shown in Fig. 158. UPE3 diglycidyl ether should be dissolved in organic solvent. However, the final product was water-soluble, meaning that the reaction condition was not suitable for this reaction, and NaOH could attack the ether linkage so that more hydroxy groups might be generated. In most cases, NaOH is used to prepare epoxy resin.

4.12.4 Resin Cure

Table 27 summarizes the cure results of modified cross-linkers (70 wt%) and reactive diluents (30 wt%). Most modified cross-linkers cured with styrene provided solid materials, while cured H-UPE1-H and H-UPE2-H were sticky. Cured, modified UPE resins with MMA and MAA showed low T_g below room temperature, and were generally poor samples that ranged from viscous liquid to a sticky, bent solid.

Table 27 Cure results of modified cross-linkers (70 wt%) and reactive diluents (30 wt%)

Unsaturated polyester	Styrene (30 wt%)	MMA (30 wt%)	MAA (30 wt%)
H-UPE1	Solid, flexible	Liquid	Shrank, bent, sticky surface
H-UPE1-H	Sticky solid		
H-UPE2	Solid, flexible		
H-UPE2-H	Sticky solid		
B-UPE1	Solid	Sticky solid	Sticky solid
B-UPE1-B			
B-UPE2			
B-UPE2-B			

The double bond in uncured and cured cross-linkers was monitored by FTIR (Figs. 164 and 165). The H-UPE1 has an unsaturated part (double bond) near 1,620 cm^{-1}. After it was cured with 30 wt% styrene, the strong intensity decreased significantly, meaning that the double bond reacted with diluents Fig. 164). The H-UPE1 cure with 30 wt% MMA showed the decrease of double bond (Fig. 165). However, a solid polymer was not formed but instead a viscous liquid was obtained. The reasons for this are unclear, but they may indicate evaporation or phase separation of the reactive components to a position outside of the FTIR beam path.

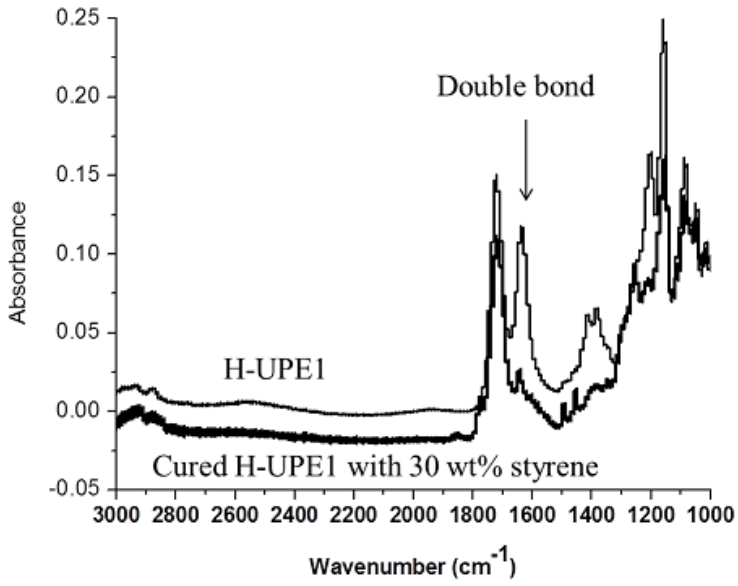

Fig. 164 FTIR spectra of H-UPE1 and cured H-UPE1 with 30 wt% styrene

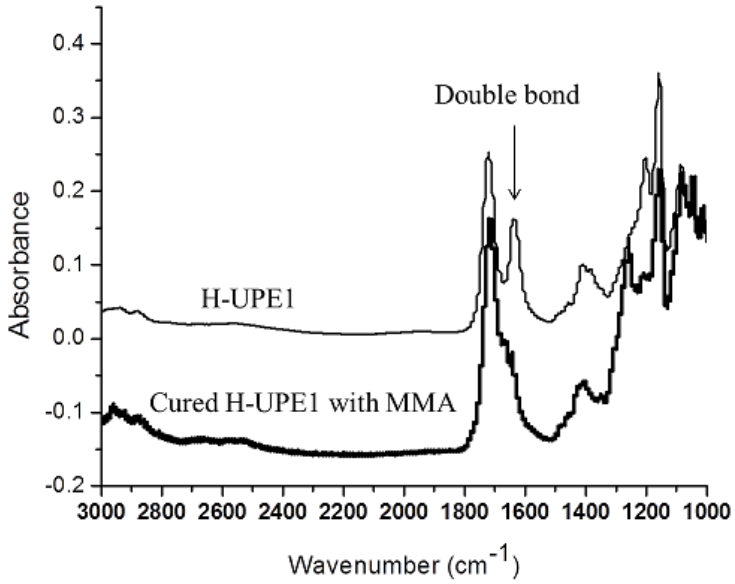

Fig. 165 FTIR spectra of H-UPE1 and cured H-UPE1 with 30 wt% MMA

4.12.5 Polymer Properties

The modified UPE cross-linkers mixed well with the 50 wt% styrene, while the unmodified UPE1 and UPE2 mixed with the styrene at a maximum concentration of 1.5 and 15 wt%, respectively. End group modification made it possible to mix the UPE cross-linkers with various amounts of styrene and prepared thermosetting resins. To investigate thermal and mechanical properties of the UPE thermosetting resins, DMA was employed to obtain the storage modulus (E′ at 25 °C) and the T_g. The summary was displayed in Table 28.

Table 28 T_g and E′ at 25 °C in cured modified UPE resins with various amounts of styrene

Unsaturated polyester	Styrene					
	30 wt%		40 wt%		50 wt%	
	T_g (°C)	E' (GPa)	T_g (°C)	E′ (GPa)	T_g (°C)	E′ (GPa)
H-UPE1	3	0.5	…	…	…	…
H-UPE2	1, 8 (2nd)	0.25	…	…	…	…
B-UPE1	43	3.2	58, 70 (2nd)	3.6	47, 70 (2nd)	2.75
B-UPE1-B	…	…	28	2.7	35	3.4
B-UPE2	26	2.2	47, 65 (2nd)	3.1	53, 80	3.6
B-UPE2-B	21	2.1	30, 42 (2nd)	3.2	40, 55 (2nd)	3.3

The storage modulus and loss modulus of H-UPE1 and H-UPE2 cured with 30 wt% styrene are shown in Fig. 166. The H-UPE1 and styrene mixed well because of the end group modification by the hexyl group, and DMA displayed one peak of the loss modulus, indicating that there were no phase separation and microphase

separation. The T_g and storage modulus at 25 °C were low, approximately 3 °C and 0.5 GPa, respectively. The T_g was determined by the peak of the loss modulus.[185] The H-UPE2 and styrene also mixed well. However, microphase separation may occur in this resin because there were 2 peaks of the loss modulus. The T_g of the cured H-UPE2 resin was similar to that of the cured H-UPE1 resin, while the storage modulus of the cured H-UPE2 was lower than that of the cured H-UPE1.

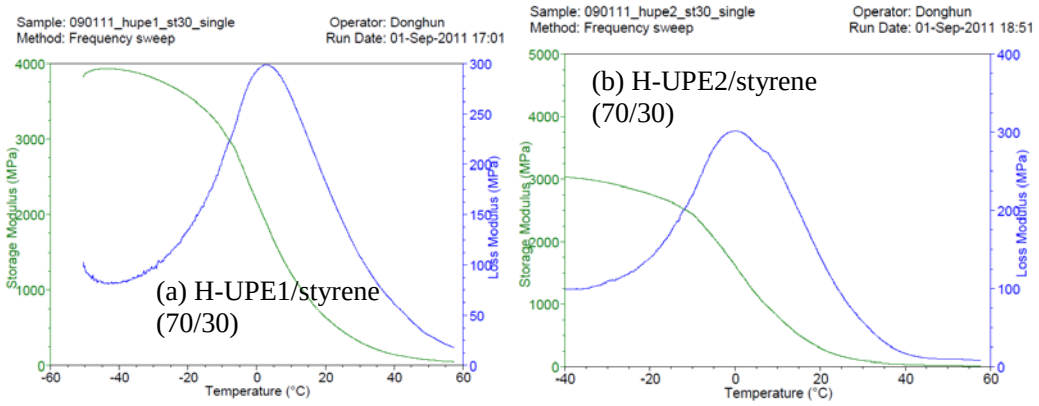

Fig. 166 DMA cross-linkers cured with 30 wt% styrene: a) H-UPE1 and b) H-UPE2

The hexyl end group could make the T_g decrease because of the plasticizer effect. Therefore, a different end group that includes a ring structure was tested to increase the thermal and mechanical properties of the thermosetting resins. In this report, the benzyl group was introduced at the end of the cross-linkers. Figure 167 shows the storage modulus and loss modulus as a function of temperature for B-UPE1 cured with various amounts of styrene, such as 30, 40 and 50 wt%. Before the cure process, the B-UPE1 and styrene mixture was clear, meaning that phase separation did not occur. Microphase separation may occur in the resins containing 40 and 50 wt% styrene because there was a peak and shoulders on the loss modulus. Overall, the benzyl end group provided higher T_g and modulus than the hexyl end group. B-UPE1 (60 wt%) with 40-wt% styrene exhibited a T_g of approximately 58 °C and a storage modulus at 25 °C of approximately 3.6 GPa while B-UPE1 (70 wt%) with 30 wt% styrene showed approximately 43 °C and approximately 3.2 GPa, respectively. The storage modulus and T_g increased when the amount of styrene was increased. These results are reasonable because the T_g of pure polystyrene is about 100 °C. However, the values decreased at the B-UPE1 (50 wt%) cured with 50 wt% styrene, and the microphase separation may occur based on the apparently broad loss modulus. In addition, there were 3 possible peaks near 25, 47, and 70 °C, suggesting that double end modification could provide better solubility of the cross-linkers and styrene.

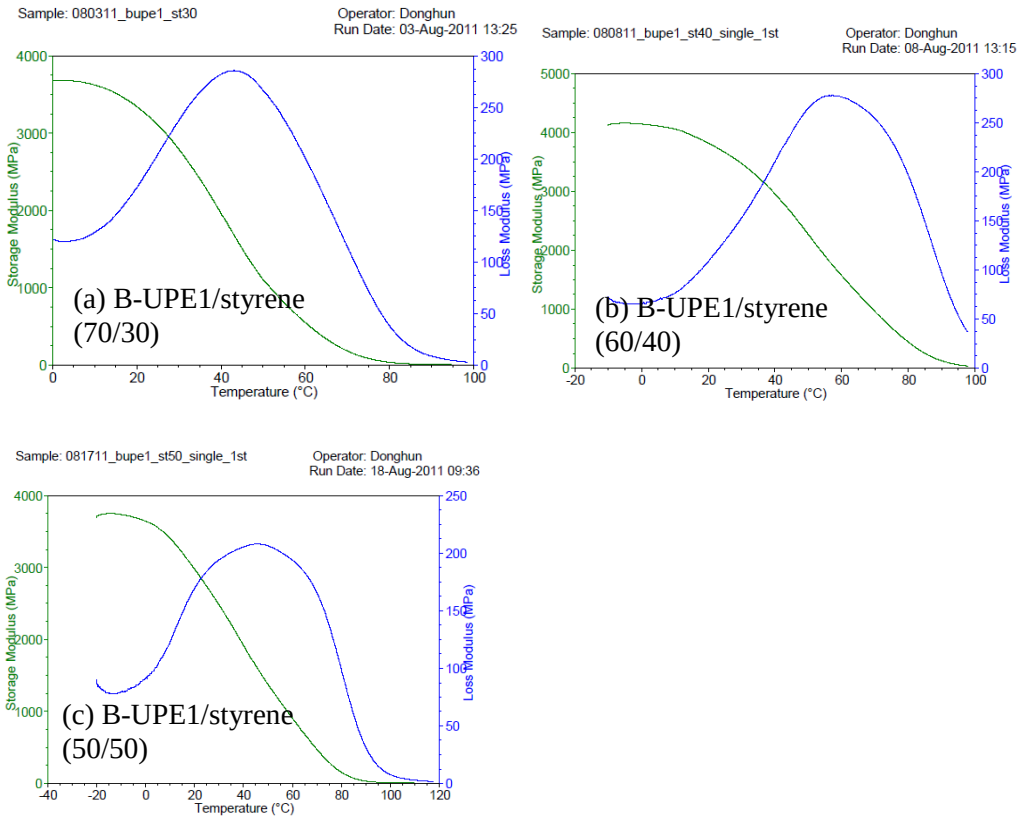

Fig. 167 DMA, the B-UPE1 resins cured with styrene of 30, 40, and 50 wt%

Figure 168 shows the DMA data of B-UPE1-B cured with 40 and 50 wt% styrene. Based on the mixture and the loss modulus of B-UPE1-B/styrene (60/40), there was no evidence of phase and microphase separation. B-UPE1-B/styrene (50/50) showed the improvement of the solubility between the cross-linker and styrene compared with B-UPE1/styrene (50/50). However, the introduction of one more benzyl group caused the reduction of T_g from approximately 47 to 35 °C, while the storage modulus at 25 °C is from approximately 2.75 to 3.4 GPa.

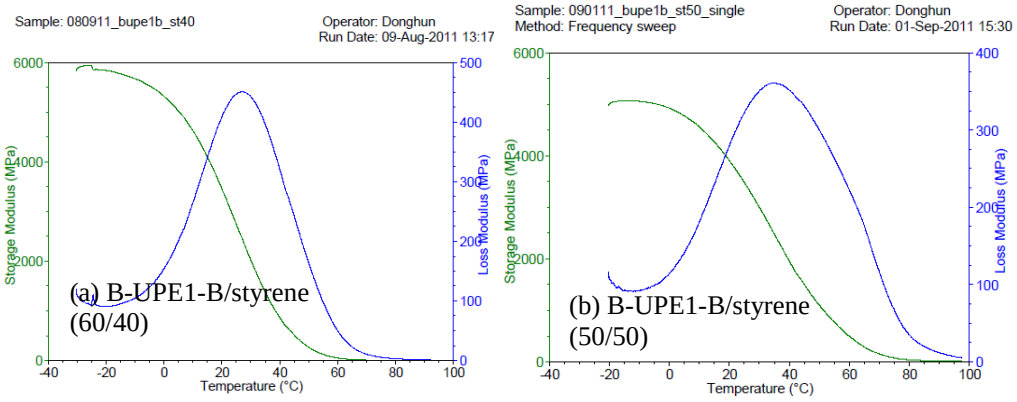

Fig. 168 DMA, the B-UPE1-B resins cured with 40 and 50 wt% styrene

One hydroxy end of the UPE2, the chain extended type of UPE1, was also modified by the benzyl group to improve the solubility of the UPE2 cross-linker and styrene. The B-UPE2 blended well with the 30, 40, and 50 wt% styrene to form apparently clear mixtures. After the curing process, DMA results were obtained, as shown in Fig. 169. The T_g and storage modulus at 25 °C increased when the amount of styrene was increased. The B-UPE2 resin cured with 30 wt% styrene showed a T_g of approximately 26 °C and a storage modulus of approximately 2.2 GPa at 25 °C with one peak of the loss modulus. According to the loss modulus of the B-UPE2/styrene (60/40) sample, one peak was shown at approximately 47 °C, and a shoulder appeared at approximately 65 °C. Furthermore, the shoulder turned to one peak at approximately 80 °C in the B-UPE2/styrene (50/50) sample. It was revealed that microphase separation might occur in the samples containing 40 and 50 wt% styrene. The B-UPE2/styrene (50/50) showed a T_g of 80 °C and a storage modulus of 3.6 GPa at 25 °C, which were the highest values among samples in this report. We expected that one end modification was insufficient to completely blend the UPE2 cross-linker with styrene. Therefore, both end group modifications of UPE2 were conducted; Fig. 170 exhibits storage and loss moduli of B-UPE2-B resin cured with 30, 40, and 50 wt% styrene, respectively. The modification in 2 end groups of UPE2 seemed to answer the problem of microphase separation. However, adding one more bulky end group caused a significant reduction of T_g, from 80 °C (B-UPE2 /styrene [50/50]) to 40 °C (B-UPE2-B/styrene [50/50]).

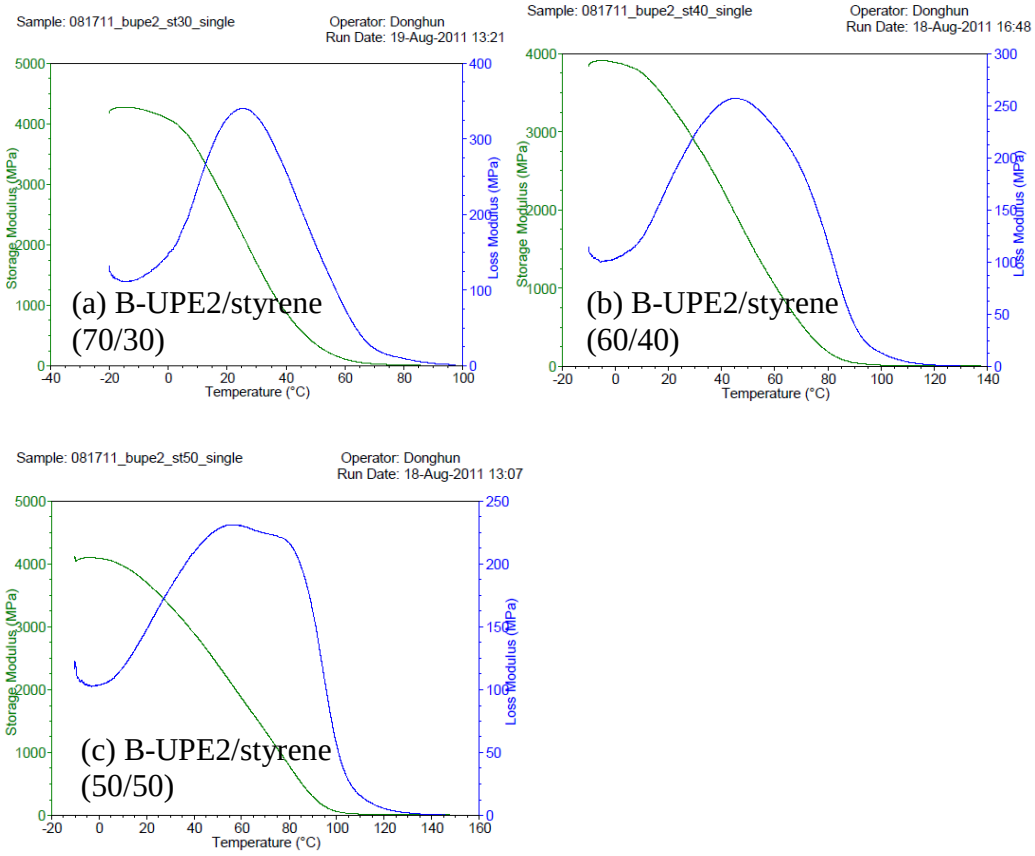

Fig. 169 DMA, the B-UPE2 resins cured with a) 30, b) 40, and c) 50 wt% styrene

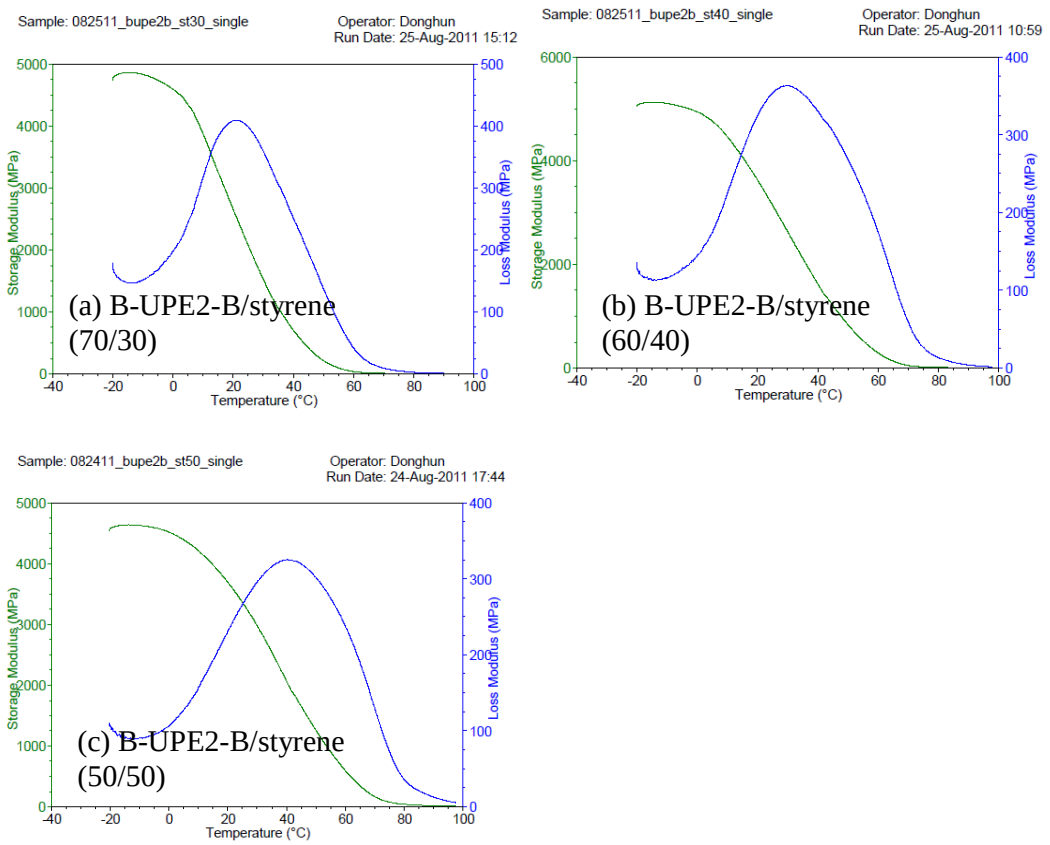

Fig. 170 DMA, the B-UPE2-B resins cured with a) 30, b) 40, and c) 50 wt% styrene

4.12.6 Ternary Blends

Thus far, this section has covered the properties of biobased UPE thermosetting resins cured with styrene. As a reactive diluent, styrene has been used for several decades because of its low cost and excellent properties. Recently, scientists have been researching a replacement for styrene that uses renewable sources. Because styrene is a HAP and VOC, the EPA presented legislation to limit styrene emission from composite manufacturing.[24] La Scala et al.[1] reported that fatty acid–based monomers were used as a styrene replacement to reduce styrene emissions. A methacrylated fatty acid monomer was prepared by the reaction between lauric acid (one of the fatty acids) and glycidyl methacrylate with 1 wt% of AMC-2 at 90 °C. The synthesized monomer was symbolized as MLau. The MLau efficiently replaced about 15 wt% styrene while maintaining proper thermal and mechanical properties of thermosetting resins. The MLau was received and used for this research.

The ternary blend of B-UPE1 (60 wt%), styrene (30 wt%), and MLau (10 wt%) was cured. The T_g was obtained by modulated DSC (Fig. 171), showing that the T_g determined from the reversible heat flow curve was approximately 60 °C.

B-UPE1/styrene/MLau (60/30/10) should be compared to B-UPE1/styrene (60/40). Therefore, the effect of 10 wt% styrene replacement was found.

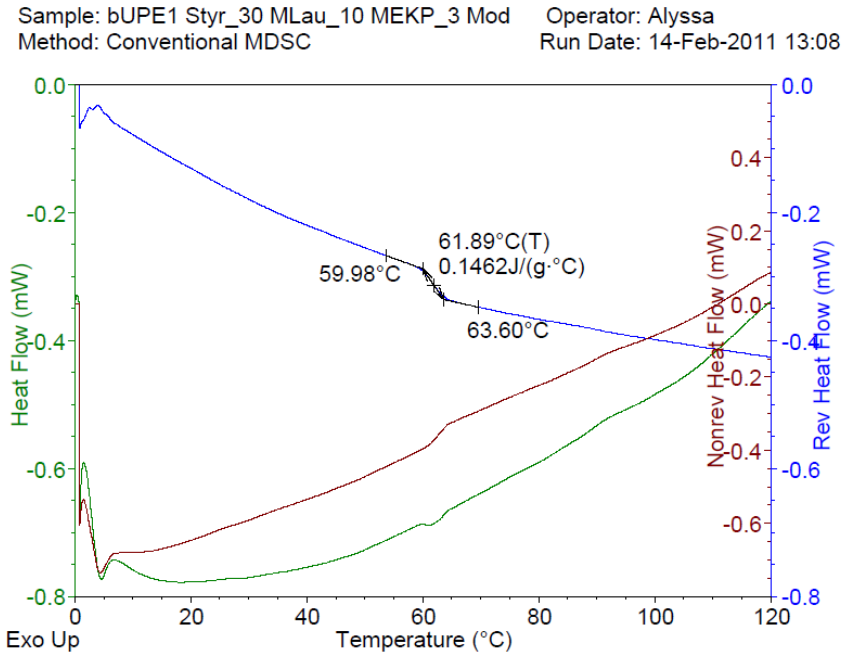

Fig. 171 MDSC thermograms, B-UPE1/styrene/MLau (60/30/10)

From B-UPE1/styrene (60/40) (Fig. 170b), a shoulder at approximately 72 °C and a peak at approximately 60 °C were recognized as T_g. The biobased reactive diluent (MLau) did not show a significant decrease in T_g, and the result suggested that the fatty acid–based monomer would be a promising candidate as a styrene replacement.

4.12.7 Conclusions

Biobased UPE cross-linkers were prepared via the reaction between isosorbide and MA. The cross-linkers of a monomer type (UPE1), a chain-extended type (UPE2), and a sequence-inversed type were confirmed and characterized by NMR, MS, and GPC. However, the cross-linkers did not mix well with reactive diluents such as styrene and MMA. To improve the blending of cross-linkers and styrene, the hydroxy end on cross-linkers were converted to hydrophobic ends such as hexyl and benzyl group. We conducted 1- and 2-end modifications to prepare thermosetting resins. Based on loss modulus results, 1-end modification showed microphase separation, while 2-end modification provided the improvement. However, 2-end modification caused the reduction of T_g compared to 1-end modification. A fatty-acid based monomer was used as a styrene replacement to reduce styrene emissions. The styrene replacement of 10 wt% was applied with

B-UPE1/styrene (60/30), and there was no significant reduction in T_g compared to B-UPE1/styrene (60/40).

4.13 Isosorbide as the Structural Component of BioBased Unsaturated Polyesters for Use as Thermosetting Resins

4.13.1 Introduction

Unsaturated polyesters using isosorbide as the diol component for rigidity were prepared and characterized. The results are described within Sadler and La Scala's work:

- Sadler J, Toulan R, Nguyen T, Kayea R, Ziaee S, Palmese G, La Scala J. Isosorbide as the structural component of bio-based unsaturated polyesters for use as thermosetting resins. Carbohydrate Polymers. 2014;100(SI):97–106. http://dx.doi.org/10.1016/j.carbpol.2013.04.036

4.13.2 Highlights from the Publication

A one pot synthesis, common for UPE preparation, was used to prepare the bio-UPEs as shown in Fig. 172. Isosorbide (0.103–0.308 mol), ethylene glycol (0.103–0.308 mol), MA (0.127-0.246 mol), and a diacid (adipic, suberic, or sebacic 0.127–0.246 mol) were suspended in xylenes and melted together at 55 °C before adding *p*-toluenesulfonic acid (5.0 wt%) and refluxed with aid of a Dean-Stark attachment. The progress of the reaction was monitored by AN titration, and once the desired AN had been reached, the reaction was fitted with a vacuum distillation adapter and distilled at ambient pressure for 2 h and then under reduced pressure (–680 mbar) for 0.5 h. Hydroquinone was added to the molten resin and allowed to stir for 15 minutes before placing in a vacuum oven at 55 °C at –30 mbar for 18 h and allowing to cool. Resins appeared as yellow to amber semi-solids with varying stiffness/viscosity. This resulted in UPEs with the model structure shown in Fig. 173.

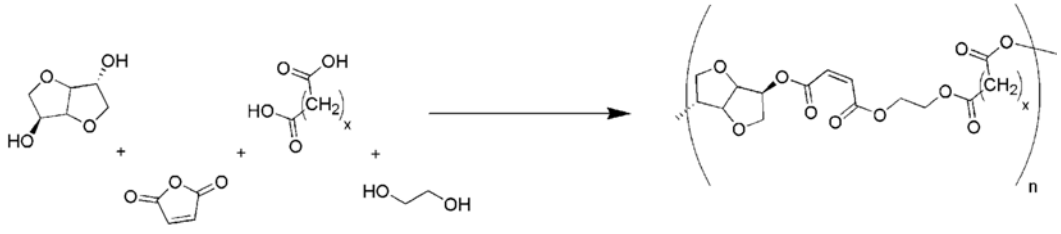

Fig. 172 Schematic of the isosorbide UPE preparation

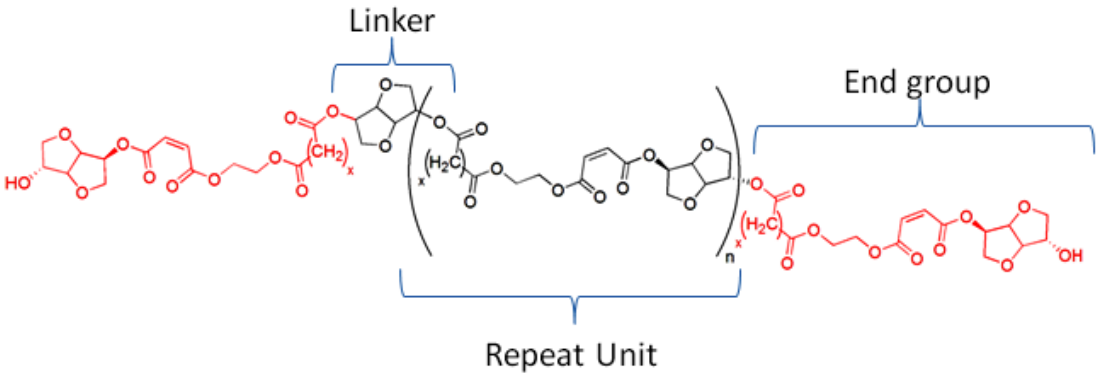

Fig. 173 Model UPE structure

Because of the differences in chemical versus standard UPE resins, these isosorbide-based UPEs solubility in common reactive diluents, such as styrene and MMA, was reduced and likely affects its solubility in other reactive diluents. When solubility parameters are used, the solubility of UPEs in reactive diluents was predicted as a function of degree of polymerization and chemical composition. Figure 174 shows the effects of these parameters on the solubility of isosorbide UPEs in styrene. The higher the relative energy difference (RED), the more insoluble the UPE is in the solvent or reactive diluent. A value RED less than one indicates likelihood of solubility. Our experimental results indicated that RED values of approximately one had limited solubility and values of 0.75–0.8 were required for good levels of solubility.

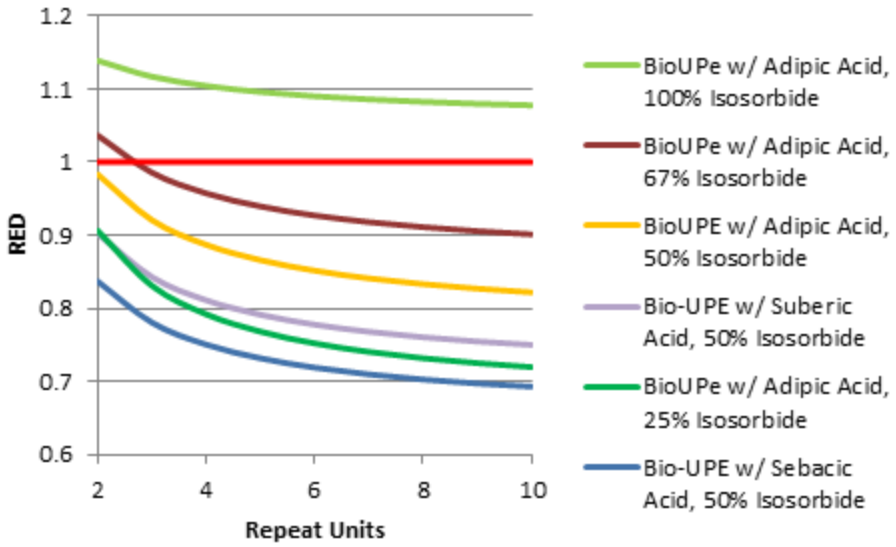

Fig. 174 Predicted structural effects on RED for UPE in styrene

The isosorbide UPE resins had viscosities comparable to that of commercial resins but clearly increased as isosorbide content increased (Fig.175).

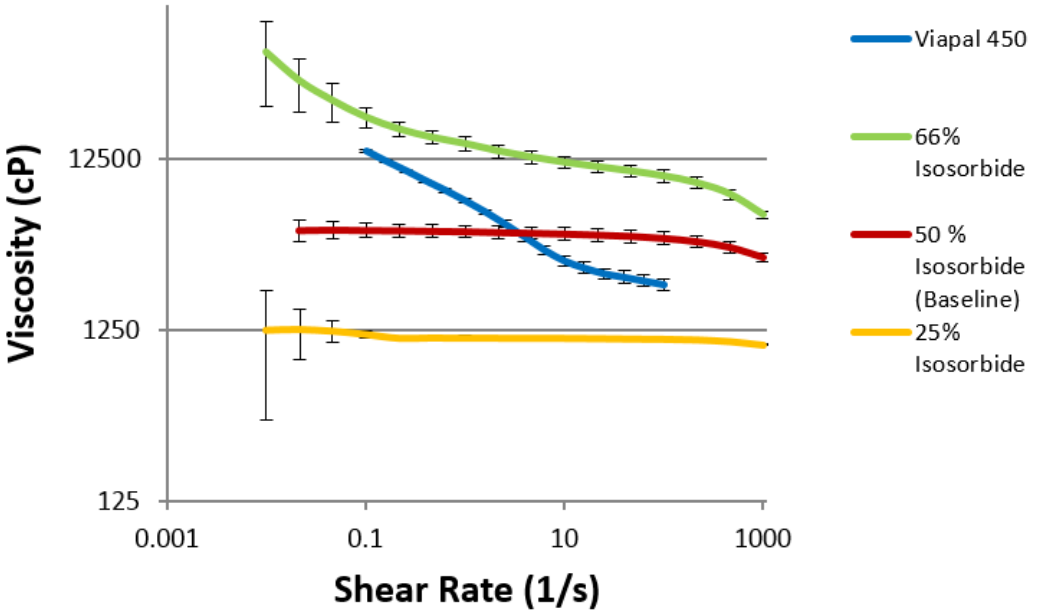

Fig. 175 Isosorbide effect on the viscosity of BioUPE resin blends

The thermomechanical properties of the isosorbide-UPEs increased as the isosorbide content increased, exhibiting both higher modulus and higher glass transition temperature as shown by the peak of tan δ in Fig. 176. Yet, the resultant UPEs had overall low T_g's and are not high-performance resins. The reason for this is that the diacid component used were linear aliphatic monomers providing no structural integrity. Thus, the next section uses isorsorbide as an additive to UPE resins with more standard formulations that use more rigid diacid components.

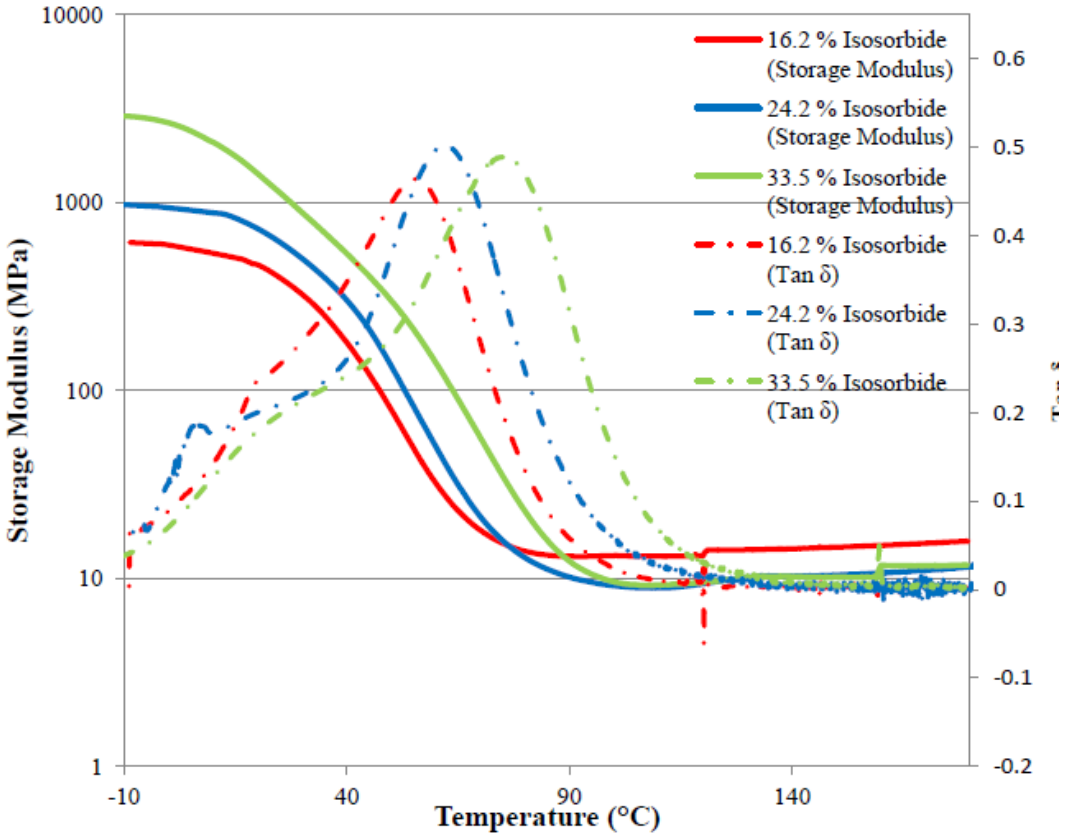

Fig. 176 Tan d of UPEs as a function of UPE isosorbide content

4.13.3 Summary and Conclusions

These results have shown that biobased UPE resins have the potential to be developed as useful thermosetting resins and that isosorbide can be used as a structural constituent of unsaturated polyester resins from the diol component. Our investigations into BioUPE resins have not identified a formulation using isosorbide that possess solubility in common reactive diluents and having thermomechanical properties that would be amenable to high-performance applications. However, these resins do have viscosities that fall within the necessary ranges for composite application and adequately compare to some commercial UPE resins. These basic BioUPE resins have the potential to be leveraged as thermosetting plastics and composites in applications that do not require stricter performance standards. In general, we showed that compositional effects created significant effects in BioUPE viscosity and thermomechnical properties. In particular, our studies have shown that increased isosorbide content does have an effect on viscosity, T_g, and storage modulus but reduced solubility in styrene and would be an invaluable tool for novel resin development. However, isosorbide has proved to be intractable, and to produce resins with properties desirable for high-performance applications, it would be necessary to use concentrations of isosorbide

that would make the resin insoluble in any potential reactive diluents. Although current formulations are inadequate for high-performance thermosetting applications, it may be possible to use isosorbide in the future to improve current aromatic-based UPEs. Such UPEs would have rigid diacid and diol components, potentially enabling the attainment of properties higher than that of any current UPE.

4.14 Unsaturated Polyester Resins for Thermoset Applications Using Renewable Isosorbide as a Component for Property Improvement

This work has been published in the following journal paper and only a summary of the work is provided herein:

- Sadler JM, Toulan FR, Palmese GR, La Scala JJ. Unsaturated polyester resins for thermoset applications using renewable isosorbide as a component for property improvement. Journal of Applied Polymer Science. 2015;132(30):42315.

UPE resins are used in a variety of thermosetting applications due to the reduced cost when compared to epoxy resins; however, UPE resins also have reduced thermomechanical performance. Investigating avenues to improve the performance of UPEs has led to the use of biobased starting materials as structural components of the synthesized prepolymers as a result of their advantageous structural features. Isosorbide, a compound derived from renewable feedstocks, has been used to provide additional stiffness from the diol component for novel unsaturated polyesters resins. These resins have been shown to possess T_g's (32–72 °C) and storage moduli (540–2200 MPa) that are in the desired range for composite materials with viscosities (1.2–25 Pa·s) amenable to a variety of liquid molding techniques.

4.15 Isosorbide-Based Polyurethanes

This work has been published in the following journal paper and only a summary of the work is provided herein:

- Toulan FR, Sadler JM, La Scala JJ. Bio-based polyurethane containing isosorbide for use in composites and coatings. Aberdeen Proving Ground (MD): Army Research Laboratory; 2015 Apr. Report No.: ARL-TR-7259.

The purpose of this research is to formulate polyurethane 1) for use in composites or coatings that contain isosorbide as part or all of the polyol phase and 2) that can be easily molded or cast into a film at ambient conditions. Solubility studies were

conducted to determine the maximum amount of isosorbide that could remain in solution with other diols. Formulation of polyurethanes using isosorbide as part or all of the polyol phase combined with monomers such as toluene diisocyanate (TDI) and isophorone diisocyanate (IPDI) in the isocyanate phase. TDI reactivity at ambient conditions was too extreme, while IPDI was not reactive enough. Prepolymerized polyisocyanates were studied with isosorbide and compared with a commercial polyurethane coating. The dynamic mechanical analysis showed that isosorbide as a drop-in replacement for the commercial polyol increased the T_g 17 °C (Fig. 177). However, UV exposure revealed that the polyurethane containing isosorbide does not perform as well as the commercial product with defects such as brittleness and delamination (Fig. 178).

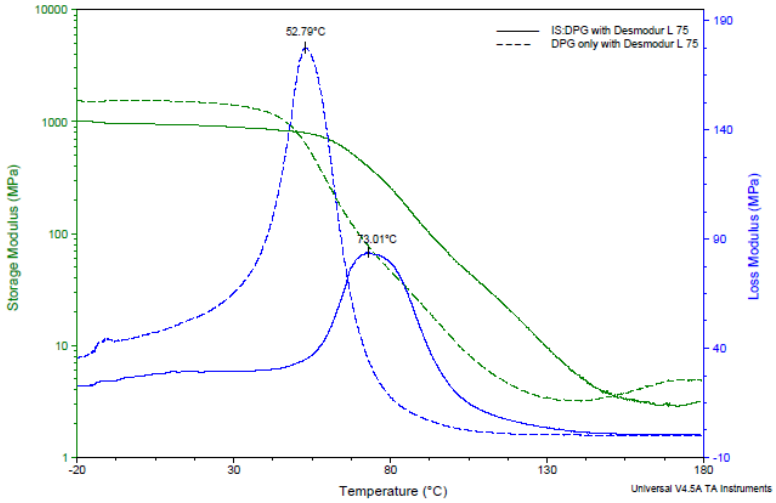

Fig. 177 DMA comparison of Desmodur L 75 blends with isosorbide and DPG

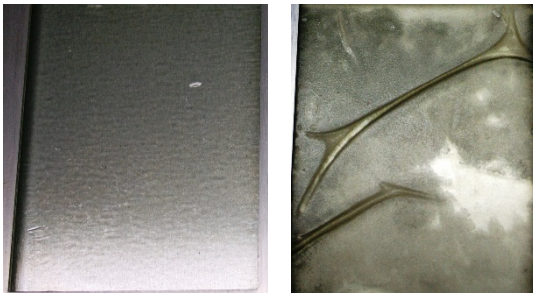

Fig. 178 Commercial coating (left) and isosorbide coating (right) after QUV exposure

4.16 Other Carbohydrate-Based Monomers*

4.16.1 Introduction

As previously discussed, biobased VE and epoxy resins are desired to make more sustainable composites. The previous section shows that anhydrosugars can be used to produce excellent resins. While these anhydrosugars can be used to produce high-performing resin and are based on renewable resources, the drawback to these derivatives is that they still require extensive chemical modification to produce the parent scaffold, which drives up the base cost of the novel resin. The natural carbohydrate derivatives for these anhydrosugars have a wealth of functionality that can be modified by similar chemical means to generate a new class of resins. Oligosaccharides, when viewed as potential candidates, as a core scaffold have a great deal of structural features that would promote the development of high-performance, low-cost, and renewable cross-linking thermosetting resins.

In 2002, global sugar production was estimated to be approximately 143 million ton annually, with the United States responsible for 3% of the total production. Historically, the price of sugar per pound fluctuates, but in recent years the price has been around $0.25–$0.30/lb, which equates to roughly $600/ton. Unrefined carbohydrates potentially could offer a low-cost highly cross-linking resin that could be used in a number of applications. Thus, this section investigates the use of sugar-derived VE and epoxy resins.

4.16.2 Chemistry and Formulation of Bio-Y Epoxies

Synthesis of BIO-Y-1. A methacrylated carbohydrate derivative was prepared as detailed in Fig. 179. Triethylamine was added to a stirred suspension carbohydrate derivative in dichloromethane and cooled to 0 °C before methacryloyl chloride was slowly added and warmed to room temperature. After 18 h, the solid had been completely dissolved, and the reaction was quenched with water (100 mL) and allowed to stir for an additional 30 min. The layers were partitioned, and the aqueous layer washed with an aliquot of DCM. The combined organic layers were washed sequentially with water (2 × 75 mL), sodium bicarbonate (50 mL), and brine (50 mL), dried over magnesium sulfate, and condensed under reduced pressure. The product appeared as a dark brown tacky gel. FTIR spectroscopy analysis indicated the presence of –OH functionality, meaning that the reaction had

* Portions of this section were originally published in La Scala et al. Biobased carbon fibers and high-performance thermosetting resins for use in U.S. Department of Defense applications. Aberdeen Proving Ground (MD): Army Research Laboratory (US); 2012 Jun. Report No.: ARL-SR-245.

not proceeded to completeness. ^{1}H NMR spectroscopy showed that there were 5.75 methacrylates per molecule.

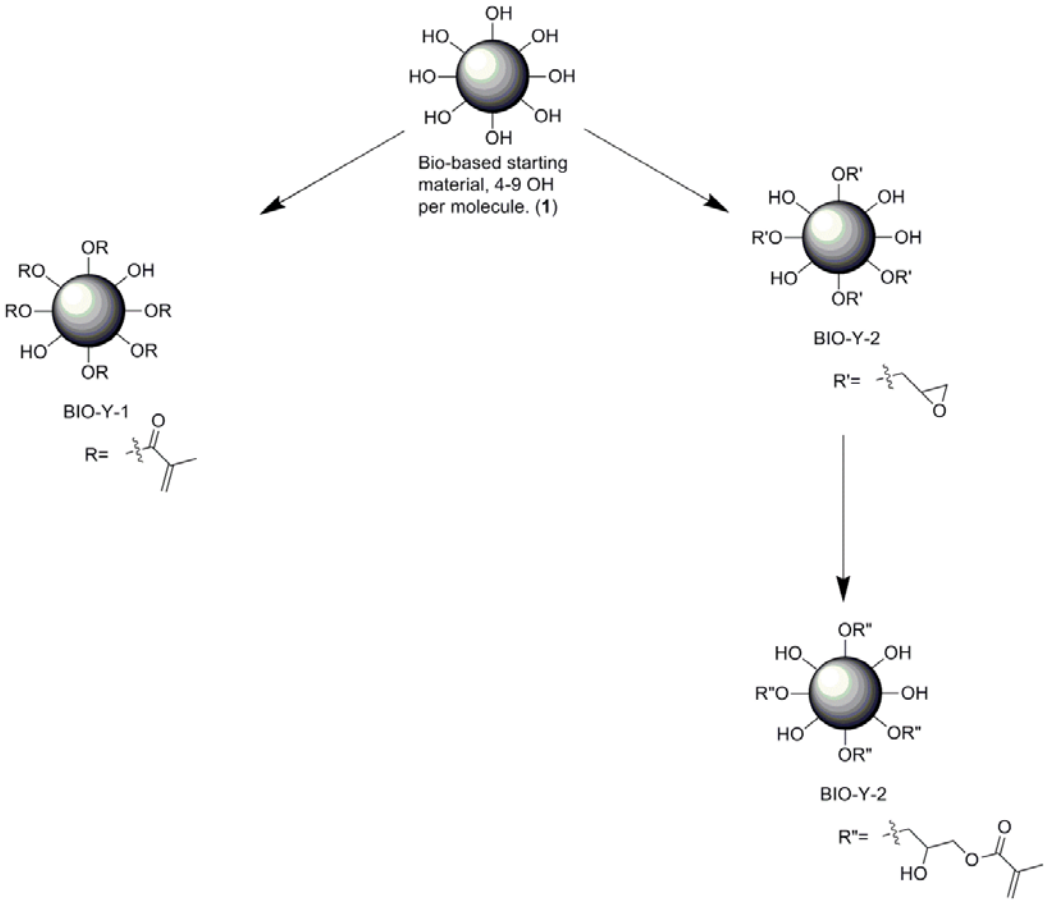

Fig. 179 Schematic of sugar-based cross-linkers

Synthesis of BIO-Y-2. Carbohydrate derivative (5.0 g, 14.61 mmol) and tin (II) fluoride (958.6 mg, 6.118 mmol, 3.0 mol% based on OH content) were suspended in excess epichlorohydrin (20.0 mL, 255.34 mmol) and refluxed for 24 h before removing the excess epichlorohydrin under reduced pressure. The dark reddish-orange oil was diluted with toluene (10 mL) before NaOH was added dropwise in water (5.245 g, 131.125 mmol in 10.0 mL) and stirred at room temperature for 12 h. The reaction mixture was poured into water (300 mL) and extracted with ethyl acetate (3 × 200 mL). The combined organic layers were washed sequentially with water (3 × 100 mL) and then brine (3 × 100 mL), dried over magnesium sulfate, and then condensed under reduced pressure.

Synthesis of BIO-Y-3. BIO-Y-2 (3.0249 g, 3.8274 mmol) and MAA (2.6351 g, 30.619 mmol) were mixed together and heated to 75 °C before AMC-2 catalyst was added and allowed to react for 24 h. The reaction mixture was dissolved in ethyl

acetate (100 mL) and washed with sodium bicarbonate (4 × 50 mL), water (50 mL), and brine (100 mL), and then dried over magnesium sulfate and concentrated under reduced pressure.

Formulation and Curing of BIO-Y-1. Resin systems were blended so that their composition consisted of 65 wt% BIO-Y-1 (2) and 35 wt% styrene. The resin mixture was blended using an ARE-250 Thinky planetary mixer at 2,000 rpm for 5 to 10 min until the sample was homogeneous. Free radical polymerization of each resin was initiated with 1.5 wt% Trigonox, with 0.375 wt% cobalt naphthenate (CoNap) added as a promoter. Resins were cured overnight in a horizontal rubber mold at room temperature and then postcured at 120 °C for 2 h before any analysis was carried out.

Curing of BIO-Y-2: Epoxidized carbohydrate derivatives were produced as shown in Fig. 179. Epoxy products were characterized using NMR spectroscopy and by titration in accordance with ASTM 1652-04[52] to determine the number of epoxy groups per molecule. For this investigation, 0.2 g of epoxy was dissolved with a 1.2-M solution of tetraethylammonium bromide solution in acetic acid (9 mL) in dichloromethane (9 mL) with a crystal violet indicator. Samples were titrated with a solution of 0.1 N perchloric acid in acetic acid until the end point was reached. The epoxy number was calculated using Eqs. 5 and 6. Equation 5 allows for calculation of the weight percent epoxide for the sample; this value depends on the volume of perchloric acid in acetic acid titrated. Equation 6 allows for calculation of the epoxy equivalent weight, which accounts for the molar mass of an epoxy group as shown in Table 29 for 3 samples. This equation also allows for calculation of the epoxy number, with respect to the molecular weight of the epoxidized product.

$$E = 4.3 \times V \times \frac{N}{m_{epoxy}}, \tag{5}$$

$$W = 43 \times \frac{100}{E} = \frac{Molecular\,Weight}{Epoxy\,Number}, \tag{6}$$

where

E = weight percent epoxide (%),

V = volume of perchloric acid reagent required to titrate the standard (mL),

N = normality of perchloric acid reagent (N),

m_{epoxy} = mass of epoxy specimen used (g),

W = epoxy equivalent weight (%),

Molecular Weight = molecular mass of epoxidized product, and

Epoxy Number = number of oxirane units (epoxy groups) per molecule.

Table 29 Epoxy number calculation for Bio-Y-2

Sample no.	Mass	$V_{titrant}$	E	W	EN
1	0.3443	13.38	16.71	257.3	2.31
2	0.3212	12.40	16.60	259.03	2.29
3	0.3063	11.86	16.65	258.26	2.30

Results of the titration experiments showed that very limited substitution occurred. The desired epoxy number of 4–6 epoxies per molecule was not reached. Instead, approximately 1.7–2.2 epoxy groups were added per molecule. Once the product epoxy values were calculated using Eqs. 5 and 6, the appropriate amount of PACM amine curing agent can be calculated using Eq. 7.

$$\frac{52.5}{W} = \frac{m_{PACM}}{1g\ epoxy}. \quad (7)$$

BIO-Y-2 (4.0226 g) was mixed with a PACM amine curing agent (0.8125 g) in an orbital mixer for 5 min before the resin was poured into a horizontal DMA mold and cured at 120 °C for 3 h. The sample was then cooled at room temperature. DMA was performed, and the sample had a glass transition temperature (T_g) of 42.35 °C (loss modulus).

Formulation and Curing of BIO-Y-3. BIO-Y-3 (0.3116 g) was dissolved in styrene (0.1591 g) and free radically polymerized using Trigonox, with CoNap used as an accelerant at room temperature for 18 h and then postcured at 120 °C for 24 h. The resin cured into a hard dark brown material.

4.16.3 Results and Discussion of Bio-Y Epoxies

Syntheses of the primary resins were accomplished starting from a single starting material and then modified in a single reaction step that can add polymerizable functionality to the numerous sites arranged around the core molecule. For the synthesis of the first novel resin, BIO-Y-1, the core scaffold was directly methacrylated using either methacryoyl chloride or methacrylic anhydride in dichloromethane. These highly reactive reagents were ideal for modifying this structure and easily esterified a number of the free hydroxyl groups. Initially, the starting material was not soluble in organic solvent; however, as the reaction progressed, the product slowly increased in solubility and dissolved in the reaction solvent. By the conclusion of the reaction, no solid starting material remained. This

qualitatively indicated that the highly hydrophilic character of the starting material had been modulated and that the desired methacrylate “caps” had been installed. NMR analysis of the product showed that of the 8 potential sites for modification, we were successful in adding methacrylate groups to an average of 4.5–5.5 hydroxyls around the structure. Because of the highly functionalized nature of the starting material and the lack of specificity of the reaction, we cannot determine which hydroxyl groups were substituted and if the same groups are modified from molecule to molecule. For the purposes of our investigation, this is not important; as long as there is a mixture of compounds with similar reactivity, we can formulate a biobased resin system.

Initial formulations dissolved the tacky BIO-Y-1 resin in 35% styrene and cured using a standard CoNap and Trigonox package with a room temperature methodology. The cured resins hardened into dark opaque materials and were subjected to DMA. The preliminary results indicated that the novel resin system had a T_g of 64 °C (Fig. 180) with reactive diluent. As seen in Fig. 180, the material showed interesting characteristics, but the testing was incomplete because the sample failed at moderate temperatures.

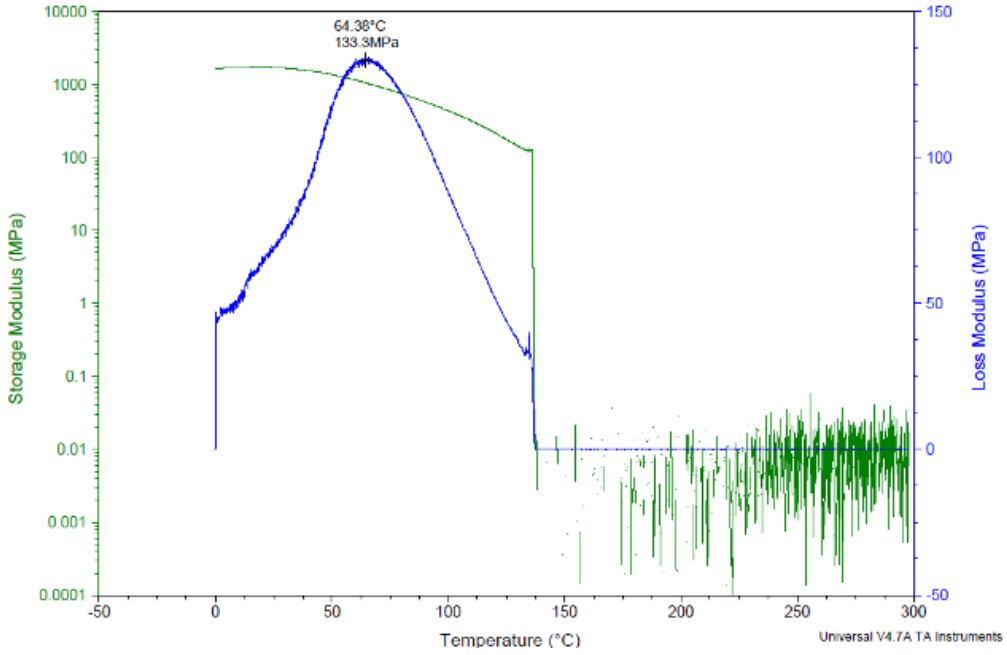

Fig. 180 DMA of BIO-Y-1

The synthesis of resin BIO-Y-2 proved to be more challenging than originally envisioned. Common epoxy synthesis is carried out on a substrate using excess epichlorohydrin in aqueous NaOH; however, when this methodology was applied to the starting material, no reaction was observed and the starting material was

unrecoverable because of alkaline degradation. Once alternate methods were used, the synthesis of BIO-Y-2 was realized when the starting material was treated with the Lewis acid tin fluoride in refluxing epichlorohydrin. Subsequent base treatment reformed the oxirane ring, completing the synthesis of BIO-Y-2. We were not able to accurately determine the degree of epoxidation using NMR; thus, we turned to epoxy titrations as described in ASTM 1652-04.[52] The results of those experiments indicated that we had on the order of 1.2–1.5 epoxide groups per molecule—a significant difference from the goal of 4–6 per molecule or the maximum of 8. The development of this synthesis is only in the beginning stages, and our investigations will continue in an effort to optimize the conditions. Ideally, the resulting optimization studies will allow us to tailor the reaction to produce a range of resins with varying degrees of substitution that will result in different materials.

With the limited success that was experienced with the initial synthesis of BIO-Y-2, materials characterization of the cured resins began in earnest. The results of the epoxy titration allowed us to calculate the appropriate equivalent weight of the PACM amine curing agent. The cured BIO-Y-2 resin hardened into clear reddish-brown material and was subjected to DMA. The resulting material had a modest T_g of 42 °C (Fig. 181) with a storage modulus of 2.7 GPa at 25 °C, indicating a potential for higher-performing materials as more epoxy substituents are added. Materials characterization will continue as the synthesis is refined and new resin systems result.

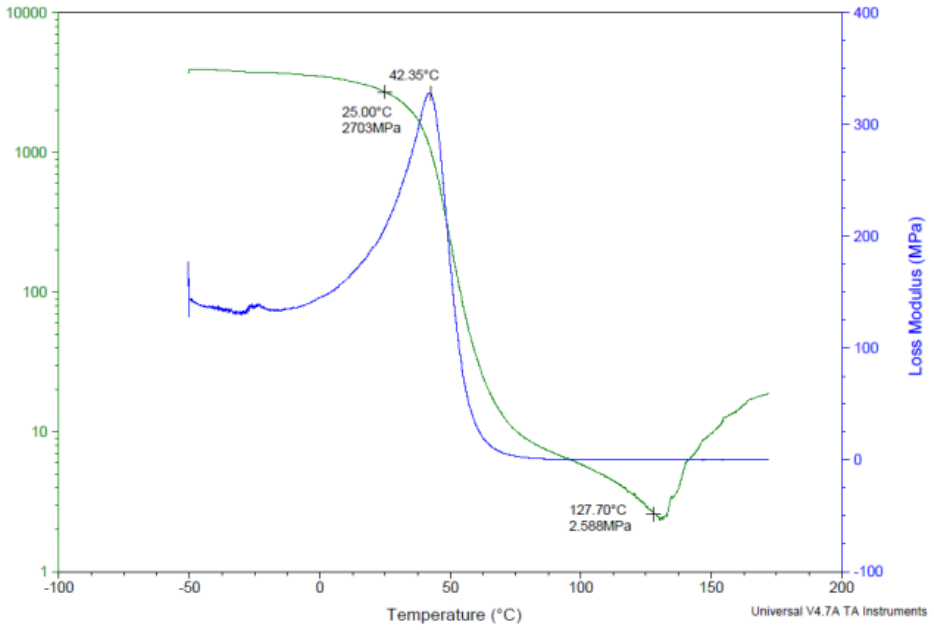

Fig. 181 DMA BIO-Y-2

4.16.4 Other Biobased Monomers

4.16.4.1 Sucrose Amines (Chitin-Like Analogues)

Concept for the conversion of sucrose's hydroxyls into amine functionalities (2 to 7 groups) for use as amine curing agents for epoxy resins is shown in Fig. 182. Changing this functionality also opens the door to making sucrose-based polyisocynates and other resins the utilized amine groups.

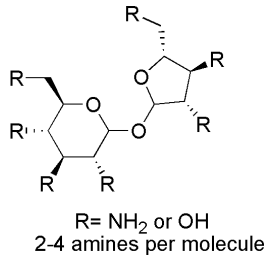

Fig. 182 Amines based on sucrose

4.16.4.2 Diels-Alder Products from Furfuryl Alcohol and Maleic Anhydride (MA)

The bioderived furan rings undergo a Diels-Alder reaction when dienophiles are present—in our case, MA. This unique structure has a number of fused rings that could be used in a number of applications.

Trifunctional Aromatic Structures. The Diels-Alder product that is formed was successfully modified in a 2-step sequence, first to form the aromatic ring and then to reduce the acid/anhydride functionality to obtain a trishydroxymethyl structure. This synthesis was completed and works; however, we did not go back and attempt to scale it or optimize the product yields. This concept should be able to be adapted to the bHMF molecule that would result in a tetra functional molecule (Fig. 183). These hydroxyl functional groups could easily be converted to give methacrylate, epoxy, or glycidyl methacrylate groups to make thermosetting resins. Additionally, the polyol nature of these molecules can also be used in polyesters, unsaturated polyesters, and polyurethane resins.

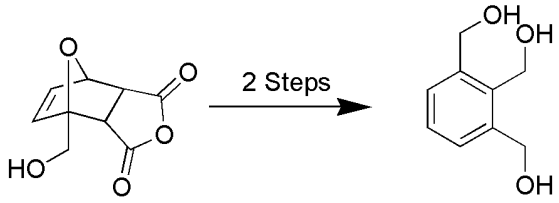

Fig. 183 Diels-Alder products from furfuryl alcohol and MA

Ring-Opening Metathesis Polymerization (ROMP). The double bond in the fused ring system offers the opportunity for ring-opening metathesis with Grubb's catalyst

to develop new polymeric material (Fig. 184). A common substrate for ROMP is dicyclopentatidene (DCPD), which is structurally similar to the Diels-Alder adduct that we have obtained the laboratory. DCPD polymers have been shown to have high impact resistance and be chemically resistant. These biobased Diels-Alder products have the potential to display similar attributes while the various side chain could be modified to produce polymers with novel characteristics.

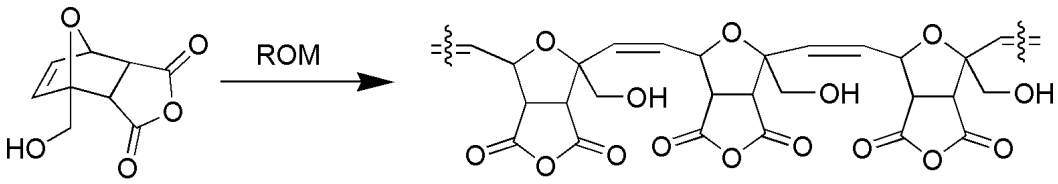

Fig. 184 Diels-Alder polymers through ROMP

Polyimide Oligomer End Cap Units. Polyimide resins are used in high-temperature applications and are typically made from petroleum-derived subunits. Methylene dianiline and benzophenone-3,3′,4,4′-tetracarboxylic dianhydride are oligomerized and bicyclo[2.2.1]hept-5-ene-2,3-dicarboxylic anhydride is added as a capping unit to control molecular weight of the oligomeric material and cross-link the resin through a reverse Diels-Alder reaction to the cured polymide resin. The biobased furfuryl alcohol D-A product that we have isolated in our laboratory is structurally similar to this capping unit and offers the potential for replacement and formulation of novel polyimide resins (Fig. 185). This product has the same anhydride functionality that is necessary for capping that amine group on the oligomeric chain. It also possesses the same bicyclic ring system needed for the reverse Diels-Alder to cross-link the polyimide resins at high temperature.

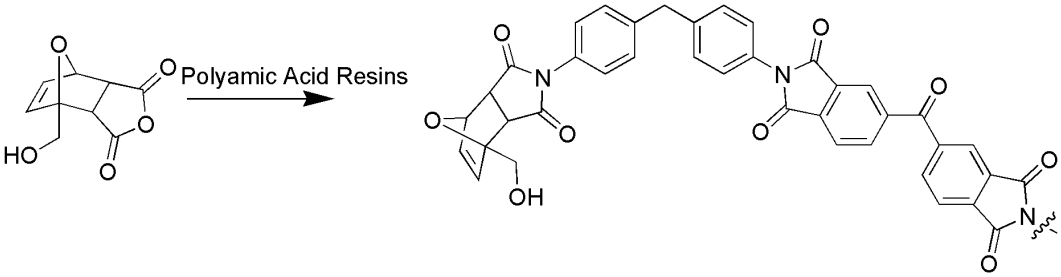

Fig. 185 Polyimide polymers based on Diels-Alder products from furfuryl alcohol and MA

4.16.4.3 BioNovolac Cross-Linking Resins

Expanding on our work with biobased phenolic resins, where we polymerize furfuryl alcohol with an acid catalyst, we designed a series of novel bionovolac cross-linkers that can be used as novolac resin replacements (Figs. 186 and 187). Novolac resins are one of the most ubiquitous classes of resins in the commercial industry, with the BPA derivative being the most well known. This class of resins

and monomers can be found as constituents of polyurethanes, polycarbonates, polyester resins, epoxy, and VE resins to name a few. The chemistry to make these molecules is well known, with the limiting step of adding formaldehyde to phenol, forming the more reactive hydroxymethyl group that readily adds another phenol (or other aromatic subunit). The reaction can be controlled to stop with 2 aromatic groups, yielding BPA and its derivatives, or it can be extended to make higher-molecular-weight novolac oligomers. Many bioderived materials that have been identified by our laboratories for resin development have this reactive hydroxy methyl group already installed, making the need for formaldehyde addition (HAP generator) unnecessary. We have designed variants that would be easily described as substituted BPA derivatives as well as furan-seperated phenols that are a new division within the novolac family.

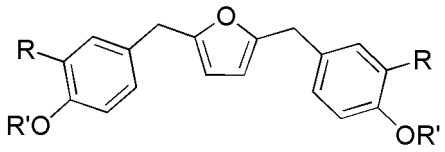

R= H or OMe or Me
R'= Methacrylate, Epoxy,
Glycidyl Methacrylate

Fig. 186 Biofuran separated phenols

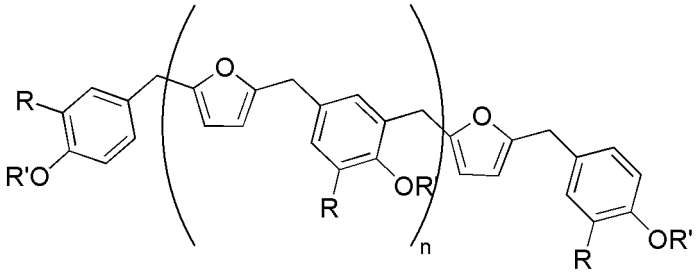

R= H or OMe or Me
R'= Methacrylate, Epoxy,
Glycidyl Methacrylate

Fig. 187 Biofuran separated phenol oligomers

4.16.4.4 Vinyl Furan as a Potential Biobased Reactive Diluent

Synthesis was completed using the reaction scheme outlined in Fig. 188. Vinyl furan was obtained in good yield, but we were not able cure vinyl furan using free-radical polymerization. The literature suggests that this molecule may be polymerized using anionic means; however, we did not pursue it further.

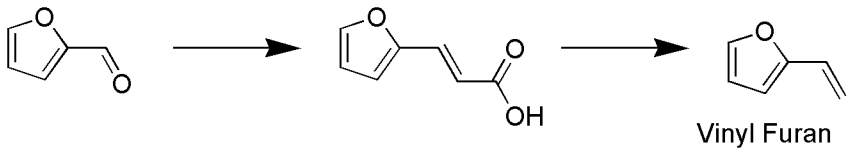

Fig. 188 Vinyl furan

4.16.4.5 bHMF-Methacrylate

We synthesized the molecule using a number of different methods (anhydride, acid chloride, MMA transesterification) and completed a test cure see the resulting material (Fig. 189). No further progress has been made on this molecule to date; other avenues were pursued instead. We intend to revisit this resin in other efforts.

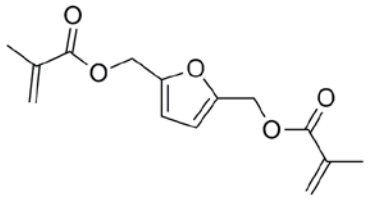

Fig. 189 bHMF-methacrylate

4.16.4.6 Polycarbonates and Polyurethanes

We conceptualized the structures shown in Fig. 190; however, we were not able to pursue this avenue. We were not authorized to acquire the chemicals necessary to pursue investigation.

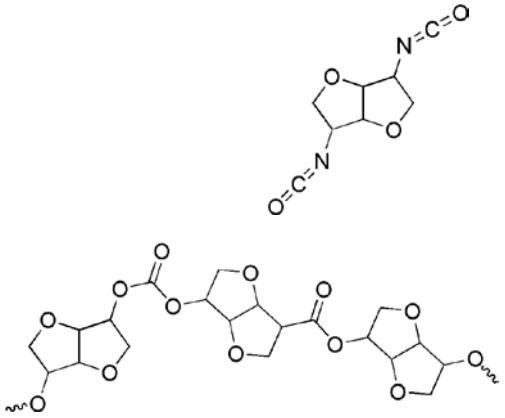

Fig. 190 Isosorbide isocyanate and resulting polymer from reaction with isosorbide

4.16.5 Conclusions

Thus far, we have successfully synthesized a new class of carbohydrate-based resins. Future synthetic efforts will focus on optimizing the reactions to control the degree of functionalization that can be attained. By synthesizing these resins with controlled degrees of functionality, we should be able to produce cured material that exhibits different properties.

Initial DMA of the resins shows materials with low T_g's, but they were promising for future development. These resins need to continue to be developed and formulated to produce materials that can be used in commercial applications.

In this avenue of novel resins, we have only begun to discover the possibilities. Methodologies developed to modify these base structures can be used to modify simpler or more complex carbohydrates. Modification of monosaccharides, polysaccharides, or even cellulose can open a new avenue for resin systems that can offer renewable solutions for the needs of future polymers.

4.17 Biobased Diamines

4.17.1 Introduction

Epoxy resin systems are often used to manufacture high-performance thermosetting polymers as the matrix for fiber-reinforced composites. These resins often feature desirable properties, such as strength, toughness, low cost, low weight, and viscosities amenable for easy processing. The major drawback to the manufacture and development of these resins is that they are derived from petroleum resources, making them nonrenewable, and the costs associated with their manufacture increase as oil reserves begin to dwindle, making future use of these resins cost prohibitive.

Epoxy resins and hardener systems derived from renewable sources can reduce dependency on petroleum. They have become an imperative for continued use and development of thermosetting polymers and composites. The biorefining industry has developed new chemicals and materials from biomass that can lead to the development of sustainable VE and epoxidized products. For example, biorefining triglycerides and carbohydrates has produced a wealth of new fine chemicals that are useful for the development of biobased polymers. Fatty acids and triglycerides have also been successfully developed into materials ranging from toughening agents to cross-linkers in thermosetting resins.

Triglycerides and fatty acids were the first foray into producing biobased resins systems; they found utility in application requiring low- to mid-ranged

thermomechanical properties. Cellulose- or carbohydrate-derived monomers have also been explored for use in thermosetting resins. Derivatives of sugars are useful building blocks because they provide a rigid core structure that can be used to provide stiffness and rigidity. Lignin is another source of biobased material rich in aromatic ring systems that is known to produce rigid high-performance materials. Carbohydrate- and lignin-derived materials have been shown to produce polyurethane, polyester, VE, and epoxy thermosetting resins with excellent thermomechanical properties, driving the development of biobased resins. In an effort to develop wholly biobased thermosets, we have begun work on synthesizing a series of diamine compounds that are derived from isosorbide and lignin-model compounds for use as epoxy curing systems.

4.17.2 Experimental Details

4.17.2.1 Chemistry

Synthesis of Isosorbide Ditosylate: Isosorbide (15.0 g, 103 mmol) and p-toluenesulfonyl chloride (43.6 g, 229 mmol) were suspended in dichloromethane pyridine (49.05 g, 620.1 mmol) separately and slowly added and allowed to react at room temperature for 24 h. The reaction mixture was then concentrated under reduced pressure, and the resulting oily solid was dissolved in ethyl acetate (500 mL) and the solids removed by vacuum filtration. The filtrate was washed with additional ethyl acetate (2 × 500 mL), and the combined organic layers were washed sequentially with aqueous HCl (1 M, 3 × 300 mL), water (500 mL), and brine (500 mL). The layers were then dried over magnesium sulfate and condensed under reduced pressure. The resulting product appeared as a white crystalline solid (46.1 g, 101 mmol, 98.8%) and was used without further purification.

Synthesis of Isosorbide Diazide: Isosorbide ditosylate (46.1 g, 101 mmol) and tetrabutyl ammonium bromide (2.23 g, 6.69 mmol) were dissolved in DMF (120 mL) and heated to 85 °C before adding sodium azide (14.7 g, 226 mmol). The suspension was stirred for 18 h before being cooled to room temperature and the DMF removed under reduced pressure. The crude oil was dissolved in ethyl acetate and partitioned with water. The aqueous layer was washed with ethyl acetate, and the combined organic layers washed with brine (500 mL) and dried over magnesium sulfate and condensed under reduced pressure. The resulting product appeared as an off-white crystalline solid (33.3 g, 97.56 mmol, 96.2%) and was used without further purification.

Synthesis of Isosorbide Diamine: Palladium on carbon was suspended in a solution of isosorbide diazide in methanol and pressurized with 40 psi of H2 gas. The

reaction vessel was agitated for 3 h, and the reaction progress was monitored by TLC. When the reaction was complete, the catalyst was removed by vacuum filtration and the organic solution condensed under reduced pressure.

4,4'-Methylenebis(2-Methylaniline) (Fig. 191): In a 500-mL round-bottom flask, 2-toluidine (20.0 g, 186.9 mmol), HCl (37%) (50 mL), DI water (100 mL), and paraformaldehyde (1.4 g, 46.7 mmol) were combined. The reaction mixture was heated to 90 °C for 3 h. The reaction mixture was then cooled to 0 °C, and solid NaOH was added portionwise over 20 min until the pH reached 9–10. The mixture was extracted with dichloromethane (CH_2Cl_2). The organic extract was dried ($MgSO_4$) and concentrated. The residual was triturated with hexanes and filtered to obtain 4,4'-methylenebis(2-methylaniline) (10.6 g, 98% yield) as an off-white powder: TLC R_f (40%EtOAc/Hexanes) = 0.50.

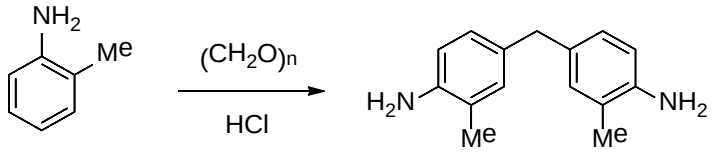

Fig. 191 Coupling reaction to prepare methyl substituted dianilines from anilines

4,4'-methylenebis(2-methoxyaniline) (Fig. 192): In a 500-mL round-bottom flask, 2-anisidine (20.0 g, 162.6 mmol), HCl (37%, 50 mL), DI water (100 mL), and paraformaldehyde (1.21 g, 40.6 mmol) were combined. The reaction mixture was heated to 90 °C for 3 h. The reaction mixture was cooled to 0 °C, and solid NaOH was added portionwise over 20 min until the pH reached 9–10. The mixture was extracted with CH_2Cl_2. The organic extract was dried ($MgSO_4$) and concentrated. The residual oil was chromatographed to obtain 4,4'-methylenebis(2-methoxyaniline) (5.01 g, 47% yield) as a light-orange powder: TLC R_f (40%EtOAc/Hexanes) = 0.50.

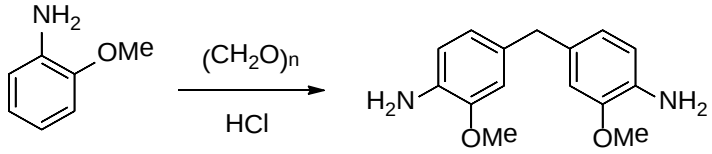

Fig. 192 Coupling reaction to prepare methoxy substituted dianilines from anilines

4.17.2.2 Resin Curing

Solid diamine was dissolved in a minimum amount of methyl ethyl ketone (MEK, 50–75 wt%, Amine Hydrogen Equivalent Weight [AHEW] calculated based on diamine and amount of solvent used) before blending with an appropriate amount

of EPON 828 (epoxy equivalent weight = 187). The resin was blended with the curing agent in a Thinky planetary mixer at 2000 rpm for 5 min before molding in a horizontal silicone mold. The resins were cured at room temperature for 18 h and postcured at 135 °C for 2 h.

4.17.2.3 Rheological Characterization

Thus far, these materials have been crystalline solids that need to be dissolved in solvent to be blended with epoxy resin for curing. Neither the solids nor the amine solution has been analyzed rheologically.

4.17.2.4 Dynamic Mechanical Analysis

Thermomechanical properties of the postcured thermosets were measured using a TA Instruments Q800 DMA in a 17.5-mm single cantilever clamp geometry. Bars were cut into nominal dimensions of 17.5 × 12 × 3 mm^3 and were sanded on both sides to ensure uniform cross-sectional area. The samples were tested at 1 Hz with a deflection of 7.5 μm while subjected to a temperature sweep at a rate of 3 °C/min starting at –20 °C and ending at 210 °C. Two temperature ramp experiments were run for each sample.

A sample of 4,4'-methylenebis(2-methylaniline) was run on DMA and found to have the following properties:

E' @ 25 °C: 1.5 GPa

E'': 125 °C

Tan δ: 129 °C

4.17.3 Conclusions and Future Work

This work is primarily the focus of the SERDP WP-2402 and thus will be reported in future reports for that project. However, the application to SERDP WP-1758 is obvious: to make biobased epoxies with high biocontent, the epoxy *and* diamine content must be bioderived. Future results will determine whether these biobased scaffolds provide benefits for the diamine component.

4.18 Processing of Composites Containing Acetylated Softwood Kraft Lignin (Ace-SKL)-Derived Carbon Fibers

4.18.1 Scale-up of Ace-SKL Carbon Fiber Production

To produce mini-composite specimens derived from lignin-based carbon fibers, a larger amount of carbon fibers was generated from Ace-SKL precursor.

Purification, acetylation, and solution spinning were done following the previously described procedure. For stabilization, 130–140 mg of as-spun Ace-SKL fibers were mounted on each tow (as contrasted with only 30 mg/tow in earlier years).

There is a limitation of dead-weight that could be applied during batch carbonization experiments (performed during the course of this research project) because of the shape and volume of the current graphite fixture. Also, there is a limitation of bonding force of the ceramic based glue used for mounting fiber tows before carbonization. Weights larger than about 65 g led to a separation of the glue from the graphite end-tab during carbonization, which caused a loss of tension. Even then, the average tensile strength from single-filament tests was measured around 800 MPa. Thus, 18 carbon fiber tows around 125 mm long were generated with each tow consisting of 120–150 mg of carbon fibers, as shown in Fig. 193. Application of tension in a continuous process is done by speeding up the take-up roll relative to the feed-roll. Thus, application of adequate tension or debonding of the adhesive will not be a problem in a scaled-up continuous process.

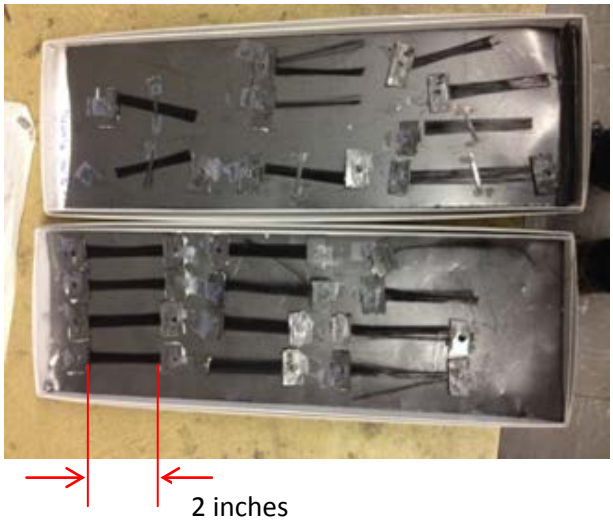

Fig. 193 Carbonized Ace-SKL carbon fiber tows

4.18.2 Composite Fabrication Using Ace-SKL Carbon Fibers and Epoxy

Individual carbon fiber tows derived from Ace-SKL were processed into composites with the vacuum infusion method. Silicone molds with sample thickness of 0.5–1 mm were made with RTV 664 Pail Kit. Fibers were aligned unidirectionally in the mold and PT1271 resin was filled around. Surface of resin was covered with porous Teflon nonstick film and breather film, and the whole system was sealed around the edges, and connected to vacuum. The mold and resulting composite is illustrated in Fig. 194. Also, commercial PAN-based T300 carbon fiber were fabricated into composites as control samples.

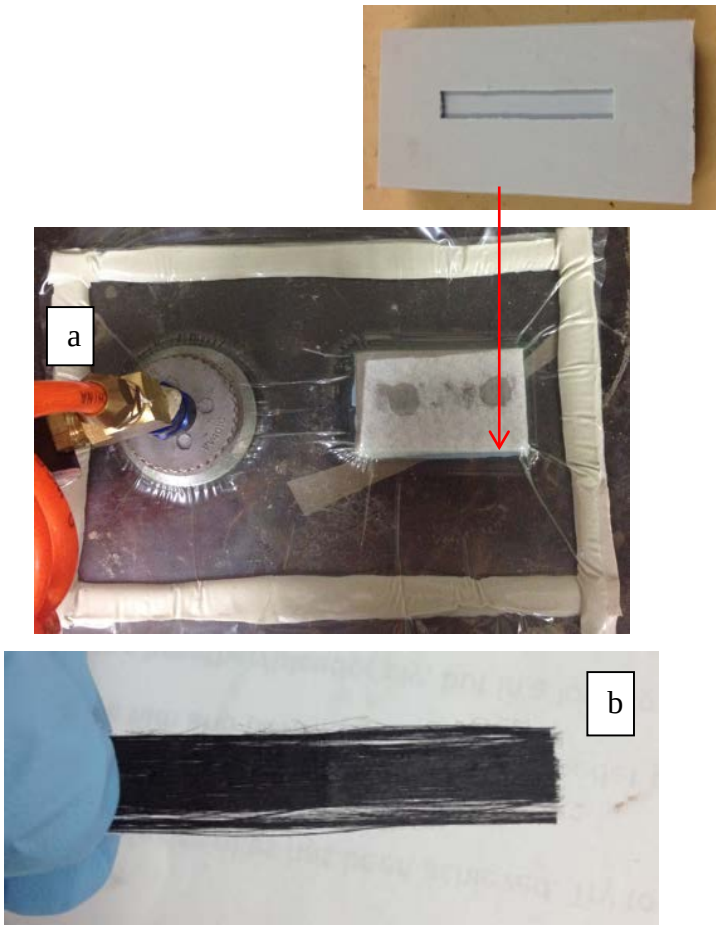

Fig. 194 a) Composite production with vacuum-assisted infusion; b) Ace-SKL carbon fiber composite

All of the experimental composites thus produced are shown in Fig. 195. Vacuum infusion in the 1-mm-deep cavity resulted in composite samples with least bubbles.

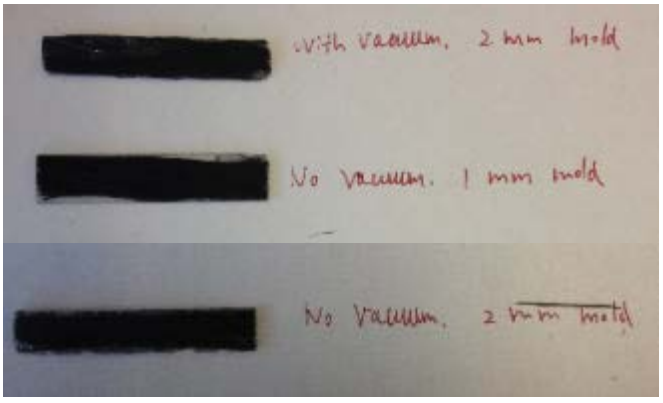

Fig. 195 Composites produced from commercial T300/epoxy

One end of the composite samples from a 1-mm cavity was cut, and the cross-sectional area was polished. The optical microscope image of polished cross-sectional area of an Ace-SKL carbon fiber–based composite is shown in Fig. 196. In Fig. 196a, a region with a higher density of fibers is observed, whereas in Fig. 196b, a region with very low fiber content is seen. Figures 196c and 196d are higher magnifications (200× and 500×) of the region displayed in Fig. 196a. The uneven distribution of fibers was caused by limited amount of Ace-SKL carbon fibers fabricated in the composite.

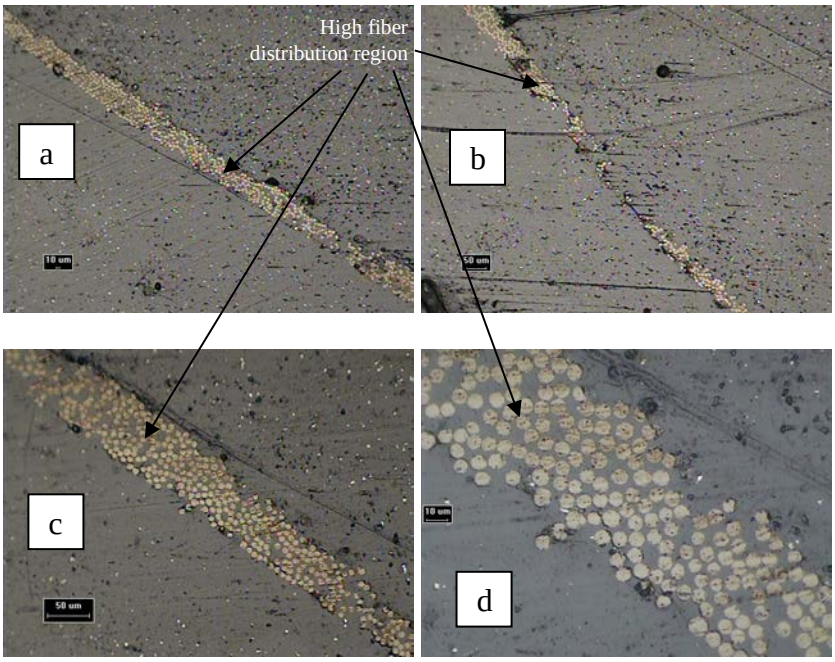

Fig. 196 Optical microscopy images of polished Ace-SKL carbon fiber composite cross-sectional area: a) 100× magnification of region with higher fiber content; b) 100× magnification of region with lower fiber content; c) and d) 200× and 500× magnification of image a), resptectively.

The edge of the epoxy matrix of the composite could not be clearly observed in this image because it blended with the background of the epoxy mounting compound, and the overall volume fraction of fibers could not be obtained from these optical images. Thus, it was calculated from the density of the composite (ρ) as measured by sample mass (m), length (L), thickness (D) and width (w). The total cross-sectional area of fibers $A_f = m / \rho / L$, and volume fraction of fibers $V\% = A_f / (D \cdot w)$.

The fiber volume fraction was calculated at 28 vol%, which is lower than commercial carbon fiber composites (ca. 60%). However, in several local regions as shown in Fig. 196d, the local fiber volume fraction was calculated at 56 ± 2%,

which is very close to the commercial composite. An example of a light micrograph used for local volume fraction calculation is shown in Fig. 197. It is expected that with increased fiber production, an Ace-SKL carbon fiber composite with good fiber distribution could be obtained.

Fig. 197 Optical image processed for local fiber volumn fraction calculation

The flexural modulus was measured using the 3-point bending test. A T300 carbon fiber–based composite sample mounted in the rheometer is shown in Fig. 198. A strain sweep was applied from 0%–0.1% to determine the linear viscoelastic regime, and the results are shown in Fig. 199. The measured modulus is generally consistent with that reported in the literature for composites containing a relatively small fiber volume fraction of about 14%. The Ace-SKL carbon fiber-based composite samples were also attempted, but they were much thinner compared with T-300-based carbon fiber composite and were not rigid enough to be tested in the 3-point bending fixture. Instead, these were tested in tension as described next.

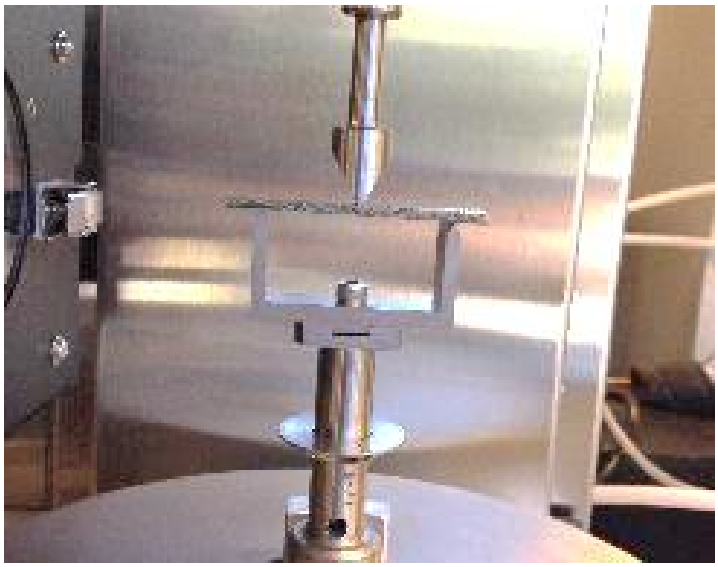

Fig. 198 Three-point bending test of T-300-based carbon fiber composite

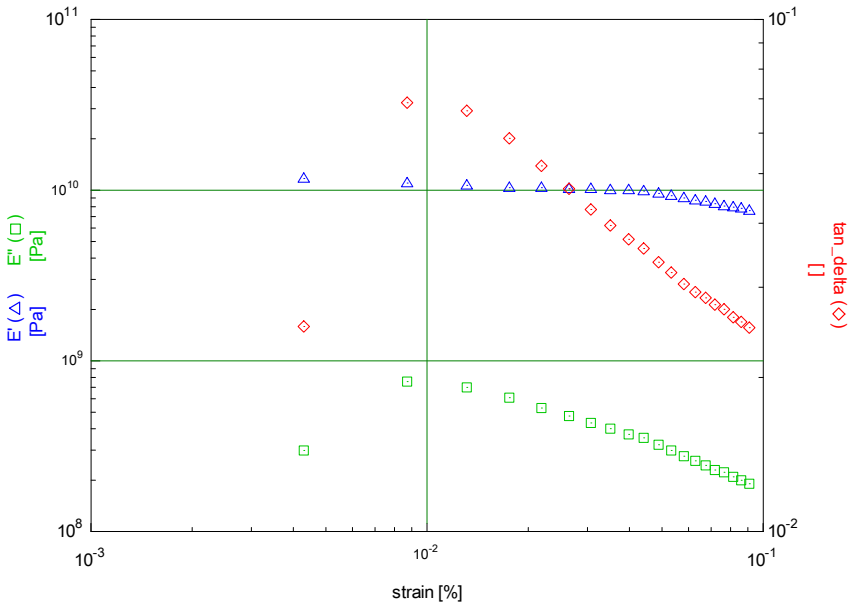

Fig. 199 Three-point bending results for T-300/epoxy mini-composite

For the tensile test, a layer of resin was applied to both ends of the composites. However, slippage occurred when the applied force was around 18 lb. This confirms the need to generate a thicker layer of resin to reduce slippage in future experiments.

To test the tensile strength of the Ace-SKL carbon fiber composite, epoxy resin end tabs were painted on both ends of the composite sample, as displayed in Fig. 200a. Composites were mounted in a wedge-action tensile fixture, and a crosshead speed was set to 0.1 inch/min (Fig. 200b). In some regions of the sample, breakage occurred along the fiber direction, as is sometimes observed for unidirectional composites, as shown in Fig. 200c. In contrast, a clear breakage was observed for the sample shown on the right side of Fig. 200d. The tensile strength for a sample containing 28 vol% fiber composite was just under 200 MPa. For greater volume fractions of carbon fibers and with better automated composite processing techniques, the composite strength will be higher. The clear breakage in Fig. 200d and microscope image in Fig. 200e are indications of excellent fiber/matrix bonding.

Fig. 200 (a) Ace-SKL carbon fiber composite specimen with pure epoxy resin end-tabs; (b) composite specimen during tensile testing; (c) composite specimen fractured halves after tensile testing showing partial failure along the length for (a); (d) breakage after tensile testing with clear tensile failure.

For tensile testing, the sample was mounted in a wedge-action fixture, but slippage occurred when the applied force reached about 80 N. This indicated the need for adequate end-tabs to reduce slippage during tensile experiments. Thus, epoxy resin end-tabs were applied to both ends of the composite sample, as displayed in Fig. 200a. These end-tabs helped in successful testing of the composites, as shown in Fig. 200b, at a crosshead speed of 0.1 in/min. As shown in Fig. 200c, in some regions of the sample breakage occurred along the fiber direction, as is sometimes observed for unidirectional composites. In contrast, a clear breakage was observed

for the sample shown in Fig. 200d. The tensile strength for a sample containing 28 vol% fibers composite was approximately 200 MPa. For greater volume fractions of carbon fibers and with better automated composite processing techniques for fiber alignment, greater composite strength can be achieved. The clear breakage in Fig. 200d is an indication of good fiber/matrix bonding.

SEM micrographs of the fractured cross sections are displayed in Fig. 201. Fiber pull-out is observed for several fibers, with some resin stuck to the other fiber surfaces. This is not surprising because these experimental carbon fibers were not surface treated to enhance bonding with epoxy resin. For commercial fibers, surface modification is an important step. Thus, with additional processing steps, it will be possible to enhance the fiber-matrix bonding and composite strength further.

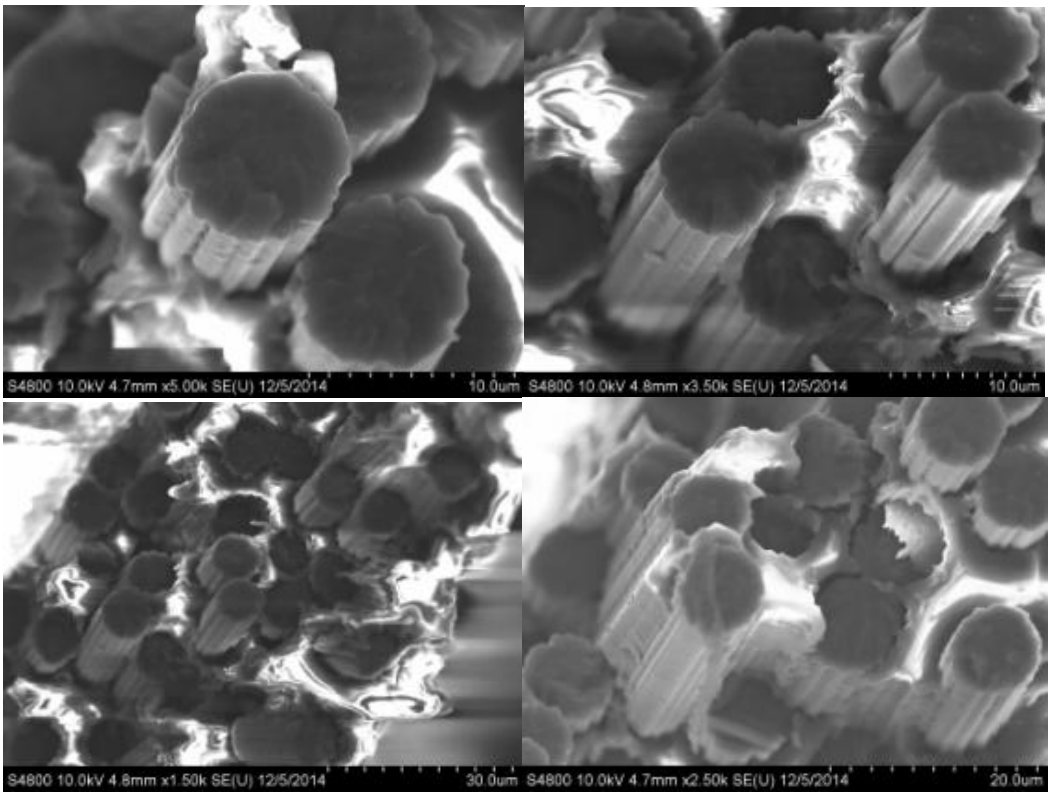

Fig. 201 SEM image of composite breakage after tensile test

4.18.3 Biobased Resins and Carbon Composites

Finally, as a proof-of-concept, the biobased (Ace-SKL) carbon fibers were infused with bioderived BOF and BOB resins to produce true biobased composites. These composites were prepared using the same method as previously described.

The composites were tested for tensile strength, and a tested sample is displayed in Fig. 202. The clear/smooth fracture surface indicates good bonding between fiber

and epoxy matrix. It was observed that there was significant misorientation of fibers within the composite likely caused by the flow of the resin during the vacuum infusion step.

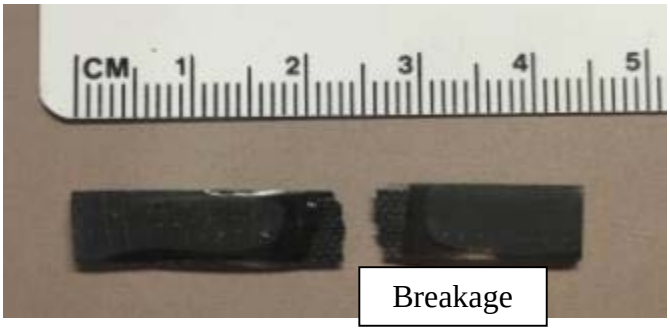

Fig. 202 Ace-SKL CF / BOF composite sample halves after tensile testing

The tensile strengths for Ace-SKL/BOF and Ace-SKL/BOB composites containing 8–10 vol% fibers were 230 and 210 MPa, respectively, similar to that of composites derived from synthetic resin. These tensile strength values are lower than those obtained from commercial fibers and resins. However, the commercial products are produced from synthetic precursors, whereas the current ones are from wholly biobased precursors. Thus, there exists significant potential for optimization and automation of the biobased carbon fibers and resins produced in the current research project to lead to superior properties of the composites.

4.19 Life-Cycle Cost Analysis*

4.19.1 Lignin-Based Carbon Fiber

It is expected that lignin-based carbon fibers will cost significantly less than current carbon fibers. The DOE's initiative to develop lignin-based carbon fibers to make lighter-weight, affordable automobiles is centered on the reduced costs of lignin-based carbon fibers. Their goal, although not yet realized, is lignin-based carbon fiber costing $5–7/lb. Current aerospace carbon fiber costs approximately $25/lb, and commercial-grade carbon fiber costs about $15/lb. The DOE has yet to obtain lignin-based carbon fibers with the appropriate performance, so truly assessing the feasibility of the cost is not possible at this time.

There are significant costs associated with manufacturing carbon fibers from rayon, PAN, or pitch. Figure 203 breaks down the costs of carbon fiber production. Some of the cost is the raw material, especially for rayon and PAN, but much of the cost

* Portions of this section were originally published in La Scala et al. Biobased carbon fibers and high-performance thermosetting resins for use in U.S. Department of Defense applications. Aberdeen Proving Ground (MD): Army Research Laboratory (US); 2012 June. Report No.: ARL-SR-245.

results from the manufacturing method. The high-energy process used to melt pitch fibers and oxidize and carbonize all types of carbon fibers is a large element. However, this cost is likely to be very similar for lignin-based fibers. On the other hand, PAN, in particular, generates toxic chemicals during manufacture that impose significant costs to prevent worker fatality and minimize environmental pollution. Lignin-based carbon fibers would have no need for much of these emissions control facilities and should obtain reduced costs.

An analysis done by ORNL shows the cost breakdown for low-grade PAN-based carbon fibers in Fig. 203.[186] These carbon fibers cost approximately $10/lb. The PAN precursors are by far the largest cost component and represent an even higher share of the cost for aerospace-grade carbon fiber. In fact, much of the other costs in Fig. 204 remain relatively unchanged for aerospace-grade fibers. The cost of acrylontrile is only $1/lb, and the cost of low-performance acrylic fiber is only approximately $1/lb.[187,188] Thus, much of the precursor cost is the solution fiber-spinning method necessary to orient the fibers and reduce the size of the fibers to less than 30 μm in diameter. The hazardous solvents play a significant role in raising this cost.

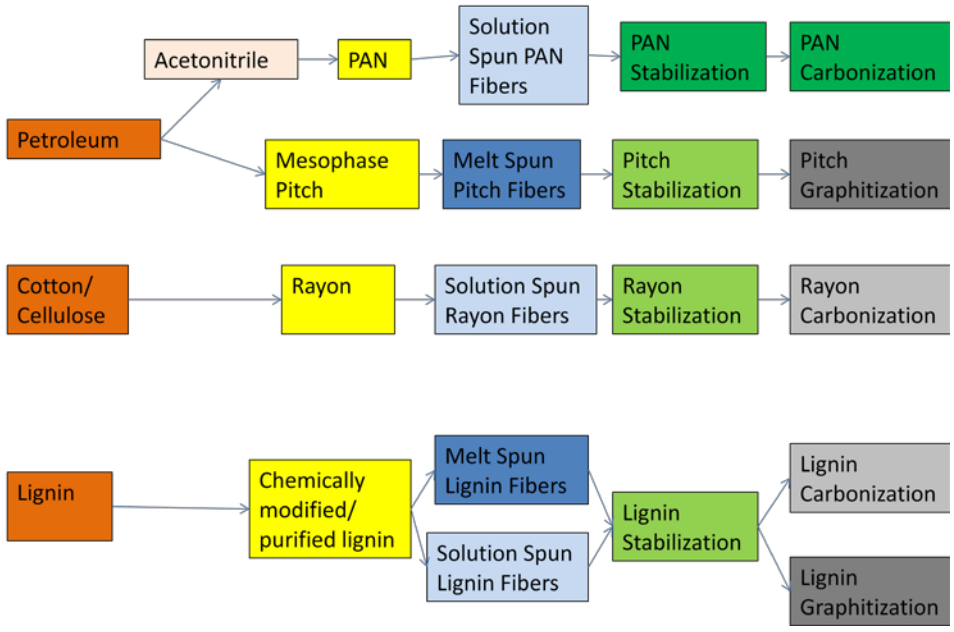

Fig. 203 Cost breakdown of carbon fiber manufacture

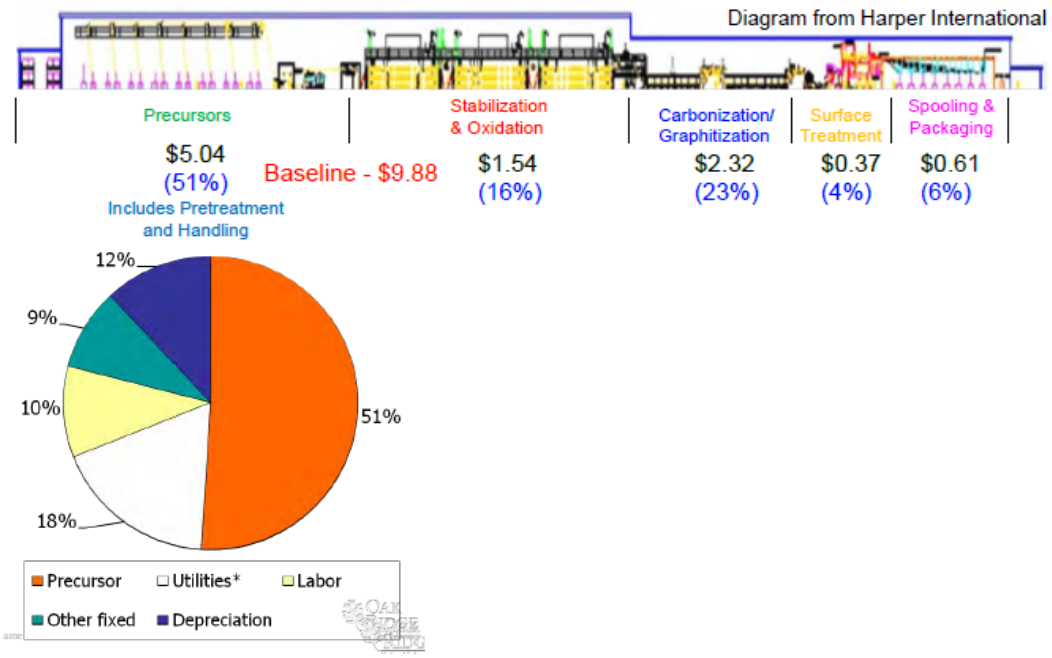

Fig. 204 Cost breakdown for low-grade PAN-based carbon fiber (reprinted from Warren[186])

Table 30 lists the potential cost savings associated with lignin-based carbon fibers. Overall, lignin-based fibers are expected to result in a cost reduction of approximately $1.5/lb.[186] A cost reduction for aerospace-grade fibers could be as high as $5/lb but will highly depend on the ability to prepare high-performance lignin-based carbon fibers shown by this work. Oxidative stabilization represents 75%–80% of fiber residence time and 18%–20% of cost.[186] Low-cost methods like UV stabilization of methacrylate functional lignin should help decrease the cost (~$0.9–$1.6/lb cost savings) potentially as much as half and reduce residence time to less than 20%–50% of the total process. Carbonization and graphitization cost nearly one-quarter of the carbon fiber cost. Lignin-based fibers should reduce or eliminate the need for emissions capture equipment to capture hydrogen cyanide and other hazardous emissions. This should decrease the cost of carbonization/ graphitization again by $0.4–0.8/lb. Surface treatment, spooling, and packaging are likely to have similar costs for lignin-based and current carbon fibers. The overall cost savings for lignin-based carbon fibers relative to PAN-based fibers is thus $2.50–$8.70/lb.

Table 30 Cost savings associated with lignin-based carbon fibers relative to current PAN-based carbon fibers

					Totals	
Processing Step	**Raw Materials**	**Utilities**	**Labor**	**Capital Depreciation**	**Minimum**	**Maximum**
Precursors	$1-5	$0-0.25	$0.1-0.5	$0-0.25	$1.10	$6.00
Stabilization	$0	$0.5-0.8	$0.1-0.3	$0.3-0.5	$0.90	$1.60
Carbonization/graphitization	$0	$0	$0.1-0.3	$0.4-0.8	$0.50	$1.10
Surface Treatment	$0	$0	$0	$0	$0.00	$0.00
Packaging	$0	$0	$0	$0	$0.00	$0.00
Total =	$1-5	$0.5-1.05	$0.3-1.1	$0.7-1.55	**$2.50**	**$8.70**

As of now, it is too soon to estimate the costs of the manufacture and purification of bacteria-decomposed lignin. These will be estimated before the end of the project. These could represent reduced or increased costs relative to chemically modified lignin-based carbon fibers. However, all the costs for lignin-based manufacture of carbon fiber should apply.

4.19.2 Process Design and Economic Analysis of Lignin-Based Carbon Fiber Production

Currently, the world production of carbon fiber is about 100,000,000 lb/yr, and the calculation is based on approximately 10% world production of carbon fiber, that is about 540 kg/h. The process flowchart is displayed in Fig. 205. The costs are calculated in the following sections based on capital costs, operational costs, and materials costs.

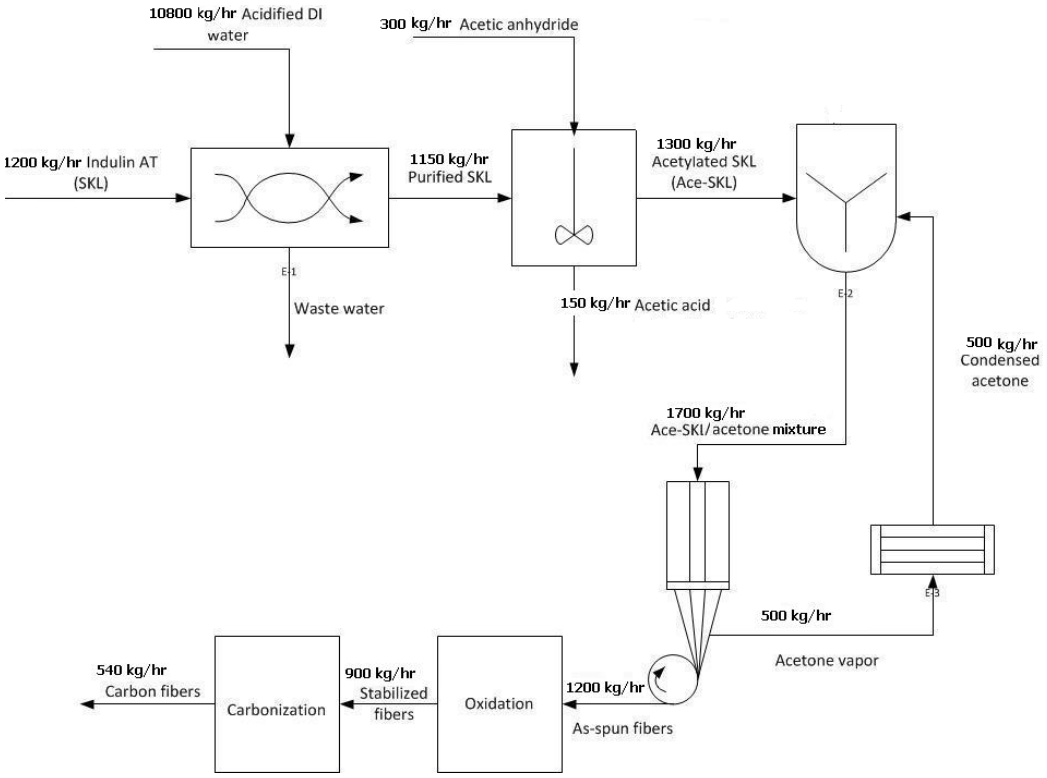

Fig. 205 Process flowchart of Ace-SKL carbon fiber production

4.19.2.1 Equipment Cost

Basis: Capital cost based on 15 years of straight-line depreciation.

Vessel for purification:

1,200 kg/h Indulin AT lignin + 10,800 kg/h of acetic acid/DI water solution (~10.8 m^3/h)

Volume = 10.8 m^3/h*1 h = 10.8 m^3

Vessel oversize by 50%

Price for a 20-m^3 vessel is \$1,000/m^3 *20 m^3*574/397 = \$ 28,917

Hourly cost = \$28,917/15 year*(1 year/365 day)*(1 day/24 h) = \$0.22/h

Evaporator for lignin drying after purification:

$Q_{acetic\ acid}$ = 405,000 J/kg*5,400 kg/h + 2,043 J/(kg·K) * (118–25) K *5,400 kg/h

= 3,212,994,600 J = 3,045,493 Btu/h

Q_{water} = 40,657 J/kg*5,400 kg/h + 4,179 J/(kg·K) * (118–25) K * 5,400 kg/h

= 2,197,385 Btu/h

Q_{total} = (3,045,493 + 2,197,385) Btu/h = 200 Btu/(ft^2·h·°F) * 9/5 °F/°C * A * (160–118) °C

A = 346 ft^2 = 32 m^2

Choose a 40-m^2 evaporator at \$3,000/m^2 * 40 m^2 * 574/397 = \$173,501

Hourly cost = \$173,501/15 year*(1 year/365 day)*(1 day/ 24 h) = \$ 1.32/h

Reactor for acetylation:

Volume = 300 kg/h / (1,080 kg/m^3) * 1/3 h = 0.1 m^3

Choose a 1-m^3 reactor, the price is \$15,000/m^3 * 1 m^2 * 574/397 = \$21,687

Hourly cost = \$21,687/15 year*(1 year/365 day)*(1 day/24 h) = \$0.17/h

Evaporator for acetic acid evaporation after acetylation:

$Q_{acetic\ acid}$ = 405,000 J/kg*150 kg/h + 2,043 J/(kg·K) * (118–25) K *150 kg/h

= 84,953 Btu/h

$Q_{acetic\ acid}$ = 84,953 Btu/h = 200 Btu/(ft^2·h·°F) * 9/5 °F/°C * A * (160–118) °C

A = 5.6 ft^2 = 0.5 m^2

Choose a 0.9-m^2 evaporator, then the price is \$100,000/m^2 * 0.9 m^2 * 574/397 = \$130,126

Hourly cost = \$130,125/15 year*(1 year/365 day)*(1 day/ 24 h) = \$ 0.99/h

Storage tank for SKL (2-day supply):

Volume = 1,200 kg/h / (1,300 kg/m^3) * 48 h = 44 m^3

Choose a 100-m^3 storage tank, the price is \$450/m^3 * 100 m^3 * 574/397 = \$65,063

Hourly cost = \$65,063/15 year*(1 year/365 day)*(1 day/24 h) = \$0.50/h

Storage tank for acetic anhydride (2-day supply):

Volume = 300 kg/h / (1,080 kg/m^3) * 48 h = 13.33 m^3

Choose a 100-m^3 storage tank, the price is \$450/m^3 * 100 m^3 * 574/397 = \$65,063

Hourly cost = \$65,063/15 year*(1 year/365 day)*(1 day/ 24 h) = \$ 0.50/h

Pumps:

For solution conveying, 10,800 kg/h solution (10.8 m^3/h, 48 gpm)

Head = 24 m

Power = 9.81 * 24 m *10,800 L * 1 / (60 s *1000) = 42.4 kW

The price of the pump is $200/kW * 42.4 Kw * 574/397 = $12,260

Hourly cost for each pump = $8,476/15 year*(1 year/365 day)*(1 day/24 h) = $0.09/h

For 4 pumps, the total cost is 0.09*4 = $0.36/h

Total equipment cost = $4.06/h

4.19.2.2 Operational Cost

Cost of DI water for purification:

$0.01/kg * 5,400 kg/h = $5.40/h

Cost of steam for lignin drying evaporator after purification:

Calculated the needed heat for evaporation in, 5.53 GJ/h

$13.28/GJ *5.53 GJ/h = $73.44/h

Cost of heating for acetylation:

Because of unknown reaction heat, the energy needed to heat up the acetic anhydride is calculated:

$Q_{\text{acetic anhy}}$ = 191.5 J/(kg·K) *1 mol/(0.102 kg) * (85–25) K *300 kg/h = 33,794,118 J/h = 0.033 GJ/h

$13.28/GJ * 0.033 GJ/h = $0.45/h

Cost of steam for evaporation of acetic acid after acetylation:

Calculated heat for evaporation = 0.089 GJ/h

$13.28/GJ * 0.089 GJ/h = $1.19/h

Cost of cooling water for acetic acid condensing after acetylation:

$0.354 GJ * 0.089 GJ/h = $0.03/h

Cost of cooling water for acetone condensing after spinning:

Q_{acetone} = 511,000 J/kg*500 kg/h + 125.5 J/(mol·K) * 1 mol/0.058 kg * (56–40) K

*500 kg/h = 0.27278 GJ

$0.354/GJ * 0.27278 GJ/h = $0.10/h

Power to run the pump:

42.4 kW * 4 = 169.6 kW

Cost/hour = $0.06/kWh *169.6 kW = $10.18/h

Total operational cost without stabilization and carbonization = $90.74/h

Stabilization and carbonization cost ($ amount adapted directly from literature sources)

$(2.32 + 1.54)/lb *1 lb/0.45 kg = $8.51/kg

4.19.2.3 Material Cost

Price of acetic anhydride: $1.85/kg

Cost/hour = $1.85/kg * 300 kg/h= $555/h

Price of lignin $1.50/kg

Cost/hour = $1.50/kg * 1,200 kg/h= $1,800/h

Total cost material cost = $2,355/h

4.19.2.4 Total Cost

The total cost to make carbon fibers from lignin using the methods discussed in this work amount to the sum of the amortized capital costs, operational costs, and materials costs:

Total cost = $(2,355 + 90.74 + 4.06)/h / (540 kg/h) + $8.51/kg = $13.05/kg = $5.92/lb

These costs are consistent with what is found in Table 30. However, to enable profit, the price of the lignin-based carbon fibers should likely be double that cost at approximately $12/lb. Although this cost is relatively low, it is still above the cost threshold of $5–7/lb set by the DOE. Furthermore, the properties of these lignin-based carbon fibers are not at the level expected for that cost basis.

In a recent development, Japan is now allowing its manufacturers to sell their products to the DOD. With this and the higher production rate of carbon fiber, because of projects like the Boeing 787 Dreamliner, the cost of carbon fiber has recently fallen steeply for the US and the DOD. The cost for high-performance T800 carbon fibers is approximately $4/lb. In light of this, there is no longer a need

for lignin-based carbon fibers. Furthermore, there is no need for a US program on low-cost carbon fibers, as that milestone has already been achieved.

4.19.3 Biobased Resins

4.19.3.1 Baseline Monomer Costs

The baseline costs of commercial thermosetting epoxy, VEs, UPEs, and their components are shown in Table 31. UPEs are among the cheapest resins, with prices ranging from $1 to $2/lb. UPE monomers themselves are a bit more expensive, but the price of styrene is quite low at $0.7–$1.2/lb. VE monomers cost more than $4/lb, and their resulting styrenated resins cost anywhere from $2 to $4/lb. Epoxy resins are far more expensive at $5–$50/lb depending on the performance level. Epoxies that perform lower than VEs cover the lower scale, while epoxies that perform similar to VEs cost $10–$15/lb. Epoxies with high-temperature performance (>200 °C) cost more than $20/lb and up to $50/lb. Polyurethanes cost $2–$6/lb.

Table 31 Cost of commercial monomers and resins

Resin/monomer	Price (min)	Price (max)	Source
VE resins	$2.00	$4.00	Composites one 2010 and 2015
VE monomers	$4.00	$5.00	Calculation
Styrene	$0.60	$1.10	Alibaba 2015
MMA	$0.65	$1.20	Alibaba 2015
UPE resins	$1.00	$2.00	Composites one 2010 and 2015
UPE monomers	$1.50	$2.50	Calculation
Epoxy	$2.00	$4.00	Composites one 2010 and 2015
High-temperature epoxy	$5.00	$15.00	Composites one 2010 and 2015
Amines	$4.00	$20.00	Air products 2010 and 2015
Polyurethanes	$2.00	$6.00	Bayer 2010 and 2015
Polyols	$1.00	$5.00	Bayer 2010 and 2015
Isocyanates	$3.00	$7.00	Bayer 2010 and 2015

4.19.3.2 Material Costs

The estimated price of biobased resins was calculated using the weighted costs of the reactants and the costs of the reaction, and establishing a price markup for profit. First, the material cost for the monomers was calculated based on the reactants used. The reactants costs are listed in Table 32 as determined through web searches (Alibaba, Markitizer, ICES, and Index Mundi) and literature.[189] The stoichiometry to produce the reactions was used to determine the biobased monomer costs in Table 33. These costs were compared to that of the baseline monomers. Because there is a range of prices for the baseline monomers, the 50% markup price for the baseline monomers is just the average cost of that monomer. Based on monomer costs alone, we can see that various monomers appear to have favorable costs (most biobased VE monomers) while others have unfavorable costs (reactive diluents and bis-aromatic scaffolds). Yet, this is not the full story. It is possible that based on reaction costs and environmental savings, the life cycle cost of these resins can change.

Table 32 Reactant costs

Reactant	Min Cost ($/lb)	Source	Date	Max Cost ($/lb)	Source	Date
Adipic Acid	$ 1.03	ICES/Alibaba	2010/2015	$ 1.05	ICES/Alibaba	2010/2015
BPA	$ 1.04	Alibaba	2015	$ 1.13	Alibaba	2015
Epichlorohydrin	$ 0.82	ICES/Alibaba	2010/2015	$ 0.91	ICES/Alibaba	2010/2015
Ethylene Glycol	$ 0.83	ICES	2010	$ 1.07	ICES	2010
Furfuryl methacrylate	$ 0.45	Alibaba	2015	$ 45.36	Alibaba	2015
Furoic Acid	$ 0.26	Alibaba	2015	$ 0.36	Alibaba	2015
Glycidyl methacrylate	$ 3.27	Alibaba	2015	$ 4.00	ICES	2010
GM	$ 3.18	Alibaba	2015	$ 3.63	Alibaba	2015
GM	$ 2.81	Alibaba	2015	$ 3.45	Alibaba	2015
Guaiacol	$ 0.45	Alibaba	2015	$ 0.68	Alibaba	2015
HMF	$ 0.45	Alibaba	2015	$ 0.49	Iowa State	2007/2009
Isosorbide	$ 2.27	Alibaba	2015	$ 4.00	ICES	2010
Maleic Anhydride	$ 0.45	Alibaba	2015	$ 0.91	Alibaba	2015
Methacrylic Acid	$ 0.66	ICES/Alibaba	2010/2015	$ 1.84	ICES/Alibaba	2010/2015
Methacrylic Anhydride	$ 1.32	Markitizer	2015			
Methacryloyl chloride	$ 0.75	Alibaba	2015	$ 2.00	ICES	2010
Methyl Methacrylate	$ 0.65	ICES/Alibaba	2010/2015	$ 1.20	ICES/Alibaba	2010/2015
Phthalic Acid	$ 0.91	ICES/Alibaba	2010/2015	$ 1.36	ICES/Alibaba	2010/2015
Sucrose	$ 0.14	ICES/Alibaba	2010/2015	$ 0.40	ICES	2010
Terephtahic acid	$ 0.16	ICES	2010	$ 0.49	Iowa State	2007/2009
Vanillyl alcohol	$ 0.91	Alibaba	2015	$ 13.61	Alibaba	2015

Table 33 Monomer costs and price based on materials, reaction, and markup arranged by monomer type

Monomer	Monomer Type	Baseline?	Monomer Min. Cost ($/lb)	Monomer Max. Cost ($/lb)	Monomer Reaction Cost ($/lb)	Full Monomer Cost ($/lb)	Monomer Price (50% markup) ($/lb)
VE Resins	VE Resin	Yes	$ 2.00	$ 4.00		$ 3.00	$ 3.00
MV-DGM	VE Resin		$ 2.16		$ 0.87	$ 3.03	$ 4.55
Methacrylated Bio-Oil	VE Resin		$ 1.35		$ 0.87	$ 2.22	$ 3.33
VE Crosslinkers	VE	Yes	$ 4.00	$ 5.00		$ 4.50	$ 4.50
Sucrose tetraepoxy-tetramethacrylate	VE		$ 1.38		$ 0.87	$ 2.25	$ 3.37
Sucrose tetramethacrylate	VE		$ 1.29		$ 0.87	$ 2.16	$ 3.24
IM	VE		$ 2.20		$ 0.87	$ 3.07	$ 4.60
VE-bFdE	VE		$ 1.31		$ 1.00	$ 2.31	$ 3.47
VE-bF	VE		$ 1.26		$ 0.87	$ 2.13	$ 3.19
VE-DGEBGF	VE		$ 1.17		$ 1.00	$ 2.17	$ 3.26
VE-BGF	VE		$ 1.47		$ 0.87	$ 2.34	$ 3.51
VE-DGEVA	VE		$ 1.23		$ 1.00	$ 2.23	$ 3.35
VE-dVA	VE		$ 1.63		$ 0.87	$ 2.50	$ 3.75
Styrene	Reactive Diluent for VE/UPE	Yes	$ 0.70			$ 0.70	$ 0.70
Methyl Methacrylate	Reactive Diluent for VE/UPE	Yes	$ 0.73			$ 0.73	$ 0.73
MG	Reactive Diluent for VE/UPE		$ 1.30		$ 0.87	$ 2.18	$ 3.27
FA-GM	Reactive Diluent for VE/UPE		$ 1.96		$ 0.13	$ 2.09	$ 3.14
UPE Crosslinkers	UPE	Yes	$ 1.50	$ 2.50		$ 2.00	$ 2.00
UPE Crosslinkers - Calc cost	UPE	Yes	$ 0.39		$ 0.87	$ 1.27	$ 1.90
Isosorbide UPE	UPE		$ 1.01		$ 0.87	$ 1.88	$ 2.82
Vanillyl alcohol UPE	UPE		$ 0.59		$ 0.87	$ 1.46	$ 2.20
Epon 828	Epoxy	Yes	$ 2.00	$ 4.00		$ 3.00	$ 3.00
High Temp epoxies	Epoxy	Yes	$ 5.00	$ 15.00		$ 10.00	$ 10.00
Isosorbide-epoxy	Epoxy		$ 1.89	$ 3.11	$ 0.87	$ 3.37	$ 5.06
BOF	Epoxy		$ 0.91	$ 2.22	$ 0.87	$ 2.44	$ 3.66
bFdE	Epoxy		$ 0.76	$ 1.62	$ 0.87	$ 2.06	$ 3.09
DGEVA	Epoxy		$ 0.71	$ 1.46	$ 0.87	$ 1.96	$ 2.94
DGEBGF	Epoxy		$ 0.59	$ 1.40	$ 0.87	$ 1.87	$ 2.80
BPA	Bis-Aromatic Scaffold	Yes	$ 1.04	$ 1.13		$ 1.09	$ 1.09
BVA	Bis-Aromatic Scaffold		$ 0.91		$ 0.87	$ 1.78	$ 2.67
BGF	Bis-Aromatic Scaffold		$ 0.76		$ 0.87	$ 1.63	$ 2.44
BF	Bis-Aromatic Scaffold		$ 0.47		$ 0.87	$ 1.34	$ 2.01

4.19.3.3 Estimated Cost of BOF Production

To obtain a cost estimate for the manufacture of BOF, a group of chemical engineering students designed a chemical plant for its manufacture and conducted an economic analysis of the process. The process consists of 2 main steps: 1) converting HMF to bHMF and 2) converting bHMF to BOF, as detailed in Fig. 206. The first step is hydrogenation of HMF in a continuous plug flow reactor using Raney nickel as a catalyst. The second step is the batch epoxidation of the diol bHMF using epichlorohydrin and tetrabutylammonium hydrogen sulfate as the catalyst. The overall chemical reaction scheme for this process is shown in Fig. 206. The plant was designed to produce 60 million lb of BOF with 95% purity a year. This would account for 1.2% of the world's epoxy market. The projected lifetime of the plant was assumed to be 20 years.

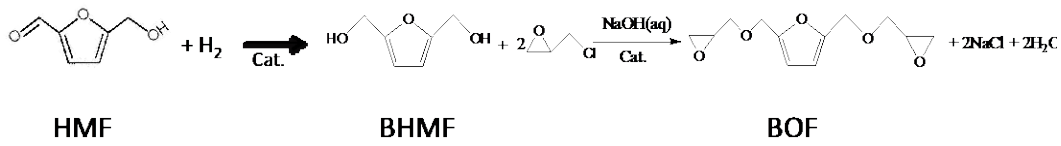

Fig. 206 The 2 reaction steps used for converting HMF to BOF

The complete process shown in Fig. 207 uses 2 plug flow reactors, 5 batch reactors, 6 sets of mixers and settlers, and 3 distillation towers. The first 2 blocks represent the hydrogenation and epoxidation steps. The rest of the steps are extraction and distillation steps used to separate products and unreacted materials for recycle. The 2 output streams are the product BOF and a water waste stream that is sent to a water treatment facility. One batch cycle lasts 16 h; no risks of toxic release were identified.

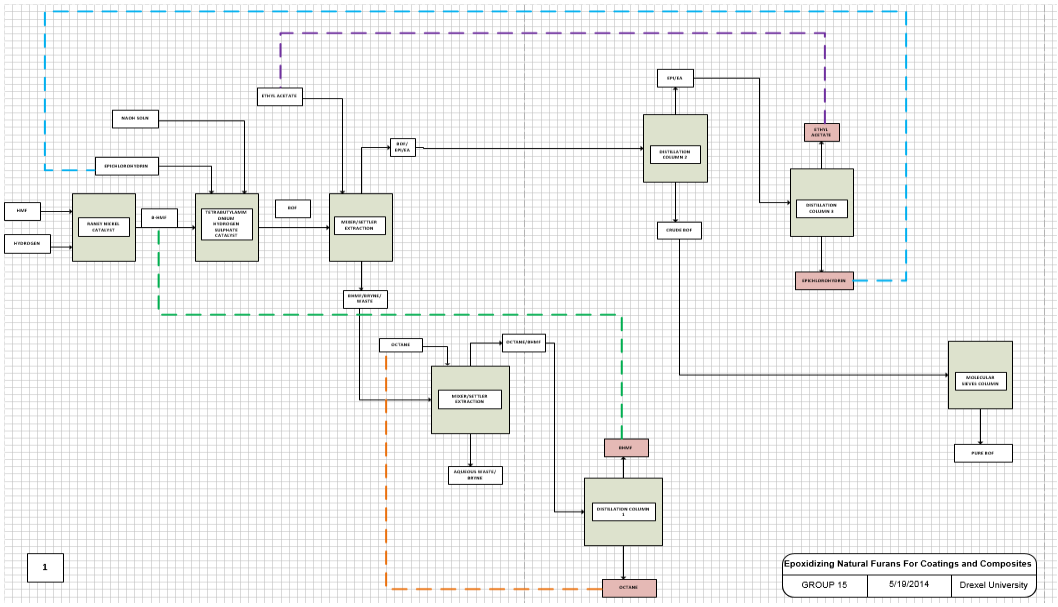

Fig. 207 Block flow diagram of process for converting HMF to BOF. The process includes 2 reaction steps: first for the hydrogenation of HMF to bHMF and second the epoxidation of bHMF to BOF. Separations are conducted to obtain the product; unreacted materials and solvents are recycled.

The capital investment including land was estimated to be $18 million. The cost of manufacturing (COM) was estimated to be $76 million/yr and includes depreciated capital expense, raw materials costs, cost of utilities, waste treatment costs, and costs of operating labor. By far the greatest portion of the COM can be attributed to raw materials: $66 million/yr or 87%. The estimated cost per pound to produce BOF at the 60 million pound per year capacity is therefore $1.10/lb. The main raw materials cost driver is HMF since it was estimated to be $1.26/lb and represents

38% of the raw materials cost. Moreover, the cost of this HMF is uncertain since it is currently only available from pilot scale sources. A doubling of its price would result in a $1.78/lb cost for BOF production.

4.19.3.4 Reaction Costs

The reaction costs were calculated as detailed in the previous sections for all of the monomers. Most of the reactions are a single step and thus follow the same reaction methodology as for BOF. The cost of this reaction, including energy and labor, to run the reaction and purify the product was calculated to be $0.87/lb. VE produced from epoxy resins is a 2-step reaction. However, the second reaction is a simple addition reaction with no separation, and its cost is small at about $0.13/lb.[186] The FA-GM reaction is one very simple step with no separation, and thus the costs should be approximately $0.13/lb.[190] Table 34 lists these reaction costs for each monomer and lists the total monomer cost. A 50% mark-up for the monomer is assumed. Based on that, the cost of the monomer was compared to that of the baseline monomers. The color coding in the table indicates whether the biobased monomer is favorable in terms of cost (green colors), slightly unfavorable (yellow), and highly unfavorable (red). Most of the biobased VE monomers have favorable costs. The epoxies are mixed, with some being favorable and some not. However, these costs do not factor in environmental savings that are detailed in the following section.

4.19.3.5 Environmental Savings

Carbon credits are approximately $30/ton of carbon dioxide (CO_2) emissions.[191] This amounts to $0.03/lb for each 100% biobased resin. However, most of the resins are not fully biobased. The biobased fraction multiplied by the $0.03/lb was the savings associated with each biobased resin. Table 34 lists these cost savings per biobased resin.

Table 34 Monomer modified price based on life cycle savings

Monomer	HAP Emissions Savings ($/lb)	Greenhouse Gas Emissions Savings ($/lb)	Bio-Content (mol%)	CO_2 Savings ($/lb)	Monomer - Mod Price ($/lb)
VE Resins	$ -	$ -	0%	$ -	$ 3.00
MV-DGM	$ 0.30	$ 0.12	33%	$ 0.02	$ 4.11
Methacrylated Bio-Oil	$ 0.30	$ 0.12	52%	$ 0.03	$ 2.88
VE Crosslinkers	$ -	$ -	0%	$ -	$ 4.50
Sucrose tetraepoxy-tetramethacrylate	$ -	$ -	37%	$ 0.01	$ 3.36
Sucrose tetramethacrylate	$ -	$ -	50%	$ 0.01	$ 3.23
IM	$ 0.30	$ 0.12	46%	$ 0.03	$ 4.16
VE-bFdE	$ -	$ -	47%	$ 0.01	$ 3.46
VE-bF	$ -	$ -	60%	$ 0.02	$ 3.18
VE-DGEBGF	$ -	$ -	49%	$ 0.01	$ 3.25
VE-BGF	$ -	$ -	62%	$ 0.02	$ 3.49
VE-DGEVA	$ -	$ -	52%	$ 0.02	$ 3.33
VE-dVA	$ -	$ -	64%	$ 0.02	$ 3.73
Styrene	$ -	$ -	0%	$ -	$ 0.70
Methyl Methacrylate	$ -	$ -	0%	$ -	$ 0.73
MG	$ 0.30	$ 0.12	59%	$ 0.03	$ 2.82
FA-GM	$ 0.30	$ 0.12	44%	$ 0.03	$ 2.69
UPE Crosslinkers	$ -	$ -	0%	$ -	$ 2.00
UPE Crosslinkers - Calc cost	$ -	$ -	0%	$ -	$ 1.90
Isosorbide UPE	$ -	$ -	25%	$ 0.01	$ 2.81
Vanillyl alcohol UPE	$ -	$ -	25%	$ 0.01	$ 2.19
Epon 828	$ -	$ -	0%	$ -	$ 3.00
High Temp epoxies	$ -	$ -	0%	$ -	$ 10.00
Isosorbide-epoxy	$ -	$ -	56%	$ 0.02	$ 5.04
BOF	$ -	$ -	53%	$ 0.02	$ 3.64
bFdE	$ -	$ -	69%	$ 0.02	$ 3.07
DGEVA	$ -	$ -	73%	$ 0.02	$ 2.92
DGEBGF	$ -	$ -	71%	$ 0.02	$ 2.78
BPA	$ -	$ -	0%	$ -	$ 1.09
BVA	$ -	$ -	100%	$ 0.03	$ 2.64
BGF	$ -	$ -	100%	$ 0.03	$ 2.41
BF	$ -	$ -	100%	$ 0.03	$ 1.98

Resins that emit HAPs, including all commercial and VE and UPE, require emissions capture or other expensive methods to mitigate emissions if composite production is on a large scale. The cost of this equipment was estimated to be approximately $0.30/lb in previous work.[190] Furthermore, these equipment operate continuously regardless of composites operations and thus must continuously burn natural gas. This results in the greenhouse gas savings in Table 34, as that amount of methane would not be required at $0.1/lb. This also adds to the CO_2 savings for HAP-emitting resins.

Toxicity costs are not counted in this work. As a result, the toxicity associated with styrene (HAP), MMA (HAP), BPA, and so on, is not quantified. For example, even though Bisguaiacol F and other such bis-aromatic scaffolds are more expensive than BPA, the life cycle cost counting toxicity may make these favorable. A more in-depth study required to determine this is outside of the scope of this work. In addition, biobased VE monomers are favorable, and when formulated with biobased reactive diluents, the resins system as a whole would have a comparable price to that of commercial resins, while being wholly biobased and producing little emissions.

Although some of the resins are benefited by the environmental offset costs, most are not affected much. Furthermore, the results clearly show that the raw material costs dominate the price of these resins. Therefore, the best way to reduce resin cost is to drive down the price of the starting chemicals. The price of the biobased chemicals has dropped and should continue to drop over the next few years as production increases. For example, the price of isosorbide was approximately $4.0/lb in 2010 and now in 2015 is $2.27/lb. Cost reductions in this and other biobased starting chemicals should make most of these monomers and resins profitable.

4.19.4 Conclusions

These results show that lignin-based carbon fibers are inexpensive based on the original project. However, they do not quite meet the price threshold set by the DOE. More importantly, recent changes to the carbon fiber market resulted in commercial high-performance carbon fibers that are cheaper than the threshold. As such, there is no longer a need for lignin or any low-cost carbon fibers, as this has already been achieved.

Biobased resins have promise, with costs that are similar to that of baseline resin systems. Currently, production of the biobased starting chemicals will likely limit production and will affect viability of such biobased resins. There is significant potential for these changes, but leadership must first be taken in commercial industry. Unfortunately, the recent reduction in the cost of oil will undermine these changes in the near term.

5. Conclusions and Implications for Future Research

5.1 Summary of Accomplishments

Our accomplishments during the course of this project include the following:

- Bacteria can successfully decompose lignin into useable structures for carbon fiber formation. Approximately 300 strains of bacteria that decompose lignin were identified, including *Pseudomonas*.
- The results of this work indicate that 2 unknown species of *Serratia* bacteria are the most effective at decomposing lignin. As a side aspect of this project, we have identified 2 unknown species of bacteria (*Serratia*) that happen to have good ligninolytic behavior.
- The scale-up of microbial decomposition of lignin is feasible given personnel with the right skills, but given the low cost of commercial carbon fiber, there is little driving force toward this.
- We have chemically fractionated lignin to alter its molecular weight distribution and usefulness for separating chemically modifying lignin.
- Various chemical modifications of lignin have been successful for use in carbon fiber development. These methods, which include acetylation and methacrylation, have developed separation strategies to produce good carbon fiber precursors.
- Both melt-spinnable and solution-spinnable lignin-based fibers were produced. Thermo-oxidation and UV curing were successful stabilization methods for these fibers.
- Carbon fibers were produced from a few types of lignin and chemically modified lignin. We have developed the highest-performing lignin-based carbon fibers to date, including the highest attainable strength (1 GPa), modulus (35 GPa), highest strain to failure (2.0%), and lowest electrical resistivity (14 μm).
- We reduced the cost of lignin-based carbon fibers to approximately $6/lb with an expected price of approximately $12/lb.
- The resulting mechanical properties of the lignin-based carbon fibers are relatively poor versus commercial carbon fibers. Furthermore, the cost of commercial carbon fibers has decreased steeply recently. As a result, the nation's effort to produce low-cost carbon fibers has already been achieved

commercially with standard carbon fibers, and thus it is recommended for no additional effort on lignin-based carbon fibers.

- We have advanced the state of the art with respect to renewable VE, epoxy, UPE, polyurethane, and various other high-performance polymers.
- We have developed isosorbide methacrylate with the highest ever glass transition temperature (T_g) of greater than 250 °C for a VE system.
- We have developed numerous reactive diluents and viscosity reducers for VE and UPE technology based on fatty acids, lignin, and isosorbide. The isosorbide-based viscosity reducer and lignin-based reactive diluents are promising for scale-up and commercialization.
- We have developed highly biobased resins based entirely on lignin with high atomic efficiency that are good for the lower end of high-performance composites and most coatings applications.
- We developed promising furan epoxies with good thermomechanical properties and very high toughness, making them excellent candidates for composites and coatings applications.
- We have developed higher-performing UPE resins using isosorbide as an additive or component, but the feasibility for scale up is low because of the long reaction times required.
- We have developed resins with significantly reduced toxicity and reduced emissions relative to commercial resins technology.
- We have performed life cycle analysis to show that various resin technologies have lower or similar cost relative to commercial resins and thus have high potential for commercial transition.

5.2 Conclusions

We have attained both significant price reduction and property improvement of lignin-based carbon fibers and renewable resins technology. Regarding lignin-based carbon fibers, we have pushed the technology beyond that of any researcher or organization to achieve the highest-performing materials to date. However, we do not recommend further investigation because of their significantly higher cost and their lower performance versus commercial fibers, and low potential for significant further reductions in cost or improvement in properties. In addition, we have advanced the state of the art in renewable resins technology, achieving performance with renewables and resins technology in general that was previously

thought unfeasible. Through targeting rigid scaffolds to replace BPA, we have developed new scaffolds capable of advancing numerous high-performance polymers. In particular, isosorbide methacrylates, epoxies, and diamines; BGF polymers in general; lignin-derived methacrylates as reactive diluents; VA-based epoxies, methacrylates, and diamines; and furan-based epoxies, methacrylates, and diamines all have demonstrated high performance and significant potential for technology transition for high-performance polymers, composites, and coatings applications.

5.3 Future Work

Future work was generally discussed throughout this report for the particular research areas. Thus, in this section, we generalize the future work discussion.

Much of the future work involves completing the final details of the work presented within this report, which involves completing publications, dissertations, and so on. To ensure there are few holes in the work, we understand the formation of the polymer network as best as possible, determine as many properties as possible, determine structure-property relationships as best as we can, and begin using the polymers in composite parts to assess their performance. Much of the work on this last point will be through transition efforts as previously discussed. In addition, all researchers partnering with ARL will be required to follow ARL's standard process description on resin characterization to enable full structure-property evaluation of high-performing materials.

Microbial decomposition of lignin has been successful. Approximately 300 different bacterial strains have been identified but have not yet quantified the characteristics of the more successful lignolytic bacteria, including Gram staining, to what extent they degrade lignin, and how fast they degrade lignin. To produce carbon fibers, larger-scale production of the bacteria-decomposed lignin must be prepared. Someone who has the skills and capabilities to perform this work could use this technology to make precursors for carbon fiber or chemicals for polymers or other applications.

The use of furans was explored in the production of carbon fibers, but none of the materials provided had the appropriate properties for this work. For this work to be successful, a 1-week to 1-month visit of ARL researchers to Clemson or vice-versa is required. In addition, DuPont has been developing tannins for use in phenolic resins. It seems possible to use tannins, which are already smaller polymers of lignin, for use in making carbon fibers. However, because of the low cost of commercial carbon fibers, neither of these areas of research are high priorities.

Isosorbide-unsaturated polyester research should not continue in university or government labs. Work in this area should be transitioned or shelved.

Isosorbide polyurethane oligomers need to be prepared to achieve high biocontent, reduce foaming, and make isosorbide amenable for composites and coatings applications. This will be performed using ARL mission funding in 2015.

Isosorbide methacrylate needs to be scaled up and made into larger specimens for mechanical testing and various composites formulations for composite testing and evaluation. In summary, the technology readiness level (TRL) of this resin should be increased to increase the feasibility to transition this technology to commercial industry.

Other isosorbide resins—in particular, epoxides—should be examined for use in coatings because they are aliphatic (non-UV sensitive) and thus could be used as topcoats or primers.

Furan epoxides have excellent toughness and should be scaled up to enable preparation of larger-scale coatings and composites. In summary, the TRL of this resin should be increased to increase the feasibility to transition this technology to commercial industry.

Lignin-based reactive diluents have shown promise, but their low extent of cure limits their performance. Methods to affect their cure would prove beneficial in reducing the use of styrene in VE and UPE resins. Field effects should possibly be considered to increase the reactivity of these monomers.

Lignin-based diphenols will have continued development as replacements for BPA for various high-performance polymers. ARL is working this using mission funding through internal research and support of Rowan University and the University of Delaware. In addition, these universities will continue seeking funding support to further these polymer systems.

Diamines from furans, isosorbide, and lignin-derivatives have excellent potential and are the subject of SERDP WP-2402 for use in polyimide technology. However, these monomers will also have tremendous application toward epoxy resin technology for coatings and composites, which will drive the market toward use of these materials.

Life cycle analysis of processes, carbon fibers, and resins will be continually (at least cursorily) assessed while ARL and its partners have funding for relevant technology to identify when any of these technologies have a greater need for transition to commercial industry.

5.4 Technology Transition

This project resulted in nearly 100 scientific publications and presentations. A full listing of scientific/technical publications are listed in Appendix B. Other supporting material can be found in Appendix C, including the numerous awards members of this project team have won. The advancements in technology that we have achieved in this project have caught the interest of our technology transition departments in our team's organizations. In addition, some of the technologies have interested commercial partners. For example, Drexel and PPG are partners on ARL-sponsored coatings research. Through this, Drexel/ARL are working to transition furan-based epoxies for coatings technology. If successful products can be developed, the door to the composites market will open very easily. PPG is also interested in the BGF technology for coatings and composites applications.

Dixie Chemicals has expressed interest in the isosorbide technology, and we are working through Drexel University to transition this technology. The lignin-based resins and reactive diluents are promising for transition, but we currently do not have supply of relevant lignin-derived chemicals at sufficient level to attract commercial transition partners. We will look for transition partners regarding the isosorbide-UPE technology, but we doubt this will be transitioned because of the long reaction times required. ARL is working on a marketing strategy for renewable resins to educate companies on technologies they can take advantage of with little investment on their behalf. Such technologies will allow them to gain high potential, high performance resins technology.

We have some interest in lignin-based carbon fibers from Meade-WestVaaco and other companies, but we do not think this will pan out given the recent reduction in commercial carbon fiber costs. Nonetheless, efforts will be pursued to transition this technology further.

Regardless of the current status, the team is in a good position to continue to work to transition resins technology to commercial industry. ARL still has a mission program devoted to renewable resins technology. ARL/Drexel/PPG have a few years of funding for coatings technology research that should allow the team to successfully transition epoxy and acrylate technology for coatings and possibly composites applications. ARL/Drexel are also partnered on SERDP WP-2402, which will be used to develop and transition diamine technology. ARL has various other partnerships with coatings companies, including some through SERDP/ESTCP, and will use these to push advanced and biobased resins technology. In addition, ARL has worked internationally to increase the advancement and potential transition of renewable resins technology. Through The Technical Cooperation Program, Materials Group, Technical Panel 6 (TTCP-MAT-

TP6) on polymers, we recently completed an operating assignment on biobased resins, where we collaborated on the isosorbide methacrylate paper. We are now beginning a new operating assignment on renewable resins for coatings and composites. We also have a new collaboration with Argentina coming online in early 2015 to do lignin and furan development work.

6. References

1. La Scala JJ, Sands JM, Orlicki JA, Robinette EJ, Palmese GR. Fatty acid-based monomers as styrene replacements for liquid molding resins. Polymer. 2004;45:7729–7737.
2. Khot SN, La Scala JJ, Can E, Morye SS, Williams GI, Palmese GR, Kusefoglu SH, Wool RP. Development and application of triglyceride-based polymers and composites. J. Applied Polym. Sci. 2001;82:703–723.
3. Pilato L, Michno M. Advanced Composite Materials. New York (NY): Springer; 1994.
4. Quilter A. Composites in aerospace applications. IHS White Paper, 2004.
5. Potter P. Amptiac. 2003;7:37–40.
6. Ackerman R. Stiletto cuts a swatch to new navy technologies. Signal. 2006 March.
7. Griffiths B. Composites Tech. August 2006;12(4):60–62.
8. AGY. Product specification sheet for S-2 glass fiber. Aiken (SC): AGY; 2004.
9. Hexcel Corporation. Product specification sheet for magnamite AS4C carbon fiber. Stamford (CT): Hexcel Corporation; 2002.
10. Hexcel Corporation. Product specification sheet for magnamite IM7 (5000) carbon fiber. Stamford (CT): Hexcel Corporation; 2002.
11. Fitzer E, Manocha LM. Carbon Reinforcements and Carbon/Carbon Composites. Berlin (Germany): Springer-Verlag Publishers; 1998.
12. Buckley JD, Edie DD. Carbon-Carbon Materials and Composites. Park Ridge (NJ): Noyes Publications; 1993.
13. Mukundan T, Bhanu VA, Wiles KB, Johnson H, Bortner M, Baird DG, Naskar AK, Ogale AA, Edie DD, McGrath JE. Polymer. 2006;47:4163–4171.
14. Paiva MC, Kotasthane P, Edie DD, Ogale AA. Carbon. 2003;41:1399–1409.
15. Naskar AK, Walker RA, Proulx S, Edie DD, Ogale AA. Carbon. 2005;43:1065–1072.
16. Traceski FT. Assessing industrial capabilities for carbon fiber production. Acquisition Review Quarterly. Spring 1999:179–194.

17. Warren CD. Future low cost carbon fiber for autos: international scale-up and what is needed. Oak Ridge(TN): Oak Ridge National Laboratory; September 2008.

18. Fowler P, Hughes JM, Elias RJ. Science Food Agriculture. 2006;86:1781–1789.

19. Kvien I, Oksman K. Applied Physics A. 2007;87:641–643.

20. Pascault JP, Sautereau H, Verdu J, Williams RJJ. Thermosetting polymers. New York (NY): Marcel Dekker; 2002.

21. Malik M, Choudhary V, Varma IK. Rev Macromol Chem Phys. 2000;C40:139–165.

22. Ziaee S, Palmese GR. J Polym Sci B: Polym Phys. 1999;37:725–744.

23. La Scala JJ, Orlicki JA, Winston C, Robinette EJ, Sands JM, Palmese GR. Polymer. 2005;46:2908–2921.

24. Environmental Protection Agency. National emissions standards for hazardous air pollutants: reinforced plastic composites production. 40 CFR Part 63. Federal Register. 2003;68(76):19375–19443.

25. Sanderman H Jr, Scheel D, Trenck TV. D. Metabolism of environmental chemicals by plants – copolymerization into lignin. In: Sarko A, editor. Proceedings of the Ninth Cellulose Conference, Part I; New York (NY): John Wiley and Sons, Inc; 1983.

26. Lee YY, Lee BH. Solvent-phase thermal cracking of lignin for production of potential liquid fuels. J Industrial Eng Chemistry. 1998;4:334–339.

27. Xiang Q, Lee YY. Applied Biochemistry and Biotechnology. 2000;84–86:153–162.

28. Greene AK. Biodegradation of lignin by mutants of Erwinia spp. [master of science thesis]. [Baton Rouge (LA)]: Louisiana State University; 1985.

29. Axegard P. STFI-Packforsk AB. Forest Based Sector Technology Platform Conference. Lahti, Finland; 2006 Nov 22–23.

30. Amit K, Naskar DW. Lower cost carbon fiber precursors. Presentation of Oak Ridge National Laboratory. 2012 May 16. Project ID# LM004.

31. Dye DW. The inadequacy of the usual determinative tests for the identification of xanthomonas spp. N Z J Sci. 1962;5:393–416.

32. Mörck R, Yoshida H, Kringstad K. Holzforschung. 1986;40:51–60.

34. Hortling B, Turunen E, Eokkonen P. Handbook of size exclusion chromatography and related techniques. 2nd ed. Wu C, editor. New York (NY): Marcel Dekker, Inc.; 2004. p. 355–383.

35. Bonini C, D'Auria M, Ferri R. Photochemical and Photobiological Sciences. 2002;1:570–573.

36. Pouchert CJ, editor. The Aldrich library of infrared spectra. 3rd ed. Milwaukee, (WI): Aldrich Chemical Co.; 1981.

37. Pouchert CJ, editor. Aldrich library of NMR spectra. Vols. 1 and 2. Milwaukee (WI): Aldrich Chemical Co.; 1983.

38. Garcia AA, Bonen MR, Ramirez-Vick J, Sadaka M, Vuppu A. Bioseparation process science. Malden (MA): Blackwell Science; 1999; p. 181–183.

39. ASTM D3461. Standard test method for softening point of asphalt and pitch (Mettler cup-and-ball method). West Conshohocken (PA): ASTM International; 2014.

40. ASTM D5630. Standard test method for ash content in plastics. West Conshohocken (PA): ASTM International; 2013.

41. Kundu S, Grecov D, Ogale AA, Rey AD, Shear flow induced microstructure of a synthetic mesophase pitch, Journal of Rheology, 53(10), 85-113, 2009.

42. Gupta A, Ogale AA. Polymer Composites. 2002;23(6):1162–1170.

43. ASTM C693. Standard test method for density of glass by buoyancy. West Conshohocken (PA): ASTM International; 2013.

44. ASTM D3379-75(1989)e1. Standard test method for tensile strength and young's modulus for high-modulus single-filament materials (withdrawn 1998). West Conshohocken (PA): ASTM International; 1975.

33. Thielemans W, Wool RP. Biomacromolecules. 2005;6:1895–1905.

45. Carey FA. Organic chemistry. 2nd ed. New York (NY): McGraw-Hill; 1992.

46. Lu J, Khot S, Wool R. Polymer. 2005;46:71–80.

47. Kamm B. Biorefineries – industrial processes and products: status quo and future directions. Gruber PR, Kamm M, editors. Weinheim (Germany): Wiley-VCH; 2006.

48. La Scala JJ, Wool RP. J Am Oil Chem Soc. 2002;79:59–63.

49. Dumitriu S. Polysaccharides: structural diversity and functional versatility. 2nd ed. Boca Raton (FL): CRC Press; 2004.

50. Rupley JA. Biochimica et Biophysica Acta. 1964;83:245–255.

51. La Scala JJ, Sands JM, Orlicki JA, Robinette EJ, Palmese GR. Fatty acid-based monomers as styrene replacements for liquid molding resins. Polymer. 2004;45:7729–7737.

52. ASTM D1652-04. Standard test method for epoxy content of epoxy resins. West Conshohocken (PA): ASTM International; 2004.

53. Brill RP, Palmese GR. J Appl Polym Sci. 2000;76:1572–1582.

54. Palmese GR, McCullough RL. J. Appl. Polym. Sci. 1992;46(10):1863–1873.

55. Flory PJ. Principles of polymer chemistry. Ithaca (NY): Cornell University Press; 1953; p. 432–493.

56. ASTM D790. Standard test methods for flexural properties of unreinforced and reinforced plastics and electrical insulating materials. West Conshohocken (PA): ASTM International; 2010.

57. ASTM D5045. Standard test methods for plane-strain fracture toughness and strain energy release rate of plastic materials. West Conshohocken (PA): ASTM International; 2014.

58. Jeffries TW. Biodegradation of lignin and hemicelluloses. In: Ratledge C, editor. Biochemistry of microbial degradation. London: Kluwer Academic Publishers; 1993.

59. Campbell MM, Sederoff RR. Variation in lignin content and composition mechanisms of control and implications for the genetic improvement of plants. Plant Physiol. 1996;110:3–13.

60. Whitman WB, Coleman DC, Wiebe WJ. Perspective prokaryotes: the unseen majority. Proc Natl Acad Sci. 1998;95:6578–6583.

61. Torsvik V, Goksoyr J, Daae FL. High diversity in DNA of soil bacteria. Appl Environ Micro. 1990;56(3):782–787.

62. Bach HJ, Tomanova J, Schloter M, Munch JC. Enumeration of total bacteria and bacteria with genes for proteolytic activity in pure cultures and in environmental samples by quantitative PCR mediated amplification. J Microbiol Methods. 2002;49:235–245.

63. Sharma R, Ranjan R, Kapardar RK, Grover A. Unculturable bacterial diversity: an untapped resource. Current Science. 2005;89(1):72–77.

64. Belgacem MN, Gandini A, editors. Monomers, polymers and composites from renewable resources. Oxford (UK): Elsevier; 2008.

65. Higson A. NNFCC renewable chemicals factsheet: lignin. [accessed 2011 Nov]. http://www.nnfcc.co.uk/publications/nnfcc-renewable-chemicals-factsheet-lignin.

66. Wool RP, Sun XS. Biobased polymer and composites. 1st ed. New York (NY): Elsevier; 2005.

67. Lora JH, Glasser WG. J Polymers Environment. 2002;10:39–48.

68. Thielemans W, Wool RP. Composites Part A: Applied Science and Manufacturing. 2004;35:327–338.

69. Li Y, Sarkanen S. Macromolecules. 2002;35:9707–9715.

70. Calvo-Flores FG, Dobado JA. ChemSusChem. 2010;3:1227–1235.

71. Gandini A. Green Chemistry. 2011;13:1061–1083.

72. Voitl T, Rudolf von Rohr P. ChemSusChem. 2008;1:763–769.

73. Zakzeski J, Weckhuysen BM. ChemSusChem. 2011;4:369–378.

74. Binder JB, Gray MJ, White JF, Zhang ZC, Holladay JE. Biomass and Bioenergy. 2009;33:1122–1130.

75. Jia S, Cox BJ, Guo X, Zhang ZC, Ekerdt JG. ChemSusChem. 2010;3:1078–1084.

76. Petrocelli FP, Klein MT. Industrial and Engineering Chem. Product Research and Development. 1985;24:635–641.

77. Silva EABD, Zabkova M, Araújo JD, Cateto CA, Barreiro MF, Belgacem MN, Rodrigues AE. Chem Engineering Research and Design. 2009;87:1276–1292.

78. Chakar F, Ragauskas AJ. Industrial Crops and Products. 2004;20:131–141.

79. Mialon L, Pemba AG, Miller SA. Green Chemistry. 2010;12:1704–1706.

80. Sergeev AG, Hartwig JF. Science. 2011;332:439–443.

81. Marton W. In: Lignins: occurrence, formation, structure and reactions. Sarkanen KV, Ludwig CH, editors. New York (NY): Wiley-Interscience; 1971. p. 639–694.

82. Schrodi Y, Ung T, Vargas A, Mkrtumyan G, Lee CW, Champagne TM, Pederson RL, Hong SH. CLEAN - Soil, Air, Water. 2008;36:669–673.

83. Ferré-Filmon K, Delaude L, Demonceau A, Noels AF. European J Organic Chem. 2005;2005:3319–3325.

84. Scholl M, Ding S, Lee CW, Grubbs RH. Organic Letters. 1999;1:953–956.

85. Gallivan JP, Jordan JP, Grubbs RH. Tetrahedron Letters. 2005;46:2577–2580.

86. Bonini C. Industrial Crops and Products. 2004;20:243–259.

87. Bonini C, D'Auria M, Ferri R. Photochemical and Photobiological Sciences. 2002;1:570–573.

88. Lanzalunga O, Bietti M. J Photochemistry and Photobiology B, Biology. 2000;56:85–108.

89. Holladay JE, White JF, Bozell JJ, Johnson D. Top value-added chemicals from biomass - volume II - results of screening for potential candidates from biorefinery lignin. Richland (WA): Pacific Northwest National Laboratory (US); 2007. Report No.: PNNL-16983.

90. Stanzione J. Lignin-based monomers: utilization in high performance polymers and the effects of their structures on polymer properties. Newark (DE): University of Delaware; 2013.

91. Otani S, Fukuoka Y, Igarashi B, Sasaki K, inventors. Method for producing carbonized lignin fiber. United States patent US 3,461,082. 1969 Aug 12.

92. Sudo K, Shimizu K. A new carbon fiber from lignin. J Appl Polym Sci. 1992;44:127–134.

93. Uraki Y, Kubo S, Nigo N, Sano Y, Sasaya T. Preparation of carbon fibers from organosolv lignin obtained by aqueous acetic acid pulping. Holzforschung. 1995;49:343–350.

94. Kubo S, Uraki Y, Sano Y. Preparation of carbon fibers from softwood lignin by atmospheric acetic acid pulping. Carbon. 1998;36:1119–1124.

95. Kadla J, Kubo S, Venditti R, Gilbert R, Compere A, Griffith W. Lignin-based carbon fibers for composite fiber applications. Carbon. 2002;40:2913–2920.

96. Warren CD, Paulauskas FL, Baker FS, Eberle C, Naskar AK. Development of commodity grade, lower cost carbon fiber-commercial applications. SAMPE Journal. 2009;45:24–36.

97. Baker FS, Visiting O. Low cost carbon fiber from renewable resources. EERE. US Dept of Energy Project ID No. lm_03_baker, 2009.

98. Eckert RC, Abdullah Z, inventors. Carbon fibers from Kraft soft wood lignin. United States patent US 7,678,358. 2010 Mar.

99. Morales MS, Ogale AA. Carbon fibers derived from UV-assisted stabilization of wet-spun polyacrylonitrile fibers. J Appl Polym Sci. 2014;131.

100. Plackett D, Dunningham E, Singh A. Weatherig of chemically modified wood. Holz als Roh-und Werkstoff. 1992;50:135–140.

101. Heitner C. Light-induced yellowing of wood-containing papers: an evolution of the mechanism. In: Heitner C, Scaiano JC, editors. Photochemistry of lignocellulosic materials. ACS symposium series 531 (Washington, DC): American Chemical Society; 1993 Jun 11. Chapter 1, p. 2–D)

102. Feist WC, Rowell RM, Ellis WD. Moisture sorption and accelerated weathering of acetylated and methacrylated aspen. Wood Fiber Sci. 1991;23:128–136.

103. Report on carcinogens. 12th ed. Washington (DC): US Department of Health and Human Services, Public Health Service, National Toxicology Program; 2011.

104. La Scala JJ, Ulven CA, Orlicki, JA, Jain R, Palmese GR, Vaidya UK, Sands JM. Clean Technologies and Environmental Policy. 2007;9:265–279.

105. Campanella A, La Scala JJ, Wool RP. Polymer Engineering and Science. 2009;49:2384–2393.

106. Campanella A, La Scala JJ, Wool RP. Journal of Applied Polymer Science. 2011;119:1000–1010.

107. Palmese GR, La Scala JJ, Sands JM. Fatty acid monomers to reduce emissions and toughen polymers. United States Patent 7,525,909. 2009 Apr 28.

108. Sarkanen KV, Ludwig CH. Lignins: occurrence, formation, structure and reactions. New York: John Wiley and Sons, Inc.; 1971; p. 639–694.

109. Lanzalunga O, Bietti M. Photo- and radiation chemical induced degradation of lignin model compounds. Journal of Photochemistry and Photobiology B: Biology. 2000;56:85–108.

110. Rogers D. Lignin-derived thermosetting vinyl ester resins for high performance applications [master's thesis]. [Glassboro (NJ)]: Rowan University; 2015.

111. Holmberg AL, Reno KH, Wool RP, Epps TH II. Biobased building blocks for the rational design of renewable block polymers. Soft Matter. 2014;10:7405–7424.

112. Stanzione JF, Giangiulio PA, Sadler JM, La Scala JJ, Wool RP. Lignin-based bio-oil mimic as biobased resin for composite applications. ACS Sustainable Chem Eng. 2013;1:419−426.

113. Bisphenol a market for polycarbonates, epoxy resins and other applications - global industry analysis, size, share, growth and forecast 2013 – 2019. Albany (NY): Transparency Market Research; 2013 Nov; 64 pages.

114. Erler C, Novak JJ. Pediatr Nurs. 2010;25:400.

115. Chemical Weekly. 2009:205.

116. Borrell, B. Nature. 2010;464:1122.

117. Nelson AM, Long TE. Polym. Int. 2012;61:1485.

118. Reno KH, Stanzione JF III, Sadler JM, La Scala JJ, Wool P. U. Provisional Patent Application 62/003,115, 2014.

119. Mooney, BP. Biochem J. 2009;418:219.

120. Harmer MA, Sun Q Appl Cat A: General. 2001;221:45.

121. Carvill BGK, Roland M. General Electric Company: United States. United States patent US 7132575 B2. 2006.

122. Reno KHS., JF III; Epps TH, III; Wool RP. Presented at: 247th National Meeting of the American Chemical Society; 2014; Dallas, TX.

123. da Silva EAB, Zabkova M, Araujo JD, Cateto CA, Barreiro MF, Belgacem MN, Rodriques AE. Chem Eng Res Des. 2009;87:1276.

124. Saito T, Brown RH, Hunt MA, Pickel DL, Pickel JM, Messman JM, Baker FS, Keller M, Naskar AK. Green Chem. 2012;14:3295.

125. Jegers HE, Klein MT. Ind Eng Chem Process Des Dev. 1985;24:173.

126. Mohan D, Pittman CU, Steele PH. Energy and Fuels. 2006;20:848.

127. Brodin I, Sjoholm E, Gellerstedt G. J Anal Appl Pyrol. 2010;87:70.

128. Workgroup, B. A.; Agency, U. S. E. P., Ed.; U.S. Environmental Protection Agency: Washington, DC, 2000.

129. Wool RP. In 17th Annual Green Chemistry and Engineering Conference; Washington DC; 2013.

130. Anastas PT, Warner JC. Green chemistry: theory and practice. New York: Oxford University Press; 1998.

131. Hatem A B H., U K Mahalingam; United States: Sabic Innovative Plastics; 2010; vol. US2010/0010273 A1.

132. Meylemans HA, Groshens TJ, Harvey G. ChemSusChem. 2012;5:206.

133. Stanzione JF, Sadler JM, La Scala JJ, Reno KH, Woo, RP. Green Chem. 2012;14:2346.

134. Liu J, Ishida H. Macromolecules. 2014;47:5682.

135. Stanzione JF., III, Giangiulio PA, Sadler JM, La Scala JJ, Wool RP. ACS Sustainable Chemistry and Engineering. 2013;1:419.

136. Stanzione JF, Sadler JM, La Scala JJ, Wool RP. ChemSusChem. 2012;5:1291.

137. Weapons O. f. t. P. o. C., editor. the Technical Secretariat of the Organization for the Prohibition of Chemical Weapons; 2005.

138. Taherimehr M, Pescarmona PP. J. Appl. Polym. Sci. 2014;131:41141.

139. Sakakura T, Kohn, K. Chemical Communications. 2009;1312.

140. Stanzione I., JF. Presented at: 16th ACS Green Chemistry and Engineering; 2012; Washington, DC.

141. Wool RP, Khot SN, LaScala JJ, Bunker SP, Lu J, Thielemans W, Can E, Morye SS, Williams GI. In ACS Symposium Series; ACS Publications: 2002; 823:177.

142. Auvergne R, Caillol S, David G, Boutevin B, Pascault J-P. Chemical Reviews. 2013.

143. Gandini A. Macromolecules. 2008;41:9491.

144. Gandini A, Silvestre AJ, Neto CP, Sousa AF, Gomes MJ. Polym. Sci. Part A: Polymer Chemistry. 2009;47:295.

145. Lavill, C, Alla A, de Ilarduya AM, Munoz-Guerra S. Biomacromolecules. 2013,14:781.

146. Noordover BAJ, van StaalduinenVG, Duchateau R, Koning CE, van Benthem R, Mak M, Heise A, Frissen AE, van Haveren J. Biomacromolecules. 2006;7:3406.

147. Lavilla C, Munoz-Guerra S. Green Chem. 2013;15:144.

148. Jiang M, Liu Q, Zhang Q, Ye C, Zhou G. J Polym Sci Part A: Polymer Chemistry. 2012;50:1026.

149. Shirahama H, Kawaguchi Y, Aludin M. S, Yasuda H. J Appl Polym Sci. 2001;80*:*340.

150. Schug TT, Abagyan R, Blumberg B, Collins TJ, Crews D, DeFur PL, Dickerson SM, Edwards TM, Gore AC, Guillette LJ, Hayes T, Heindel JJ, Moore, A, Patisaul HB, Tal TL, Thayer KA, Vandenberg LN, Warner JC, Watson CS, vom Saal FS, Zoeller RT, O'Brien KP, Myers JP. Green Chem. 2013;5:181.

151. Eiler S, Gangloff M, Duclaud S, Moras D, Ruff M. Protein expression and purification. 2001;22:165.

152. US Environmental Protection Agency, 2012.

153. Trott O, Olson AJ. Journal of Computational Chemistry. 2010;31:455.

154. Sadler JM, Nguyen A-PT, Toulan FR, Szabo JP, Palmese GR, Scheck C, Lutgen S, La Scala JJ. Isosorbide-methacrylate as a biobased low viscosity resin for high performance thermosetting applications. J Mater Chem A. 2013;1:12579–12586.

155. Kamm B, Gruber PR, Kamm M, editors. Biorefineries-industrial processes and products. Weinheim (Germany): Wiley-VHC; 2010.

156. High-Intensity Sweeteners. Washington (DC): US Food and Drug Administration; 2014 May 19. [accessed 2015 May 5]. http://www.fda.gov /Food/IngredientsPackagingLabeling/FoodAdditivesIngredients/ucm397716 .htm.

157. Kricheldorf HR, Mardomol J. Sci Rev Macromoll Chem Phys. 1997;37:599–631.

158. Sadler JM, Toulan FR, Nguyen A-PT, Kayea RV II, Ziaee S, Palmesae GR, La Scala JJ. Isosorbide as the structural component of bio-based unsaturated polyesters for use as thermosetting resings. Carbohydr Polym. 2013;100:97–106.

159. Noordover BAJ, van Stallduinen VG, Duchateau R, Koning CE, van Benthem RATM, Mak M, Heise A, Frissen AE, van Hvernen J. Co- and terpolyesters based on isosorbide and succinic acid for coating applications: synthesis and characterization. Biomacromolecules. 2006;7:3406–3416.

160. Noordover BAJ, Duchateau R, van Benthem RATM, Ming W, Koning CE. Enhancing functionality of biobased polysester coating resins through modification with citric acid. Biomacromolecules. 2007;8:3860–3870.

161. Okada M, Okada Y, Aoi KK. Polym Sci Part A: Poly Chem. 2010;48:2813–2820.

162. Jasinska L, Koning CE. Unsaturated, biobased polyesters and their cross-linking via radical copolymerization. J Poly Sci Part A: Polym Chem. 2010;48(13):2885–2895.

163. CognetGeorjon E, Mechin F, Pascault JP. New polyurethanes based on 4,4' diphenylmethane diisocyanate and 1,4:3,6 dianhydrosorbitol 2: synthesis and properties of segmented polyurethane elastomers. Macromol Chem Phys. 1996;197:3593–3612.

164. Feng X, East AJ, Hammond WB, Zhang Y, Jaffe M. Polym overview of advances in sugar-based polymers. Polymers for Advanced Technology. 2011;22(1):139–150.

165. Romanski J, Nowak P, Kosinski K, Jurczak J. High-pressure transesterification of sterically hindered esters. Tetrahedron Letters. 2012 July.

166. Benito-Lopez F. High pressure: a challenge for lab-on-a-chip technology [PhD thesis]. [Enschede (The Netherlands)]: University of Twente; 2007.

167. Netravali A, inventor. Starch based composites and their manufacture. United States Patent. Appl. US 20100291822. 2010 Nov 18. p. 30.

168. Pinto G, Maaroufi AK, Benavente R, Pereña JM. Electrical conductivity of urea–formaldehyde–cellulose composites loaded with copper. Polymer Composites. 2011;32:193–198.

169. Vacková T, Kroisová D, Špatenka P. Water desorption kinetics of polymer composites with cellulose fibers as filler. Journal of Macromolecular Science Part B. 2008;48:68–76.

170. Guigo N, Mija A, Vincent L, Sbirrazzuoli N. Eco-friendly composite resins based on renewable biomass resources. Polyfurfuryl Alcohol/Lignin Thermosets. European Polymer Journal. 2010;46:1016.

171. Zaske OC, Goodman SH. Unsaturated polyester and vinyl ester resins. In: Goodman SH, editor. Handbook of thermoset plastics. Westwood (NJ): Noyes Publications; 1998. p. 97.

172. Claffey DJ, Case MF, Finan PA. Glycosylation of l,4:3,6-dianhydro-d-glucitol (isosorbide). Carbohydrate Research. 2004;339:2433–2440.

173. Fenouillot F, Rousseau A, Colomines G, Saint-Loup R, Pascault JP. Polymers from renewable 1,4:3,6-dianhydrohexitols (isosorbide, isomannide and isoidide): a review. Progress in Polymer Science. 2010;35:578–622.

174. Okada M, Tsunoda K, Tachikawa K, Aoi K. Biodegradable polymers based on renewable resources IV enzymatic degradation of polyesters composed of 1,4;3,6-dianhydro-D-glucitol and aliphatic dicarboxylic acid moieties. J Appl Polym Sci. 2000;77:338.

175. Chatti S, Schwarz G, Kricheldorf HR. Cyclic and noncyclic polycarbonates of isosorbide. Macromolecules. 2006;39:9064.

176. Braun D, Bergmann M. Polymers from 1,4;3,6-dianhydrosorbitol. J Prakt Chem. 1992;334:298.

177. Cognet-Georjon E, Mechin F, Pascault JP. New polyurethanes based on diphenylmethane diisocyanate and 1,4;3,6-dianhydrosorbitol 1 model kinetic studies and characterization of the hard segment. Macromol Chem Phys. 1995;196:3733.

178. Beldi M, Medimagh R, Chatti S, Marque S, Prim D, Loupy A, Delolme F. Characterization of cyclic and non-cyclic poly(ether-urethane)s bio-based sugar diols by a combination of MALDI-TOF and NMR. European Polymer Journal. 2007;43:3415.

179. Philip B, Sreekumar K. Synthesis and characterization of chiral main chain polyesters with polar segments tailored for second harmonic generation. J Mater Sci. 2003;38:1573.

180. Caouthar AA, Loupy A, Bortolussi M, Blais JC, Dubreucq L, Medour A. Synthesis and characterization of new polyamides based on diphenylaminoisosorbide. J Polym Sci. Part A: Polym Chem. 2005;43:6480.

181. Caouthar AA, Roger P, Tessier M, Chatti S, Blais JC, Bortolussi M. Synthesis and characterization of new polyamides derived from di(4-cyanophenyl)isosorbide. European Polymer Journal. 2007;43:220.

182. Kamm B, Gruber PR, Kamm M. Biorefineries–industrial processes and products: status quo and future directions. Weinheim (Germany): Wiley-VCH; 2006.

183. Jasinska L, Koning CE. Unsaturated, biobased polyesters and their cross-linking via radical copolymerization. Journal of Polymer Science Part A: Polymer Chemistry. 2010;48:2885–2895.

184. Van Walsem J, Anderson E, Licata J, Sparks K, Mirley C, Sivasubramanian MS, inventors. Process for producing a monomer component from a genetically modified polyhydroxyalkanoate. United States patent US 20120315681 A1. 2012 Dec 13.

185. Sadler JM, McAninch IM, Toulan FR, Levine F, La Scala JJ. Resin characterization. Aberdeen Proving Ground (MD): Army Research Laboratory (US); 2015 June. Report No.: ARL-SR-0323.

186. Warren CD. Low cost carbon fiber overview. Oak Ridge (TN): Oak Ridge National Laboratory; 2011 May.

187. Alibaba.com. http://price.alibaba.com/price/priceLeafCategory.htm?categoryId=100001628 [accessed 26 Apr 2012].

188. Warren CD. Future low cost carbon fiber for autos: international scale-up and what is needed. Oak Ridge (TN): Oak Ridge National Laboratory; 2008 Sep.

189. Patel AD. Techno-economic analysis of Di-butyl ketone, Dimethyl furan and Hydroxymethyl furfural production from biomass based resources [master's thesis]. [Ames (IA)]: Iowa State University; 2009.

190. La Scala J. Final report: low HAP/VOC compliant resins for military applications. Aberdeen Proving Ground, MD: Environmental Security Technology Certification Program; 2011 Sep. Report No.: ESTCP WP-0617.

191. World Bank Group. State and trends of carbon pricing, 2014. Washington (DC): World Bank Group; 2014 May. Report No.: 88284.

Appendix A. Supporting Data: Isolation and Characterization of Ligninolytic Bacterial Species

INTENTIONALLY LEFT BLANK.

Appendix B. List of Scientific/Technical Publications

B.1 Articles in Peer Review Journals

Journal Papers Publications

The team has 17 journal publications on this work.

1) A. A. Ogale, M. Zhang, and J. Jin, Recent Advances in Carbon Fibers Derived from Bio-based Precursors, *Journal of Applied Polymer Science*. 2016, DOI: 10.1002/APP.43794, May 2016

2) Eric D. Hernandez, Alexander W. Bassett, Joshua M. Sadler, John J. La Scala, and Joseph F. Stanzione, Synthesis and Characterization of Bio-based Epoxy Resins Derived from Vanillyl Alcohol, *ACS Sustainable Chem. Eng.*, **2016**, *4* (8), pp 4328–4339.

3) M. Zhang and A. A. Ogale*, "Effect of temperature and concentration of acetylated-lignin solutions on dry-spinning of carbon fiber precursors", J. APPL. POLYM. SCI. 2016, DOI: 10.1002/APP.43663, March 2016

4) F. Hu, S. Kumar Yadav, J.J. La Scala, J.M. Sadler, G.R. Palmese, Preparation and Characterization of Fully Furan-Based Renewable Thermosetting Epoxy-Amine Systems, *Macromolecular Chemistry and Physics*, 216 (13), 1441-1446, (2015).

5) Sadler, J. M.; Toulan, F. R.; Palmese, G. R.; La Scala, J. J., Unsaturated polyester resins for thermoset applications using renewable isosorbide as a component for property improvement, *Journal of Applied Polymer Science*, 132(30), 42315 (2015)

6) M. Zhang, J. Jin, and A. A. Ogale*, "Carbon Fibers from UV-Assisted Stabilization of Lignin-Based Precursors", Fibers, 3, 184-196, 2015. DOI:10.3390/fib3020184

7) J.J. La Scala and J.F. Stanzione, Richard P. Wool, PhD, Professor, FRSC In memoriam, *Journal of Applied Polymer Science*, 132(37), 42525 (2015)

8) Hu F, La Scala JJ, Sadler JM, Palmese GR. Synthesis and characterization of thermosetting furan-based epoxy systems, macromolecules. May 2014;47(10):3332–3342. http://pubs.acs.org/doi/abs/10.1021/ma500687t

9) Holmberg AL, Reno KH, Wool RP, Epps TH II. Biobased building blocks for the rational design of renewable block polymers. Soft Matter.

2014;10:7405–7424.
http://pubs.rsc.org/en/content/articlelanding/2014/sm/c4sm01220h

10) M. Zhang and A. A. Ogale*. Carbon fibers from dry-spinning of acetylated softwood kraft lignin. CARBON 69, 626-29 (2014). http://www.sciencedirect.com/science/article/pii/S0008622313011573.

11) Sadler J, Toulan R, Nguyen T, Kayea R, Ziaee S, Palmese G, La Scala J. Isosorbide as the structural component of bio-based unsaturated polyesters for use as thermosetting resins. Carbohydrate Polymers. 2014;100(SI):97–106. http://dx.doi.org/10.1016/j.carbpol.2013.04.036

12) Sadler JM, Nguyen T, Toulan FR, Szabo JP, Palmese GR, Scheck C, Lutgen S, La Scala JJ. Isosorbide-methacrylate as a bio-based low viscosity resin for high performance thermosetting applications. Journal of Materials Chemistry A. 2013;1(40):12579–12586. http://pubs.rsc.org/en/content/articlelanding/2013/TA /c3ta12918g#!divAbstract

13) Stanzione JF III, Giangiulio PA, Sadler JM, La Scala JJ, Wool RP. Lignin-Based bio-oil mimic as biobased resin for composite applications. Sustainable Chemistry & Engineering. 2013;1:419–426. http://pubs.acs.org/doi/abs/10.1021/sc3001492

14) La Scala J, Wool RP. Fundamental thermo-mechanical property modeling of triglyceride-based thermosetting resins. Journal of Applied Polymer Science. 2013;127(3). http://onlinelibrary.wiley.com/doi/10.1002/app.37927/abstract

15) Stanzione JF III, Sadler JM, La Scala JJ, Wool RP. Vanillin-based resin for use in composite applications. Green Chemistry. 2012;14(8):2346– 2352. http://pubs.rsc.org/en/content/articlelanding/2012/gc /c2gc35672d#!divAbstract

16) Sadler JM, Nguyen AP, Greer SM, Palmese GR, La Scala JJ. Synthesis and characterization of a novel bio-based reactive diluent as a styrene replacement. Journal of BioBased Materials and BioEnergy. 2012;6:86–93. http://www.ingentaconnect.com/content/asp/jbmb/2012/00000006 /00000001/art00009?token=004d1c7dc4bd36d5512139412f415d7678 255f45514a2f42384259253033294876c47b8945a83

17) Stanzione JF III, Sadler JM, La Scala JJ, Wool RP. Lignin model compounds as bio-based reactive diluents for liquid molding resins. ChemSusChem. 2012;5(7):1291–1297. http://onlinelibrary.wiley.com /doi/10.1002/cssc.201100687/abstract

Draft Journal Papers

The group has a number of other journal publications in the works including the following one.

18) Chambers SD, Hayes MM, Zhang Y, Bodine AB, Rodgers RS, Greene AK. Putative lignolytic *serratia* 1 sp. isolated from Louisiana environmental samples. Draft.

B.2 Technical Reports

This work has resulted in 4 technical reports, including one international technical report through TTCP. One more technical report is expected based on the final SERDP WP-1758 report.

19) Faye R Toulan, Joshua M Sadler, and John J La Scala, Bio-Based Polyurethane Containing Isosorbide for Use in Composites and Coatings, ARL-TR-7259, April 2015.

20) La Scala J, Rider A, Harman A, Szabo J, Scheck C, Lutgen AP, Nguyen Lam S, Sadler J, Toulan FR, Palmese G. MAT‐TP6‐O39, thermomechanical properties of bio-derived resins. TTCP MAT Group; 2014 May 1. Report No.: TR-MAT-TP6-3-2014.

21) Cureton L, La Scala J. Synthesis and characterization of furanic compounds. Aberdeen Proving Ground (MD): Army Research Laboratory (US); 2013 Sep. Report No.: ARL-TR-6668.

22) John La Scala, et al. Biobased carbon fibers and high-performance thermosetting resins for use in US Department of Defense applications. Aberdeen Proving Ground (MD): Army Research Laboratory (US); 2012 Jun. Report No.: ARL-SR-245.

23) La Scala J. et al. Biobased carbon fibers and high-performance thermosetting resins for use in US Department of Defense applications, SERDP WP-1758 final report. Draft.

B.3 Conference Proceedings

24) Craig M. Paquette, Joshua M. Sadler, John La Scala, Bio-based replacement monomers for PMR-15, High Temple Workshop, Florence, AL, 3 FEB 2015

25) Joshua M. Sadler, Faye R. Toulan, John J. La Scala, Characterization of bio-based phenolic analogs for use as novel resins for high performance materials, High Temple Workshop, Florence, AL, 3 FEB 2015

26) Joseph F. Stanzione, III, Eric D. Hernandez, Joshua M. Sadler, John J. La Scala, Vanillyl Alcohol: A Renewable Epoxy Resin Building Block, Green Chemistry & Engineering Conference, Bethesda, MD, 15 JUL 2015.

27) Craig Paquette, Joshua Sadler, Raven Toulan, Ian McAninch, Benjamin Harvey, Gregory Yandek, William Eck, F. Hu, S.K. Yadav, G.R. Palmese, and John J. La Scala, Environmentally Friendly High Performance Bio-Based Polymers for DOD Applications: Diamines with Improved Sustainability, Green Chemistry & Engineering Conference, Bethesda, MD, 15 JUL 2015.

28) Invited: J.J. La Scala, Bio-Based Thermosets Inspired by Richard Wool, from Plant Oil-Based Resins to Ligno-Cellulose-Derived Polymers, Green Chemistry & Engineering Conference, Bethesda, MD, 15 JUL 2015.

29) In-Chul Yeh, Berend C. Rinderspacher, Tanya Chantawansri, Yelena Sliozberg, Tim Sirk, Robert M. Elder, LaShonda T. Cureton, John J. La Scala, and Jan W. Andzelm, Computational modeling of bio-based furan polyamides and furfuryl alcohol polymers, Green Chemistry & Engineering Conference, Bethesda, MD, 15 JUL 2015.

30) Invited: Kaleigh H. Reno; Eric D. Hernandez; Dakota Hanemann-Rawlings; Joshua M. Sadler; Joseph F. Stanzione, III; John J. La Scala; Chan Ho Jang; Changqing Wu; Thomas H. Epps, III; and Richard P. Wool, Exploration of bisguaiacols derived from lignin as potential BPA alternatives, Green Chemistry & Engineering Conference, Bethesda, MD, 15 JUL 2015.

31) Invited: J.J. La Scala, Introduction to D. Mielewski, Green Chemistry & Engineering Conference, Bethesda, MD, 15 JUL 2015.

32) Invited: J.J. La Scala, Environmentally Friendly High Performance Bio-Based Polymers for DOD Applications, SERDP Webinar – invited, 22 Jan 2015.

33) Hernandez ED, Sadler JM, La Scala JJ, Stanzione JF. Synthesis, characterization, and bimodal blend studies of renewable bio-based epoxy resins from vanillyl alcohol. 249th ACS National Meeting & Exposition; 2015 Mar 22–26; Denver, CO.

34) Stanzione JF, Wool RP. Next-generation renewable polymers from lignin, ACS Division Proceedings [PMSE Division: Next-Generation Renewable Polymers Symposium]; 2012 Mar; San Diego, CA.

35) Stanzione JF, Sadler JM, La Scala JJ, Wool RP. Functionalized lignin model compounds utilized in bio-based resins. Society for the advancement of material and process engineering (SAMPE) Proceedings [Natural, Green, Bio-Materials and Reinforcements Technology and Applications Symposium]; 2012 May; Baltimore, MD.

36) Sadler J, Phuong A, Nguyen T, Toulan FR, La Scala JJ. Development of bio-based resins from carbohydrate derived compounds for use in renewable composites. 2012 SAMPE Spring Conference; 2012 May 21; Baltimore, MD.

37) Zhang M, Ogale AA. Carbon fibers from bio-derived precursors. Society for the advancement of material and process engineering (SAMPE) Proceedings [Natural, Green, Bio-Materials and Reinforcements Technology and Applications Symposium]; 2012 May; Baltimore, MD.

38) La Scala JJ, Sadler JM, Nguyen AP, Stanzione JF, Wool RP, Koo D, Geng X, Palmese GR. Environmentally friendly bio-based resins for military applications. Proceedings of the Army Science Conference, 2010 Nov, Orlando, FL.

B.4 Abstracts/Presentations

39) J.J. La Scala, O49 Thermomechanical Properties of Bio-Derived Resins, TTCP MAT-TP-6 Annual Meeting, Portsdown West, UK, 25 Mar 2015

40) J.J. La Scala, Changquing Wu, Joseph Stanzione, Kaleigh Reno, Joshua Sadler, SusChem: BPA Replacements with Non-Toxic Biobased Monomers, Briefing to Polymers Program Director, Division of Materials Research, NSF, Newark, DE, 15 Apr 2015.

41) J. Sadler, R. Toulan, J. Stanzione, F. Hu, K. Reno, I-C. Yeh, C. Paquette, C. Annunziato, I. McAninch, W. Eck, B. Harvey, G. Yandek, M. Staehle, R. Wool, G. Palmese, J. Andzelm, & John La Scala, High Performance Bio-Based Polymers for Army Applications, Bio TAB, 10 JUN 2015.

42) J.J. La Scala, J.M. Sadler, High Performance Bio-Based Polymers, Open Campus Open House, Adelphi, MD, 9-10 Dec 2014.

43) J.J. La Scala, Resins Technology for Coatings and Composites, Rowan University, 7 Nov 2014.

44) J.J. La Scala, Resins Technology for Coatings and Composites, Drexel University, 7 Nov 2014.

45) Zhang M., Ogale A. A., UV-assisted stabilization of modified softwood kraft lignin fibers. Oral presentation at AICHE conference, Atlanta, November, 2014

46) La Scala J. Bio-based polymers. ARL-DuPont CRADA Meeting; 2014 May; Wilmington, DE.

47) La Scala J. O39 thermomechanical properties of bio-derived. TTCP-MAT-TP-6; 2014 Mar 20; Melbourne, AS.

48) La Scala JJ. High performance bio-based carbon fibers & thermosetting resins for use in DOD composites applications. SERDP WP-1758, SERDP IPR; 2014 Feb; Arlington, VA.

49) La Scala J. High performance bio-based polymers for DOD applications. Presentation at the ICB review; 2014 May 21; Santa Barbara, CA.

50) La Scala J. Bio-based polymers. Rowan University, 2014 April 11.

51) La Scala J, Sadler J, Paquette C, Toulan R, Annunziato C. Bio-based polymers. EPA; 2014 Sep 17; Aberdeen Proving Ground, MD.

52) Sadler JM, La Scala JJ. Bio-based polymers. Briefing to Bob Grubbs and Brian Stoltz, Cal Tech, 2013 Sep 4, Invited.

53) Zhang M., Ogale A. A., Carbon Fibers Derived from Sustainable Precursors. Poster at SPE ACCE conference, Detroit, September 2013

54) Stanzione J, Sadler JM, La Scala JJ, Wool RP. Lignin-derived resin for high-performance composite applications. 2013 Spring Meeting of ACS; New Orleans, LA.

55) Stanzione J, Sadler JM, Reno K, La Scala J, Wool RP. Getting a handle on vanillin: green modifications. 17th Annual Green Chemistry and Engineering Conference; 2013 Apr 29; West Bethesda, MD.

56) Zhang M., Ogale A. A., Acetylated-lignin as a biopolymer precursor for carbon fibers. Oral presentation at ACS conference, New Orleans, April 2013.

57) Stanzione J, Sadler JM, La Scala JJ, Wool RP. Lignin-derived reactive diluents and their influence on thermosetting resin properties. 17th ACS Green Chemistry & Engineering Conference; 2013 Jun Washington, DC.

58) Stanzione J, Sadler JM, La Scala JJ, Wool RP. Renewable thermosets derived from lignin. 2013 AkzoNobel Student Award in Applied Polymer Science at the Fall ACS meeting; 2013 Sep; Indianapolis, IN.

59) Sadler JM, La Scala JJ. Bio-based carbon fibers & thermosetting resins for use in DOD composites applications. Composites 2013; 2013 Feb 26; Orlando, FL. Invited.

60) La Scala J. Bio-based polymers. DuPont. 2012 Oct 31; Wilmington, DE. Invited.

61) Dowding B, La Scala J. DEA Korea – Bio-based polymeric fibers, 2012 Oct 23.

62) La Scala J. ARL Overview of sustainment and environmentally friendly materials, Hon Undersecretary Hammack; 2012 Oct 11; Aberdeen Proving Ground, MD.

63) La Scala JJ, Sadler J, Lam P, Stanzione J, Wool RP, Palmese G, Zhang M, Greene A, Ogale A. Bio-based polymers and fibers for defense applications. Bioenvironmental Polymers Symposium; 2012 Sep 23; Denton, TX.

64) Stanzione JF, Sadler JM, La Scala JJ, Wool RP. Methacrylated lignin model compounds as monomers for use in high performance polymers. 244th ACS National Meeting & Exposition; 2012 Aug 12; Philadelphia, PA.

65) Sadler JM, Toulan FR, Ziaee S, La Scala JJ. Development and characterization of carbohydrate derived furanic resins as phenolic analog. 244th ACS National Meeting & Exposition; 2012 Aug 12; Philadelphia, PA.

66) Zhang M., Ogale A. A., Carbon Fibers from Bio-Derived Precursors. Oral presentation at SAMPE conference, Baltimore, May 2012

67) Stanzione JF (invited speaker). Next-generation renewable polymers from lignin. 243rd ACS National Meeting and Exposition; 2012 Mar; San Diego, CA.

68) Sadler JM, Toulan FR, Kayea RV, La Scala JJ. Development of bio-based resins from carbohydrate derived compounds for use in renewable composites. 243rd ACS National Meeting and Exposition; 2012 Mar; San Diego, CA.

69) Stanzione JF, Wool RP. Lignin-derived monomers utilized in bio-based resins. 243rd ACS National Meeting and Exposition; 2012 Mar; San Diego, CA.

70) La Scala JJ. Environmentally friendly composite materials for DOD application. Natick Soldier Center, Invited Seminar, 2011 Mar.

71) La Scala J (invited speaker). Environmentally friendly composite materials for DOD application. CUNY, Invited Seminar, 2011 Sep.

72) Sadler JM, Nguyen AP, Greer SM, Koo D, Palmese GR, La Scala JJ. Synthesis and characterization of isosorbide based unsaturated polyester resins as a renewable alternative for petroleum derived resins. ACS Green Chemistry & Engineering Conference; 2011 Jun; Washington, DC.

73) Nguyen AP, Sadler JM, Greer SM, La Scala JJ. Formulation and characterization of thermosetting resins with low VOC and HAP contents using bio-based furanic reactive diluents. ACS Green Chemistry & Engineering Conference; 2011 Jun, Washington, DC.

74) Stanzione JF, Sadler JM, La Scala JJ, Wool RP. Methacrylated lignin-model compounds as reactive diluents in bio-based resins. ACS Green Chemistry & Engineering Conference; 2011 Jun; Washington, DC.

75) La Scala J (invited speaker). Bio-based composite resins. 241st ACS National Meeting & Exposition; 2011 Mar; Anaheim, CA.

76) Stanzione JF (invited speaker). Sadler JM, La Scala JJ, Wool RP. Methacrylated kraft pine lignin for use in high-performance bio-based resins. 241st ACS National Meeting & Exposition; Mar 2011; Anaheim, CA.

77) Sadler JM, Nguyen AP, Greer SM, Koo D, Palmese GR, La Scala JJ. Synthesis, formulation and characterization of bio-based unsaturated polyester resin. 241st ACS National Meeting and Exposition; 2011 Mar; Anaheim, CA.

78) Sadler JM, Nguyen AP, Palmese GR, La Scala JJ. Synthesis and characterization of thermosetting isosorbide-based resins. 241st ACS National Meeting and Exposition; 2011 Mar; Anaheim, CA.

79) La Scala JJ, Sadler JM, Nguyen AP, Stanzione, JF, Wool RP, Koo D, Geng X, Palmese GR. Environmentally friendly bio-based resins for military applications. Army Science Conference; 2010 Nov; Orlando, FL.

80) Stanzione J. Lignin-derived monomers for use in high-performance bio-based resins. ACS Summer School on Green Chemistry and Sustainable Energy; 2010 Aug; Boulder, CO.

81) Stanzione J. Lignin-derived monomers for us in thermally resistant bio-based resins. 14th Annual ACS Green Chemistry & Engineering Conference; 2010 Jun; Washington, DC.

B.5 Textbooks and Chapters

82) M. Zhang and A. A. Ogale, "Carbon fibers derived from acetylated softwood kraft lignin" Chapter 6 in “Polymer Precursor-Derived Carbon”, Editors: A. K. Naskar and W. Hoffman, pp. 137-168, American Chemical Society, ACS Publishing, USA, 2014. Doi: 10.1021/bk-2014-1173.ch006

B.6 Dissertations and Theses

This work supported 4 PhD students, 3 master’s students, and 1 BS student at 3 universities.

83) Fengshuo Hu, Structure versus Property Relationship of Thermosetting Polymer Materials Derived from Biobased Feedstocks, Ph.D. Dissertation, Drexel University, Philadelphia, PA, December 2016.

84) Meng Zhang (PhD), Carbon Fibers Derived From Dry-Spinning of Modified Lignin Precursors, Clemson University, Clemson, SC, May 2016.

85) Daniel Rogers. Lignin-Derived Thermosetting Vinyl Ester Resins for High Performance Applications, Master's Thesis, Rowan University, Glassboro, NJ, December 2015.

86) Eric D. Hernandez, Synthesis and Characterization of Vanillyl Alcohol Based Thermosetting Epoxy Resins, Master's Thesis, Rowan University, Glassboro, NJ, August 2015.

87) Joseph F. Stanzione, Lignin-based monomers: utilization in high performance polymers and the effects of their structures on polymer properties, Ph.D. Dissertation, University of Delaware, Newark, DE, 2013.

One additional dissertation is expected from K Reno in 2017 on BGF resins and polymers. This work also supported the education of one master's student at Clemson University who is expected to complete a thesis in 2017/2018.

INTENTIONALLY LEFT BLANK.

Appendix C. Other Supporting Materials

C.1 Patents/Applications

The group has 8 patents/applications for this work.

88) G.R. Palmese, J.J. La Scala, J.M. Sands, X Geng, "Toughening Cross-linked Thermosets," U.S. Patent 9,102,807, 11 Aug 2015.

89) K. Reno, J.F. Stanzione, J.M. Sadler, E. Hernandez, J.J. La Scala, R.P. Wool, "Bisphenol Alternatives Derived from Renewable Substituted Phenolics and Their Industrial Application," PCT/US2015/032583, 27 May 2015.

90) Palmese GR, Hu F, Geng X, La Scala JJ. Toughening of epoxy thermosets. US Provisional Patent Application US 62,049,806. 2014 Sep 12.

91) Geng X, Palmese G, Sands J, La Scala J. Toughening cross-linked thermosets. US Patent Application No. 14,320,698, Divisional Patent Application. 2014 July 10.

92) Reno K, Stanzione J, Sadler J, La Scala J, Wool R. Bisphenol alternatives derived from renewable substituted phenolics and their industrial, application. US Provisional Patent 62,003,115. 2014 May 27.

93) La Scala J, Sands JM, Palmese GR. Fatty acid monomers to reduce emissions and toughen polymers. US patent 8,372,926. 2013 Feb 12.

94) Sadler JM, Lam P, Palmese GR, La Scala JJ. Renewable bio-based (meth)acrylated monomers as vinyl ester crosslinkers. PCT Patent Application PCT/US2012/050235.

95) Sadler JM, Lam AP, La Scala JJ, Palmese GR. Renewable bio-based (meth)acrylated monomers as vinyl ester cross-linkers. Provisional Patent Application No. 61,521,981. 2011 Aug.

C.2 Protocols/User Guides

96) Joshua Sadler, Ian M McAninch, Faye R Toulan, Felicia Levine, and John J La Scala, Resin Characterization, ARL-SR-0323, June 2015

C.3 Awards

Of most significance, members of the team have won significant awards for their technology development. Richard P Wool was the winner of the 2013 Presidential Green Chemistry Challenge Award for Sustainable Polymers and Composites:

Optimal Design. Three team members, Dr. Stanzione, Ms. Reno, and Dr. La Scala, were noted contributors to the award and received certificates for their contributions. In addition, Ms. Meng Zhang won outstanding student paper award at the Automotive Composites Conference (ACCE), Society of Plastics Engineers, in 2013. Dr. Stanzione won an ACS Award for best paper, enabling him to attend the ACS Green Chemistry Conference in 2013 and giving him a 2-week experience at the National Renewable Energy Laboratory in Colorado.

C.4 Publicity/News Articles/Social Media:

Enclosed below are links to various websites, blogs, etc., related to developments in SERDP WP-1758 and somewhat to SERDP WP-2402. We list items regarding awards, web articles/blogs, and SERDP WP-1758 affiliated personnel web pages.

Award Announcements

EPA Presidential Green Chemistry Award

- http://www2.epa.gov/green-chemistry/2013-academic-award
- http://www.arl.army.mil/www/default.cfm?article=2421

Web Articles

- http://www.rsc.org/chemistryworld/2014/03/green-safe-bpa-substitute-bgf-lignin-paper
- http://www.healthline.com/health-news/cancer-renewable-bpa-alternative-found-031614
- http://www.acs.org/content/acs/en/pressroom/newsreleases/2014/march/potentially-safer-greener-alternative-to-bpa-could-come-from-papermaking-waste.html
- http://greenchemicalsblog.com/2014/03/18/video-lignin-based-alternative-to-bpa/
- http://news.yahoo.com/bpa-alternative-made-paper-waste-coming-near-161000279.html
- https://twitter.com/biogarage/status/445430019096322048 (I don't speak German, but after clicking on the link I am not going out on much of a limb…)

- http://www.plasticstoday.com/articles/lignin-derived-compound-replace-potentially-harmful-bisphenol-plastics
- http://www.foodqualitynews.com/Industry-news/BPA-replacement-within-the-next-few-years

Collaborator Profiles and Group Websites

- http://www.chemeng.drexel.edu/palmesegroup/
- http://www.chemeng.drexel.edu/Faculty/Individual/palmese/Default.aspx
- http://www.che.udel.edu/research_groups/wool/index.html
- http://www.che.udel.edu/directory/facultyprofile.html?id=471
- http://www.clemson.edu/ces/chbe/faculty_staff/ogale_a.html
- http://www.rowan.edu/colleges/engineering/faculty_staff/listing/moreinfo.cfm?id=826

List of Symbols, Abbreviations, and Acronyms

1MIN	1-methylimidazole
2-D	2-dinensional
3-D	3-dimensional
ABP	acryloyl benzophenone
Ace-SKL	acetylated softwood Kraft lignin
Ace_Soda	acetylated soda (protobind 1000) lignin
AHEW	Amine Hydrogen Equivalent Weight
Al_2O_3	aluminum oxide
AN	acid number
ARL	US Army Research Laboratory
B-UPE	benzyl end group modified UPE
bAMF	2,5-bis(aldehydyemethyl)furan
BGF	bisguaiacol F
BGP	bisguaiacol P
bHMF	2,5-bis(hydroxymethyl)furan
bNMF	2,5-bis(aminomethyl)furan
BPA	bisphenol A
Bio-R	proprietary reactive diluent
Bio-X	proprietary anhydrocellulose cross-linker
Bio-Y	proprietary carbohydrate cross-linker
BOB	1, 4-bis[(2-oxiranylmethoxy)methyl]-benzene
BOF	2, 5-bis[(2-oxiranylmethoxy)methyl]-furan
BPA	bisphenol A
Bu_4NBr	tetra-n-butylammonium bromide
CAEFF	Center for Advanced Engineering Fibers and Films

$CDCl_3$	deuterated chloroform
CH_2Cl_2	dichloromethane
CO_2	carbon dioxide
COM	cost of manufacturing
CoNap	cobalt naphthenate
COSY	correlation spectra (NMR)
DCPD	dicyclopentatidene
DGEBA	lycidyl ether of bisphenol A
DEGBG	diglycidyl ether of BG
DGEGD	gastrodigenin
DGEVA	diglycidyl ether of vanillyl alcohol
DI	deionized
DM	dimethacrylate
DMA	dynamic mechanical analysis
DMAP	4-dimethylaminopyridine
DMF	dimethyl formamide
DMSO	dimethyl sulfoxide
DMSO-d_6	dimethyl sulfoxide with six (all) deuterated protons
DOD	Department of Defense
DOE	Department of Energy
DPI	diaryliodonium hexafluoroantimonate
DSC	differential scanning calorimetry
E	modulus of material
E’	storage modulus
E”	loss modulus
ECN	brand of organosolv lignin
EEW	epoxy equivalent weight

EPA	Environmental Protection Agency
EPI	Estimation Program Interface
ESTCP	Environmental Security Technology Certification Program
FA-GM	furoic acid-glycidyl methacrylate
FTIR	Fourier transform IR spectroscopy
FY	fiscal year
GDM	glycerol dimethacrylate
GPC	gel permeation chromatography
H-UPE	hexyl end group modified UPE
HAP	hazardous air pollutant
HCl	hydrochloric acid
HCN	hydrogen cyanide
HMF	5-hydroxymethylfurfural
HSQC	heteronuclear single quantum coherence
IM	isosorbide methacrylate
Indulin AT	brand of softwood Kraft lignin
IPA	isopropyl alcohol
IPDI	isophorone diisocyanate
IR	infrared
KBr	potassium bromide
KPL	Kraft pine lignin
LD50	lethal dose
LMC	lignin model compound
M4PG	4-propyl-2-methoxyphenyl methacrylate
MA	maleic anhydride
MA_Ace_SKL	methacrylated and acetylated softwood Kraft lignin
MAA	methacrylic acid

MBO	bio-oil mimic
MDS	molecular docking simulation
MDSC	modulated differential scanning calorimetry
ME	methacrylated eugenol
MEKP	methyl ethyl ketone peroxide
Meth_KPL_UD	methacrylated Kraft pine lignin from the University of Delaware
Meth_SKL	methacrylated softwood Kraft lignin
MG	methacrylated guaiacol
$MgSO_4$	magnesium sulfate
MLau	methacrylated lauric acid
MLMC	methacrylated lignin model compound
MMA	methyl methacrylate
M_n	number average molecular weight
MP	mesophase pitch
MS	mass spectrometry
MV	methacrylated vanillin
MVGDM	methacrylated vanillin glycerol dimethacrylate
M_w	weight average molecular weight
N_2	nitrogen
$NaHCO_3$	sodium bicarbonate
$NaNO_2$	sodium amide
NaOH	sodium hydroxide
NIR	near IR
NIST	National Institute of Standards and Technology
NMR	nuclear magnetic resonance
NSWCCD	Naval Surface Warfare Center Carderock Division

O_2	oxygen
ORNL	Oak Ridge National Laboratory
P_2O_5	phosphorus pentoxide
PACM	Bis(p-aminocyclohexyl) methane, Air Products
PAN	polyacrylonitrile
PDI	polydispersity index
PI	photoinitiator or principal investigator
Protobind 1000	soda lignin
Pt	platinum
RED	relative energy difference
ROMP	ring-opening metathesis polymerization
SEC	size exclusion chromatography
SEM	scanning electron microscopy/microscope
SERDP	Strategic Environmental Research Development Program
SKL	softwood Kraft lignin
Tan(δ)	ratio of loss modulus to storage modulus
TBAB	tetrabutyl ammonium bromide
T_g	glass transition temperature
T_m	melting temperature
TDI	toluene diisocyanate
TGA	thermogravimetric analysis
THF	tetrahydrofuran
THPM-GE	tris-hydroxyphenylmethane glycidyl ether
TiPED	tiered protocol for endocrine disruption
TLC	thin-layer chromatography
TRL	technical readiness level

TTCP-MAT-TP6	The Technology Cooperation Program, Materials Group, Technical Panel 6
UPE	unsaturated polyester
UV	ultraviolet
VA	vanillin alcohol
VE	vinyl ester
VE828	vinyl ester 828
VER	vinyl ester resin
VOC	volatile organic compound
WAXD	wide-angle X-ray diffraction
wt%	weight-percent

1 (PDF) DEFENSE TECHNICAL INFORMATION CTR DTIC OCA

2 (PDF) DIRECTOR US ARMY RESEARCH LAB RDRL CIO L IMAL HRA MAIL & RECORDS MGMT

1 (PDF) GOVT PRINTG OFC A MALHOTRA

1 (PDF) CLEMSON UNIV DEPT OF CHEM & BIOMOLECULAR ENGRG A OGALE

1 (PDF) DREXEL UNIV G R PALMESE

1 (PDF) ROWAN UNIVERSITY J F STANZIONE

1 (PDF) SERDP WEAPONS SYS & PLATFORMS SERDP & ESTCP PROG OFC R NISSAN

2 (PDF) NOBLIS B LEWIS L MILLER

ABERDEEN PROVING GROUND

10 (1 HC) (9 PDF) DIR USARL
RDRL SER
W BENARD
RDRL WM
J ZABINSKI
RDRL WMM
M VANLANDINGHAM
R DOWDING
RDRL WMM A
J LA SCALA (1 PDF, 1 HC)
J SANDS
E WETZEL
RDRL WMM C
J SNYDER
RDRL WMM G
J LENHART
APG MD 21005-5069

INTENTIONALLY LEFT BLANK.